PROTEIN AND CELL THERAPY FOR LECITHIN–CHOLESTEROL ACYLTRANSFERASE (LCAT) DEFICIENCY

By

Jee Keem Low

A thesis submitted in partial fulfilment of the requirements for the degree of

Doctor of Medicine

Royal Free University College
Medical School
2008

Royal Free University College Medical School

DECLARATION

I, Dr Jee Keem Low, confirm that the work presented in this thesis is my own. Where information has been derived from other sources, I confirm that this has been mentioned in the thesis.

Signature:……

ABSTRACT

PROTEIN AND CELL THERAPY FOR LECITHIN–CHOLESTEROL ACYLTRANSFERASE (LCAT) DEFICIENCY

Lecithin-cholesterol acyltransferase (LCAT) is an enzyme principally secreted by the liver into the circulation where it esterifies cholesterol and plays a key role in high-density lipoprotein (HDL) metabolism. In familial and acquired (liver disease) LCAT deficiency, the failure to esterify cholesterol causes many cellular and metabolic disturbances. Here, I describe the purification of recombinant LCAT and assess two approaches to treat LCAT deficiency. Human LCAT cDNA was cloned into a selectable expression vector and used to generate a stably–transfected Chinese hamster ovary (CHO) cells secreting human LCAT tagged with 6 histidine residues. Productive clones were selected, monitoring LCAT activity by a modification of a radioactive enzymic assay for plasma, and the enzyme purified from culture medium by immobilised cobalt affinity chromatography. The pure LCAT, as judged by SDS-PAGE, was used to raise monoclonal antibodies in LCAT knockout mice for future development of a sensitive immunoassay. For therapy, I evaluated injection of pure LCAT into the peritoneal cavity of LCAT knockout mice using single and repeat dose regimes. LCAT activity was measurable in plasma post-injection and the percentage of esterified cholesterol increased, while agarose gel electrophoresis confirmed a rise in HDL levels. In a second approach, I encapsulated the recombinant CHO cells in biocompatible and semipermeable alginate-polylysine microcapsules using a syringe pump extrusion method. A study *in vitro* showed that, after an initial lag phase, LCAT was secreted for over 90 days with the capsules remaining intact. These microencapsulated cells were implanted into peritoneal cavities of LCAT-deficient mice. LCAT activity was detected in mice plasma one week post-implantation; the relative amount of esterified cholesterol was increased and lipoprotein profile was improved. I conclude that injection of recombinant enzyme or of encapsulated LCAT-secreting cells are feasible therapies for familial and acquired LCAT deficiency.

DEDICATION

I would like to dedicate this thesis to my wife, mother, brothers and sisters for all their love and support and encouragement through the years; my late father who did not live to see the thesis come to fruition.

TABLE OF CONTENTS

LIST OF FIGURES

LIST OF TABLES

LIST OF ABBREVIATIONS

ALF……Acute liver failure

Apo…….Apolipoprotein

BSA……Bovine serum albumin

CE……...Cholesteryl ester

CETP……..Cholesteryl ester transfer protein

CHO……Chinese hamster ovary cells

DHFR…….Dihydrofolate reductase

ECACC……...European Collection of Animal Cell Cultures

EGTA……. Ethyleneglycol-aminoethyl-tetra-acetic acid

FCS…….Foetal calf serum

FED…… Fish-eye disease

FLD…… Familial LCAT deficiency

HDL……High density lipoprotein

HIC…….Hydrophobic interaction chromatography

HRP…….Horse radish peroxidase

IDL……. Intermediate density lipoprotein

IMAC……. Immobilized metal affinity chromatography

LCAT……. Lecithin cholesterol acyltransferase

Mtx……. Methotrexate

NTA……Nitrilotriacetic acid

OLT……Orthotopic liver transplantation

PAGE……. Polyacrylamide gel electrophoresis

PBS…….Phosphate buffered solution

PCR…….Polymerase chain reaction

PFM……Protein free medium

PLL…….Poly-L-lysine

SFM……Serum free medium

SDS…….Sodium dodecyl sulphate

UC……...Unesterified cholesterol

VLDL……. Very low density lipoprotein

X-gal.....5-bromo-4-chloro-3-indolyl-β-D-galactopyranoside

CHAPTER 1

INTRODUCTION

1. INTRODUCTION

1.1 Lipoprotein Metabolism

1.1.1 Introduction

Lipoproteins are macromolecular complexes that consist of a hydrophobic core of triglyceride and cholesteryl ester surrounded by an amphipathic monolayer of phospholipids, free cholesterol and proteins. The major lipids cholesterol and triglycerides are insoluble in aqueous solutions and are transported in blood as lipoproteins. Lipoproteins are classified on the basis of their density, electrophoretic mobility, and relative lipid and protein content (Gotto *et al*., 1986), into five major classes: (1) Chylomicrons are very large particles that float even on standing and have a density of $\leq$ 0.95 g/mL; they remain at the origin on electrophoresis. (2) Very-low-density lipoprotein (VLDL) floats at a density of 0.95-1.006 g/ml and migrate to a "pre-beta" position on paper electrophoresis. (3) Intermediate-density lipoprotein (IDL) floats in the density range 1.006-1.019 g/ml. (4) Low-density lipoprotein (LDL) floats in the density range 1.019-1.063 g/mL and migrates in the beta position. (5) High-density lipoprotein (HDL) floats between 1.063 and 1.21 g/mL and migrates furthest on electrophoresis to the alpha position.

Apoproteins or apolipoproteins are the protein components of lipoproteins and are important in regulating lipid transport. There are at least nine apolipoproteins that are distributed in significant amounts in different human lipoproteins. They are water soluble and have high alpha- helix content.

1.1.2 Function of lipoproteins

Chylomicrons

In humans, chylomicrons are lipoproteins that transport dietary fats, cholesterol and fat soluble nutrients. The chylomicron surface is composed of phospholipid, apoB48 and apoAI, AII and AIV. Triglyceride makes up 90 % of the core weight and is less dense than the plasma. The chylomicrons, which carry these triglycerides, appear only after a fatty meal. They are assembled in intestinal mucosal cells and released into the lacteals of intestinal villi. The chylomicrons reach the general circulation via the thoracic duct. After entry into the plasma, the chylomicrons acquire apoC and apoE

from the surface of HDL. Free cholesterol, cholesteryl esters and phospholipids from HDL are transferred to chylomicrons. In the extrahepatic tissues, the chylomicron's triglyceride is hydrolyzed to free fatty acids and 2-monoacylglycerol by lipoprotein lipase (LPL). As hydrolysis proceeds, decreasing core volume, the surface area is also reduced by the transfer of phospholipid, free cholesterol and apoC lipoproteins back to HDL. The remaining remnant particles are enriched with cholesteryl ester and apoE can interact with receptors on hepatocytes (Gotto *et al*., 1986). The uptake of chylomicron remnants involves interaction with heparin sulphate proteoglycans followed by binding to the LDL-receptor or the LDL-receptor-related protein (LRP). This binding requires apoE. After binding to one of the receptors, the remnant particle is endocytosed and its constituent lipids and proteins are hydrolyzed by lysosomal enzymes.

Very-low-density lipoproteins

VLDL is synthesized in the liver and transport mainly triglyceride in the fasting state. They contain 10 - 15 % of total serum cholesterol and are precursors for LDL. Nascent VLDL contains apoB-100 and small amounts of apoE and apoC. Like the chylomicrons, VLDL later acquires more apoE and apoC by transfer from HDL. ApoB, apoE and apoC play a significant role in VLDL catabolism via their interactions with enzymes, cell surface proteoglycans and specific receptors. Like chylomicrons, VLDL is metabolized initially by LPL on endothelial cell surfaces. As lipolysis proceeds, VLDL become smaller and denser and is converted to IDL. Triglyceride hydrolysis is accompanied by the transfer of surface cholesterol, phospholipids and apolipoproteins to HDL, but like chylomicron remnants, VLDL remnants possess apoE, which mediates their uptake into liver.

The term VLDL remnant has been used along with IDL to describe the product of LPL-mediated VLDL triglyceride catabolism. Larger VLDL remnants containing multiple copies of apoE are removed from the plasma by the liver, whereas the smaller denser VLDL are targeted for conversion to IDL and eventually remodelled to LDL (Packard *et al*., 1984). The catabolism of VLDL remnant is affected by hepatic lipase (HL). Studies suggest that HL play a role in removing triglycerides from partially catabolised VLDL or IDL and LDL (Deckelbaum *et al.*, 1992). In addition, HL facilitates the uptake of VLDL remnants by hepatocytes.

Low-density lipoprotein production and catabolism

LDL is a major carrier of cholesterol and cholesteryl esters. They contain about 70 % of total serum cholesterol and function to deliver cholesterol to peripheral tissues in the body, where it is used for synthesis of cell membranes and steroid hormones.

LDL is mainly produced as a result of catabolism of VLDL and IDL. Studies in humans (Arad *et al*., 1990) and animals have demonstrated that some may also be produced independently of VLDL or IDL via direct secretion from the liver. Its lipid component includes a high proportion of cholesterol and cholesterol esters. The metabolism of LDL is intimately connected to cholesterol metabolism. Although cholesterol is a necessary component of mammalian cell membranes, excess synthesis and failure to clear cholesterol results in a greatly increased risk of cardiovascular disease.

LDL circulates in the blood on average for 3 days as its metabolism is sluggish. The LDL-receptor is a glycoprotein with a molecular weight of 160 kD and is present on the cell surfaces of nearly all tissues in the body. Approximately two-thirds of the LDL is taken up by the liver and one-third by the extrahepatic tissues. LDL acquired through the LDL-receptor is the major external source of cholesterol (Goldstein and Brown, 1985). After binding of LDL apoB-100 to the LDL-receptor, the particle is internalized and delivered to lysosomes. Within the lysosomes, apolipoproteins are degraded to amino acids by proteases. Cholesteryl ester is converted to free cholesterol via the action of an acid lipase.

The majority of LDL (60 % to 80 %) is cleared by LDL-receptor mediated pathways. Macrophages and some endothelial cells possess alternative lipoprotein receptors collectively known as the scavenger receptors. There are several of them with various affinities for native and chemically modified LDL. Their main function is the removal of aberrant or aged lipoproteins that are no longer ligands for other lipoprotein receptors.

High-density lipoprotein metabolism

HDL is responsible for transporting about 20 % of cholesterol. It is an important carrier for reverse cholesterol transport which involves the transfer of membrane cholesterol to HDL, its conversion to cholesteryl esters and its ultimate transfer to LDL and the liver (Bruce and Tall, 1995). High levels of HDL-cholesterol are associated with a reduced risk for atherosclerosis (Barter and Rye, 1994).

Nascent HDL is secreted by the liver and intestine. They are small, cholesterol-poor, phospholipids-rich particles, which resemble a disc of lipid bilayer with apolipoproteins at the edge. Nascent HDL from liver contains apoAI, apoAII, apoE and the apoC but the HDL from intestine has only apoAI as its principal apolipoprotein, the rest being acquired later by the transfer from other lipoproteins.

Once in the circulation, nascent HDL adsorbs free, unesterified cholesterol both from other lipoproteins and from cell membranes and become HDL_3 particles. Recent work suggests that ATP-binding cassette transporter, class A1 (ABCA1), a membrane protein, mediates the efflux of cholesterol across peripheral cell membranes and indirectly function as a cholesterol efflux regulatory protein (Oram and Lawn, 2001; Owen and Mulcahy, 2002). The effluxed cholesterol is transferred to extracellular lipid-poor apoAI. Cell surface transporter ABCG1, have been implicated in the transfer of additional cholesterol to nascent HDL and HDL_3 (Wang *et al.*, 2004; Zannis *et al*., 2006). The cell- derived cholesterol is converted to cholesteryl esters through the action of lecithin-cholesterol acyltransferase (LCAT), an enzyme that is activated by the HDL component apoAI. The hydrophobic cholesteryl esters formed migrate to the centre of the particle and increase the capacity of the HDL_3 surface to accept more free cholesterol. The original discoidal HDL expands into a spherical particle. As the HDL_3 enlarges, they accommodate apoCII and apoCIII as well as more phospholipid on their surfaces. HDL also acquires apoE at this time and all these processes lead to the formation of HDL_2. When they reach the liver, they are taken up by endocytosis.

Cholesteryl ester transfer protein (CETP) mediates the transfer of cholesteryl ester from HDL to other lipoproteins (chylomicrons and VLDL) (Tall, 1990) either alone or exchanged for triglycerides. As the chylomicron and VLDL remnants are taken up by the liver via LDL or other receptor-mediated pathways, the CETP-transferred cholesteryl esters are also removed. Cholesterol uptake from HDL by cells is mediated by scavenger receptor class B, type 1 (SR-B1), which is localised in membrane invaginations termed caveolae (Kreiger, 2001; Silver *et al*., 2001). SRB1 is highly expressed in liver, adrenal, ovaries and testes, all tissues with a high cholesterol demand for bile acid synthesis or steroidogenesis. When SR-B1 binds HDL in hepatocytes, the intact particles are taken up into endosomes. The cholesteryl esters are hydrolysed to free cholesterol, while the receptor and its lipid-depleted HDL are not degraded but recycled to the cell surface (Owen and Mulcahy, 2002).

The number of cholesterol molecules, especially esterified cholesterol in each HDL particle and the number of HDL particles determine the plasma concentration of

HDL cholesterol. However, regulatory pathways of HDL levels are still unknown. It is postulated that cholesteryl content is regulated by the ability of HDL_2 to accept cell membrane cholesterol, LCAT activity (see 1.1.3), the rate of CETP-catalysed cholesteryl transfer from HDL_2 to triglyceride rich lipoproteins (chylomicrons or VLDL) and the rate of selective cholesteryl delivery to cells. HDL particle number is affected by the direct uptake of apoE containing HDL particles to hepatocytes.

1.1.3 Lecithin-cholesterol acyltransferase

Introduction

LCAT was first recognized by Sperry in 1935. He found that when human serum was incubated the free cholesterol concentration fell markedly without a change in total cholesterol. He attributed this to enzymatic esterification of free cholesterol because the effect was abolished by heating serum to 55 – 60 ^{0} C. Subsequent work by Glomset (Glomset, 1962; Glomset, 1963; Glomset and Wright 1964) led to the identification of LCAT as a unique plasma enzyme. This enzyme is primarily synthesized in the liver and secreted into the circulation where it converts cholesterol to cholesteryl esters on the surface of HDL. The enzyme catalyses the transfer of a fatty acid from the 2-position of lecithin (phosphatidylcholine) to the 3-β-hydroxyl group of free cholesterol, forming cholesteryl ester and lysolecithin. Interest in LCAT has increased since the first family with three siblings affected with LCAT deficiency was described (Norum *et al*., 1967). The number of patients with secondary LCAT deficiency is large since many individuals with liver disease have at least some degree of LCAT deficiency. The enzyme plays a pivotal role in the metabolism of cholesterol and lipoproteins. Of particular interest is the relationship of the enzyme to the HDL and the reverse transport of tissue cholesterol and its ultimate excretion from the body. LCAT is the key enzyme involved in cholesterol homeostasis and regulating its transport in blood and this link with the pathophysiology of atherosclerosis makes the enzyme of great interest to many researchers and clinicians.

Distribution

The plasma concentrations of LCAT (about 6 μg/ml) vary little in adult humans with age, gender and smoking (Albers *et al*., 1982). Some LCAT is produced in the brain and is in cerebrospinal fluid at very low concentrations; it is also present in intestinal lymph and interstitial fluid. In plasma, LCAT binds reversibly to lipoproteins

and is found in different proportions in the HDL, LDL or lipid-free fractions, depending on the method of isolation.

Function

LCAT has several major functions with respect to plasma lipoprotein metabolism. In blood it binds to its preferred substrate, HDL and is activated by apoAI (Mclean *et al*., 1986). Cholesterol and lecithins in HDL are converted into cholesteryl esters and lysolecithin. The acyltransferase catalytic activity, which involves the transfer of a fatty acid from lecithin to the hydroxyl group of cholesterol, is responsible for the formation of essentially all plasma cholesteryl esters. The formation and accumulation of cholesteryl esters in the core of HDL not only removes cholesterol from the surface of HDL but also promotes movement of cholesterol from cell membranes into HDL. This pathway serves to transport cholesterol, in the form of cholesteryl esters, to the liver or to steroidogenic tissues for excretion or utilization in bile salt or steroid hormone synthesis. As nascent discoidal HDL acquires cholesteryl esters, they become spherical HDL (Jonas, 2000). Excess cholesteryl esters are transferred to other HDL species and then to VLDL, IDL and LDL by CETP. This process ensures that cholesteryl ester accumulation within the HDL surface does not inhibit further LCAT action.

There is a preference for LCAT to transfer the fatty acid at the *sn*-2 position of lecithin to cholesterol. Long chain and unsaturated fatty acids at the *sn*-2 position of lecithin (Sgoutas, 1972) are ideal. In addition fatty acids in the *sn*-1 position can serve as substrates for cholesteryl ester formation (Aron *et al*., 1978). The rate of cleavage of the *sn*-2 ester bond appears to be influenced by the nature of the fatty acid in the *sn*-1 position.

In the absence of an acyl acceptor LCAT also exhibits significant phospholipase acitivity (Aron *et al*., 1978). The hydrolysis of the *sn*-2 fatty acid lecithin to lysolecithin and free fatty acid is also stimulated by apoAI. The prescence of serum albumin as the acyl acceptor is calcium independent unlike the more active calcium dependent phospholipases. It is unlikely that this reaction is of physiological significance.

The third property of LCAT is the catalytic reaction of lysolecithin acyl transferase (Subbaiah *et al*., 1980). Plasma LDL is the main substrate and apoAI is not required as a cofactor. There is no net formation of either lecithin or lysolecithin.

Structure

LCAT is a 64 kDa plasma glycoprotein as determined by SDS-PAGE. Chemical sequencing of LCAT was completed in 1987 (Yang *et al*., 1987). In the mature secreted form, human LCAT has a polypeptide mass of 47 kDa and 416 amino acids. The enzyme contains six cysteine residues of which four are involved in disulphide bridges. Two disulphide bridges between C_{50}-C_{74} and C_{313}-C_{356} are important in maintaining the structure and function of the enzyme (Qu *et al*., 1993). Human LCAT has two free cysteine residues C_{31} and C_{184} which are thought to be located near the active site of the enzyme (Francone and Fielding, 1991). The loop spanned by C_{50}-C_{74} is essential for LCAT binding to lipoprotein surfaces (Jin *et al*., 1999).

Carbohydrate accounts for 25 % of the molecular mass of which 13 % is hexose (mannose and galactose), 6 % glucosamine and 5 % sialic acid. There are four N-linked glycosylation sites at Asn-20, 84, 272 and 384 (Mclean *et al*., 1986). Based on the diverse carbohydrate structures at each glycosylation position, more than 20 isoforms of the enzyme are possible. In addition to the N-linked carbohydrate chains, LCAT has two O-linked chains at T_{407} and S_{409}. Heterogeneity occurs in the carbohydrate chains, with one to three terminal sialic residues. Human LCAT expressed in animal cells is also glycosylated but the degree of glycosylation varies from one expression system to the next (Miller *et al*., 1996).

The function of the LCAT glycan chains is uncertain. They seem to increase the solubility of the enzyme, prevent non-specific binding to cell membranes and provide a removal mechanism for old enzyme from plasma. Although they are required for the efficient secretion of LCAT from cultured cells, blocking of individual carbohydrate chain sites does not interfere with the folding and secretion of the enzyme. When individual chains are removed, there is either an increase or decrease in reactivity of the enzyme with HDL substrates (Francone *et al*., 1993; Qu *et al*., 1993).

The Functional Domains

The catalytic site of LCAT has been identified from studies with specific chemical modifications, by sequence homology with other lipases and by site-directed mutagenesis. The active site of the enzyme was identified as serine on position 181 (Farooqui *et al*., 1988) according to its homology with other serine-type esterases which have a common structure of glycine-variable amino acid-active serine-variable amino acid-glycine (Gly-X-Ser*-X-Gly).

ApoAI is the most potent activator of LCAT followed by apoAIV (Fielding *et al*., 1972; Steinmetz and Utermann, 1985). Other apolipoproteins such as apoCI, apo CII, apo CIII, apoAII, and apoE have been shown to activate LCAT to various extents but less effectively than apoAI (Jonas, 1991). Several mechanisms have been proposed for the activation of LCAT reaction by apolipoproteins, specifically by apoAI. The latter concentrates the lipid substrates in the vicinity of LCAT where it specifically binds and presents the lipid substrates in an optimal conformation to LCAT. In addition, apoAI removes the products of enzyme reaction and promotes the final dissociation of LCAT from the lipid surface (Jonas, 1998).

1.2 LCAT Deficiency

1.2.1 Genetic Mutations of LCAT

The human LCAT gene is localized in the q21-22 region of chromosome 16 (Tiesberg *et al*., 1975) and is principally expressed in the liver. It consists of 6 exons separated by 5 introns and encompasses a total of 4.2 kilobases. Human LCAT mRNA consists of approximately 1550 bases and encodes a protein of 416 amino acids with a hydrophobic leader sequence of 24 residues (McLean *et al*., 1986).

LCAT deficiency arises as a consequence of either a defect in the enzyme, or in its synthesis and secretion or a mutation in the major plasma activator, apoAI, which results in an inability to stimulate the reaction. Mutations in the human gene are the basis for either familial LCAT deficiency (FLD) or fish-eye disease (FED). About 40 natural mutations in the LCAT gene have been identified and many involve single amino acid substitutions, located throughout the LCAT molecule. All these substitutions significantly reduce the LCAT activity. Four classes of either complete or partial human LCAT deficiency syndromes have been characterized at the molecular level (Kuivenhoven *et al*., 1997).

(1) The first class of LCAT gene mutations is a null mutation resulting in a clinical phenotype of FLD with total loss of catalytic activity and virtual absence of LCAT mass. (2) The second class is characterized by missense mutations (a total of 18 have been described) causing FLD, with reduced plasma LCAT concentrations (most cases) and virtual absence of LCAT activity (Owen *et al*., 1996). (3) A third class of missense mutations or minor deletions cause an intermediate phenotype in between those described for classes (1), (2) and FED. This class is characterized by a partial loss

of activity using LDL as substrate or combined partial loss of activity against both HDL and LDL (Kuivenhoven *et* al., 1995) associated with a reduction in plasma LCAT mass. Only three mutations with this phenotype have been reported. (4) The fourth class of mutations cause the classical FED phenotype as a result of specific loss of activity against HDL analogues with a normal or reduced LCAT mass (Kuivenhoven *et al*., 1997). The LCAT activity from some class (3) and (4) mutants still retain the capability to esterify cholesterol on LDL and VLDL. This finding explains the relatively normal cholesterol esterification rates in fish-eye disease (FED) as opposed to the FLD subjects with severely reduced levels of cholesteryl esters.

1.2.2 Familial LCAT deficiency

FLD was first described in a Norwegian family in 1967 by Norum and Gjone. It is characterized by low or undetectable concentrations of LCAT in plasma, or by absence of LCAT activity in all lipoprotein substrates. The disorder is characterised by HDL deficiency, abnormal triglyceride-rich VLDL and LDL and markedly reduced cholesteryl ester contents of lipoproteins. Erythrocytes have abnormal structures and elevated cholesterol contents. The major clinical findings were anaemia, corneal opacity, premature atherosclerosis, proteinuria and renal disease.

Corneal opacities are common in genetic disorders affecting HDL metabolism e.g. deficiency of apoAI or apoCIII, Tangier disease (Chu *et al*., 1979) and in FED (Carlson, 1982). Patients with FLD have corneal opacities in their early childhood. The whole cornea appears cloudy and consists of numerous minute, grayish dots in the parenchyma. A dense accumulation of the dots near the limbus form a prominent annular opacity. Despite these changes, the patients have normal visual acuity. Ultrastructural examination of sections obtained from superficial keratectomy revealed the presence of many vacuoles containing electron-dense membranous deposits. The exact nature of the deposits is not known but the tissue contains an excess of free cholesterol and phospholipid.

Renal disease is common and is a major cause of morbidity and mortality in FLD. Proteinuria is one of the earliest findings in these patients but the pathogenesis of glomerulosclerosis is poorly understood. Some studies have suggested that the renal changes seen in FLD may be immune–complex and complement mediated (Borysiewicz *et al.,* 1982; Lager *et al.,* 1991) and may be further exacerbated by the accumulation of oxidised phospholipids in the glomeruli. Large LDL particles and Lp-X found in

capillary loops have been implicated to induce endothelial and vascular injury in the kidneys of FLD patients (Norum *et al.,* 1971; Gjone *et al.,* 1974; Imbasciati *et al.,* 1986). Ultimately this may lead to renal failure in the fourth or fifth decade of life.

Despite low HDL levels, FLD patients do not appear to have an increased risk for developing cardiovascular disease (Kuivenhoven *et al*., 1997). However, premature coronary heart disease has been found in a subset of these patients (Kuivenhoven *et al*., 1996). It has been found in the aorta and large arteries of many patients. Renal arteries and arterioles also show early atherosclerotic changes (Hovig and Gjone, 1973). Electron-microscopy of sections of arteries shows lipid accumulation, similar to those found in other organs. They are present together with foam cells in all layers of the vessel wall. Only 35 % of the total cholesterol is esterified in contrast with 75 % in atheromas of typical vascular disease. Furthermore, the fatty acid pattern in these atherosclerotic lesions differs from the common lesions as it contains a markedly increased ratio of oleic to linoleic acid. It resembles the abnormal pattern found in plasma and mimics the pattern in cells as a result of the action of acyl-coenzyme A:cholesterol acyltransferase.

The pathology of this early atherosclerosis is unknown and one possible explanation is that reduced plasma LCAT activity impairs the transport of cholesterol from peripheral cells, including macrophages, to the liver for excretion (Assman and Jabs, 1985). A second possibility is the deposition of excess cholesterol after cellular uptake of abnormal lipoproteins, such as LDL found in familial LCAT deficiency (Gjone, 1974) and in obstructive jaundice (Agorastos *et al*., 1978). The accumulation of cholesterol in erythrocyte and platelet membrane raises a third possibility. Nucleated cells such as macrophages also take up cholesterol from cholesterol-rich lipoproteins by a non-receptor pathway, bypassing the LDL receptor (Brown and Goldstein, 1983). Through this unregulated process, the net transport of cholesterol to cells may contribute to the premature atherosclerosis of familial LCAT deficiency and to the xanthomata of patients with prolonged biliary obstruction.

1.2.3 Fish-eye-disease

FED or partial LCAT deficiency was extensively studied by Carlson and Philipson in two unrelated families of Swedish origin (Carlson and Philipson, 1979; Carlson, 1979; Carlson, 1982). There were two sisters from a village in northern Sweden who had corneal opacities, as did their father. Villagers said that they had ‘fish

eye' disease because their eyes resembled those of boiled fish. It is characterised by HDL deficiency, elevated LDL, VLDL and triglyceride. LCAT concentration is partially decreased and its activity is significantly reduced in plasma particularly with HDL substrates despite near normal esterification rates (Carlson *et al*., 1985). However, cholesteryl ester levels in plasma are almost normal because of the predominant LCAT action with LDL. More specifically, the cholesteryl ester content of HDL was very low whilst the relative cholesterol ester content of VLDL and LDL was normal. These features clearly distinguished this disorder from FLD.

. Carlson and Holmquist originally suggested that two types of LCAT activities normally exist in plasma, one that esterifies HDL cholesterol (α-LCAT activity) and one that esterifies LDL and VLDL cholesterol (β-LCAT activity). Furthermore, they proposed that FED was due to deficiency of α-LCAT and that FLD was due to the lack of both alpha and beta LCAT activity. However, it is now clear that only one gene for LCAT is present and that certain mutations in this gene cause FLD, whereas others cause FED.

In contrast to FLD, the partial LCAT deficiency in FED has no major clinical manifestations, except for corneal opacity. Poor vision is developed late in life and both cornea are opaque with the irises visible only as indistinct shadows. The peripheral cornea is most opaque and although there is no distinct arcus, a thin yellow ring-shaped opacity is present superficially. Microscopically, small white-yellow dots form a mosaic pattern present in all layers of the cornea. It is interesting to note that the disease does not cause an apparent increase in atherosclerosis.

1.2.4 Acquired liver disease

The liver plays a key role in the synthesis and secretion of VLDL and of (nascent) HDL; it is also the major site for the synthesis of several enzymes including LCAT (Osuga and Portman, 1971; Nordby *et al.,* 1976) and apolipoproteins (Guo *et al*., 1982) that regulate lipoprotein metabolism in the plasma and peripheral tissues. Furthermore, the liver is involved in the uptake of intermediates and products of plasma lipoprotein catabolism and functions in the final degradation of these remnant lipoproteins. It regulates total body cholesterol stores via the disposition of cholesterol and other lipids into bile.

In liver disease, LCAT mRNA is reduced substantially compared with the mRNA of other secreted proteins (Bingle *et al.,* 1991*).* As LCAT protein mass is

reduced, it is common to find low plasma LCAT enzymic activity in acute and chronic liver diseases (Floren *et al.*, 1987) and in medical illness which secondarily affect liver function. Cholesterol esterification is reduced resulting in a profound lipid and lipoprotein abnormalities, which predominantly reflect those seen in familial LCAT deficiency (Day *et al*., 1979; Seidel, 1987). Abnormal circulating lipoprotein particles in liver disease result in the change of membrane lipid composition and this in turn affects the ability of membrane proteins to function because cholesterol deposited in the membrane reduces the fluidity of the lipid bilayer (Owen, 1990). As this mechanism tends to affect many cells, it has been proposed that many of the cellular disturbances and metabolic abnormalities accompanying liver disease result from, or are exacerbated by, lipoprotein-induced changes in membrane lipid composition and function. Examples of clinical problems in which membrane lipid abnormalities appear to play a significant role include anaemia, variceal bleeding and renal dysfunction in liver disease (Owen, 1990). A wide spectrum of liver disease exists and many of the underlying disorders having acute and chronic presentations.

Acute presentation

Acute liver failure (ALF) is defined as the onset of hepatic encephalopathy because of severe liver injury in patients and in the absence of pre-existing liver disease (O' Grady *et al.,* 1993). Although a rare disorder, it is rapidly progressive with devastating consequences. It is characterised by a sudden cessation of normal hepatic function, which triggers a multi-organ response and is reflected by haemodynamic instability, cerebral oedema, susceptibility to infection, renal failure, coagulopathy and profound metabolic disturbances. However, it is potentially reversible and the rapidity of onset is an important indicator of prognosis (Nevens, 1997).

ALF in its most severe form continues to carry a high mortality rate because of multi-organ failure. Unless emergency orthotopic liver transplantation (OLT) can be performed, many patients do not survive. Currently, a worldwide shortage of donor organs limits the applicability of OLT in the setting of ALF (Riordan and Williams 2000). Those on long-term pharmacological immunosuppression who had successful transplantation are still at risk of serious side effects.

In view of the potential for complete recovery of native liver in ALF, new modalities of providing temporary liver support based on extracorporeal devices (artificial or biological) or hepatocyte transplantation (Strom *et al*., 1997), either as a

"bridge" to OLT or, ideally, to obviate the need for it by promoting native liver regeneration and reversing multi-organ failure would theoretically be the best treatment option. Hence, this has led to my work on encapsulating recombinant cells that secrete LCAT to reverse some of the abnormal cell and metabolic functions in patients, as this should help them over acute episodes of hepatocellular dysfunction and or improve metabolic states prior to surgery in jaundiced patients.

Chronic presentation

Primary biliary cirrhosis is a disease of unknown aetiology associated with a profound immunological disturbance resulting in progressive destruction of intra-hepatic bile ducts (Gershwin *et al*., 1991). It typically presents as cholestatic jaundice. Primary sclerosing cholangitis (PSC) on the other hand is characterised by chronic fibrosing inflammation of the bile ducts which results in obliteration of the biliary tree and ultimately in biliary cirrhosis (Lee *et al*., 1995, Cullen and Chapman, 2005). Another common cause of cirrhosis in the western world is alcoholic liver disease. The latter can progress and lead to the development of hepatocellular carcinoma and liver failure. At the advanced stage of all these diseases, the only effective therapeutic option is liver transplantation.

Hepatitis viruses A, B, C, D or E can cause acute hepatitis. The majority of infections with hepatitis viruses of all types is asymptomatic or result in anicteric illnesses that may not be diagnosed as hepatitis. All forms of viral hepatitis have a basic pathological lesion, which is an acute inflammation of the entire liver. Hepatitis B and C virus are parenterally transmitted and cause most cases of chronic viral hepatitis, which is defined as a chronic inflammatory reaction in the liver continuing without improvement for at least 6 months. About 20 % of patients presenting with chronic viral hepatitis go on to develop liver cirrhosis. The detection of cirrhosis is important as patients are at risk of complications, including variceal bleeding and hepatocellular carcinoma and even fulminant liver failure

Haemochromatosis and Wilson's disease are both autosomal recessive metabolic disorders where there is an increased iron absorption in the former and impaired biliary copper excretion in the latter. Due to increased deposition of iron and copper in tissues, an inflammatory fibrous reaction occurs that results in end organ (e.g. liver and pancreas) damage and causes cirrhosis, hepatocellular carcinoma and diabetes.

1.2.5 Lipoprotein abnormalities in liver disease

As the liver plays an important role in the synthesis and degradation of lipoproteins (Cooper, 1985), it is not surprising that liver disease is accompanied by abnormalities in lipoprotein structure and composition. Differences and similarities exist when we compare the changes in obstructive jaundice with those of parenchymal liver disease. The similarities appear to be related to the reduction in the concentration of LCAT in plasma.

Lipoproteins in obstructive jaundice

In obstructive jaundice, the total lipids tend to be high irrespective of plasma LCAT activity (Agorastos *et a*l., 1978). There is marked increase in plasma free cholesterol and phospholipids (mainly lecithin), and triglyceride. In those with normal or high LCAT, the individual lipoprotein fractions contain particles with near normal composition and structure. However, when the LCAT activity is low there are striking changes especially in LDL and HDL.

Three types of particles are found in the LDL fraction when separated by column chromatography. One is an abnormal lipoprotein which has been designated as lipoprotein-X (Lp-X) (Seidel *et al*., 1972). It is rich in phospholipids and free cholesterol and complexed with albumin and apoC, a normal constituent of VLDL. Triglyceride and cholesteryl esters are virtually absent. Under electron microscopy, Lp-X appears as disc shaped (40-60 nm in diameter) surrounded by a lipid bilayer and the individual particles tend to form rouleaux. The origin of Lp-X remains unclear, but may be due to regurgitation of biliary lipids with interaction of bile and serum constituents, particularly albumin (Manzato *et al*., 1976). It is removed by the cells of the reticuloendothelial system. Detection of Lp-X in the serum of patient is a sensitive and specific clinical chemical parameter for the diagnostic confirmation of obstructive jaundice (Narayanan, 1984). A second large particle (30-70 nm), rich in triglyceride and containing apoB and apoC is present when LCAT activity is low (Kostner *et al*., 1976). Finally, there are spherical particles of the same size as LDL from normal subjects (20 nm) but with abnormal composition; they are triglyceride rich and cholesteryl ester depleted.

HDL concentrations are not always reduced in cholestasis. Patients with relatively early primary biliary cirrhosis have raised HDL levels especially HDL_2. This contrasts with reduced HDL found in advanced disease and in patients with acute biliary obstruction and due to other causes (Clifton *et al*., 1988). When LCAT is low in

obstructive jaundice, three peaks may be seen within HDL on column chromatography (Agorastos *et al*., 1978). In the first, the material looks like normal HDL in size and appearance but is triglyceride and free cholesterol rich and depleted in cholesteryl esters and phospholipid. The other peak is rich in free cholesterol and phospholipid but poor in cholesteryl esters and has the appearance of stacked discs or rouleaux under the electron microscope. They resemble nascent HDL (Hamilton *et al.*, 1976) and the HDL of patients with familial LCAT deficiency (Norum *et al*., 1971). In some patients small spherical particles rich in triglyceride and phospholipid are found in a third small peak. They are also seen in familial LCAT deficiency and are thought to be intestinal in origin.

VLDL can be isolated in the ultracentrifuge but they have β mobility on agarose because they are deficient in apoA (Seidel *et al*., 1972). They are rich in free cholesterol and phospholipid but lack cholesteryl esters and triglyceride (Agoratos *et al*., 1978).

These abnormalities in plasma lipids and lipoproteins in obstructive jaundice are similar to those found with familial LCAT deficiency. This suggests that acquired LCAT deficiency may be important in their genesis. In obstructive jaundice, only patients with reduced LCAT activity show these changes. Patients with normal LCAT activity have marked hyperlipidaemia but lipoproteins of normal composition and electrophorectic ability.

The apolipoprotein content of lipoproteins also changes. The most striking abnormality in HDL apolipoproteins in obstructive jaundice is an increase in apoE (Floren and Gustafon, 1985). Both apoAI and apoAII are quantitatively reduced in cholestasis with a disproportionate reduction in apoAII.

Lipoproteins of parenchymal liver disease

Hypercholesterolaemia and hypertriglyceridaemia are common in parenchymal liver disease. The most characteristic abnormality in plasma lipids is a decrease in the concentration of cholesteryl esters as a result of LCAT deficiency. This is possibly due to inadequate synthesis or loss of the enzyme secondary to hepatocyte necrosis (McIntyre *et al*., 1974) and results in changes in most lipoprotein fractions, which become depleted in cholesterol esters and enriched in triglycerides and phospholipids. Furthermore, the apolipoprotein composition and content of the lipoprotein particles are abnormal.

Patients with normal or high LCAT activity have normal plasma lipid levels and lipoprotein fractions of normal structure, electrophoretic mobility and composition.

However, when LCAT activity is low, there are several HDL abnormalities (Day *et al*., 1979). For example, the HDL level is reduced and is similar to those found with familial LCAT deficiency and in those with obstructive jaundice who had low LCAT levels. In these patients, as revealed by electron microscopy, nascent HDLs appear like the stacked discs observed in obstructive jaundice. These are low in cholesteryl ester but rich in free cholesterol, phospholipid and triglyceride. Their protein content was reduced with marked decrease in the levels of apoAI and apoAII. As in cholestatic jaundice, the HDL fraction was rich in apoE. Small HDL particles found in obstructive jaundice and familial LCAT deficiencies are not found in parenchymal liver disease.

In addition, patients with low LCAT activity have abnormal LDL composition being deficient in cholesteryl ester and rich in triglyceride (Day *et al*., 1979). These LDL are similar to LDL fractions found in obstructive jaundice (and low LCAT) and with familial LCAT deficiency. VLDL levels were markedly reduced in patients with parenchymal liver disease and low LCAT. Lastly, low levels of VLDLs are found in these patients. This may be due to failure in VLDL synthesis and release, either because of malnutrition or because of damage to parenchymal cells responsible for the manufacture of VLDL (McIntyre, 1978).

1.2.6 Clinical implications of dyslipoproteinaemia in liver disease

Lipoprotein abnormalities are sensitive indicators of metabolic insufficiency in liver but the biochemical changes are not usually of diagnostic significance. HDL-cholesterol level decreases as primary biliary cirrhosis advances and thus may be a useful marker in disease progression (Jahn *et al*., 1985). Lp-X is present consistently in cholestasis but is of no diagnostic value in distinguishing between intra or extrahepatic cholestasis.The degree of LCAT deficiency may be of some prognostic significance since patients with low activity appear to have a greater impairment of liver function and therefore a worse prognosis than patients with lesser degrees of impaired LCAT activity (Gjone *et al*., 1971). Some attempts have been made to predict allograft viability and assess early allograft function by measuring plasma LCAT activity in organs and recipients following liver transplantation (Higashi *et al*., 1990; Shimada *et al*., 1989). LCAT activity is significantly higher in the donors with good allograft function than in ones with fair or poor function. A significant correlation was found between mean LCAT activities during the first 24 hour orthotoptic liver transplantation (OLT) and early allograft function.

Thus, although a few overt clinical consequences of the plasma lipoprotein abnormalities are found with liver disease, there are a number of indirect consequences which may be of considerable biological importance. In particular, many of the metabolic disturbances seen in patients with liver disease may be secondary to changes in the composition and function of cell membranes as described in the next section.

1.2.7 Extrahepatic manifestations exacerbated by dyslipoproteinaemia

The surface composition of plasma lipoproteins is markedly altered in severe liver disease. LCAT secretion by the liver is decreased leading to accumulation of cholesterol and lecithin. There is a reduced proportion of arachidonate in phospholipid and the apolipoprotein composition of the lipoprotein subfractions, particularly HDL is abnormal. As cholesterol and phospholipid molecules in the surface lipids of lipoproteins tend to exchange and equilibrate with their counterparts in cell surface membranes, similar lipid abnormalities can be found in cell membranes. Membrane function may be altered by membrane abnormalities through change in membrane fluidity, altered binding of charged substances to phospholipid groups, interaction of hydrophobic substances with the interior of the membrane, changing the state of water at the surface and in the interior of the membrane and by reducing the concentration of arachidonic acid which is a precursor of prostaglandins and thromboxanes (Owen *et al*., 1982). Changes in membrane fluidity affect many membrane properties such as membrane permeability and may alter the activity of membrane proteins which act as receptors, transport of proteins or enzymes.

We now know that lipoproteins influence cell functions, independently of lipids. Important functional effects may be due to changes in the apolipoprotein composition. In patients with severe liver disease, HDL is rich in apoE. This competes with apoB of LDL for binding to the LDL receptor present in cell surfaces (Owen *et al.*, 1984). This receptor controls the cellular uptake of LDL, the major carrier of plasma cholesterol, which provides cells with this essential nutrient. Reduced cellular uptake of LDL has important implications for cellular cholesterol metabolism.

Renal failure occurs in familial LCAT deficiency. Large amounts of cholesterol and phospholipids accumulate in the renal cortex and glomeruli. This has been demonstrated in $LCAT^{-/-}$ mice (Lambert *et al.,* 2001) and in rat kidneys with experimental liver disease. In chronic biliary obstruction, there was an increased C:PL ratio in kidney brush border membranes. In advanced liver failure when LCAT activity

is low (Gjone, 1981), renal failure with similar histological changes also occurs. Moreover, a reduction in renal plasma membrane arachidonic acid, which in the precursor for synthesis of the vasodilator prostaglandin, PGE_2, was observed in rats with liver failure (Folkert *et al.*, 1984). Renal prostaglandins, including the vasodilator prostaglandin E_2, seem to play a role in regulating renal vascular resistance, to affect renal Na^+ and water excretion, and to interact with the rennin-angiotensin system and may be an important factor causing impaired free water clearance and renal failure in cirrhotic patients (Arroyo *et al*., 1983; Perez-Ayuso *et al*., 1984). In bile-duct ligated rats, there was an increased Na^+-dependent *D*-glucose uptake by the renal cortical brush border membrane 3 days after ligation compared with non-ligated animals. There was a positive correlation between Na^+/glucose co-transport and the C:PL ratio in the renal brush border membrane.

The life span of erythrocyte is diminished in familial LCAT deficiency and in liver disease. Enrichment of erythrocyte with cholesterol is associated with reductions in membrane fluidity (Owen *et al.*, 1982) and cell deformability (Cooper *et al*., 1985). In liver disease patients, HDL with abnormal apolipoprotein (rich in apoE) composition causes echinocyte (spur cells) formation. The shape change involves the occupation of binding sites on the cell surface by abnormal HDL. These abnormalities may underlie the premature removal of the cells from the circulation and predispose to haemolytic anaemia.

Platelet aggregation is reduced in severe liver disease and this may be related to a reduced amount of arachidonic acid in the platelet phospholipids (Owen *et al*., 1981), since this can result in diminished production of proaggregatory thromboxane A2. These findings may implicate abnormal lipoproteins in the cause of abnormal clotting seen in severe liver disease and may be an important factor in variceal bleeding (Laffi *et al*., 1986). Binding of normal LDL by platelet surfaces stimulates agonist-induced aggregation. However, abnormal apolipoprotein E rich-HDL from jaundiced patients are known to compete with LDL for binding by the LDL receptor on nucleated cells and thus contribute to the platelet hypo-aggregability (Owen *et al*., 1984). In addition, inhibition of platelet aggregation has been correlated to the high apolipoprotein E content of HDL in patients with liver cirrhosis (Desai *et al.*, 1989).

Abnormal HDL of liver disease inhibits lymphocyte transformation and appears to be due to binding of HDL apolipoproteins (Owen *et al.*, 1984). Patients with severe liver disease have increased susceptibility to infection and show abnormalities of humoral and cellular immunity (Owen *et al*., 1984).

In cirrhosis, cardiovascular function is deranged. It has been demonstrated that inotropic and chronotropic responses to β-adrenergic stimulation are substantially reduced in both cirrhotic patients and animal models of cirrhosis (Ramond *et al*., 1986; Lee *et al*., 1990). The cardiac membrane in cirrhotic rats were found to be more rigid than controls primarily due to an increase in membrane cholesterol content and C:PL ratio. As a result, there is an associated decrease in β-adrenoceptor function (Ma *et al*., 1994; Liu *et al*., 2006).

Cutaneous xanthomata occur when plasma free cholesterol and phospholipids are very high, as in chronic obstructive jaundice. A large proportion of cholesterol ester, with some free cholesterol is usually present in the deposit. There may be scanty or there may be widespread eruption with a characteristic distribution in the palmar creases, in the skin of the palms and soles, around the eyes and over the elbows, buttocks and knees. Nucleated cells seem to take up and accumulate cholesterol from cholesterol-rich lipoproteins by a non-receptor pathway. It has been shown that when LDL in liver disease was added to the culture medium of human fibroblasts, the cells increased their rate of cholesterol esterification and accumulated cholesteryl ester (Owen and Gillet, 1983). In addition, plasma LDL is not cleared by the normal route because apoE-rich HDL from jaundiced patients are known to compete with LDL for binding by the LDL receptor on nucleated cells (Owen *et al.*, 1984)

1.2.8 Animal Models of LCAT Deficiency

Given the gaps in our knowledge of LCAT deficiency and the associated difficulties with using human subjects, animal models play an important role in research. In order to understand the pathophysiology and evaluate the potential forms of treatment in LCAT deficiency, various animal models have been used. They range from animal models of liver failure to genetically engineered animals.

Several mouse models to study liver failure have been described and they include surgical (hepatic resections), devascularisation procedures, and pharmacological manipulations such as the administration of hepatotoxic drugs. The criteria for a satisfactory animal model of acute liver failure include: (1) induced liver failure should be reversible, (2) liver damage should be reproducible, (3) selective liver damage should occur that leads to death during an interval similar to that seen clinically, (4) death should occur long enough from the insult to provide a suitable therapeutic window, (5) a

large animal model should be used, and (6) any method used should pose minimal hazard to personnel (Terblanche and Hickman 1991).

Two Models of Liver Injury

Liver injury in animal models may be induced by either using a toxic agent or a surgical disconnection of the bile duct. Although not ideal, for the purposes of this study these models simulate to some extent the biochemical and metabolic disturbances in liver failure.

(i) *Galactosamine hepatitis*. Keppler and Decker in 1971 first described the hepatotoxic effects of galactosamine in rats. Subsequently a reproducible study was substantiated using galactosamine on a strain of rabbits (Blitzer *et al.,* 1978). Coma preceded the death of the majority of rabbits between 21 and 44 hour following injection. Serum biochemistry and liver histology resembled the findings seen in acute liver failure in humans. Our laboratory has studied the membrane lipid changes in erythrocytes, liver and kidney, after inducing liver disease in rats by administering intraperitoneal D-galactosamine hydrochloride (1g/kg body weight) dissolved in saline on the 1^{st} and 3^{rd} days (Kawata *et al*., 1986). Control rats were given saline alone and all were killed on the 4^{th} day. D-galactosamine is a selective hepatotoxin, an amino sugar metabolized by the galactose pathway in the liver. This leads to depletion of intracellular uridine nucleotides, which in turn disturbs hepatocyte RNA metabolism, ultimately leading to hepatocyte necrosis (Keppler *et al.,* 1968; Farber *et al*., 1973; Keppler and Decker 1969; Shinozuka *et al.,* 1973).

(ii) *Bile duct ligation*. Under diethyl ether anaesthesia, the common bile duct of rats was doubly ligated and divided between the two ligatures. Other rats were subjected to sham-operations and both groups were studied 3 weeks after operations.

Plasma LCAT activity was significantly reduced in both galactosamine-treated and bile duct-ligated rats. As expected, in both these animal models there was a significant increase in the proportion of plasma total cholesterol present as free cholesterol and in the cholesterol : phospholipid molar ratio, C:PL. There was an accumulation of cholesterol in lipoprotein surfaces and a modest rise in C:PL (15%) in red cell membranes. The increased cholesterol content of such erythrocytes correlates closely with a reduced membrane fluidity and with impaired carrier-mediated membrane transport of cations and anions. In addition, rats with chronic (3 weeks) biliary obstruction accumulated cholesterol in renal cortical brush-border membranes resulting in significant increases in cholesterol content and C:PL ratio, which correlated

with decreased membrane fluidity and contribute to renal dysfunction (Kawata *et al*., 1987). Kidney brush border membrane and red cell membrane from obstructed rats were deficient in arachidonate and thus PGE_2 synthesis would diminish.

Transgenic Mice and Rabbits that Overexpress Human LCAT Gene

The generation of transgenic animals overexpressing LCAT has helped to answer some questions regarding the role of LCAT in lipoprotein metabolism. They are (1) Is LCAT rate-limiting in the metabolic pathways of plasma HDL and LDL? (2) How does overexpression of LCAT influence the lipoprotein profile? (3) Are there other gene products acting synergistically with LCAT in controlling lipoprotein metabolism? (4) Can modification of plasma LCAT activity alter the reverse cholesterol transport and atherosclerosis?

Recent work on overexpression of human LCAT gene in mice and rabbits has reported changes in plasma lipids, lipoproteins and the susceptibility to diet-induced atherosclerosis in these animals. LCAT activity increases from 3-100 folds in these transgenic animals (Vaisman *et al*., 1995). Similarly, levels of total cholesterol, HDL cholesterol, apoA-I apoA-II and apoE increase significantly. Large HDL was present in mice but apoB containing lipoproteins decreased in both mice and rabbits. With a decreased LDL- and increased HDL-cholesterol, the lipoprotein profile appears antiatherogenic. However, when these two animal models were fed high cholesterol, atherogenic diet, unexpected results were observed. Mice transgenic for the human LCAT gene became more prone to develop atherosclerosis than control mice (Berard *et al*., 1997), whereas the transgenic rabbits became less susceptible to diet-induced atherosclerosis than their controls (Hoeg *et al*., 1996). The species difference is apparently due to the presence of CETP in rabbits, which is absent in mice. Consequently, there is an impaired transport of newly formed cholesteryl esters to LDL, and they accumulate in HDL (Berard *et al*., 1997). Indeed, coexpression of simian CETP with human LCAT in mice does reduce diet-induced atherosclerosis (Foger *et al*., 1999). CETP appears to reduce the level of large proatherogenic HDL found in the LCAT transgenic mice. When CETP was absent, large HDL persists in the circulation (Brousseau *et al*., 1996) due to slow liver clearance (Berard et al., 1997). Indeed, when transgenic mice containing both human LCAT and CETP genes were crossbred, they were significantly protected against diet-induced atherosclerosis (Foger *et al.,* 1999).

LCAT-Deficient Mouse

To evaluate the role that LCAT plays in modulating HDL metabolism, reverse cholesterol transport, and atherosclerosis, a mouse model had been created for human LCAT deficiency by performing targeted disruption of the LCAT gene in mouse embryonic stem cells (Sakai *et al*., 1997). Homozygous $LCAT^{-/-}$ mice were born healthy and fertile. Compared with age-matched wild-type littermates, the LCAT activity in heterozygous and homozygous knockout mice was reduced by 30 and 99 % respectively. The $LCAT^{-/-}$ mice had a complete deficiency of both α- and β-LCAT activities in plasma indicating that biochemically these were most similar to patients with classical LCAT deficiency but with no evidence of corneal opacities or renal insufficiency.

LCAT deficiency resulted in significant reductions in plasma concentrations of total cholesterol, HDL cholesterol and apoAI in $LCAT^{-/-}$ mice to 25, 7 and 12 % of normal levels respectively. The cholesteryl ester/total cholesterol ratio in $LCAT^{-/-}$ and wild type were 34-52 % and 79-81 % respectively reflecting the absence of LCAT-mediated cholesterol esterification in the plasma of homozygous mice. The residual cholesteryl esters remaining in $LCAT^{-/-}$ mice plasma may originate from intracellular pools in the intestine and liver formed by the enzyme acylCoA: cholesterol acyltransferase. In addition, plasma triglycerides were significantly higher in male homozygous knockout mice compared with wild-type animals but remained normal in female $LCAT^{-/-}$ mice.

$LCAT^{-/-}$ mice that were fed on a high-fat high-cholesterol diet had reduced plasma levels of the proatherogenic apoB-containing lipoproteins through upregulation of the LDL-receptor and an increase in plasma apoE. Reduced atherosclerosis in spite of low HDL levels can be explained by the compensatory reduction in the plasma levels of the proatherogenic apoB containing lipoproteins in $LCAT^{-/-}$ mice. A marked reduction in aortic atherosclerosis was seen in these mice. No ocular abnormalities were found in the $LCAT^{-/-}$ mice even though corneal opacities were found in several syndromes associated with HDL deficiency.

In addition to severe hypoalphalipoproteinaemia, and hypertriglyceridaemia, $LCAT^{-/-}$ mice also present with a clinical phenotype similar to patients with FLD, including normochromic normocytic anaemia and glomerulosclerosis. Anaemia is probably due to altered red cell membrane lipids resulting in mild haemolysis. The presence of Lp-X in these mice appears to be associated with the development of glomerulosclerosis (Lambert *et al*., 2001). They developed renal lesions similar to those

previously described in patients with FLD. Proteinuria, being one of the earliest findings in FLD patients was detectable in LCAT$^{-/-}$ mice fed on a high fat/high cholesterol diet.

1.3 Molecular Therapies

1.3.1 Recombinant Protein Therapy

The basis for recombinant therapeutic proteins was laid when the first gene technology experiment was published in 1973 (Cohen *et al*, 1973). Over the past 20 years, recombinant proteins have gained increasing importance as therapeutic agents. They are becoming more attractive compared with conventional drugs because the time required to develop protein drugs is considerably shorter (Bienz-Tadmor *et al*, 1992; Struck, 1994).

Proteins by nature are neither carcinogenic nor tetratogenic and are specific in their function. They have lower toxicity compared with chemical substances. Therefore, they have less potential for development of idiosyncratic reactions or interference with unrelated biochemical pathways. The specificity of protein actions is usually reflected in the specificity of their expression and sequestration within tissues or organs. Their development into a medicinal product involves fewer safety issues compared with chemical products once its biological mode of action has been identified and its medical application described.

Greatest research effort in developing new protein drugs is being devoted to cancer. Other therapeutic areas include AIDS, asthma, diabetes, heart disease, multiple sclerosis, rheumatism, stroke and viral disease. Monoclonal antibodies comprise the largest group of products whilst vaccines make up the second largest group. The latest form of protein production is gene therapies, whicn involves restoring or enhancing the normal functioning proteins to the body, most commonly by viral or nonviral gene transfer. Gene therapy was originally developed as a treatment modality for the management of hereditary defects such as adenosine deaminase deficiency (Mullen *et al*, 1996). Now it is being developed for the treatment of acquired diseases such as cancer or AIDS.

The first generation therapeutic proteins were naturally occurring proteins that had been produced and made available by gene technology methods. The majority of proteins currently on the market belong to this category. They include insulin, growth hormones, interferons, erythropoietin, factor VIII, granulocyte/macrophage colony

stimulating factor and tissue plasminogen activator. Recombinant production allows the manufacture of a drug that cannot be produced by conventional means e.g. erythropoietin. Large quantities of a drug can also be produced, which otherwise would only be available in limited amounts, e.g. insulin or growth hormone. Finally, the products e.g. factor VIII or hepatitis vaccines are free from human pathogenic viruses

Second generation proteins are described as the products of 'protein engineering'. They are the result of either minor or larger modifications related to manufacturing processes or pharmaceutical formulation, or to protein fusions with combined or new functions. Some examples of specific constructions are binding domains of ligands that are used as receptor antagonists, or fusions between antibody domains and new functions such as toxin fragments for tumour therapy.

Proteins have the great advantage of having been developed by nature as highly potent, specific agents and thus are ideal medicines. However, the problem is that proteins have to be administered from outside the body for therapeutic purposes. Usually proteins have to be injected as they cannot be administered orally. But even then problems can arise with the natural potency of proteins. Exogenous administration results in fluctuating drug concentrations that can differ from the natural state. Systemic administration may not be effective because of the interaction of protein with cells of the immune system. In theory, some of these problems can be overcome by *in vivo* expression of proteins, in other words by gene transfer and production within the body. Despite this, considerable technical difficulties exist and have yet to be overcome. Some of the major challenges are: (1) efficient gene transfer into cells, (2) the antigenicity of vectors, (3) cell and tissue specific gene transfer (targeting), (4) cell and tissue specific gene expression, (5) efficient and sustained *in vivo* gene expression, (6) regulatable gene expression, and (7) stable, directed integration of vectors (Gunzburg and Salmons, 1996).

1.3.2 Viral Gene Therapy

In the late 1950s, the discovery that viruses have an intrinsic capability to transfer their genetic material into infected cells gave birth to the idea of gene therapy. One of the main viral vectors used in gene therapy is the adenovirus. The high efficiency of adenoviral-mediated gene transfer results from (1) the availability of adenovirus stocks of sufficient titer to transduce a large number of cells in the liver, (2)

the affinity of adenovirus to infect mammalian cells, (3) the capacity of adenovirus to infect and express encoded genes in both actively dividing and nondividing cells and (4) the ability of adenovirus particles to access hepatocytes via the pores in the fenestrated endothelium of the liver (Wilson, 2001).

Basic Biology of Adenovirus

More than 50 different serotypes are known, and the most frequently utilized for gene therapy are type 2 and type 5. Adenovirus can infect a broad range of mammalian cell types and the group of adenoviruses associated with human diseases (typically diseases of the respiratory system) is suitable for use as gene transfer vectors. The capacity for foreign DNA is up to 8.5 kb, which suffices for most therapeutic genes and these can be inserted at a variety of sites in the adenovirus genome to generate recombinant vectors. Transduction into recipient cells and internalization is mediated through fiber protein anchored to the vertex of the adenovirus capsid. Adenovirus enters cells via an endocytic mechanism that is mediated by $\alpha 1$ integrin binding to the viral penton protein (Wickham *et al*, 1993). During lytic infection, the viral genome is replicated and the DNA packaged into virions by self-assembly of the major capsid proteins. This takes place within the nucleus of infected cells.

Three generations of adenoviral vectors have been developed in order to decrease cytopathic effects and immune responses. The first generation has a deletion in the E1 region encoding viral replication and DNA synthesis (Stillman, 1986). However, these E1 deleted viruses can be complemented by co-infection of another DNA virus. Moreover, there was still low-level replication and notable immunogenicity of the first generation (Yang *et al*., 1994) and thus led to the preparation of the second generation, which was constructed by deletion of other viral regions, either E2 or E4 (Halbert *et al*., 1985; Medghalchi *et al*., 1997). This second generation has a significantly reduced cytopathic effects and immune responses. The third generation, called “gutless vectors” was developed by deleting all viral genes except inverted terminal repeats and packaging signal and is characterized by reduced immunogenicity (Morsy and Caskey, 1999). These vectors have a capacity of 34 kb but are not able to replicate unless complemented and so are often termed, helper dependent (Gao *et al*., 1996).

These viruses have a relatively favourable safety profile and have not been associated with human malignancies or persistent infections. The viral particles can be purified and concentrated to high titre (about 10^{11} plaque-forming units/ml), making

systemic clinical administration feasible. Adenovirus rarely integrates into the host chromosome and replicates in an extra chromosomal state. This reduces the risk of insertional mutagenesis but renders a transient expression of foreign delivered genes (Silman and Fooks, 2000).

The immune system plays an important role in adenovirus-mediated gene transfer (Yang *et al*., 1996). Exposure to adenovirus infection is common and the majority of the population carry antibodies against the different serotypes. Therefore, when adenovirus vectors are injected, more than 85 % are degraded before they reach target cells. Acute-phase responses after injection are usually caused by capsid protein resulting in release of pro-inflammatory cytokines (Ritter *et* al., 2002), whereas inflammatory responses involve the activation of B and T-helper cell–mediated immunity. Ultimately, this influences the efficiency of gene delivery (DeMatteo *et al*., 1997). Different approaches are being explored to inhibit the inflammatory responses against adenoviral vectors and to circumvent the degradation of adenoviral particles. Using vectors with capsid proteins derived from different adenoviral serotypes seem to give promising results (Chia *et al*., 2004).

Adenovirus Gene Transfer to Liver

The liver is an attractive target for somatic gene transfer. *Ex vivo* gene therapy of liver is based on transplantation of autologous genetically modified hepatocytes and has been extensively developed in animal models. *In vivo* gene therapy is a more practical and potentially effective strategy for genetic reconstitution in the liver. The hepatocyte is accessible to parenterally administered gene transfer agents via large pores called fenestrae in the microcirculation of the liver. The feasibility of using recombinant adenovirus for liver-directed gene therapy has been demonstrated in mice (Imai *et al*., 2005), rabbits (Rashid *et al*., 2003), dogs (Wang *et al*., 2000; Mount., *et al* 2002) and Rhesus monkeys (Haegel-Kronenberger *et al*., 2004). It is a highly efficient process that can result in transduction frequencies in excess of 90 % (Herz and Gerard, 1993) and is much higher than that achieved with other vector systems such as recombinant retroviruses, liposomes or molecular conjugates.

1.3.3 Microencapsulated-artificial cells

The concept of artificial cells was first demonstrated by Chang in 1964 (Chang 1964). Preparation of these cells involved encapsulating charcoal, enzymes, genes

within microscopic, semipermeable containers. A number of potential medical applications of 'artificial tissue/organ' have been developed, including red blood cell substitutes (Chang *et al*., 2003), artificial liver for detoxification (Chang, 1992), artificial kidney (Chang and Malave, 2000) and immunosorbent and drug delivery systems. Encapsulation of living cells represents another important aspect of the artificial cell concept. Whole cells were first encapsulated to treat diabetes mellitus (pancreatic β cells) (Lim and Sun, 1980), and later hepatocytes were used for liver failure (Balladur *et al*., 1995) and parathyroid cells for hypocalemia (Picariello *et al*., 2001). Potentially, encapsulated cell technology can offer a solution to the problem of donor organ shortage. It not only enables the transplantation of human cells and tissues without immunosuppressant but also can permit the use of cells isolated from animals (Lanza and Cooper, 1998).

A useful application of the artificial cell concept is encapsulation of genetically modified cells which represents an alternative approach to somatic gene therapy. It has broad application to treat diseases such as cancer (Lohr *et al*., 2001; Joki *et al*., 2001; Xu *et al.*, 2002) and a wide range of other disorders resulting from functional defects of native cell systems. However, the main obstacle impeding progress in this field is the inability to achieve efficient gene transfer and persistent gene expression in appropriate somatic cells (Palmer *et al*., 1991; Puthenveetil and Malik, 2004).

Principles of Action of Microcapsules

Small molecules including peptides produced inside the microcapsules can diffuse across the membrane into the 'extracellular' environment. Biologically active materials retained inside microcapsules can act on smaller molecules outside to diffuse across the membrane of the microcapsule. The principle factors determining the rate of diffusion are the type and size of a solute, interactions between the solute and the membrane, and the membrane thickness (Uludag *et al*., 2000).

A further advantage of microcapsules is that capsule contents are protected from immune rejection because the capsule is designed to be impermeable to leukocytes and antibodies (Cirone *et al*., 2004). This allows allogeneic or even xenogeneic cells to be implanted into the host organism. The encapsulated cells are sustained by an external supply of oxygen and nutrients that can diffuse into, and their secreted products out of, the microcapsules to fulfil their functions.

Microcapsules offer a number of distinct advantages over the use of other encapsulation devices, including: (1) greater surface to volume ratio, (2) ease of implantation.

Alginate-polylysine-alginate Microcapsule

Sodium alginate (composed of mannuronic and guluronic dimers) is commonly used as the polyanion and poly-L-lysine (PPL) as polycation for microcapsule design (Orive *et al*., 2004). Since undergoing many modifications, the present form of the capsular membrane is composed of PLL sandwiched between two alginate layers (alginate-polylysine-alginate or APA) (Thu *et al*., 1996). In a typical process, encapsulation begins with the formation of alginate droplets containing cells which are produced by forcing alginate and cells to flow through a needle. The diameters of the droplets are controlled either by regulated air flow or by a high-voltage pulse around the tip of the needle. Next, the beads are formed by gelling of the alginate in a calcium-rich medium (Smidrod and Skjak-Broek, 1990). Subsequently, the beads are coated with a PLL membrane by suspending them in a PLL solution. During this step, PLL binds with mannuronic and guluronic acids in the alginate molecules to form complexes consisting of alpha-helical polypeptide cores surrounded by super helically orientated polysaccharide chains. By varying molecular weight, concentration of the PLL and incubation time, one can modulate the porosity of the capsule membrane (van Schilfgaarde and de Vos, 1999). The biocompatibility of APA biocapsules has been demonstrated in numerous *in vivo* transplantation experiments involving microencapsulation of pancreatic islets. (Soon-Shiong, 1999; Uludag *et al*., 2000).

Capsular construction is critical and capsular size is an important factor in the kinetics of biologic substances released by encapsulated cells and in the easy access to nutrients and oxygen. Smaller capsules have the following advantages: (1) encapsulated cells have quicker access to oxygen and nutrients and thus promote cell survival, (2) reduced dead space allows faster cell responses to physiological fluctuations and (3) less susceptibility to cell overgrowth on capsular surfaces, as the smaller capsules have greater mobility.

Although APA microcapsules have been widely used in microencapsulation of cells, its membrane function is still limited by mechanical fragility, low tensile resistance against swelling, immunogenicity and cytotoxicity. A recent study of alginate microcapsules coated with three different polycations, PLL, poly-D-lysine and poly-L-ornithine evaluated their performance in relation to morphology, osmotic resistance,

mechanical stability and viability of the immobilized C2C12 myoblasts cells. Poly-D-lysine and poly-L-ornithine did not show any significant improvement over the PLL microcapsules (De Castro *et al.*, 2005).

Microencapsulation of Hepatocytes

The survival following conventional treatment of fulminant hepatic failure (FHF) is only in the range of 10 - 20 %. Although liver transplantation has good results with more than 90 % 1 year survival and 50 % 5 year survival, it is still a major procedure that is limited by the shortage of donor livers and is associated with rejection complications. Transplantation of microencapsulated hepatocytes is potentially a simpler, less hazardous treatment and allows large stocks of hepatocytes to be shared for future use. The feasibility of encapsulated hepatocytes to treat FHF has been investigated previously (Sun, 1997). Initially, viable hepatocytes were encapsulated in APA membranes. Encapsulated rat hepatocytes were shown to survive and function for more than one week *in vitro* and up to one month *in vivo* in both normal rats and rats with galactosamine-induced FHF. In addition, encapsulated hepatocytes were found to produce urea. In an extended study, free hepatocytes were harvested from normal rat livers and encapsulated in APA membranes before they were implanted into the peritoneal cavities of rats with galactosamine-induced FHF. The control group of animals received empty capsules. A statistically significant improvement in survival at seven and fourteen days was demonstrated in those FHF rats with hepatocyte implantation. Following transplantation of encapsulated hepatocytes, the liver began to regenerate. By 21 days post-transplantation, this regeneration had reached a point where the viability of the encapsulated hepatocytes was no longer critical to the survival of the rats. *In vitro* studies showed that encapsulated hepatocytes continued to synthesise albumin for up to 3 weeks and they remained viable up to 30 days (Wong and Chang, 1986; Cai *et al*., 1989). The results of this study prove that allograft of encapsulated hepatocytes can take over some functions of the damaged liver caused by toxins, drugs or acute disease whilst allowing the liver time to regenerate or recover fully. In future, microencapsulated hepatocytes could potentially provide a useful method to treat acute or chronic liver failure as well as a therapeutic bridge prior to liver transplant (Benoist and Nordlinger, 2001; Ambrosino *et al*., 2003).

Implantation of Encapsulated Genetically Engineered Cells

A novel approach to gene therapy which avoids problems associated with the use of autologous tissue is the use of genetically engineered cell lines to secrete the desired therapeutic gene product. However cell lines have the potential problems of rejection by the immune system. Immunoisolation of transplanted cells is a promising way to avoid immune rejection. The technique involves expanding clones of transduced cell lines showing stable integration and sustained expression of the therapeutic gene and encapsulating them in a semipermeable biocompatible membrane such as APA. Implantation of microencapsulated cells would have the following advantages: (1) durable capsules will limit cell growth preventing uncontrolled cell line proliferation in recipient animals, (2) immunosuppressive therapy is not needed, and (3) the transplantation requires minimal surgery. The feasibility of delivery of therapeutic gene products from encapsulated recombinant cells has been demonstrated in both *in vivo* and *in vitro* (see Table 1.1).

Long-term Function of Encapsulated cells and genetically engineered cells after implantation

The encapsulations of endocrine cells, hepatocytes and genetically engineered cells have yielded promising results. Further research is focused on improving the safety and long-term feasibility of implantation. Of major interest is increasing mass transfer efficiency (Coromili and Chang, 1993; Dionne *et al*., 1996) and biocompatibility (Lanza and Cooper, 1998). When microcapsules are recognised as foreign, a foreign body reaction is triggered resulting in coating by giant cells and fibrous tissues that decreases the mass transfer of oxygen, nutrients and metabolites and eventually lead to death of the encapsulated cells (Soon-Shiong *et al*., 1991; Clayton *et al*., 1991; Vandenbossche *et al*., 1993; Fritschy *et al*., 1994). In relation to immunological acceptance, microcapsules can exclude recruited leukocytes (T lymphocyte sub-population i.e. $CD8^{+}$) preventing cell-to-cell contact between encapsulated cells and the host's immune system during allograft immunity. In addition, access to antibodies as well as complement fractions released during xenograft immunity is restricted by the microcapsule. However, if small molecules (~ a few kD) or antigens released cross the microcapsule membrane, a significant inflammatory cell reaction will result. Cytokines, nitric oxide and free oxygen radicals released from the inflammatory cells may destroy the encapsulated cells (Strand *et al*., 2001). Highly purified biocompatible polymers with minimal endotoxin and protein content are necessary to prevent graft rejection.

More research is still needed to improve the biocompatibility of microcapsules. Although lack of biocompatibility does not appear to pose a problem in microcapsules transplanted over a short time, a number of problems still need to be addressed before microencapsulated cells can be routinely implanted into humans for longer periods.

Table 1.1 Some therapies based on the implantation of microencapsulated genetically engineered cells

Cell Type	Gene	Type of Capsule	Mode of Action	Disease	References
Hamster kidney cells	Ciliary neurotrophic factor (CNTF)	Polymer	Secrete CNTF	Amyotrophic lateral sclerosis	Aebischer *et al.*, 1996
Mouse fibroblasts	Human growth hormone (hGh)	APA	Secrete hGh	Dwarfism	Basic *et al*., 1996
Neuro2A cells	Pro-opio melanocortin (POMC)	Polymer	Secrete β-endorphin	Chronic pain	Saito *et al*., 1995
SK2 hybridoma		APA	Secrete monoclonal antibodies Secrete human interleukin 6	IgG_1 plasmacytosis	Okada *et al*., 1997
Mouse fibroblasts	Factor XI	APA	Secrete human factor XI	Haemophilia	Hortelano *et al*., 1995
Hamster kidney fibroblasts	Human nerve growth factor (hNGF)	Polymer	Secrete hNGF	Parkinson's disease	Date *et al*., 1996
Xenogeneic Baby Hamster Kidney cells	Human nerve growth factor	Polymer	Secrete hNGF	Axotomised septal cholinergic neurons	Winn *et al., 1994*

1.4 Aims of Thesis

The aim of this thesis is to ascertain the feasibility of two proposed approaches to treat LCAT deficiency in animal models, namely infusion of recombinant protein and encapsulated cell therapy. Studies performed *in vitro* and *in vivo* were set out with the following four aims:

Aim 1: *To establish a method to purify histidine-tagged human LCAT from medium collected from genetically modified CHO (LCAT-CHO cells).*

Aim 2: *To determine whether purified LCAT is biochemically active and can reverse dyslipoproteinaemia when injected into LCAT $^{-/-}$ mice.*

Aim 3: *To investigate whether LCAT-CHO cells can survive in a microencapsulated environment and secrete LCAT.*

Aim 4: *To determine whether implantation of encapsulated LCAT-CHO cells into the peritoneum of LCAT $^{-/-}$ mice can correct their plasma lipoprotein abnormalities.*

CHAPTER 2

METHODS AND MATERIALS

2. METHODS AND MATERIALS

2.1 Cell Culture

2.1.1 Materials

Iscove's modified Dulbecco's Modified Eagle's Medium (DMEM), CHO-S-Serum Free Medium II (SFM), CHO-III-Protein Free Medium (PFM) and CD-CHO medium were purchased from Life Technologies. In searching for an ideal medium from which to isolate pure LCAT, the cells were cultured in these different media. Iscove's modified DMEM, the basic growth medium was supplemented with dialysed fetal bovine serum (FBS, Sigma-Aldrich Co, Dorset, UK). All media were supplemented with glutaMAX, penicillin, streptomycin and non-essential amino acids (all from Life Technologies), while phosphate buffered saline (PBS), trypsin-EDTA solution and methotrexate were purchased from Sigma-Aldrich Co, Dorset, UK.

2.1.2 Cell Growth

The CHO-H6LCAT cells were grown in Iscove's modified DMEM media supplemented with 2 mM glutaMAX, 100 U/ml penicillin, 100 µg/ml streptomycin, 1% non-essential amino acids and 5% heat-inactivated dialysed FBS. The cells were cultured as a monolayer in 75 cm^2 tissue culture flasks (T-75) at 37 ^{0}C in a humidified atmosphere of 5% CO2 and 95% air.

2.1.3 Passaging of cells

When the cells were nearly confluent, they were trypsinized and passaged. The spent medium in the flask was removed and discarded. The cells were washed once with 5 ml PBS and trypsin-EDTA (2-3 ml) was added to cover the entire monolayer of cells. After incubating the flask in the incubator for 2-3 min, the cells were detached from the surface of the flask by gentle agitation, which was confirmed by inspection under the microscope. The trypsin was neutralised by addition of growth medium. The cells were then split by volume, usually 1:6, by adding pre-warmed medium (37 ^{0}C) and were resuspended and distributed into new flasks (15 ml per T-75 flask).

2.1.4 Freezing of cells

Stocks of cells were stored frozen in liquid nitrogen without compromising their function. A flask of near-confluent cells was trypsinized as above. The trypsin was neutralised with growth medium after the cells were made into a suspension and an aliquot (100 μl) was used to estimate cell density (see 2.2.5). The recommended number of cells for freezing = 1 x 10^6 cells/ml. The remainder was centrifuged at 2,000 x g in a sterilin tube for 3 min at 22 ^{0}C. The freezing medium was FBS and 10 % DMSO, filtered through a 0.2 μm acrodisc prior to use. The pelleted cells were resuspended in freezing medium at 10^6 cells/ml and were aliquoted (0.5 ml) into cryovials. The vials were gradually cooled at approximately 1 ^{0}C/min to avoid excessive stress to the cells and after 2-3 h transferred to a liquid nitrogen storage tank.

2.1.5 Thawing of cells from liquid nitrogen

An aliquot of 15 ml of growth medium (not prewarmed) was added to a 20 ml sterile tube. The required frozen cryovial of cells was transferred from the liquid nitrogen to a 37 ^{0}C waterbath and was rapidly thawed. It was then sprayed with ethanol and placed into the tissue culture hood. The cell suspension was transferred immediately into the growth medium and the cells resuspended. Usually the cell suspension was transferred directly into a T-75 flask for incubation, but in some cases I first removed the toxic DMSO by centrifuging the tube and resuspending the pellet in a new batch of medium.

2.1.6 Estimation of cell numbers

Trypan blue staining and a haemocytometer were used to determine total cell counts and viable cell number. The underlying principle is that live (viable) cells take up and excrete trypan blue dye, whereas dead (non viable) cells absorb but cannot excrete the dye and therefore appear blue.

Equal volumes of cell suspension (50 μl) and 0.4% (w/v) trypan blue (50 μl) were mixed together and were allowed to stand for 5-15 min. With the coverslips in place, a small amount of the mixture was transferred to both chambers of the haemocytometer by carefully, touching a drop to the edge so that filling was by capillary action.

Starting with chamber 1 of the haemocytometer, all the cells in the 1 mm corner squares and centre were counted. Non-viable cells stained blue and a separate count of these was made. The same procedure was repeated for chamber 2 and a minimum of 8 squares were counted. As 1 cm^3 = 1ml, each square of the hemocytometer with coverslip in place represents a total volume of $0.1mm^3$ or 10^{-4} cm^3. Cells per ml were calculated as average count per square x dilution factor x 10^4.

If Average Count = 94.5 per square

= 94.5 x 2 (dilution factor) $x10^4$

= 1.89×10^6/ml

The total cell number was calculated as cells per ml x the original volume of medium containing the cells e.g. for 8 ml = 15.12×10^6. The percentage of viable cells (%) was calculated as total viable cells (unstained) ÷ total cells (stained + unstained) x 100.

2.1.7 Screening Cells for Mycoplasma Infection

The incidence of mycoplasma infections of cell cultures is variable. Mycoplasma infections may be transmitted from laboratory staff (M. *orale*) and infected bovine serum (M. *arginini*, M. *hyorhinis*, A. *laidlawii*) or from other mycoplasma-infected cell cultures. The infection cannot be detected by naked eye but may be evident by signs of general deterioration in culture, such as a decrease in protein production by the cell line. Mycoplasma within cells grows slowly and does not destroy host cells; hence it is important to regularly screen for covert contamination of established cell lines. There are several techniques to detect mycoplasma infection in cell culture.

DAPI (4', 6-Diamidine-2'-phenylindole dihydrochloride) method

This is a fluorescent dye that selectively binds to DNA and forms strongly fluorescent DNA-DAPI complexes with high specificity. When DAPI is added to tissue culture medium, it is readily taken up by the cells yielding fluorescent nuclei with a dark cytoplasmic background. When the cells are contaminated with mycoplasma, discrete fluorescent foci are seen in the cytoplasm and intercellular spaces.

The cells to be tested were grown in antibiotic-free media for at least two passages on coverslips in petri-dishes. At 50-70 % confluence, the medium was discarded and the cells washed once with DAPI-methanol (1 μg/ml). The cells were incubated with DAPI-methanol for 15 min at 37 ^{0}C. The staining solution was removed

and the cells were washed with methanol. The inverted coverslip was mounted on a microscope slide with glycerol and examined under a fluorescence microscope (Nikon) with 340/380 nm filter and LP 430 barrier filter.

PCR to detect Mycoplasma infection

The polymerase chain reaction (PCR) is one of the most powerful tools in molecular biology and amplifies a DNA or cDNA template many thousand- or million-times quickly and reliably. It is a relatively simple, but sensitive technique. The PCR process amplifies short (usually 100-500 bp) segments of a longer DNA molecule. A typical amplification reaction includes the sample target DNA, a thermostable DNA polymerase, two oligonucleotide primers, deoxynucleotide triphosphates (dNTPs), reaction buffer and magnesium. The components of the reaction are mixed and the reaction is placed in a thermal cycler and exposed to a series of different temperatures for varying amounts of time, referred to as one cycle of amplification. This consists of three steps: 1) production of single-stranded DNA templates by denaturing the DNA, 2) annealing with an excess of two oligonucleotide sequences (the primers), each complementary to a stretch of DNA at the target DNA and 3) synthesis of a copy from each strand of template by DNA polymerase. Each PCR cycle theoretically doubles the amount of targeted template sequence in the reaction.

Materials

PCR primers used to amplify the 16S rRNA, found specifically in mycoplasma were: GPO-3 forward primer: GG GA GCAAA CAGGA TTAGA TA CCCT (10 μM) and MGSO reverse primer: TGGCACCATCTGTCAC TCTGTTAACCTC (10 μM). The primers were added to a 2 μM cocktail of dNTPs (dATP, dTTP, dGTP and dCTP), thermostable DNA polymerase e.g. Pfu or Taq (5 U/μl), thermostable DNA polymerase reaction buffer (10 x stock concentration) and sterile filtered water. The final mixture was overlaid with mineral oil. A contaminated cell culture lysate was used as a positive control.

Methods

The test medium was collected from a 70 - 100 % confluent adherent culture and 1 ml was centrifuged for 10 min at 13,000 rpm. Most of the supernatant was removed,

the tube recentrifuged and any remaining supernatant discarded. The pellet was resuspended in 100 μl of water and transferred to PCR tubes and incubated in a PCR machine for 10 min at 95 ^{0}C to completely lyse the cells. It was further centrifuged for 2 min at 13,000 rpm and the supernatant containing the templates was kept for the PCR reaction.

A master mix for amplification was prepared by adding the reagents in the order and proportions shown below to 0.2 ml thin-walled PCR tubes (Table 2.1). Tube contents were covered with 20 μl of mineral oil and incubated in a Stratagene PCR Robocycler (Stratagene Ltd; Cambridge UK) as follows:- After heating at 95 ^{0}C for 5 min, amplification was programmed for 35 cycles, with denaturation for 1 min at 95 ^{0}C, annealing of primers for 1 min at 55 ^{0}C and extension for 1 min at 72 ^{0}C. Finally, the reaction was completed by a further extension step at 72 ^{0}C for 10 min.

Table 2.1 Composition of the PCR reaction

Component	Volume (μl)	Final concentration
GPO-3 primer	5	1 μM
MGSO primer	5	1 μM
dNTP's	5	0.2 μM
Buffer 10 x stock	5	1 x stock
Water	27.5	___
Template	2	___
Polymerase	0.5	2.5 units
Total volume	50	

Agarose gel electrophoresis of DNA

The PCR reaction was analysed using agarose gel electrophoresis, followed by staining the DNA with ethidium bromide and visualization by UV irradiation of the gel. The minigel apparatus (Horizon minigel apparatus, Life Technologies) was set up as recommended by the manufacturer. Table 2.2 outlines the separation ranges for typical gel concentrations. The required weight (1.5 g) of agarose (AquaPor LE GTAC agarose; National Diagnostics, Hull, UK) was added to the appropriate amount (100 ml) of 1 x Tris-Acetate EDTA (TAE) buffer from a 10 x stock; National Diagnostics) to make a 1.5% gel. The mixture was heated in a microwave oven until the agarose just dissolved (usually 2 min) with mixing at regular intervals. The solution was cooled to 50 - 60 ^{0}C and ethidium bromide was added (1 μg/ml) before pouring into the cast. The gel was allowed to set for ~ 30 min at room temperature. The comb and blocks were removed and a sufficient volume of 1 x TAE buffer was added until the gel was completely immersed. The PCR products were mixed 4:1 with 10x loading buffer (10 mM Tris.HCL, pH 7.5 containing 50 mM EDTA, 10% Ficoll 400, 0.25% xylene cyanol FF) and loaded (10 - 20 μl) into the wells. A 100 bp DNA ladder (5 μl; Life Technologies, UK) was used as a marker. The gel was run at a constant voltage of 125 V for ~30 min or until the dye front had migrated 2 cm from the bottom of the gel. After electrophoresis, the gel was removed, visualised and photographed under UV lightbox.

Results

During one routine test, a batch of CHO-H6LCAT cells (Fig 2.1, lane 5) was positive for a PCR product of ~ 300 bp, suggesting the presence of mycoplasma as this was also in the positive control (lane 1). The negative control (lane 2) and a second batch of CHO-H6LCAT cells (lane 4) did not demonstrate any PCR product. As expected the LCAT secretion from the infected CHO-H6LCAT cells had fallen, from a normal production of 6 - 10 μg/ml/48 h to less than 1 μg/ml/48 h. These cells were immediately discarded and replaced by a new batch of CHO-H6 LCAT cells, negative for mycoplasma.

Table 2.2 Separation ranges for typical agarose gel concentrations

DNA Size (bp)	Gel Concentration
100 - 3000	2.00 %
150 - 4000	1.75 %
200 - 5000	1.50 %
300 - 8000	1.25 %
400 - 12000	1.00 %
1000 - 23000	0.75 %

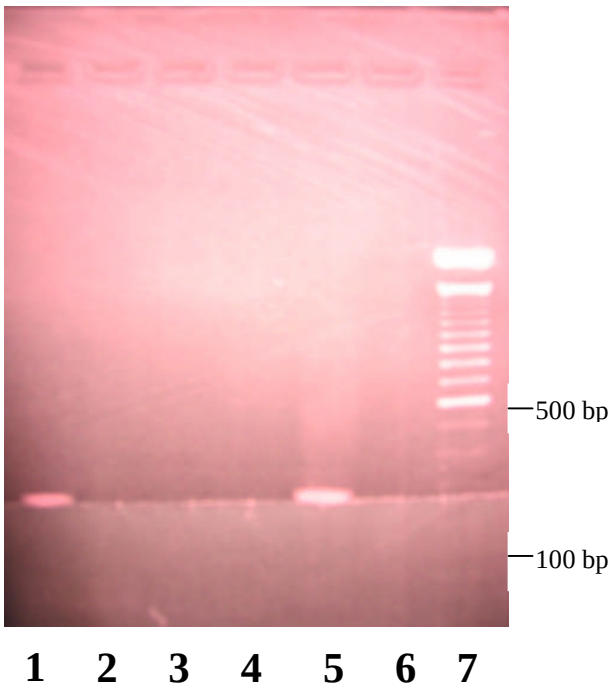

LANES

1. Positive control
2. Negative control
3. Blank
4. Uninfected CHO-H6LCAT cells
5. Infected CHO-H6LCAT cells
6. Blank
7. Marker

Figure 2.1 Testing cultured CHO-H6LCAT cells for mycoplasma contamination using PCR

The PCR products were run on 1.5% agarose gel. The marker (100 bp DNA ladder) for DNA sizes is in lane 7. Lane 5 was the test sample which had a similar band (~300 bp) as lane 1 (positive control). It confirms the presence of mycoplasma in the test sample.

2.2 LCAT assay

2.2.1 Background

Although there is a definite potential for the clinical use of LCAT assays, its measurement is not widespread, being now limited to the diagnosis of deficiency syndromes, such as classical LCAT deficiency and Fish Eye disease. Several clinical conditions such as liver and renal disease are associated with low and even absent levels of plasma LCAT. It is reported that LCAT measurement is more sensitive than conventional liver function tests and is a good prognostic indicator in liver transplantation (Shimada *et al*., 1989); its assay may also be useful in studies of hyperlipidaemias. In man the percentage of plasma total cholesterol as cholesteryl ester is remarkably constant (70 - 74%) and any reduction will invariably indicate low LCAT activity.

The LCAT reaction in plasma consists of three phases. Each of them can be influenced by reaction conditions during an *in vitro* assay. The availability of unesterified cholesterol and its transfer from various compartments of the plasma pool may affect the esterification rate thus affect the final result. These stages are as follows:

1. Activation of the phospholipid bilayer by a protein or peptide. This takes place primarily in HDL and is mostly due to the presence of apolipoprotein AI (apoAI).

2. Release of a fatty acid by hydrolysis of lecithin (mostly in the *sn*-2 position) by phospholipase A2-like activity. The esterification rate depends on the composition of lecithin, particularly on the acyl-chain lengths and their degree of saturation.

3. Transfer of the fatty acyl chain to an acceptor, the 3β-hydroxyl group of cholesterol.

The current methods of measuring LCAT can be divided into those estimating LCAT protein (mass) in plasma either directly (immunoassay) or indirectly by assaying LCAT activity using exogenous substrates (proteoliposomes or heat-inactivated plasma); and those measuring the rate of cholesterol esterification in plasma using the subject's own plasma or plasma depleted of apoB-containing lipoproteins (HDL-plasma). Because heat-inactivated plasma has low sensitivity and low reproducibility, this source of the reaction substrate has been mostly abandoned. The assay described below is based on the proteoliposome method for the measurement of enzyme activity (Gillet and Owen, 1992). This assay uses a highly efficient substrate for LCAT, a proteoliposome containing apoAI: lecithin: labelled unesterified cholesterol, in the

molar ratio of 0.8: 250: 12.5 (Chen and Albers, 1982), so that any influence of endogenous lipoproteins is bypassed. This method is considered to reflect the LCAT mass in the plasma sample. LCAT enzymic activity is then measured by counting the conversion of radiolabelled cholesterol to cholesteryl ester.

2.2.2 Substrate for LCAT activity test

Materials

Tritium (^{3}H)-labelled cholesterol (1 μCi/μl), L-α-phosphatidylcholine (100 mg/ml), fatty acid- free bovine serum albumin (BSA), β-mercaptoethanol and free cholesterol (1 μg/ml) were all purchased from Sigma-Aldrich. ApoAI was isolated from plasma in our laboratory; sodium cholate and sodium chloride were purchased from Merck. Amberlite beads (AD-2 nonionic polymeric adsorbent, 20-60 mesh) were purchased from Sigma-Aldrich.

Solvents

The solvents used for LCAT assays such as chloroform, methanol, hexane, diethylether, acetic acid and cocktail T scintillation fluid were all purchased from Sigma-Aldrich, UK. In addition whatman TLC plates 60 ^{0} A (Fisher Scientific, UK), drying block (Techne, UK) and nitrogen gas were required.

Control plasma

Pooled human plasma was used as a standard source of LCAT activity and was obtained from normal adult volunteers. Blood was drawn into vacutainer tubes containing sodium-EDTA (1 mg/ml) as anticoagulant and plasma was obtained after centrifugation at 4 ^{0}C. It was pooled and heated at 56 ^{0}C for 30 min, prior to batching and storing at –20 ^{0}C until required.

Preparation of dialysis tubing

Dialysis tubing (10,000 MWCO) was treated to remove metal ions and other substances that may have adverse effects on the LCAT substrate. The tubing was initially immersed in 1 mM EDTA solution and slowly warmed to 80-90 ^{0}C. It was then warmed to 90 ^{0}C in 0.1 % $NaHCO_3$. The tubing was then washed thoroughly in deionised water and finally stored in 0.5 % sodium azide solution at 4 ^{0}C.

Preparation of substrate proteoliposomes

In a 50 ml glass tube with a teflon-lined screw cap, 348 μl L-α-phosphatidylcholine (100 mg/ml) and 820 μl free cholesterol (1 μg/ml) were mixed and 36 μCi ^{3}H labelled cholesterol was added. The solution was evaporated under nitrogen gas and "freeze dried" for 2 h to ensure all solvent traces were removed. ApoAI (4 mg in 10.8 ml PBS) was added and, while vortexing 1.36 ml of 0.725 M of sodium cholate was added dropwise to give a clear solution. The proteoliposomes were dialysed at 4 ^{0}C in the cold room for 24 h against 4 litres of 0.9 % NaCl with 5 - 6 changes to remove cholate.

A solution of fatty acid-free BSA (0.5 g in 25 ml PBS) was heat-inactivated for 30 min at 56 ^{0}C. Then the solution was centrifuged at 2,000 rpm for 10 min and the supernatant filtered through a 0.22 μm membrane. Dialysed proteoliposomes were transferred to a 100 ml beaker and PBS added until the volume was 64.8 ml. BSA (22.5 ml) and 31.4 μl of β-mercaptoethanol were then added to the proteoliposomes.

Amberlite beads (1 g) were washed with 20 ml of methanol at room temperature for 15 min on a roller-mixer. The supernatant was discarded and the beads washed with 3 x 20 ml water for 5 min each followed by 3 x 20 ml PBS washes. The Amberlite beads were added to the proteoliposomes and incubated on a roller-mixer at 4 ^{0}C. After 24 h, the substrate was further incubated with fresh beads to ensure that all traces of cholate were removed. It was then batched into aliquots of 242.5 μl and stored at –70 ^{0}C.

Results and Discussion

Serum albumin as a component of the substrate is thought to enhance apoAI stimulated LCAT activity by stabilising the enzyme and or binding lysolecithin to minimise product inhibition (Chen and Albers, 1982).

Large stocks of porcine apoAI were available in our own laboratory and were also tested as a substrate constituent. However, they only gave an esterification of less than 2 %/h with human plasma and therefore were a poor substitute for human apoAI (10 - 12 % esterification/h (Chen and Albers, 1982)). Other studies have also demonstrated that *in vitro* activation of LCAT by apoAI is species-specific (Chen and Albers, 1983).

Plasma LCAT activity increases as apoAI concentration increases in the proteoliposome with maximal activity obtained at 0.8 nmol of apoAI (Chen and Albers,

1982). ApoAI may exert a cofactor activity by interacting reversibly with the enzyme at water-lipid interfaces. This may lead to activation of the enzyme and the optimal orientation of substrate molecules for enzymatic reaction. Coexistence of apoAI on substrate vesicles promotes the structural integrity of the active site by preventing the excessive unfolding of the enzyme at the vesicle surface (Furukawa and Nishida, 1979).

During each step of the preparation as outlined in Table 2.3, a volume of 242.5 μl was sampled and the substrate quality was measured by adding a defined amount of enzyme (7.5 μl of plasma). The results were expressed as percentages of cholesterol esterification (% CE). Despite adding apoAI, the activity of plasma LCAT was still low giving a CE of 0.55 % (Table 2.3). This is still turbid and therefore not a true liposome. Sodium cholate is necessary for lipid solubilisation and formation of a proteoliposome solution. However, sodium cholate strongly inhibited enzyme, resulting in no LCAT activity. Prolonged dialysis (> 24 h) of the substrate in sodium chloride solution was avoided as this was found to cause precipitation and an inactive substrate. Unexpectedly, a 24 h dialysis with several changes gave a very poor substrate (0.07 % of cholesterol esterified), although addition of mercaptoethanol did increase this to 0.74 % (Table 2.2). Reducing agents are known to stabilise LCAT activity by maintaining cysteine residues in the reduced (-SH) state. Thus low concentrations of β-mercaptoethanol enhance enzyme activity with a maximal effect at approximately 4 mM mercaptoethanol (Furukawa and Nishida, 1979).

Incubation of the substrate with Amberlite beads was an important step in making it fully active. Although the LCAT activity at 4 h was slight, there was a marked increase following 24 h incubation (6.83 % CE). The role of the beads was to help ensure complete removal of sodium cholate which strongly inhibits LCAT activity. When the substrate was stored at –20 ^{0}C, esterification decreased over one month period (from 6.44 % to 2.98 %). However, when it was stored at –70 ^{0}C, the substrate maintained its esterification for at least 2 months.

The substrate made using the above method achieved a desired esterification of 5 - 15 %/h using 7.5 μl of human plasma as the source of LCAT enzyme. This method enabled me to prepare a large amount of stable, homogeneous proteoliposome vesicle substrate for a rapid and sensitive determination of LCAT activity in plasma and in culture medium.

Table 2.3 The evolutionary stages of substrate preparation and its esterification by plasma LCAT

Preparation Stage	**LCAT activity (%CE/h)**
After adding ApoAI	0.55
After adding Sodium Cholate	0.00
After 24 h of dialysis against 0.9 % NaCl	0.07
After adding BSA	0.17
After adding β-mercaptoethanol	0.74
After 4 h incubation with Amberlite beads	0.44
After 24 h incubation with Amberlite beads	6.84
Thawed after storage at –70 ^{0}C	7.09

This table illustrates a typical pattern of LCAT catalytic activity at different stages of substrate preparation. A volume of 242.5 µl was sampled for use in an LCAT assay with 7.5 µl of human plasma. A significant increase in esterification was observed after 24 h incubation with the Amberlite beads. There was no loss of esterification after storage at –70 ^{0}C.

2.2.3 Standard LCAT assay

Previously prepared substrate (proteoliposomes) was thawed in water bath at 37 ^{0}C**.** For each test sample an aliquot containing LCAT e.g. 7.5 μl of plasma was transferred into 242.5 μl of the substrate. The mixture was placed in a water bath and incubated at 37 ^{0}C for 1 h before transfer to a glass tube containing 4 ml of chloroform-methanol (1 : 1). The mixture was vortexed again. The assay can be stopped here temporarily and the sample mixture stored at 4 ^{0}C.

To continue, 1.2 ml of deionised water was added to each tube. They were vortexed and centrifuged for 10 min at 2000 g at 4 ^{0}C; alternatively, they can be left to stand overnight when they will also separate into layers. At the top was the aqueous methanol phase whereas separated by a thin interphase layer of protein, the bottom was largely chloroform containing the lipids. Using the Pasteur pipettes, the chloroform phases were transferred into small glass tubes each containing 5-6 drops of methanol; the latter helps in removing water traces when drying under nitrogen gas. The tubes were placed in the wells of the Drying Block preheated at 40 ^{0}C and dried under nitrogen gas. Chloroform-methanol (200 μl 1:1) was then added and the evaporation process repeated. The dry residue was dissolved in chloroform (10 μl).

TLC Whatman chromatogram plates were marked out for each sample. The concentrated lipid extracts were applied onto the chromatogram silica about 2 cm from the bottom of the plate (i.e. higher than the level of the running solvent). The thin-layer chromatography chamber was prepared by lining the walls with Whatman (3 mm) paper and adding 40 ml of solvent. The solvent was prepared using hexane, diethyl ether and acetic acid in the ratio of 90 : 20 : 1, by volume.

The chromatogram plate was placed in the chamber and the solvent was allowed to rise to 1-2 cm from the top. The plate was dried at room temperature for 1-3 min and was stained by exposing to iodine vapour. The band second from the top was the cholesteryl esters (CE) and the band just above the origin unesterified cholesterol (UC), as verified by comparison with lipid standards as markers in one lane (Fig 2.2).

Scintillation vials were prepared by adding 8 ml of cocktail-T (toluene-based) to each plastic vial. The CE and UC bands were scrapped off and transferred into separate vials and the radioactivity counted in a Beckman βeta counter. As CE has a low disintegration per min (d.p.m.) it was counted for 10 min whilst UC with a high d.p.m. was counted 1 min. After the radioactivity was counted in the CE and UC fractions, the percentage of CE was calculated as follows:

$$\frac{\mathbf{CE}_{\mathbf{d.p.m.}}}{\mathbf{UC}_{\mathbf{d.p.m.}} + \mathbf{CE}_{\mathbf{d.p.m.}}} \mathbf{X\ 100\%}$$

The result is then subtracted from control reactions containing no enzyme which were run simultaneously to correct for nonenzymic reaction. The final value represents the LCAT activity of the test sample, expressed as the percentage of cholesterol esterified per hour (% CE/h).

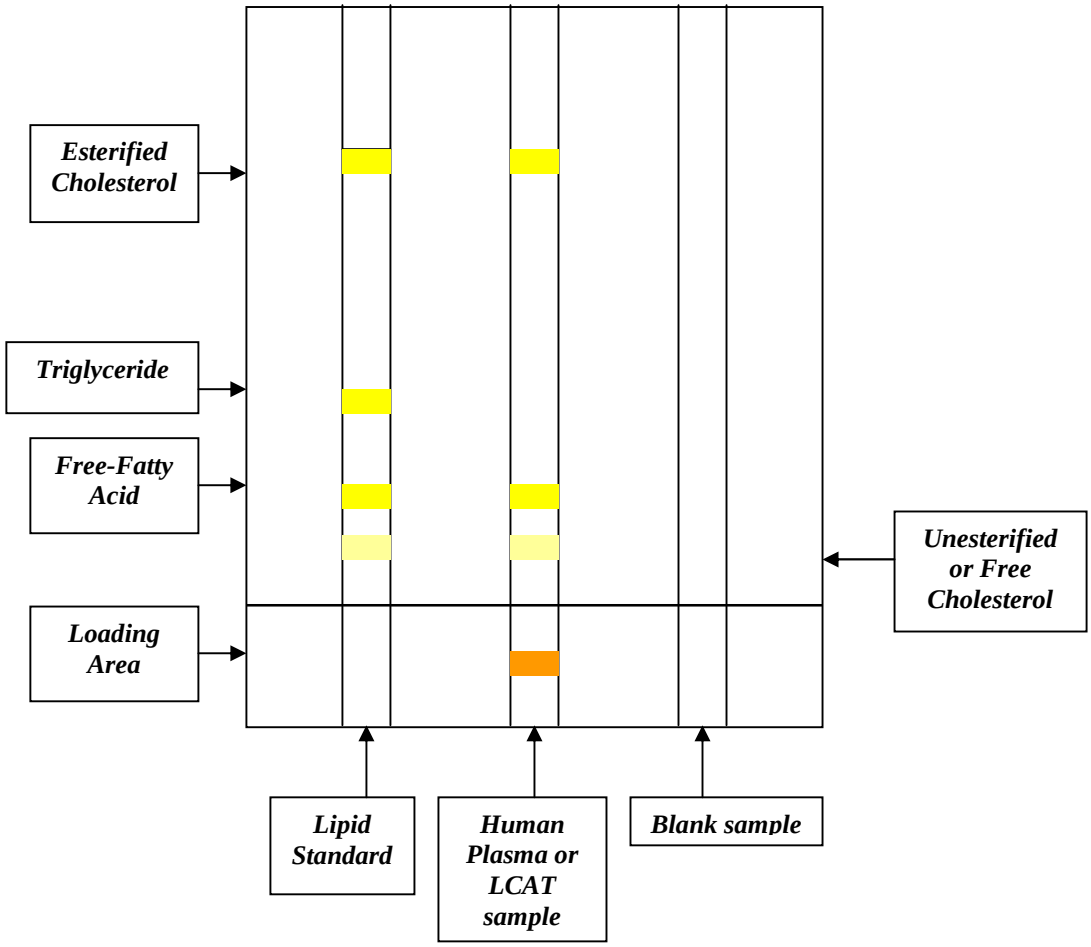

Figure 2.2 Diagram showing the separation of neutral lipids on a silica-coated TLC plate

After a lipid sample is loaded onto the Whatman Chromatogram plates, cholesterol, free- fatty acid, triglyceride and esterified cholesterol migrate and separate out in order of increasing distance from the loading point with esterified cholesterol being furthest away.

2.3 Characterisation of the LCAT Assay

2.3.1 Linearity of LCAT assay

This experiment was done in triplicate. The test plasma volume (with varying LCAT mass) used ranged from 0.5-25 μl and heat-inactivated plasma was added to make the volume of each sample to 25 μl and therefore the total volume was constant throughout this study. The assay was performed in the standard way (section 2.2.3). The percentage of esterified cholesterol was plotted against increasing plasma volume (Figure 2.3).

From the observation, there is a linear relationship of LCAT activity from 2.5-15 μl of plasma in the presence of heat-inactivated plasma (Fig 2.3). For example, as the % CE in 5 μl was twice that in 2.5 μl plasma and 10 μl twice that in 5 μl plasma. This implies that there is a good correlation between LCAT mass and enzymic activity (% CE) using this proteoliposome substrate. At higher volumes (20 and 25 μl), there was some loss of linearity, perhaps because the products of the enzymatic reaction, cholesteryl esters and lysolecithin, accumulate to inhibit LCAT catalytic activity by negative feedback. These become significant when % CE exceeds about 5 - 6 %.

In the original Alber's method (Chen and Albers, 1982), 7.5 μl of plasma was used together with 242.5 μl of substrate as the standard LCAT enzyme reaction. Since this volume corresponded to a % CE value that falls within an estimated linear slope between plasma volumes 2.5 to 15 μl, it was decided that this would be the standardised volume for the plasma control in subsequent experiments.

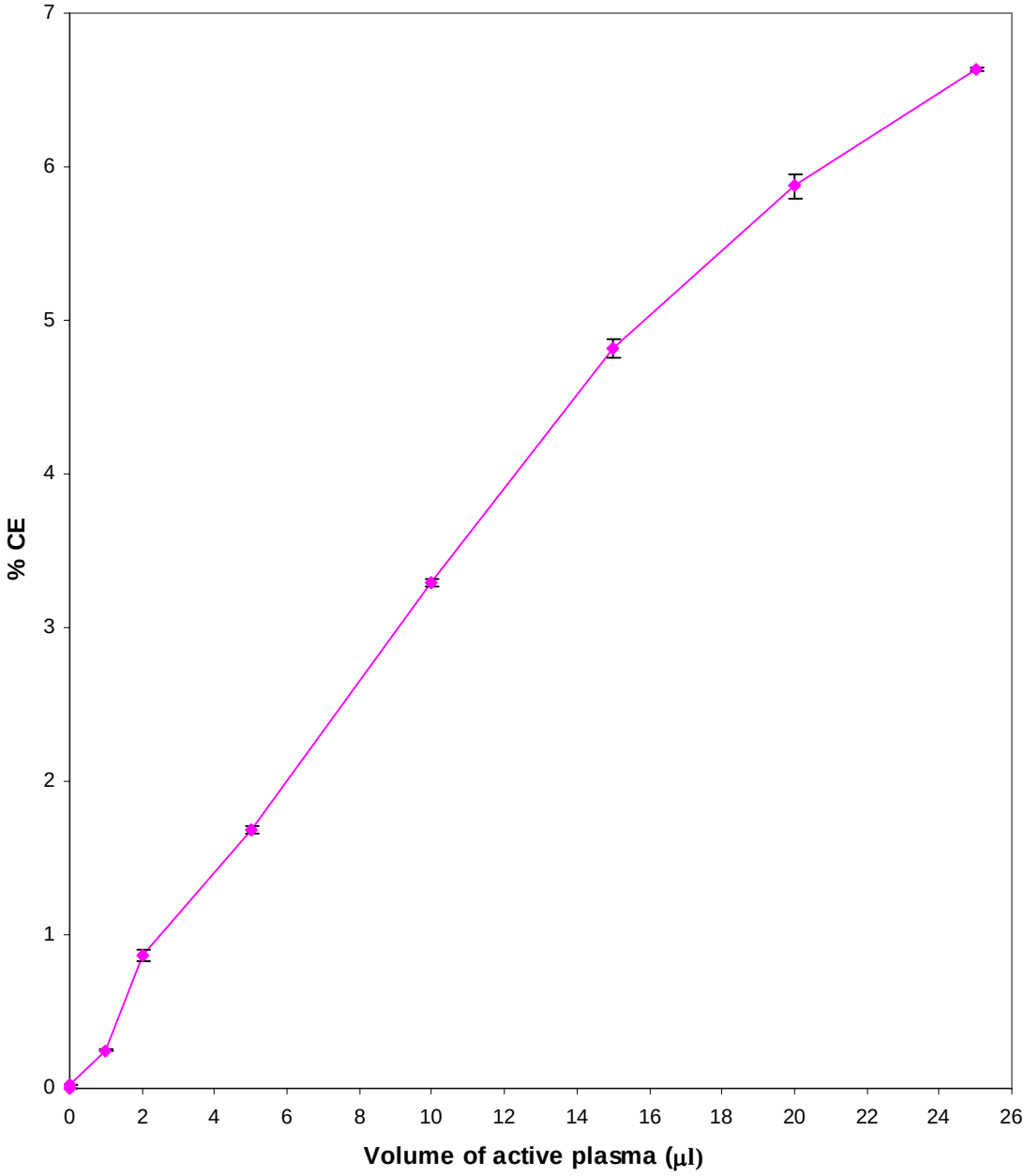

Figure 2.3 Linearity of the LCAT assay

Various amounts of plasma (µl) were added to proteoliposome substrate and the LCAT activity determined as described in section 2.3.3. Heat- inactivated plasma was added to make the total volume constant (25 µl). Each value is the mean of 3 determinations ± s.e.

2.3.2 The effect of increasing volume of CD-CHO containing LCAT on esterification of cholesterol

The LCAT assay is reported to be most sensitive for samples in which the level of LCAT activity is low e.g. culture medium. Therefore it is ideal for use to monitor LCAT production in different medium, during each LCAT purification step and assaying mice plasma following LCAT treatment. However, the effect of test sample volume on LCAT activity is not known. To investigate this factor, I have chosen CD-CHO medium as the test sample here as it is a sample commonly assayed for LCAT activity, and whose volume varies considerably.

The volume of conditioned CD-CHO medium containing LCAT (CD-CHO.H6LCAT used ranged from 5-195 μl and native CD-CHO medium was added to make up the volume of each sample to 195 μl, keeping the total volume constant throughout. The LCAT assay was performed as before (section 2.2.3).

As expected, the % CE increased in a linear manner as the proportion of CD-CHO.H6LCAT medium was increased (Fig 2.4). This was true when the diluent was CD-CHO medium alone. In practical terms, LCAT activity is proportional to the LCAT mass available in the test sample and is dependent of its volume within the range, 0-195 μl.

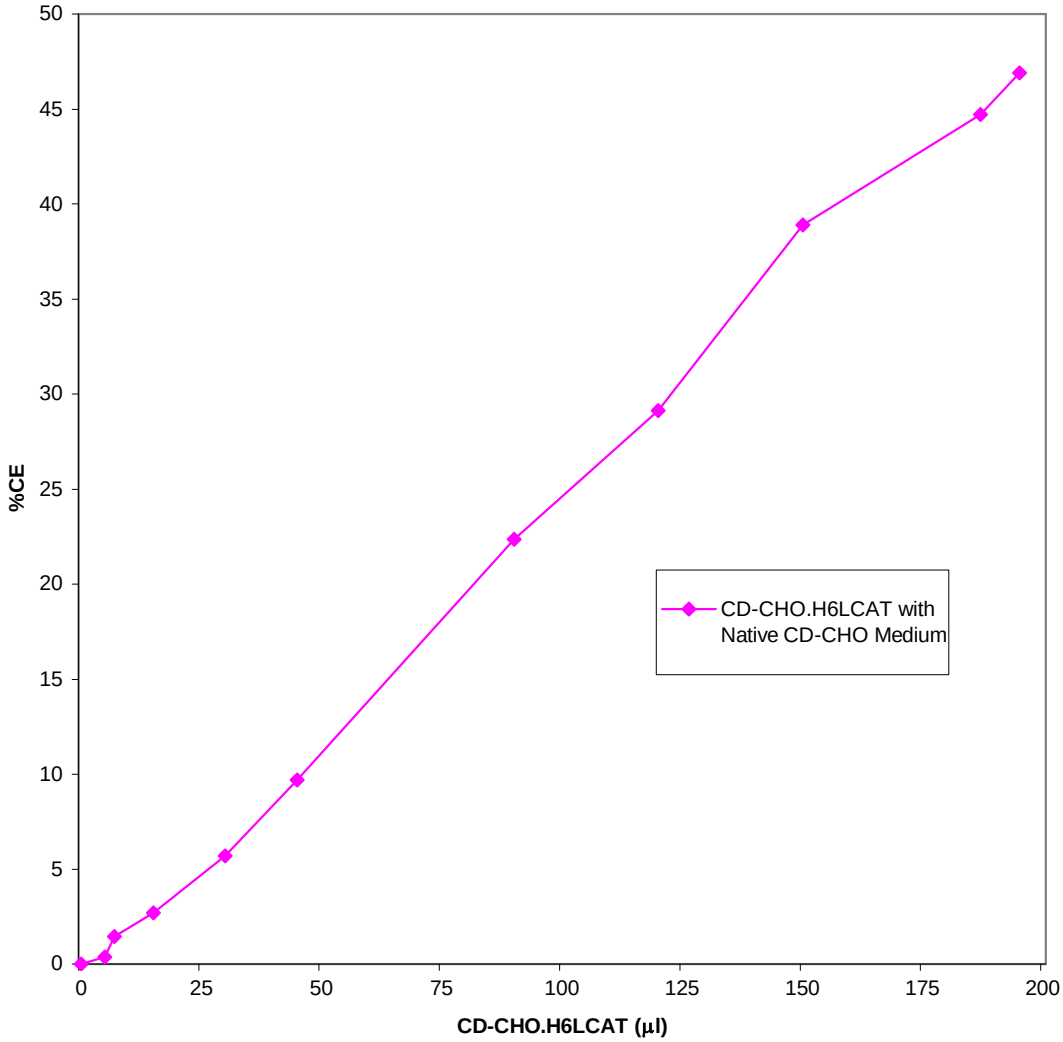

Figure 2.4 LCAT activities with increasing volume of CD-CHO.H6LCAT

CD-CHO.H6LCAT medium was collected after 48 h and a range of volumes (0-195 µl) was assayed for LCAT activity using the proteoliposome substrate method. Native CD-CHO medium was added to make up to a total of 195µl.

2.3.3 The effect of heat-inactivated plasma on concentrated CD-CHO.H6LCAT medium

Pooled human plasma has been used as a source of LCAT and as a reference standard in my experiments. It is not clear whether the amount of LCAT in test sample e.g. CD-CHO medium, is directly equivalent to the amount in human plasma given the fact that human plasma bar LCAT may have a small effect on LCAT activity (Fielding *et al.,* 1971; Albers *et al.,* 1981). To evaluate whether this effect exist, heat-inactivated (HI) plasma was added to CD-CHO medium.

Conditioned CD-CHO.H6LCAT medium was collected after 48 h interval and concentrated by a factor of 6 using Vivaspin columns (MWCO 30,000). The volume of this medium used ranged from 0.5-25 μl and heat-inactivated plasma or native CD-CHO medium was added to make up the volume of each sample to 25 μl. The assay was performed in the standard way.

The esterification of cholesterol was approximately linear whether heat-inactivated plasma or neat CD-CHO medium was the diluent, although the % CE was lower in the presence of heat-inactivated plasma (Fig 2.5). This suggest that the amount of LCAT in CD-CHO medium does not equate directly with LCAT in plasma i.e. constituents in plasma suppressing enzymic activity. Since I routinely use plasma as a reference standard, then there is a need to use heat-inactivated plasma to correct for this inconsistency.

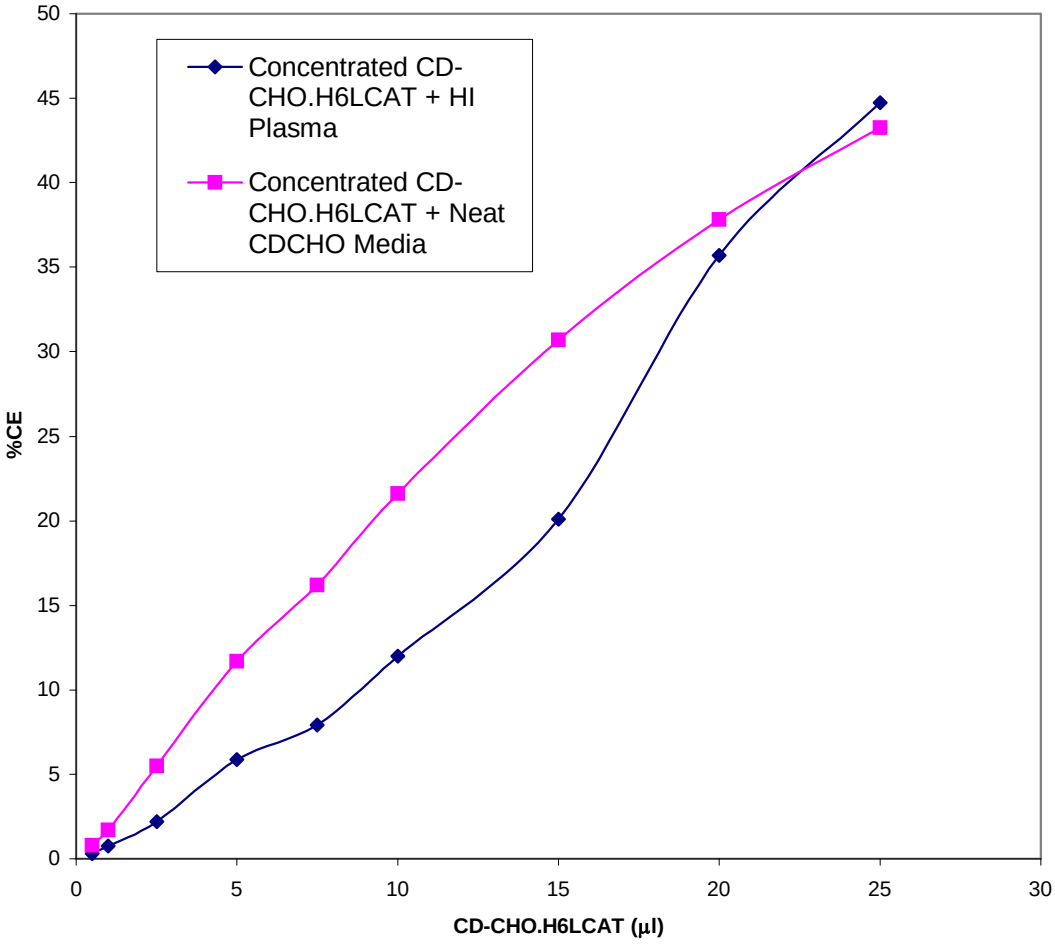

Figure 2.5 Concentrated CD-CHO.H6LCAT with and without HI plasma and its effect on cholesterol esterification

CD-CHO.H6LCAT medium was collected after 48 h interval and concentrated 6 fold. A range of volume of this medium was added to 242.5 µl of proteoliposome substrate for measurement of LCAT activity. Native CD-CHO medium or heat-inactivated plasma was added to make the total volume of each test sample constant (25 µl).

2.3.4 The effect of enzymatic activity in varying volumes of CD-CHO with constant amount of LCAT

A 48 h collection of CD-CHO.H6LCAT medium was concentrated ~ 6-fold. LCAT assays were performed using 7.5 μl of the concentrate containing LCAT and a constant volume of heat-inactivated plasma (7.5 μl), whilst adding increasing volumes of native CD-CHO medium to a maximum of 300 μl.

Keeping the amount of LCAT constant, the esterification was between 4.4-6.0 % despite increasing the total volume of the test medium by 10 fold (30-300 μl) (Fig 2.6). Thus, varying the volume had very little effect on the enzyme activity.

Conclusion

Since human plasma has a fairly constant LCAT concentration of 6 μg/ml, we can assume that 7.5 μl of plasma would have an equivalent of 45 ng LCAT. By equating LCAT activity to its mass, it was possible to calculate the mass of LCAT in various medium by comparing the % CE with a reference pool of human plasma, using 7.5 μl of plasma/242.5 μl substrate. Therefore LCAT mass in a test sample is calculated as follows:

$$\frac{\%\ \mathbf{CE}_{\text{(test sample)}} \quad \mathbf{X} \quad \mathbf{45\ ng}}{\mathbf{\%\ CE}_{\text{(human plasma)}}}$$

Alternatively, the concentration of LCAT in test sample is calculated as shown below:

$$\frac{\%\ \mathbf{CE}_{\text{(test sample)}} \quad \mathbf{X} \quad \mathbf{(6\ \mu g/ml\ or\ 6\ ng/\mu l)}}{\mathbf{\%\ CE}_{\text{(human plasma)}}}$$

However, as my data suggest that plasma itself suppresses LCAT (Fig 2.5), all future assays of CD-CHO medium also contained 7.5 μl of heat inactivated plasma to ensure a more accurate estimate of LCAT mass. An additional point to mention is that for LCAT assay on *in vivo* experiments, the volume of plasma and substrate used was reduced by

50 % (i.e. 3.75 μl of plasma/121.25 μl substrate) as the volume of plasma obtained was limited.

When using plasma, the value of %CE should not exceed 6 % as it becomes inaccurate beyond this value (Fig 2.3). Finally, allowing for small experimental variation, LCAT activity was found to be independent of the volume of CD-CHO used as shown in Fig 2.6.

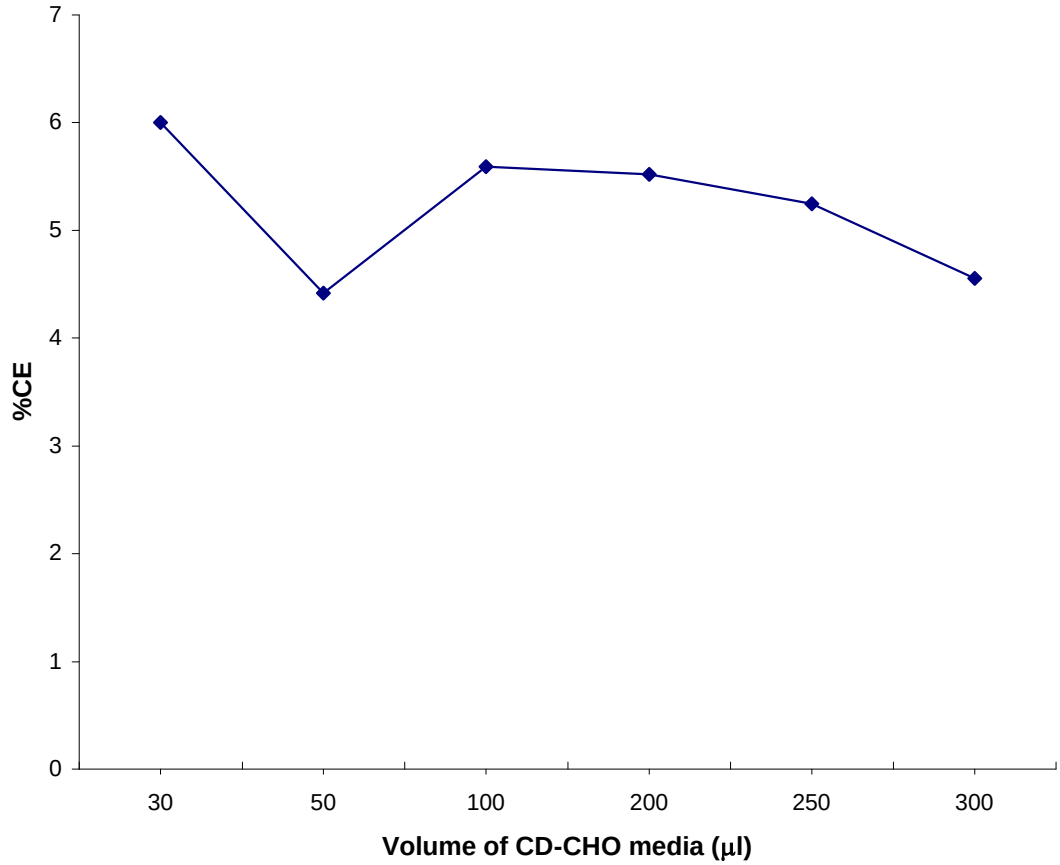

Figure 2.6 Cholesterol esterification with constant amount of LCAT in varying volumes of CD-CHO media

Using a fixed amount of LCAT (7.5 µl of concentrated CD-CHO LCAT medium, substrate and heat inactivated plasma, the esterification of cholesterol was determined in increasing volumes of CD-CHO medium. The %CE was fairly constant between 4.5-5.5%.

2.4.1 Evaluation of hexane for lipid extraction

Lipids are usually defined as those substances that are soluble in hydrophobic organic solvents (such as hexane, chloroform or ether), but are insoluble in water. The ideal solvent for lipid extraction would completely extract all lipid components, while leaving all the other components behind. In practice, the efficiency of solvent extraction depends on the polarity of the lipids present compared to the polarity of the solvent. Non-polar lipids (e.g. tri-acylglycerols) are more soluble in non-polar solvents (e.g. hexane) than in polar ones. But polar lipids (e.g. glycolipids) are more soluble in polar solvents (e.g. alcohols) than in non-polar solvents. For lipids with intermediate polarity, chloroform can serve as a good solvent. Solvents should also be inexpensive, non-toxic and be nonflammable and also of low boiling point (i.e. it can be easily removed by evaporation). No single solvent can meet all these requirements. The use of hexane here was to ascertain whether it was as efficient at extracting lipids from the LCAT assay as chloroform. As it separates above the methanol layer, it facilitates the transfer of dissolved lipids for drying.

Hexane method for extracting cholesterol

The substrate was distributed into 2 tubes, one containing 250 μl and the other 400 μl. After adding 1 ml of ethanol to each of these tubes, they were vortexed for 2 min. Then 1 ml of hexane was added to each tube and vortexed again for 2 min. The mixture was allowed to stand for 5 min to separate. From each tube, 0.5 ml of the top layer was removed and transferred to a scintillating vial each containing 10 ml of cocktail T scintillation fluid. The radioactivity in each vial was counted. Similarly, 250 μl and 400 μl of substrate were added directly to individual scintillating vial to obtain a total radioactivity count.

Most of the ^{3}H-labelled cholesterol should have dissolved in the 1 ml hexane. When 0.5 ml of the hexane (top layer) was removed from the tubes, the corrected cholesterol extracted was 77% from 250 μl of substrate and 84% from 400 μl of substrate. Although there was no significant difference in recovery rates when the volume of substrate was between 250 μl and 400 μl, it was significantly short of the expected value of 100%. Hence, it makes hexane a less attractive solvent for free cholesterol even though it was on the top layer, easily separated from ethanol.

Extraction of Cholesteryl Esters

Human plasma was added to radioactive substrate and incubated in a 37 ^{0}C water bath for 1 h. The mixture was then divided into 9 tubes of equal volume. In the first 3 tubes, the lipid was extracted and assayed using the conventional chloroform-methanol method. In 3 other tubes, the lipid was extracted using the hexane method, re-dried with 200μl of hexane and transferred to the TLC plate with 30 μl of hexane. In the remaining 3 tubes, the lipids were extracted with hexane method but were re-dried with 200 μl of chloroform and methanol and were transferred with 30 μl of chloroform to the TLC plate. The rest of the assay was the same as the method described before.

The calculated % CE averages were 7.21 ± 0.04, 8.88 ± 0.69 and 7.35 ± 0.61 for the conventional method, hexane method and hexane method of lipid extraction with conventional drying, respectively. Hexane method of extraction gave the highest % CE and one explanation may be because some free cholesterol was left behind in the aqueous ethanol, thus giving a false high value. However, the results were not statistically significant and therefore the conventional method continued to be used as the principle method for extraction of lipid in all the LCAT assays.

2.5 Lipid and Lipoprotein analysis

2.5.1 Total cholesterol assay

Principle of assay

Serum cholesterol levels can reflect the state of the hepatic function, biliary function, thyroid function, intestinal absorption, risk of coronary artery disease and adrenal disease. Cholesterol levels help in the diagnosis and classification of hyperlipoproteinaemias.

The method to assay cholesterol is based on a reaction described by Allain *et al*., 1974 which has been modified to render the reagent stable in solution.

In the assay system, the series of reactions involved are as follows:

1. Cholesteryl esters are enzymatically hydrolyzed by cholesterol esterase (CE) to cholesterol and free fatty acids.

   Cholesteryl esters $\xrightarrow{\text{CE}}$ Cholesterol + Fatty acids

2. Free cholesterol including that originally present, is then oxidized by cholesterol oxidase (CO) to cholest-4-en-3-one and hydrogen peroxide.

3. The hydrogen peroxide combines with hydroxybenzoic acid (HBA) and 4-aminoantipyrine (4AAP) in the presence of peroxidase (POD) to form a chromophore (quinonemine dye) which is quantified at an absorbance of 500-550nm. The intensity of the colour produced is directly proportional to the total cholesterol concentration in the sample.

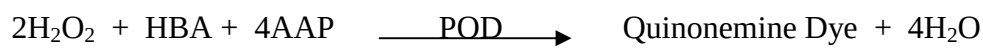

Materials

The commercial Sigma cholesterol reagent contains the following active ingredients:

Cholesterol Oxidase (CO)	> 100 U/L
Cholesterol Esterase	> 1250 U/L
Peroxidase (POD)	> 800 U/L
4-Aminoantipyrine	0.25 mmol/L
Hydroxybenzoic acid (HBA)	10 mmol

A cholesterol standard (Precinorm, 177 mg/dl), was also purchased from Sigma Diagnostics.

Method

This was based on the method described in Sigma Diagnostics procedure 401, but with some modifications. The standards were prepared as shown in Table 2.4. and were measured in duplicate by adding 10 µl to each well of a 96-well plate. Blanks were prepared by adding 10 µl of PBS to each well. The same volume of test plasma was added to each well. Finally, a multi-channel pipette was used to deliver 200 µl of cholesterol reagent to each well. The multi-well plate was then incubated at 37^0C for 10 min following which, there was a gradation of colour changes in the standard. A concentration versus absorbance calibration curve was plotted and the concentrations of the test samples were then determined from their absorbance within the linear region of the plot. The wells were read in a plate reader measuring absorbance at 490 nm; blanks were subtracted before plotting values.

Table 2.4 Preparation of the cholesterol standard curve

No.	Precinorm (μl)	PBS (μl)	Concentration of Standards (mg/dl)
1	75	25	132.75
2	50	50	88.5
3	40	60	70.8
4	30	70	53.1
5	25	75	44.25
6	20	80	35.4
7	10	90	17.7
8	5	95	8.85
9	5	195	4.425
10	50μl of No. 9 Std	50	2.213
11	25μl of No. 9 Std	75	1.106

A range of cholesterol concentrations from 1.1 to 132.7 mg/dl were being prepared by adding PBS to Precinorm, a commercial calibrated serum.

2.5.2 Free cholesterol assay

Principle

As before, cholesterol is oxidized by cholesterol oxidase to cholestenone.

Cholesterol + O2 $\xrightarrow{\text{Cholesterol oxidase}}$ Cholest-4en-3-one + H_2O_2

The hydrogen peroxide combines with 4-aminophenazone and phenol in the presence of peroxidase (POD) to form 4-(p-benzoquinone-monoimino) phenazone and water.

2 H_2O_2 + 4-Aminophenazone + Phenol $\xrightarrow{\text{POD}}$ 4-(p-benzoquinone-monoimino) phenazone + $4H_2O$

Materials

The reagents required were (A) phenol (20 mmol/L), (B) 4-Aminophenazone (2 mmol/L), (C) cholesterol oxidase (≥ 12U/ml) and peroxidase ≥ 8 U/ml and were purchased from Roche.

Method

A working reagent was prepared by mixing 10 ml of solution (A), 10ml of solution (B) and 100 µl solution (C) and stored in the dark. Standards and test samples (both 10 µl) were added in duplicate to wells of a 96-well plate. The blank was 10 µl of PBS. A multi-channel pipette was used to add 200 µl of the assay reagent to each well and the plate was incubated for 10 min. Absorbance were read in a spectrophotometer at 490 nm and, as for total cholesterol, the concentrations of test samples were calculated from the calibration curve.

2.5.3 Cholesteryl esters

Cholesteryl ester concentrations were derived by subtracting the free cholesterol values from those of the total cholesterol measurements. The percentage of total cholesterol as cholesteryl esters was then calculated.

2.5.4 Agarose gel electrophoresis

Plasma lipoprotein profiles of the injected mice were most conveniently analysed by electrophoresis on alkaline buffered (pH 8.8) agarose gels. The following

protocol was recommended by the manufacturer (Sebia, UK) and describes a typical gel analysis.

- Deionized water (177.5 ml) was added to 22.5 ml of 13.3 x stock tris-barbital buffer (2.45% barbital, 13.73% sodium barbital and 0.13% sodium azide) to make to 300 ml.
- The K20 electrophoresis chamber was prepared by loading 150 ml of 1 x tris-barbital buffer into each chamber.
- Agarose gels purchased were ready to use from the manufacturer. The 10-slit sample application template was placed on the gel, aligning the two outside slits with the arrows on the gel backing. Undiluted mouse plasma (2 μl) was transferred into each slit; human plasma was used as a marker. The samples were allowed to diffuse completely into the gel for 10 min and then template was taken off.
- The gel was placed facing down with the samples on the cathodic side and immersed about 1 cm into the buffer on each side. The gel was run at 50 V and 23 mA for 90 min. After electrophoresis, the gel was dried in the oven for about 90 min. The separated lipoproteins were stained with a lipid-specific Sudan black stain. The excess stain was removed with an alcoholic solution. The resulting gel can be evaluated visually for lipoprotein abnormalities or by densitometry to quantify relatively the individual bands.

On agarose gels, lipoproteins separate into the following fractions in order of increasing mobility:

1) Chylomicrons: these are large particles with high triglyceride content. They remain at the application point but are normally absent from plasma if the animals are fasted.
2) Low-density lipoproteins normally migrate to beta-2-globulin positions.
3) Very-low-density lipoproteins have a higher molecular weight and a density lower than LDL. As they are more mobile due to their charge, they migrate to the beta-1-globulin position (usually termed pre-beta).
4) High-density lipoproteins are the fastest fraction and they migrate in the alpha-2-globulin position.

2.5.5 Protein measurement

All protein quantification in this thesis was performed using the ‘Bio-Rad Protein Assay Kit’ (Bio-Rad, Hemel Hempstead, UK).

The Bio-Rad (Bradford) Protein Assay

This assay is based on Bradford's observation that there is a shift from 465 nm to 595 nm of the acidic solution of Coomassie Brilliant Blue G-250 as a result of its binding to proteins (Bradford, 1976). Bradford first demonstrated the usefulness of this principle (Bradford, 1976), whilst Spector demonstrated that the extinction coefficient of a dye-albumin complex solution was constant over a 10-fold range (Spector, 1978). This protein-dye binding method gives a rapid and relatively accurate but not entirely linear response over a broad range of protein concentrations.

A standard curve ranged from 0-20 μg protein/50 μl was used for every assay. This was performed by triplicate dilutions of an appropriate protein standard [usually bovine serum albumin (Sigma)] in distilled water to a final volume of 50 μl. Triplicates of the unknown samples were also diluted in 50 μl of distilled water. The standards and the unknown samples were added to appropriate wells of a 96-well plate. To each well, 250 μl of freshly diluted Bio-Rad dye reagent (final concentration 20%, v/v) was added. After 10 min incubation at room temperature, the OD_{595} versus reagent blank was measured using a Dynex plate-reader (Jencons-PLS, East Sussex, UK). The concentration of the standards versus their OD_{595} was plotted, and the test sample concentrations were determined from the standard curve.

2.5.6 SDS-Polyacrylamide gel electrophoresis (SDS-PAGE)

SDS-PAGE is one of the most commonly used methods for fractionation and characterization of proteins. It dissociates all the proteins within a complex mixture into their individual polypeptide subunits due to the presence of the ionic detergent sodium dodecyl sulphate (SDS) which was purchased from National Diagnostics (Leicestershire, UK). The presence of excess SDS in the buffer and the use of a reducing agent such as β-mercaptoethanol, denatures the proteins and facilitates their binding to SDS once the samples are heated to 100 ^{o}C. As a consequence, each polypeptide-SDS complex will have a constant negative charge per mass unit and moves towards the anode during electrophoresis. In addition, the mobilities of the complexes are inversely proportional to their molecular weights due to the molecular-sieving properties of the gels. Proteins with known molecular weights can therefore be used to determine the molecular weight of sample proteins.

In this thesis, SDS-PAGE was used to determine the size of a protein and estimate the purity of a protein in a solution (section 4.4-4.5, 4.7-4.9). Pre-cast Tris-glycine gradient gels of 4-20% (Novex gels) were purchased from Invitrogen (Paisley, UK) and prepared for electrophoresis following the instructions in the manual.

Electrophoresis

For all SDS-polyacrylamide gels, samples were prepared as follows: samples were mixed (3:1 ratio) with 4 X SDS-PAGE sample buffer [200 mM Tris.HCl (pH 6.8), 8% (w/v) SDS, 0.2% (w/v) bromophenol blue, and 20% (v/v) glycerol]. For reduced samples, β-mercaptoethanol was added to a final concentration of 2% (v/v). Reduced samples were heated in a boiling water bath for 5 min. In addition, a broad range molecular weight marker (6-175 kDa; New England Biolabs, Hertfordshire, UK) was also heated for 3 min. The samples (maximum volume of 30 μl) and the marker (15 μl) were loaded on to the gel, after which the electrophoresis chamber was filled with 1 X running buffer (Novex). When the dye front had migrated to the bottom of the gel, the gel was removed from its cassette and stained with either Coomassie blue or Silver stain or alternatively for Western blotting (section 2.5.7).

Coomassie Staining of SDS-Polyacrylamide gels

Coomassie blue staining has a sensitivity of 0.1-0.5 μg protein and is a technique that is commonly used to visualize protein bands on gels. The reagent reacts with any protein regardless of its biological activity. After polypeptide separation by SDS-PAGE, the gel was incubated on a shaker for 30 min at room temperature with 50 ml of Coomassie stain: 0.25% (w/v) Coomassie brilliant blue R-250 (Sigma), 50% (v/v) methanol, and 10% (v/v) glacial acetic acid. The gel was then destained using successive volumes of destaining solution: 30% (v/v) methanol and 10% (v/v) glacial acetic acid. The thoroughly destained gel was then washed in distilled water and either dried in a GelAir Drying Frame (Bio-Rad) for archiving purposes or used for Western blotting (section 2.5.7).

Silver Staining

Silver staining was performed on gels immediately after SDS-PAGE i.e. not previously stained with other stains. The gels were fixed by adding a solution of 30% (v/v) ethanol and 10% (v/v) glacial acetic acid for 3 x 10 min. The gel was then rinsed with deionized water for 3 x 5 min, equilibrated in silver staining solution [0.2% silver

nitrate (w/v) in 1 mM formaldehyde], rinsed with distilled water and developed using a Silver Stain Kit (Sigma) according to the manufacturer's protocol. Once the background began to darken, the reaction was stopped by adding 1% (v/v) acetic acid solution for 5 min.

2.5.7 Western blotting

Antigens present within a complex mixture of proteins are normally detected by specific antibodies. In Western blotting, electrophoretically separated proteins are transferred from a gel to a solid matrix support. This is then probed with antibodies that are specific to a particular antigenic epitope displayed by the target protein allowing the identification of specific proteins. Western blotting is summarized in Figure 2.7.

Electrotransfer for Western Blots

Proteins that were subjected to 4-20% Tris-Glycine electrophoresis were electrotransferred to a nitrocellulose membrane with the Blot module of the X-Cell II Novex electrophoresis system (25 V constant for 60 min) according to the manufacturer's protocol.

To prepare for transfer, four sheets of of 3MM absorbent paper (Whatman International Ltd., Maidstone, UK) and one sheet of nitrocellulose membrane (Amersham Biosciences) were cut to the dimensions of the gel. These were pre-soaked for 5 min in transfer buffer (Novex). The electrode plates of the cell were washed with distilled water and the transfer 'sandwich' made up on the bottom plate as follows:

- Bottom electrode
- 2 sheets of Whatman paper, pre-soaked in transfer buffer
- 1 sheet of nitrocellulose soaked in transfer buffer
- polyacrylamide gel slightly wetted in transfer buffer
- 2 sheets of Whatman paper, pre-soaked in transfer buffer

After transfer, the 'sandwich' was removed and the bottom left corner of the nitrocellulose was cut to help lane identification after immunoblotting.

Immunoblotting

Following transfer, the membrane was blocked for 45 min at room temperature or overnight at 4 °C in blocking buffer [5% (w/v) non-fat Marvel dry milk, 0.1% (v/v) Tween-20 (Sigma), 0.2% (w/v) 2-chloracetamide in PBS (Sigma)] and then

immunoblotted for the histidine residues of LCAT. Briefly, primary anti-His antibody (Clone HIS-1; Sigma) was diluted 1/1000 in PBST wash buffer [0.1% (v/v) Tween-20, 0.2% (w/v) 2-chloracetamide in PBS] and incubated with the blot for 1 h at room temperature. The blot was then washed 6 x 5 min in PBST wash buffer and incubated for 1 h with 1/10,000 dilution a secondary antibody (Sheep anti-mouse Fab–HRP; Jackson Immuno Research). After washing as before, the membrane was transferred to a dark room, developed by immersion in ECL reagent (Amersham Biosciences), wrapped in clingfilm, placed in a film cassette and exposed to autoradiographic film. Hyperfilm ECL X-ray films (Amersham Biosciences) were exposed to the membrane from 5 sec to 30 min, depending on the intensity of the signal. Exposed films were developed in an automatic X-ray film processor (Compact X4, Xograph Imaging Systems).

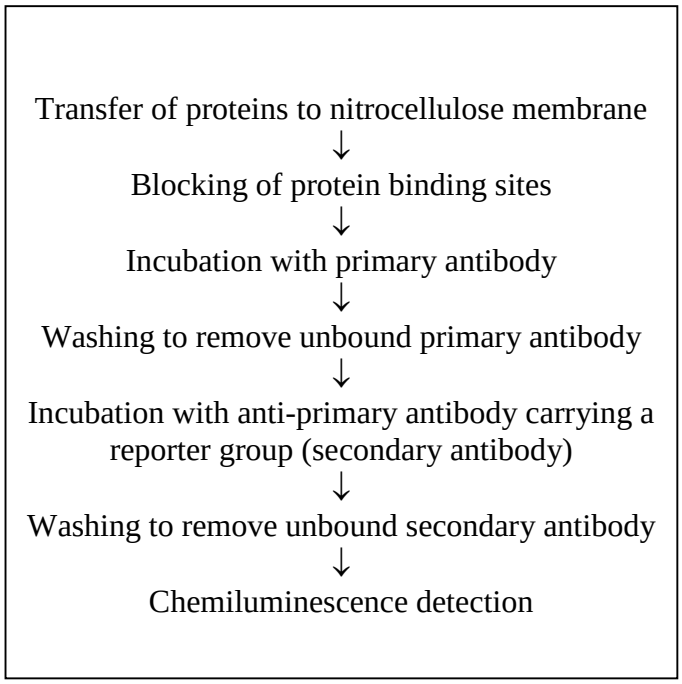

Figure 2.7 Steps required for immunoblotting technique

CHAPTER 3

PRODUCTION AND CLONING OF RECOMBINANT CELLS SECRETING LCAT

3. PRODUCTION AND CLONING OF RECOMBINANT CELLS SECRETING LCAT

3.1 Introduction

In modern biotechnology, pure, soluble and functional proteins are of high demand. Natural protein sources can rarely meet the requirements for quantity and ease of isolation. The ability of scientists to grow eukaryotic cells *in vitro* and to produce recombinant cells and the concomitant production of proteins has led to a huge increase in demand for recombinant cell factories. The proliferation of animal cells in culture has many applications, including their use as model systems for biochemical, physiological and pharmacological studies and for the production of growth factors, blood factors, monoclonal antibodies, interferon, enzymes, vaccines and hormones.

The expression of eukaryotic genes when transfected into animal cells is regulated by factors such as the number of gene copies, transcriptional control and mRNA stability. In this chapter I describe how the LCAT-secreting recombinant Chinese hamster ovary (CHO) cells were produced and grown. The mutant CHO cell line, deficient in dihydrofolate reductase (CHO-*dhfr* $^{-}$) was purchased from the European Collection of Animal Cell Cultures (ECACC). These cells which exhibit epithelial morphology, lack the *dhfr* gene and so are defective in endogenous purine and pyrimidine base synthesis; as such they have an absolute requirement for hypoxanthine and thymidine in order for purine and pyrimidine synthesis to occur by salvage pathways.

Cells were transfected with a mammalian expression plasmid containing full-length LCAT cDNA and mouse *dhfr* gene as a selectable marker. The *dhfr* gene encodes for the enzyme dihydrofolate reductase (DHFR) which is inhibited by methotrexate (Mtx). Non-transfected CHO-*dhfr* $^{-}$ cells when grown in normal selection medium lacking in hypoxanthine and thymidine would all die. However, when transfected cells are cultivated in normal selection medium which contains Mtx, the majority die, but a few cells survive because they have stably integrated the *dhfr* gene (and LCAT cDNA).

Moreover, by increasing the Mtx concentration in the medium it is potentially possible to amplify the number of *dhfr* gene copies. The number of copies of the gene of interest (LCAT) should also correspondingly increase with the marker gene. Indeed, co-amplification of two transgenes has been demonstrated (Schimke *et al*., 1978), with an

increase in concentration of Mtx, leading to more productive cell lines. However, the disadvantage of the method is the time consuming procedure of Mtx amplification, which must be done in a step-wise manner while passaging the cells.

3.2 Vector system

Different recombinant cell systems have been described previously for the production of LCAT. These include stably-transfected CHO (Miller *et al*., 1996; Jin *et al*., 1997) and baby hamster kidney (BHK) cells (Hill *et al*., 1993). The secreted LCAT displays very similar physical characteristics, (e.g. molecular weight, MW), and biologic/enzymic (i.e. specific activity) characteristics when compared to plasma LCAT. However, they are heterogeneously glycosylated in both carbohydrate sequence and structure. It has been suggested that the oligosaccharides on the protein contribute to structure and conformational stability of the protein in an aqueous environment (Yang *et al.*, 1987). LCAT has also been expressed in insect cells using the baculovirus system (Chawla and Owen, 1995) and although enzymatically active, contains much less carbohydrate than LCAT from mammalian sources. Despite relatively high productions of LCAT by these methods, isolation of the enzyme has still proved difficult and results in low yield. An alternate and theoretically more reliable method is to add an epitope tag to recombinant LCAT as an aid to purification. Our laboratory has reported that LCAT tagged with six histidine residues at the carboxyl terminus is catalytically active and immunodetectable using an anti-His_4 antibody (Vinogradov *et al*., 1998).

In our laboratory, we used a cDNA clone encoding LCAT within pUCLCAT.10 plasmid (a gift from Dr J. McLean; Genetech Inc., USA). A His_6 tag was added to the 3' end of the LCAT cDNA. The resulting fragment was digested with *Bam*HI-*Hind*III and substituted for interleukin-2 cDNA in the expression vector p7055 (generously provided by Dr B. Miloux, Sanofi Recherché, France) which was designed to express *dhfr* along with the gene of interest (LCAT). This expression construct was designated as pxLCAT. The expression system uses the SV-40 promoter reinforced by the hepatitis B virus X transactivator, while the selectable *dhfr* gene is weakened by insertion of an A+T-rich sequence derived from the 3'-untranslated region of GM-CSF mRNA. This enables us to select highly producing clones by a simple one-step procedure. Although in most cases Mtx should not be necessary, it does however increase LCAT production and may aid selection of LCAT producing clones. Dr D. Vinogradov in our laboratory

demonstrated that LCAT production increased substantially when the cells were grown in the presence of Mtx (unpublished data).

3.2.1 Transfection of CHO cells with βgal cDNA

In order to optimise transfection efficiency, I used β-galactosidase (β-gal) as a reporter gene. This is one of a series of enzymes involved in the breakdown of lactose to glucose plus galactose. It is coded by the β-gal gene which is present in the pCMVβgal plasmid. Screening for the presence and absence of β-gal involves a lactose analogue called X-gal (5-bromo-4-chloro-3-indolyl-β-D-galactopyranoside) which is hydrolysed by β-galactosidase to a product that is coloured deep blue. If X-gal (plus an inducer of the enzyme such as isopropyl-thiogalactoside, IPTG) is added, then those cells that have been transfected and hence synthesize β-gal will be coloured blue whereas non transfected cells (unable to make β-gal) will be white.

Materials

pCMVβ-gal and serum-free medium (Iscove's containing no serum, no protein supplements and no antibiotics) were purchased from Life Technologies/Gibco BRL (Invitrogen), Paisley, UK, as was growth medium (see 2.1.1). Transfectam reagent was purchased from Promega Ltd., Southampton, UK and Superfect from Qiagen Ltd., Crawley, UK. CHO-*dhfr*$^-$ *cells* were purchased from the ECACC (Salisbury, UK).

Method

CHO-*dhfr*- cells were plated onto two 12 - well plates (8 wells were plated per plate only) and incubated at 37 ^{0}C and 5% CO_2 so that the cells were 50 – 80 % confluent on the day of transfection. Two millilitres of growth medium was added to each well with an equivalent growth area of 3.83 cm^2. The cells were transfected with Transfectam or Superfect using increasing concentrations of pCMVβ-gal gene in order to determine the efficiency of the reagents. After 48 h of incubation, they were stained using an X-gal staining assay kit (catalog no. 3145000) purchased from ICN Biomedical, Bassingstoke, UK.

3.2.2 Transfection of cells using Transfectam

Transfectam is a synthetic, cationic lipopolyamine molecule called diotadecylamidoglycyl spermine (DOGS). The strongly positively charged spermine group has a high affinity for DNA and coating the DNA with a cationic lipid layer facilitates binding to the cell membrane and entry into cell.

Following the instructions from Promega, 200 μl of ethanol was added to 0.5 mg Transfectam. The mixture was vortexed and left at room temperature for 5 min and stored at 4 ^{0}C. On the day of transfection, 2 sets of solutions were set up in sterile tubes as follows:

Solution A in 3 sterile tubes:

I 2 μg (2 μl) pCMVβ-gal was added to 178 μl of serum-free medium

II 4 μg (4 μl) pCMVβ-gal was added to 176 μl of serum-free medium

III 6 μg (6 μl) pCMVβ-gal was added to174 μl of serum-free medium

Solution B in 3 sterile tubes:

I 6 μl Transfectam was added to 174 μl serum-free medium

II 12 μl Transfectam was added to 168 μl serum-free medium

III 18 μl Transfectam was added to 162 μl serum-free medium

The two solutions were immediately vortexed (AI+BI, AII+BII, AIII+BIII). The medium from one plate was removed and the cells were washed gently with 2 ml of serum-free medium per well. Then 100 μl serum-free medium was added to each well. Half of the resultant mixture from I, II and III were added to duplicate wells respectively. Thus, three different concentrations of pCMVβ-gal (1 μg, 2 μg and 3μg) were evaluated in duplicates. As a negative control, two wells were left untransfected. After 6 h of incubation, the cells were washed with 1 ml of serum-free medium before 2 ml of growth medium were added to each well.

3.2.3 Transfection of cells using Superfect reagent

Following the protocol for stable transfection of adherent cells in Qiagen's manual, three sterile tubes of solutions were prepared as below:

I 3 μg (3 μl) pCMVβ-gal was added to 147 μl serum-free medium

II 6 μg (6 μl) pCMVβ-gal was added to 144 μl serum-free medium

III 9 μg (9 μl) pCMVβ-gal was added to 141 μl serum-free medium

The solutions were each added to 15 μl of the Superfect reagent, mixed by vortexing and incubated for 5 - 10 min. In the meantime, 800 μl of growth medium was added to the transfection reagent mix. After removing the medium from the cells, half of the reagent mixes (I, II, III) were added to each well (1.5 μg, 3 μg, and 4.5 μg respectively) and incubated for 5 h. The cells were then washed with 1 ml of serum-free medium before adding 2 ml of growth medium.

3.2.4 X-Gal Staining

After incubating the cells for 48 h, the growth medium was removed from the wells and washed with PBS. The cells were fixed with the formaldehyde solution provided in the kit for 15 min and, after this was removed, 500 μl of X-gal staining solution was added to each well. After 12 h incubation, cells were washed with PBS and examined by microscopy.

3.2.5 Results

Cells that had taken up the transfected plasmid pCMVβ-gal containing the gene coding for β-galactosidase would stain blue in the wells. This was estimated by visualisation under a light microscope (using the x 10 objective lens). Counting stained and unstained cells in a field (> 50 cells) and taking the average of three fields gave the percentage of stained cells in the total population (Table 3.1). The duplicate wells using the Transfectam reagent with three different concentrations of plasmid had 50 % or less staining of its cells. Similarly those duplicate wells using Superfect with 3 and 4.5 μg of plasmid had less than 50 % of cells stained. However in the presence of 1.5 μg of plasmid, the Superfect reagent resulted in approximately 80 % of cells turning blue and was considered the optimum transfection efficiency.

Table 3.1 Efficiency of transfection using Superfect and Transfectam

Transfection Reagent	**pCMVβ-gal Plasmid (μg)**	**Well (1) % Staining**	**Well (2) % Staining**	**Wells (3a,b) Control % Staining**
Transfectam	1	30	20	0
	2	50	40	-
	3	40	30	-
Superfect	**1.5**	**80**	**80**	0
	3.0	30	30	-
	4.5	40	30	-

The transfecion experiment was performed in duplicate (Wells (1) and (2)). Wells (3a,b) containing untransfected cells acted as a control. Three different concentrations of the pCMVβ-gal plasmid for each reagent were used. Superfect with 1.5 μg of pCMVβ-gal plasmid gave the optimum transfection efficiency as 80% of the cells in the wells of a 12 - well plate were stained blue.

3.3 Transfection of CHO cells with LCAT cDNA

3.3.1 Method

In order to scale up the transfection of CHO cells with LCAT cDNA, CHO-*dhfr*- cells were plated into 3 wells (6 - well plates). The 3 wells were transfected identically, and serial collections were obtained from each and the 4th well as a control (Fig. 3.1). After 24 h, they were 80 % confluent. According to Qiagen's protocol for scale up culture formats and my previous optimization experiments with β-gal and Superfect we found that 1.5 μg DNA was optimum for a 12 - well plate (Table 3.1). Therefore for the 6 - well plate, we increased the amount of DNA accordingly to 2.5 μg of pxH6LCAT plasmid (prepared by our laboratory) which was added to 100 μl of growth medium. No plasmids were added to control wells. Ten microlitres of Superfect reagent was then added, mixed and left for 5 - 10 min at room temperature in order for the plasmid and Superfect to complex. This was followed by the addition of 600 μl of growth medium to the Superfect complex and, after mixing, was immediately transferred onto cells which already had their growth medium removed. After 5 h incubation, the cells were washed with warm PBS and 3 ml of fresh selection medium was added to each well. Regular 24 h collections of the medium from cells was commenced and continued for one month. After the 19th day there was rapid proliferation of colonies of cells believed to be stably-transfected cells, whereas the surrounding cells were slowly dying. All the samples collected were centrifuged and stored at –20 ^{0}C until the collection period was completed. A similar transfection was carried out on a T-75 culture flask of cells, using 7.5 μg of pxH6LCAT plasmid.

3.3.2 Results

LCAT assays were performed which showed that the transfection was successful with enzymic activity detectable in 2 wells on the 8th day, which slowly increased to day 11 (Fig. 3.1) where there was LCAT activitydemonstrated in all three transfected wells (well 1, 2, 3). No collection was then made until day 20, when a large rise in LCAT secretion was detected. The peak LCAT production for each well was on day 21, when most of the viable cells were likely to be LCAT-secreting. Moreover, at 28 days when the wells were over-confluent, LCAT continued to be secreted. There was no LCAT activity in the negative control throughout this period of study (Fig. 3.1).

Similarly after 3 weeks, LCAT was detected in the T-75 culture flask, when most stably-transfected cells were selected from untransfected ones. There was 150 ng/ml of LCAT in the first 48 h collection in 15 ml of medium, followed by 144 ng/ml of LCAT in the 2nd 48 h collection. Therefore, these cells were frozen for cloning to improve the yield of LCAT secretion (Table 3.2).

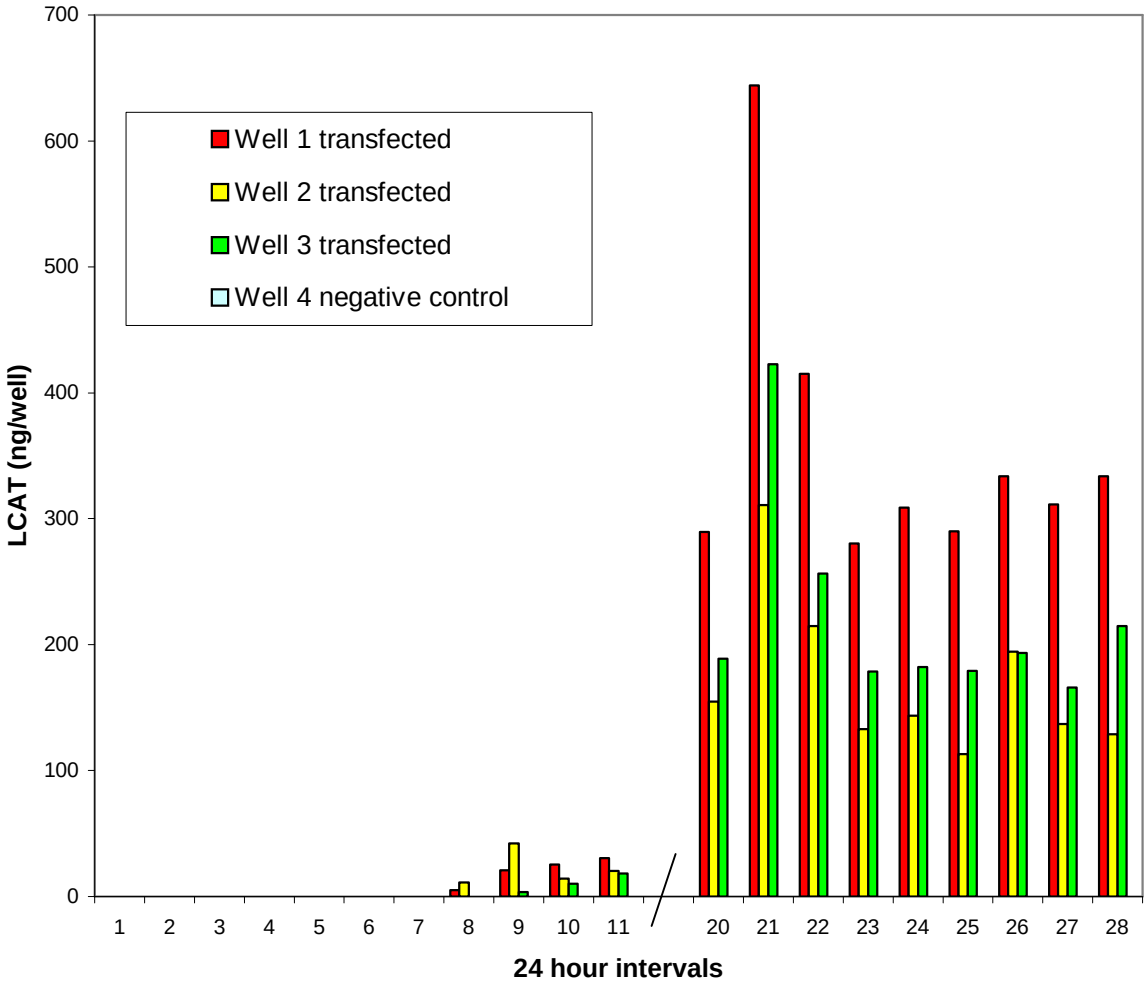

Figure 3.1 LCAT production following transfection in a 6 - well plate

CHO-dhfr- cells were plated onto 4 wells (6-well plate). Three wells of cells were transfected with LCAT cDNA and the 4th well only contained transfectam reagent but no plasmid (negative control).The medium from each well was collected and replaced every 24 h. It was sampled to assay for LCAT. The graph shows the amount of LCAT (ng) secreted in each well at 24 h interval. There was a lag phase of 7 days before LCAT was detected in the medium and this generally increased from day 8 to 11. No further collections were made until day 20 when a significant rise in LCAT secretion was detected, which most likely peaked on day 21, and sustained secretion thereafter. No LCAT activity over background control was detected in medium from 4th well at any time point.

3.4 Cloning of CHO-H6LCAT Cells

One T-75 culture flask containing a monolayer of stably transfected CHO-H6LCAT cells in selection medium was trypsinized and the cells were suspended in medium. The cells were counted and diluted to 10 cells/ml suspension, which was transferred in 100 μl aliquots to each well of a 96 - well plate. Each well then received 100 μl of growth medium containing 10 % FCS. When a colony of cells appeared after several days in the individual wells, they were picked. During this cloning some cells did not proliferate or grew very slowly and therefore these wells were discarded. Thirty six clones were transferred into 12 - well plates but only 12 clones survived. These were further expanded sequentially in 6 - well plates, and then in a T-75 culture flask (Table 3.2). LCAT secretion in clones that became confluent was checked initially in 12-well plates and later in 6 - well plates.

As shown in Table 3.3, apart from clone 1, 5 and 11, the rest of the clones were secreting LCAT. The three highest producers were clone 2, 3 and 12, each yielding more than 350 ng/ml/48h of LCAT. They were expanded in 6-well plate and then transferred into T-75 culture flasks. Clone 3 being the highest producer secreted more than 600 ng/ml/48h of LCAT. These cells were then grown and passaged with stepwise increments of Mtx concentration; commencing at 1 – 2 – 5 – 10 – 25 – 50 – 70 - 100 and finally 150 nM. I found that increasing the concentration of Mtx, showed a substantial increase in LCAT production. Further increase in Mtx concentration beyond 150 nM showed a decline in LCAT production most likely due to Mtx toxicity on the cells (data not shown). The cells that secreted maximally (> 8 μg/ml) at 150 nM of Mtx in cell media were designated as H6LCAT 150 (Table 3.4). This clone was subjected to a further round of subcloning by limiting dilution to ensure it was truly clonal and the estimated highest producer designated H6LCAT 150B.

Table 3.2 Summary of the sequence of events in cloning H6LCAT cells

CHO cells

↓

Transfection with plasmid pxH6LCAT

↓

Transfected CHO cells placed in selection medium
without hypoxanthine and thymidine supplements

↓

Stably-transfected H6LCAT cells selected
(36 clones were picked and grown in 12 – well plates)

↓

12 clones survived and grown in 12 –well and expanded into 6 – well plate

↓

Three highest producer clones picked (2, 3 & 12)
and expanded into T-75 flasks

↓

The highest producer clone 3, was subjected to Mtx amplification

↓

Cells secrete maximally at 150nM Mtx in growth medium

↓

Cells subcloned to ensure truly clonal and the highest producer (H6LCAT 150B) chosen for subsequent study

Table 3.3 Secretion of LCAT by H6LCAT clones during selection

H6LCAT Clones	LCAT Secretion (ng/ml/48h)		
	12-well plate	6-well plate	T-75 flask
1	0	0	
2	**379**	**378**	**595**
3	**511**	**473**	**616**
4	440	245	
5	0	0	
6	7	96	
7	397	334	
8	287	319	
9	158	237	
10	158	220	
11		151	
12	**491**	**432**	**482**

Thirty-six clones of cells from 96 - well plate were transferred into 12 - well plate for expansion. Twelve viable CHO-H6LCAT clones were further isolated and labeled 1 - 12 as shown in the 1st column. They were initially grown in 12 - well and 6 - well plates. The three highest producing clones 2, 3 and 12 secreted > 350 ng/ml/48h and were further expanded into T-75 flasks.

Table 3.4 Amplification of LCAT production by CHO-H6LCAT cells using Mtx

CHO-H6LCAT Clones	Mtx concentration (nM)	LCAT production (μg/ml/48h)
H6-0	0	0.6
H6-70	70	2.7
H6-150	150	8.4
H6-150B	150	8.7

Clone 3 (Table 3.3) was subjected to a stepwise increments of Mtx concentration starting with 1 nM and progressing to 150 nM. The cell media at 70 and 150 nM Mtx were collected after 48 h and assayed for LCAT. A 3 - fold increase in LCAT production from 2.7 to 8.7 μg/ml was noted. The subclone, 150B has a similar LCAT secretion compared to its original clone 150 confirming its true clonal status.

3.5 Production of LCAT in different culture medium

3.5.1 Introduction

Below are described the various cell culture media used for the growth of CHO-H6LCAT cells in my search for a medium for isolating pure LCAT. Ideally, the medium should be able to support growth and metabolism of CHO-H6LCAT cells and promote expression of LCAT in large-scale culture. Low protein content and minimal macromolecules in the medium would facilitate processing and purification of LCAT.

3.5.2 Materials

Iscove's selection medium (hypoxanthine and thymidine free), serum free medium (SFM), protein-free medium (PFM) and CD-CHO medium all prepared as before (section 2.1.2). Mtx (150 nM) was added from 40 mM stock solution for routine use in the various media.

3.5.3 Method

The highest producing clone of CHO-H6LCAT cells, which had undergone several passages, was seeded into 5 culture T-75 flasks. They were allowed to grow to confluence in 5% FCS with Mtx. Each flask was washed with PBS before different medium (15 ml) was added to each flask. The media were 5 % FCS with 150 nM Mtx, 5% FCS without Mtx, SFM, PFM and CD-CHO medium. The medium in each flask was collected 6 times at intervals of 48 h replacing with fresh medium after each collection. A LCAT activity assay (section 2.2.3) was performed on the collected medium taking 20 μl as the sample volume. Finally, LCAT production in each medium was plotted against time.

3.5.4 Results and Discussion

Cells that were grown in FCS with Mtx showed a good amount secreted from 1st (8.2 μg/ml) and peaked at 4th (11 μg/ml) collection (Fig. 3.2 A). It declined in production on 5th and 6th collection (5 μg/ml) but still gave a relatively sustainable level of secretion. Those grown in FCS without Mtx showed a similar secretion pattern ranging from 4.5 – 13.7 μg/ml during the 1st to 4th collection before declining to a

sustained secretion level of 6.4 μg/ml by the 6th collection. Those medium containing less protein nutrients (SFM and PFM) showed a general trend towards a decline in LCAT production throughout the study period (Fig. 3.2 C & D). In SFM, 4.5 μg/ml of LCAT was present in the 1st collection, which peaked on the 2nd collection (9.3 μg/ml) and subsequently declined in production to less than 1 μg/ml. LCAT production in PFM was 5.7 μg/ml in the 1st collection and declined thereafter to 0.1 μg/ml at the 6th collection, the lowest recorded (Figure 3.2 D). However, CD-CHO with the least protein contents gave a gradual increase in LCAT production from 1.4 μg/ml (1st collection) to 5.4 μg/ml (3rd collection) and LCAT production increased significantly at the 4th collection (13.4 μg/ml) (Fig. 3.2 B)) and peaked at 5th collection (14.3 μg/ml) (Fig. 3.2 B). There was a slight fall to 10.6 μg/ml on the 6th collection which is a good amount even at day 12. After this period, considerable cell detachment was observed which was most marked in the PFM and SFM but less in CD-CHO and least in FCS +/- Mtx medium. From the results, CD-CHO has emerged as a good medium to use for bulk collection. Furthermore, the absence of proteins or peptides in CD-CHO could potentially facilitate the purification of LCAT.

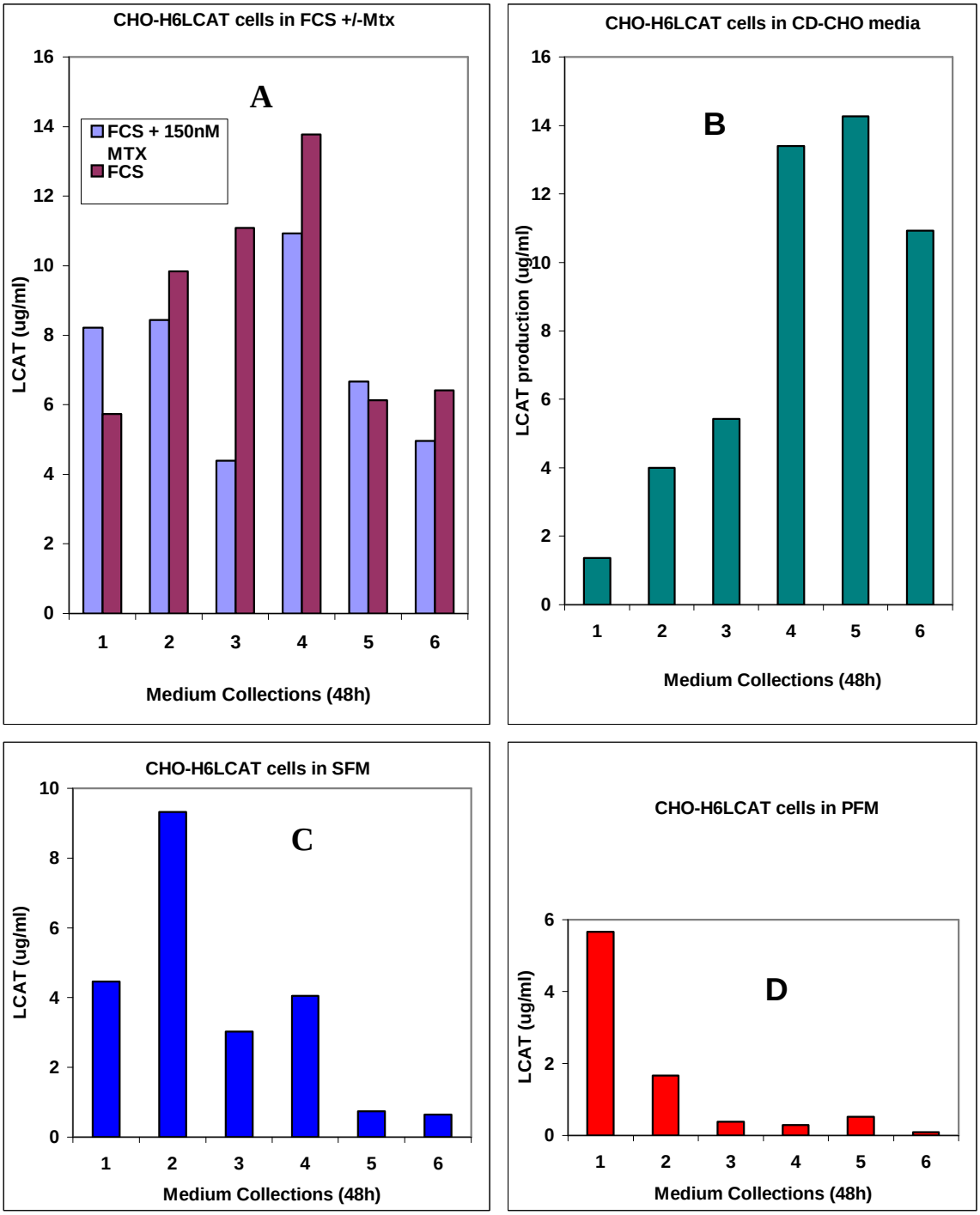

Figure 3.2 LCAT secretion by CHO-H6LCAT cells cultured in different medium

(A) *LCAT production in normal medium;* ***(B)*** *LCAT production in CD-CHO medium,* ***(C):*** *LCAT production in SFM and* ***(D)*** *LCAT production in PFM.*

Cells were grown in T-75 flasks in respective medium and changed every 48 h for LCAT assay. The amount of LCAT (μg/ml) produced in each medium were evaluated over 6 (48 h) collections.

3.6 LCAT secretion by CHO-H6LCAT cells in normal versus CD-CHO medium

3.6.1 Introduction

A good growth medium for CHO-H6LCAT cells should be able to support a sustained LCAT secretion for several collections. At the same time, a large amount of LCAT should be produced within a short interval of time. To further verify the choice of CD-CHO medium, a comparison study between LCAT production in CD-CHO medium and normal growth medium was set up. The latter consists of Iscove's selection medium (hypoxanthine and thymidine free), 5 % FCS and 150 nM Mtx.

3.6.2 Method

The CHO-H6LCAT cells were seeded into a 6-well plate and grown to confluence. Cells were then washed with PBS and three wells received 3 ml of normal medium while the other three received 3 ml of CD-CHO medium. Culture medium was collected every 48 h and completed on the 6^{th} collection. The media were assayed for LCAT as described in 2.2.3. The data were analysed and LCAT production expressed as μg/ml per 48 h collection interval.

3.6.3 Result and Discussion

The mean LCAT concentration in CD-CHO medium from the 1^{st} 48 h collection was 1.6 ± 0.3 μg/ml compared to 2.5 ± 0.2 μg/ml in normal growth medium containing 5% FCS (Fig. 3.3 A, B). LCAT production in CD-CHO medium rose steadily peaking at an average of 4.6 ± 1 μg/ml at the 5^{th} 48 h interval (Fig 3.3 C). During the 6^{th} 48 h interval, 4.5 ± 0.2 μg/ml of LCAT was detectable. However, in normal growth medium, LCAT production peaked at the 3^{rd} 48 h interval, (2.9 ± 0.5 μg/ml) and then steadily declined to 1 ± 0.1 μg/ml at the 6^{th} interval.

Although initially LCAT secretion was less in CD-CHO medium than normal growth medium, LCAT production after the 4^{th} 48 h interval was sustained at 2-3 times the initial concentration. Moreover, the maximum LCAT production in CD-CHO medium exceeded the peak production in normal growth medium.

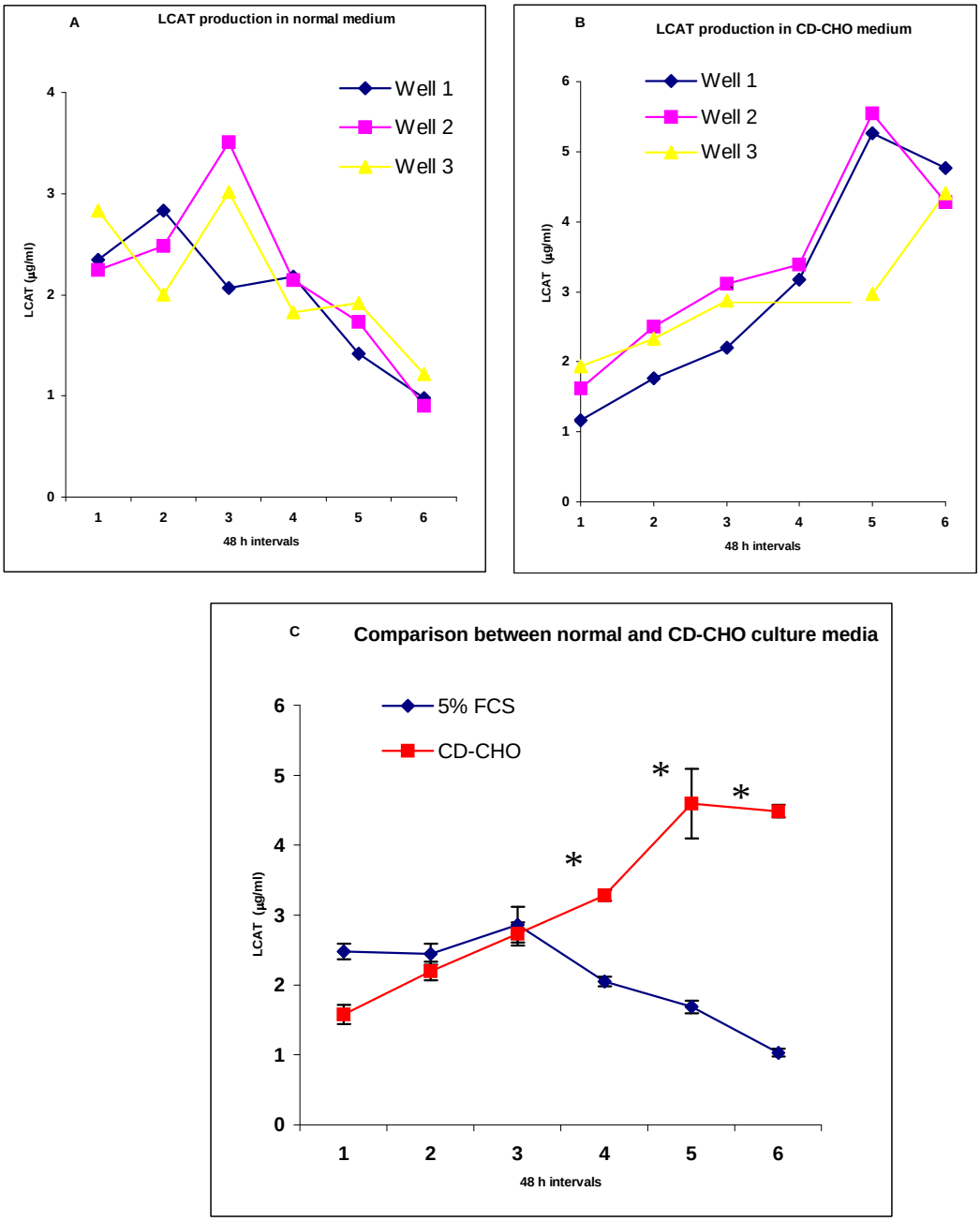

Figure 3.3 LCAT production in normal growth medium and CD-CHO medium

*LCAT production by CHO-H6LCAT cells in 3 different wells grown in (**A**) normal medium or (**B**) CD-CHO medium. The medium was collected and replaced every 48 h over a period of 12 days. LCAT level at each interval was ascertained by assay and the amount secreted expressed as µg/ml. (**C**) Mean values ± s.e. were plotted for both normal and CD-CHO culture conditions. Asterisks denote data points (LCAT production in normal vs CD-CHO medium) at time intervals (4^{th} –6^{th} 48 h interval) that were significantly different using the Student's t-test ($p < 0.05$).*

3.7 Effect of sodium butyrate on LCAT production by CHO-H6LCAT cells grown in CD-CHO media

3.7.1 Introduction

Sodium butyrate produces many reversible morphological and biochemical modifications when added to mammalian cell cultures at low concentrations. Some of them occur in all cell lines. They concern regulatory mechanisms of cell growth, cell morphology and gene expression. Butyrate reduces the growth of many cell types (Wright, 1973; Leibovitch and Kruh, 1979; Dyson *et al*., 1992); it can induce differentiation as observed with erythroleukemia cells and HeLa cells (Henneberry and Fishman, 1976; Friend *et al*., 1987) or it can lead to a growth arrest at the G_1 phase of the cell cycle as in cultured hepatoma cells (VanWijk *et al*., 1981; Gupta *et al*., 1994). In 1977, Riggs *et al*. established that cell treatment with sodium butyrate led to increased histone acetylation. This resulted from inhibition of the enzyme histone deacetylase and was reversed upon the removal of sodium butyrate (Candido *et al*., 1978; Sealy and Chalkley 1978). Reversible histone acetylation is now considered to play an important role in the regulation of chromatin structure and its transcriptional activity. The aim of this study was to evaluate whether sodium butyrate affect LCAT secretion by CHO-H6LCAT cells.

3.7.2 Methods

The CHO-H6LCAT cells were seeded into 6-well plates and grown in normal growth medium until they were confluent. They were washed with PBS and 1 ml of CD-CHO medium with Mtx was added to each well. After 24 h, sodium butyrate was added to make concentrations of 0, 1, 10, 30 and 50 mM in duplicate wells. The medium was collected after 48 h of incubation and replaced with the same medium for the second 48 h collection.

3.7.3 Results and Discussion

Upon addition of 1 mM of sodium butyrate to growth medium, LCAT production was at an average of 1.2 to 1.4 μg/ml and a negligible increase (1.23 μg/ml) was observed with 10 mM of sodium butyrate after 48 h (Fig. 3.4). The LCAT

production was smaller in 30 mM and 50 mM compared with those without sodium butyrate. In the 2nd 48 hour, the production in 1 mM was less and much smaller in 10 and 30 mM compared with control. There was no LCAT production in 50 mM sodium butyrate in the 2nd 48 h. As increasing sodium butyrate concentration led to a decrease in LCAT production, this agent was clearly not necessary for LCAT production by CHO-H6LCAT cells.

These findings are in contrast to the report of Chisholm and Parks (1999), who showed that addition of sodium butyrate (10 mM) to CHO-H6LCAT cells in protein-free complete medium (PFX-CHO) resulted in a 3-fold increase in LCAT production (15 μg/ml at 72 h), compared to PFX-CHO alone. Whilst Chisholm and Parks showed that sodium butyrate positively enhanced LCAT production at the transcriptional level, my study showed a dose-dependent decline in LCAT production from 48-96 h. Conceivably, random integration of LCAT cDNA into the CHO cell genome during transfection, may have caused sodium butyrate to suppress promoter activity in my particular cloned cells reducing LCAT synthesis. In addition, other experimental variation such as the use of different cell line (CHO-*dhfr vs* CHO-K1) and selection agent (*Mtx vs* Geneticin), expression vector or growth medium (CD-CHO *vs.* PFX-CHO) could have contributed to these results.

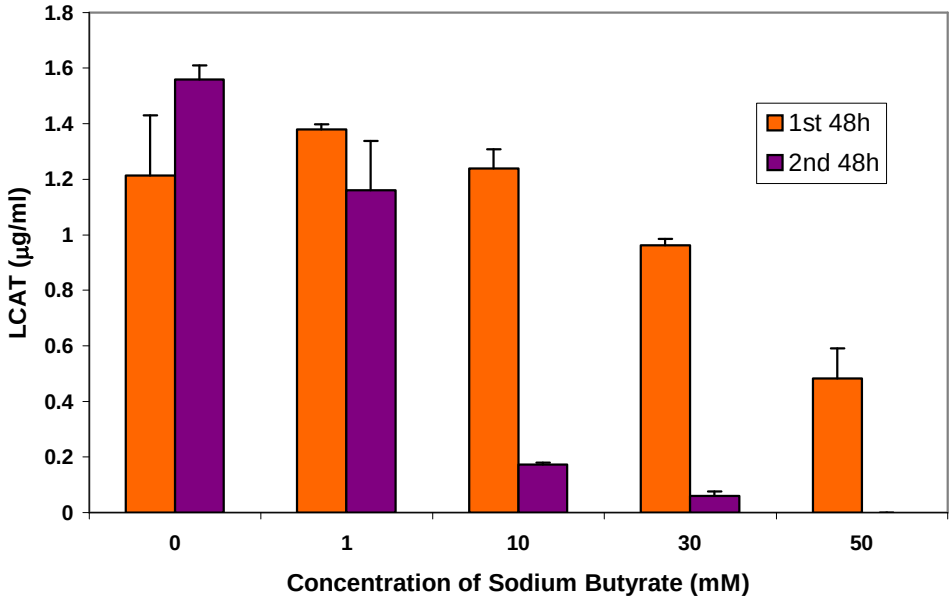

Figure 3.4 Effect of sodium butyrate on LCAT production

Histogram represents mean values of LCAT production ± s.e.(n=2) over a range of sodium butyrate during the 1st 48 h (grey) and 2nd 48 h (black). In the first 48 h, the production of LCAT remained about the same (1.2-1.4 µg/ml) in 0, 1 and 10 mM sodium butyrate. But there was reduced production in 30 and 50 mM sodium butyrate. In the 2nd 48 h, there is a general decline in LCAT production most marked in 10-50 mM concentrations.

CHAPTER 4

LCAT - PURIFICATION

4. LCAT – PURIFICATION

4.1 Immobilized metal affinity chromatography

Affinity chromatography separates proteins on the basis of a reversible interaction between a protein and a specific ligand coupled to a chromatographic matrix. Immobilized metal affinity chromatography (IMAC) was first used in 1975 as a group-specific affinity technique for separating proteins (Porath *et al*., 1975). This principle is based on a reversible interaction between various amino acid side chains and immobilized metal ions. Depending on the type of immobilized metal ions, different side chains can be involved in this reversible adsorption process. Most notably, histidine, cysteine and tryptophan side chains have been implicated in protein binding to immobilized metal ions (Porath, 1992).

Histidines exhibit highly selective coordination with certain transition metals and have great utility in IMAC. Under conditions of physiological pH, histidines bind by sharing electron density of the imidazole nitrogen with the electron-deficient orbitals of transition metals. Although three histidines may bind transition metals under certain conditions, six histidines have been shown to reliably bind transition metals in the presence of strong denaturants such as guanidium (Hochuli *et al*., 1987). These protein tags are commonly referred to as "H6" or "His_6".

Elution occurs when the imidazole nitrogen is protonated, generating a positively charged ammonium ion which is repelled by the positively charged metal ion. By adding imidazole to the elution buffer, the bound polyhistidine-tagged protein can be competitively eluted. The aim of this chapter is to identify a suitable method for LCAT purification by comparing different methods of affinity purification.

4.2 Nickel-nitrilotriacetic acid (Ni-NTA) spin columns

The recombinant CHO cells that I produced secreted LCAT that was tagged with six histidine molecules. This facilitates its binding to metal chelating resins and thus its isolation from the cell culture media. Nickel is one such ion that binds to histidine molecules.

I first evaluated ready-to-use spin columns packaged with nitrilotriacetic acid (NTA) resin, which chelates nickel. Protein purification system is based on the high selectivity of the Ni-NTA resin for recombinant proteins carrying His_6. The high

affinity of the Ni-NTA resins for proteins or peptides tagged with His_6 is due to both the specificity of the interaction between histidine residues and immobilized nickel ions and to the strength with which these ions are held by the NTA resin. The silica material in the resin has been modified to provide a hydrophilic surface and hence a reduction in nonspecific hydrophobic interactions. The spin columns allow rapid purification of a protein from cell medium under native conditions. According to the manufacturer, up to 150 μg of His_6 tagged protein can be purified in 20 min.

4.2.1 Materials and Methods

Ni-NTA spin columns were purchased from Qiagen (West Sussex, UK). The buffers required were freshly prepared on the day of the experiment. They contained 50 mM NaH_2PO_4 (pH 8.0) and 300 mM NaCl plus increasing amounts of imidazole for lysis (10 mM), washing (20 mM) and elution (250 mM).

To assess the recovery of LCAT from three different cell culture media, 48 h collections of LCAT-containing normal growth medium, SFM and PFM were thawed in a 37 ^{0}C water bath. These had previously been centrifuged at 1,500 x g for 15 min at 4^{0}C following collections and the supernatants stored at –20 ^{0}C. In the meantime, the Ni-NTA spin columns was equilibrated with 600 μl lysis buffer, and briefly centrifuged for 2 min at 700 x g.

The pre-equilibrated column was loaded with 600 μl of medium containing His_6-tagged LCAT. It was centrifuged at 700 x g for 2 min and the flow-through was collected. The Ni-NTA spin column was washed twice with 600 μl wash buffer by centrifuging for 2 min at 700 x g. Bound protein was eluted from the column with 200 μl elution buffer by centrifuging for 2 min at 700 x g. The eluate was collected for LCAT assay (section 2.2.3).

4.2.2 Results and Discussion

The three different starting media plus their respective flow-throughs, washes and eluates were assayed for LCAT (Table 4.1). Approximately 19.5 % (normal growth medium), 12.8 % (SFM) and 16.2 % (PFM) active enzyme detected in the flow-throughs, while the corresponding washes contained 15.8 %, 10.7 % and 1.5 % and all were notably very high. The majority of His_6-tagged LCAT (65-82 %) was retained by the column. When the eluate from growth medium was assayed 11.4 % of LCAT was recovered, whereas the recovery from SFM was only 2.4 % and less than 1 % from PFM.

The initial losses in the flow-throughs and washes were disappointing as the total amounts of LCAT loaded onto the columns (<7 μg; Table 4.1) were considerably less than the claimed capacity (150 μg). One explanation is that protein constituents of the medium or those released by CHO-H6LCAT cells interfere with the binding and weaken the Ni-H6LCAT interaction. This would account for incomplete capture and additional loss on washing, although the presence of imidazole at low concentration in both loading (lysis) and wash buffers should help reduce non-specific binding. Another possible factor, which was not examined, is that the LCAT had been partially inactivated or denatured because the buffers used were all at pH 8 rather than pH 7.4 of the culture mediums. This factor might also explain the low recovery of LCAT activity following elution, rather than avid retention by the column, particularly as this buffer contains a much higher concentration of imidazole (250 mM). Although recycling the flow-through and wash solutions and buffer exchange may allow a higher recovery of active LCAT, it was clear that an alternative protocol was required. Therefore, in the next sections of this chapter, I examined the purification process in more detail and also evaluated additional isolation systems.

Table 4.1 Purification of H6LCAT from different culture medium using Ni-NTA spin columns

	Normal Medium		Serum Free Medium		Protein Free Medium	
	LCAT (μg)	**Recovery (%)**	**LCAT (μg)**	**Recovery (%)**	**LCAT (μg)**	**Recovery (%)**
Start	6.70	100	3.28	100	2.60	100
Flow-through	1.30	19.4	0.42	12.8	0.42	16.2
Wash	1.06	15.8	0.35	10.7	0.04	1.5
Eluate	0.76	**11.4**	0.08	**2.4**	0.02	**0.8**

*The LCAT activities in start medium, flow-through, wash and eluate were measured by standard proteoliposome method and converted to μg of H6LCAT (section **2.3.4**). Recoveries are expressed as a percentage of each start medium.*

4.3 Binding capacity of the Ni-NTA spin columns

4.3.1 Materials and Methods

Serum-free medium was collected from CHO-H6LCAT cells after 72 h and concentrated 5-times using a membrane filter (30,000 MWCO) and centrifugation at 2,500 x g for 10 min. The final volume of concentrated medium was 2.5 ml. A Ni-NTA spin column was equilibrated in the usual way and loaded with 600 μl of concentrated medium. The flow-through was collected and the process was repeated three times, each time loading 600 μl of fresh media. Finally, the column was washed and eluted.

4.3.2 Results and Discussion

As shown in Table 4.2, there was more than 60 % loss in the 1st and 2nd flow-throughs, with more than 80 % loss in the 3rd and 4th follow-throughs. This indicated that the column had become near saturated after the 1st loading which contained 13.5 μg of LCAT. In the previous study, when 3.28 μg of LCAT in SFM was loaded, the loss was only 13 % adding further evidence to support saturation of the column (see Table 4.1). The total amount of LCAT loaded was 54 μg and the eluate contained 14.3 μg of LCAT. There was an overall loss (73.6 %) of LCAT some of which in the flow-through, the rest may be still bound to the column, inactivated or denatured during the purification process. In total, 26.4 % of LCAT was recovered. This was an improvement compared with the previous recovery of LCAT from SFM which was only 2.4 % and an accompanying overall loss of 97.6 % of LCAT with a small proportion in the flow-through (12.8 %). This does suggest that the efficiency of capturing and recovering LCAT can be enhanced by increasing the initial load of LCAT on the column at near saturation levels. Another key question is the time allowed for binding may have been insufficient. Under native conditions, it is possible to close the lid on the column and mix on a roller for 30-60 min. In addition, centrifuging the column with a closed lid may reduce the flow rate thereby further extending the binding time. Recycling the flow-through a few more times may also improve the capture of LCAT.

Table 4.2 Assessing the binding capacity of Ni-NTA spin columns for H6LCAT

Ni-NTA Column	LCAT (μg)	Loss (%)	Recovery (%)
Start Medium	13.5 x 4	-	-
Flow-through 1	8.6	63.7	-
Flow-through 2	10.4	77.0	-
Flow-through 3	11.7	87.0	-
Flow-through 4	11.6	85.9	-
Eluate	**14.3**	**-**	**26.4**

Four consecutive batches of LCAT (each 13.5 μg in 600 μl) were loaded onto the Ni-NTA colum and the flow-throughs collected. Finally, the column was washed, eluted and the LCAT in each collection was quantified by LCAT assay (section 2.2.3). The fraction of LCAT in the eluate was expressed as a percentage of the total LCAT loaded onto column capture.

4.4 Hydrophobic interaction chromatography – octyl-Sepharose column

4.4.1 Introduction

Hydrophobic interaction chromatography (HIC) separates proteins and peptides based on the interaction between the hydrophobic groups of the sample and an insoluble immobilized hydrophobic matrix containing short-chain phenyl or octyl non-polar groups. Separation on HIC matrices exploits differences in hydrophobicity between proteins is usually done in aqueous salt solutions which are generally non-denaturing. Samples are loaded onto the matrix in a high-salt buffer and elution is by a descending salt gradient. HIC depends on surface hydrophobic groups and is carried out under conditions which maintain the integrity of the proteins.

It has been noted that a 20-30 % reduction in binding strength occurs when the temperature is reduced from 20 °C to 4 °C. If the experiment is done in a cold room, the strength of the hydrophobic interactions will be lessened. Once the sample has been applied to the column, the hydrophobic protein will bind to the column and unbound protein will be washed away in the void volume. Elution of proteins is accomplished in several ways: (1) reducing the concentration of salting out ions in the buffer with a negative salt gradient; (2) eluting with a positive gradient of detergent; (3) raising the pH; and (4) reducing the temperature. HIC gels can be reused several times depending on the quality of the buffers and sample. After every chromatographic run, a wash with 6 M urea will remove tightly bound proteins.

4.4.2 Materials and Methods

Octyl-Sepharose, CL-4B was purchased from Amersham Biosciences, Buckinghamshire, UK and stored in 24 % ethanol. The chromatographic equipment used was LKB Bromma 2111 Multirac and LKB 2132 and Microperpex peristaltic pump with variable speed control.

The experiment was performed in collaboration with Dr S Schepelmann. An octyl-Sepharose suspension (40 ml) in ethanol was washed with 40 ml of water by centrifuging at 200 g for 1 min and de-gassed under a partial vacuum for 5 min. The column used had a diameter of 1.5 cm and hence a cross-sectional area of 1.77 cm^2. The octyl-Sepharose slurry was transferred into the column using a glass funnel and allowed to settle by gravity. A pump was connected to the column with the flow rate set at 90

(2.2 ml/min or 132 ml/h) and is equivalent to linear flow rate of 74.6 cm^2/h, well within the permitted maximum linear flow rate of 150 cm^2/h for packing.

The column was then washed with 10 ml of 0.5 M sodium hydroxide solution at a flow rate of approximately 2 ml/min and was left for 30 min to equilibrate with the column. Next the column was washed with deionised water followed by equilibration of the column with PBS. Non-concentrated CD-CHO H6LCAT medium (400 ml) from a 48 h collection was loaded onto the column. The pump flow rate was set at 1.175 ml/min and the chart recorder was set at 1 mm/min, 100 mV and the absorbance at 0.2 on the detector. The flow-through (400 ml) was collected and the column was washed with PBS until the indicator returned to a stable baseline. The column was eluted with deionised water, which showed a sharp peak in absorbance as protein eluted, and this was continued until the absorbance indicator returned to stable baseline. The amount of protein and LCAT at each stage of the purification was determined using Bradford (section 2.5.5) and LCAT activity assays (section 2.2.3). Protein purity in the eluate was checked by running an 8 % Tris-Glycine gel (section 2.5.6).

4.4.3 Results and Discussion

A total of 13 mg of protein in the CD-CHO H6LCAT medium was loaded onto the column. There was 8.5 mg (65 %) of protein in the flow-through, nearly undetectable proteins in the wash (20 μg) and 1.6 mg (12.5 %) in the eluate (Table 4.3). In terms of LCAT capture, the actual amount of LCAT loaded on the column was 500 μg and 108 μg (21.6 %) in the flow-through, 4.7 μg (0.9 %) in the wash and 184.8 μg (37 %) in the eluate (Table 4.3).

LCAT only made up 3.8 % of the protein at the start and hence a large proportion of non-specific proteins were loaded onto the column. From Table 4.3, 35 % of protein was presumed bound to the column after the flow-through phase, although in relative terms, more LCAT was bound (78.4 %; Table 4.3). There was virtually no protein detected in the wash, but of the 1.62 mg protein in the eluate, only approximately 0.18 mg (~ 10 %) was LCAT. It is apparent that a significant amount of contaminating proteins were bound and eluted from the column.

Gel electrophoresis analysis revealed a band of the expected size for LCAT (64 kDa; see arrow Fig 4.1). However, additional proteins marked (*) were also present. Although HIC is capable of capturing a significant amount of LCAT from culture

medium, contaminants in the eluate make it unlikely to be suitable for 1-step purification procedure.

Table 4.3 Purification of LCAT by octyl-Sepharose column chromatography

Purification Stage	Total Protein		LCAT	
	mg	**% recovery**	**μg**	**% recovery**
Start medium (400 ml)	13	100	500	100
Flow-through (400 ml)	8.5	65	108	21.6
Wash (10 ml)	0.02	< 0.1	4.7	0.9
Eluate (23.6 ml)	1.6	**12.5**	184.8	**37.0**

The amount of protein (mg) and LCAT (μg) in the start medium, flow-through, wash and eluent were estimated by Bradford and LCAT activity assays, respectively. The percentage recovery of total protein and LCAT was then calculated for each stage of the purification process.

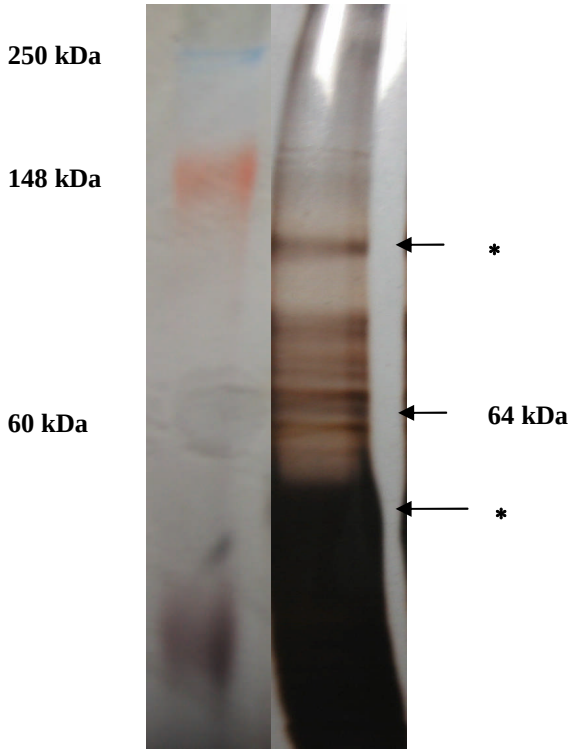

Figure 4.1 Electrophoretic purity of LCAT isolated by octyl-Sepharose column chromatography

The eluate of the column was run on a 8 % Tris-Glycine gel and silver stained. The left lane shows molecular weight markers in kDa, while the right lane is the column's eluate. A prominent band with the expected size for LCAT (64 kDa) was evident although some contaminants with higher and lower molecular weight were also present (*).

4.5 Ni-NTA spin column purification following octyl-Sepharose isolation

4.5.1 Materials and Methods

In order to reduce the impurities present following octyl-Sepharose separation, a further purification step was employed using a Ni-NTA spin column. The eluate from the octyl-Sepharose column was concentrated 10x using a Vivaspin concentrator with MWCO of 10,000 Da and dialysed against 50 mM NaH_2PO_4 buffer, pH 8.0 containing 300 mM NaCl and 10 mM imidazole. Concentrated octyl-Sepharose eluate (400 μl) was then loaded onto the Ni-NTA column to further purify LCAT as described in 4.2. The flow-through was collected and the column was washed with 600 μl of wash buffer. Finally, the column was eluted with 200 μl of elution buffer and the eluate collected. Aliquots were taken at each step of the purification for LCAT (section 2.2.3), Bradford assays (section 2.5.5) and SDS-PAGE (section 2.5.6).

4.5.2 Results and Discussion

Concentrated octyl-Sepharose eluate, which was the start material for the Ni-NTA column, had 360 μg of protein (Table 4.4). There was a loss of 204.4 μg (56.8 %) of protein in the flow-through and the protein recovered in the eluate was 46.6 μg (12.9 %). At each stage of this purification, the concentration of LCAT was also measured (Table 4.4). A total of 117.4 μg LCAT was loaded onto the Ni-NTA column. About 96.8 μg (82.4 %) was lost in the flow-through, while the eluate contained only 6.8 μg of LCAT giving a recovery of 5.8 %. SDS-PAGE showed that there was essentially pure LCAT following this two stage purification procedure (Fig 4.2).

Loss of LCAT in the flow-through was significant (82.4 %) even though the start material was relatively pure LCAT. This might be explained by the high LCAT (117.4 μg of H6LCAT) loaded onto the Ni-NTA as its binding capacity was relatively limited (Table 4.2). Earlier I showed (Table 4.2) that after loading 13.5 μg of LCAT in non-fractionated culture medium onto Ni-NTA column, the loss of LCAT in the flow-through was similarly high (63.7 %). Moreover, only 6.8 μg (5.8%) of LCAT was recovered from the eluate and this was a lower recovery compared with the previous result from the Ni-NTA column (Table 4.2). Since, this two-step method is not an

efficient way of purifying LCAT from cell culture medium, I attempted using another purification technique with His-Bind Quick cartridges, which is described in the following section (4.6).

Table 4.4 Purification of LCAT by Ni-NTA spin column following octyl-Sepharose chromatography

Purification Stage	Total Protein		LCAT	
	μg	% recovery	μg	% recovery
Start (Concentrated octyl-Sepharose Eluate) (400 μl)	360.0	100	117.4	100
Flow through (400 μl)	204.4	56.8	96.8	82.4
Wash	-	-	0	0
Eluate (200 μl)	46.6	**12.9**	6.8	**5.8**

The amount of protein (μg) in the start medium, flow-through, wash and eluate were estimated by Bradford assay. LCAT activity was determined at each step using proteoliposome substrate (section 2.2.3) and hence its corresponding amount (μg).From these values, the percentage of total protein and LCAT at each stage of Ni-NTA column purification was calculated.

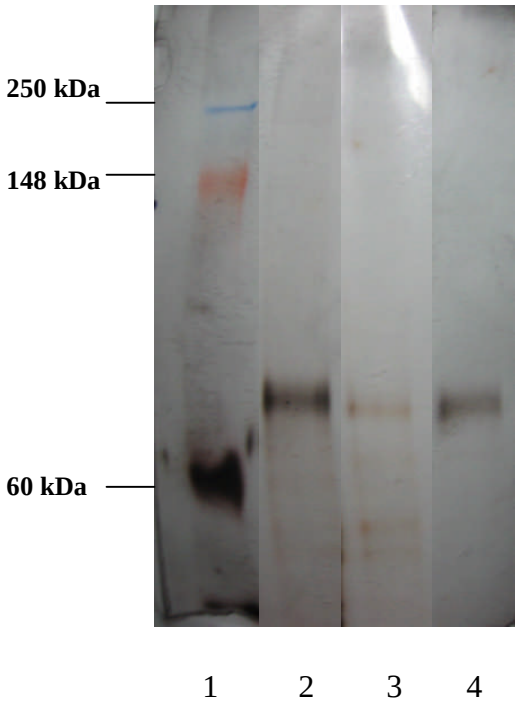

Figure 4.2 Analysis of LCAT purity SDS-PAGE following a two-stage purification using octyl-Sepharose and Ni-NTA columns

Samples from the purification process were run on a 8 % Tris-Glycine gel and silver stained. ***Lane 1*** *shows molecular weight markers in kDa****, Lane 2*** *represents the start medium ("purish"LCAT, octyl-Sepharose eluate) indicated by a thick dark band above 60kDa,* ***Lane 3*** *representing wash of Ni-NTA column with a few visible bands of unbound proteins and* ***Lane 4*** *eluate of Ni-NTA column, showing a single dark band above 60 kDa representing purer LCAT.*

4.6 His-Bind Quick Cartridges and Columns

4.6.1 Introduction

The His-Bind Quick cartridges were packed with pre-charged nickel cations resin and are designed for use with a syringe. Like the spin columns, they are suited to the rapid purification of proteins containing a histidine tag sequence. They have a large diameter cellulose matrix and have flow-rates 5–50 times faster than agarose resins, while maintaining a similar binding capacity. Target proteins can be purified from crude cell lysates in as little as 5 mins. However, the re-use of these cartridges is not recommended by the manufacturer.

4.6.2 Materials and Methods

Quick 900 Cartridges with a column volume of 2 ml and a binding capacity of 2.0 mg per run were purchased from Novagen. The His–Bind Buffer kit contains the following components:

- Binding buffer: 5 mM imidazole, 0.5M NaCl, 20 mM Tris-HCl, pH 7.9
- Wash buffer: 60 mM imidazole, 0.5M NaCl, 20 mM Tris-HCl, pH 7.9
- Elution buffer: 1 M imidazole, 0.5M NaCl, 20 mM Tris-HCl, pH 7.9

Using a 20 ml syringe, the appropriate buffer can be pushed through the cartridge at a rate of approximately 5 ml/min. According to the manufacturer's instructions, the column was initially equilibrated with 6 ml of binding buffer. The test sample was prepared by a 48 h collection of normal growth medium in a 75 cm^2 culture flask containing confluent CHO-H6LCAT cells. A sample of the medium was retained for LCAT assay and the remaining 13 ml was applied to the column. The column was then washed with 20 ml binding buffer followed by 10 ml of wash buffer. Finally, proteins were eluted with 4 ml of elution buffer. The flow-through and eluate were collected and assayed for LCAT.

4.6.3 Results and Discussion

There was 13.4 μg of LCAT in the normal growth medium loaded onto the His-Bind Quick cartridge. The amount of LCAT lost in the flow-through was 0.6 μg (4.5 %) (Table 4.5), while 3.9 μg (29.1 %) was recovered in the eluate. The rest of the

unrecovered LCAT (66.4 %) could be accounted for in the wash but a significant proportion is likely to have been inactivated. When using the Ni-NTA spin column, the starting amount of LCAT in the normal growth medium was half (6.7 μg; Table 4.1) that used here. The amount lost after the 1st flow-through was four times more (19.5 %) and the recovery of LCAT from the eluate was about one third less (11.4%) (Table 4.1) compared to the corresponding values for the His-Bind Quick cartridge (4.5 % and 29 %; Table 4.5). This suggests that His-Bind Quick cartridges are more efficient in isolating active LCAT than Ni-NTA spin column. An added advantage here is that the culture medium containing LCAT does not need to be concentrated, a step which is necessary when using spin columns.

Table 4.5 Purification of H6LCAT using His-Bind Quick Cartridge

His-Bind Cartridge	LCAT (μg)	Recovery (%)
Start	13.4	100
Flow-through	0.6	4.5
Eluate	3.9	**29.1**

The His-Bind Quick Cartridge was loaded with 13.4 μg of LCAT in 13 ml of normal growth medium. LCAT activity in the flow-through and eluate were estimated by standard assay. The LCAT recovered was calculated as a percentage of LCAT in eluate compared to the start.

4.7 Hi-Trap affinity column chromatography

4.7.1 Introduction

Hi-Trap is a ready to use, disposable column designed for affinity chromatography. The columns are 1 ml or 5 ml and have a porous top and bottom frits which allow high flow rates. The separation can be achieved using a syringe or a laboratory pump. Here, the chelating Sepharose consists of highly cross-linked agarose beads to which imino-diacetic acid has been coupled by stable ether groups. As a result of this coupling, a high capacity and performance gel is obtained, which is stable over the pH range 2-14. When charged with suitable ions, the matrix will selectively retain proteins if complex forming amino acid residues are exposed on the surface of the protein.

4.7.2 Materials and Methods

The matrix (purchased from Amersham Biosciences, UK) is supplied with 20% ethanol, free of metal ions and has to be charged with a suitable ion before use. The metal ion most commonly used is Cobalt (Co^{2+}) and the following solutions were prepared:

- Binding buffer: 50 mM Na_2 PO_4, 0.5 M NaCl, 5 mM imidazole, pH 8
- Wash buffer: 50 mM Na_2 PO_4, 0.5 M NaCl, 50mM imidazole, pH 8
- Elution buffer: 50 mM Na_2 PO_4, 0.5 M NaCl, 50 mM EDTA, pH 8

EDTA (50 mM) was used as a chelating agent to strip the metal ions from the gel and cause desorption. The charged column was stored in 20 % ethanol.

Tubing of a peristaltic pump was connected to a 1 ml Hi-Trap column and the matrix washed with 5 ml of water at 1 ml/min. About 1 ml of 0.1M cobalt sulphate was loaded to charge the column as indicated by the column turning pink, followed by 5 ml of binding buffer and then 5 ml of wash buffer. This was to elute non-specifically bound cobalt ions that might otherwise be released during elution. The column was then equilibrated with 5 ml of binding buffer. After a 48 h collection, concentrated 5 ml CD-CHO H6LCAT medium was loaded onto the column with the flow rate preset at 300 µl/min, the chart printer set to run at 1 mm/min and the absorbance at 0.2. The flow-through was collected and the column washed with 5 ml of wash buffer. Finally, the

column was eluted and the fraction of eluate (1.6 ml) corresponding to the peak absorbance was collected and assayed for LCAT activity.

The whole process of purification was repeated to obtain a duplicate result and to test the re-usability of the column. First, the column was washed with 15 ml of water at a flow rate of 1 ml/min, followed by recharging with 1 ml 0.1 M cobalt sulphate and removal of excess metal ions. A second aliquot of CD-CHO H6LCAT medium (5 ml) was then loaded onto the column, and samples from the various stages of purification were taken for LCAT assay (section 2.2.3).

4.7.3 Results and Discussion

The starting amount of LCAT was 22.7 μg in the 1st run and 18.6 μg in the 2nd run (Table 4.6). There was no loss of LCAT detectable in the flow-through and is clearly a first compared to Ni-NTA (Table 4.1), His-Bind Quick Cartridges (Table 4.3) and octyl-Sepharose columns (Table 4.4). This implies that there was 100% capture of LCAT. However, in the wash, there was 4.6 % of LCAT detected in the 1st run compared with 11.8 % in the 2nd run. In contrast, there was virtually no LCAT detected in the wash following octyl-Sepharose column chromatography and two-stage purification using octyl-Sepharose and Ni-NTA columns. The LCAT in this wash may be due to the higher concentration of imidazole (50 mM) and this loss could be reduced by lowering the concentration of imidazole. LCAT recovered were similar with 22.3 % in the 1st run and 20.5 % in the 2nd run. SDS-page gel-electrophoresis (section 2.5.6) demonstrated that pure LCAT was recovered (Fig 4.3). The purity of the LCAT obtained here was comparable to the LCAT after two-stage purification using octyl-Sepharose and Ni-NTA columns (Fig. 4.2) but less contaminant than the LCAT recovered from octyl-Sepharose column alone. However, the efficiency of LCAT purification was still relatively low at about 20 %. It is likely that the majority of LCAT was still bound to the column. An alternative to overcome this problem was to elute the protein at a lower pH (e.g. 7.2), but this may compromise the catalytic function of LCAT.

Table 4.6 Purification of H6LCAT via a reusable cobalt-charged Hi-Trap column

Hi-Trap Column	1st Run		2nd Run	
	LCAT (μg)	LCAT % recovery	LCAT (μg)	LCAT % recovery
Start Medium (5ml)	22.7	100.0	18.6	100.0
Flow through (5 ml)	0	0	0	0
Wash (30 ml)	1.1	4.6	2.2	11.8
Eluate (1.6 ml)	5.1	**22.3**	3.8	**20.5**

Concentrate CD-CHO. H6 LCAT medium was loaded onto the Hi-Trap column for the 1st run and the amounts detected in the flow-through, wash and eluate are shown in the table. Tthe column was then recharged with cobalt ions and again used to purify a similar amount of LCAT (2nd run). The percentage recovery of LCAT in the three fractions is also shown.

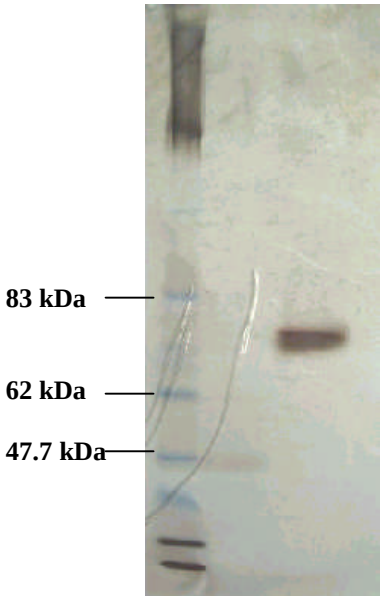

Figure 4.3 Electrophoretic purity of H6LCAT after isolation by chromatography on a cobalt-charged Hi-Trap column

The left lane shows molecular markers in kDa and eluate of the cobalt- column was run on a 8-16% Tris-Glycine gel. The gel was silver stained which showed a dark band above the 62 kDa level representing pure LCAT with very little impurities evident.

4.8 Talon resin gravity-flow columns

4.8.1 Introduction

Talon resins are durable, cobalt-based resins designed to purify recombinant His_6 proteins (Bush et al., 1991). These resins are compatible with many commonly used reagents and allow protein purification under either native or denaturing conditions. To overcome the problem of metal leakage encountered with other resins, Talon utilizes a special tetradentate metal chelator. This tightly holds the electropositive metal in an electronegative pocket, which is ideal for binding metal ions such as cobalt. It enhances the resin's protein binding capacity by making the bound metal ion accessible to surrounding polyhistidine-tagged proteins.

Nickel-base resins often exhibit an undesirable tendency to bind unwanted "background" proteins containing exposed histidine residues (Kasher et al., 1993). Talon resin is said to bind polyhistidine-tagged proteins with enhanced selectivity over nickel-based resins since it has a reduced affinity for background proteins. As a result no background proteins are expected to bind to Talon resin when the sample is applied. Therefore elaborate washing procedures are not generally required before protein elution. Another practical advantage is that His_6 proteins elute from Talon under slightly higher pH or lower imidazole concentration, less stringent conditions than from nickel-based resin.

4.8.2 Materials and Methods

Talon purification kit (#K1253-1) was purchased from Clontech laboratories. It contains the following items:

- Talon metal affinity resin supplied as a 50% (v/v) slurry in non-buffered 20% ethanol
- Disposable 2 ml gravity columns
- Extraction buffer: 50 mM sodium phosphate, pH 7.4 ; 300 mM NaCl
- Elution buffer : 50 mM sodium phosphate, pH 7.4; 300 mM NaCl; 150 mM imidazole
- 20 mM MES, pH 5; 0.1 M NaCl

CHO-H6LCAT cells were grown to confluence in a 175 cm^2 culture flask and switched to CD-CHO medium (28 ml) for a 48 h collection. One ml of Talon resin (2 ml of the 50 % slurry) has a binding capacity of at least 3 mg of tagged protein, which exceeds that of the H6LCAT in the CD-CHO medium, and the medium to resin ratio was standardized to 20:1. Therefore 1.4 ml of resin (2.8 ml of the resin suspension) was centrifuged at 1500 x g for 2 min at 4 ^{0}C, and, after removing the supernatant, the resin was equilibrated with 10-bed volumes (14 ml) of extraction buffer. The resin was sedimented again by centrifugation at 1500 x g for 2 min at 4 ^{0}C, and, after a second 10-bed volume wash, was incubated with the LCAT-containing medium on a roller mixer for 2 h at 4 ^{0}C.

After incubation, the mixture was centrifuged at 1500 x g for 2 min. The supernatant (flow-through) was removed, the resin washed twice with 25 ml of extraction buffer, pH 7.4, and then resuspended in 2 ml of extraction buffer. It was transferred into a gravity-flow column and washed with 5 bed volumes of extraction buffer (pH 7.4). The column was then eluted with 5 bed volumes of elution buffer. The elutions were collected in approximately 500 μl fractions. Finally, the resin was washed with 7 ml of 20 mM MES/0.1 M NaCl (pH 5) followed by 7 ml deionized water and stored in 20% ethanol at 4^{0}C. The samples obtained during various stages of purification were used for LCAT assay (section 2.2.3) and to assess purity by SDS-PAGE (section 2.5.6).

4.8.3 Results and Discussion

Table 4.7 summarises the results of four independent purifications using individual single-use Talon resin column to isolate H6LCAT from CD-CHO medium. Whilst the amount of LCAT varied from 19.7 – 104.0 μg, the volume of medium was kept constant at 28 ml. When 19.7 μg of LCAT was present in the medium, there was no LCAT lost in the flow-through and the recovery in the eluate was 53.9 % which was an improvement compared with previous methods of purification. The recovery was even higher (66.7 %) when the medium contained 40 μg LCAT was present in the medium but this was at the expense of a 27 % LCAT loss in the flow-through. Further increases in LCAT to 87.8 and 104 μg resulted in a decline of LCAT recovery to 54.1 and 47.2 % respectively, although the amount of LCAT protein actually isolated was nearly doubled (47.5 and 49.1 μg).

At each stage of the purification, individual fractions were run on an 8-16 % Tris-glycine gel (Novex) (Fig. 4.4). In a typical gel, Lane 1 represents the markers and lane 2 showed a prominent light band in the region of 64 kDa demonstrating the presence of LCAT in the starting medium (CD-CHO). There were other associated faint bands, which represented non-specific proteins in the medium. A faint band in lane 3 at 64 kDa indicated a negligible loss of LCAT in the flow-through. Lane 4 showing a marked dark band at 64 kDa signifying the presence of concentrated LCAT with a high degree of purity and this was confirmed by enzymic assay.

It would appear that the resin was functioning at good efficiency throughout the range of LCAT (20-104 μg) loaded onto the 1.4 ml of Talon resin which was used each time. Since more than 50 % of LCAT could be recovered from CD-CHO.H6LCAT medium, this method clearly out performed other methods of purification. Therefore, it was chosen to purify LCAT throughout the study.

To determine the feasibility of reuse, the resin is regenerated by washing with 20 mM MES buffer and was equilibrated with extraction buffer as before. CD-CHO.H6LCAT medium (28 ml) was collected over 48 h and subjected to the same purification steps as described above. There was approximately 4 % recovery of LCAT from CD-CHO.H6LCAT medium. This compared poorly with 47-66 % recovery of LCAT when the resin was used only once. There was also a significant loss in the flow-through of approximately 70% compared to less than 30% when the resin was used as fresh. This suggests that very little LCAT loaded was binding in the column. One possible way to address this problem is to use a larger volume of used resin. Alternatively, re-charge the column by passing a cobalt solution through prior to reuse. Electrophoresis of the eluate, showed a small pure band (LCAT) in the 65kDa region. Although the purity of LCAT was not compromised, the recovery was substantially less than expected and therefore it was not cost effective to reuse the resin.

Increasing LCAT in the starting medium would involve concentrating greater volumes of medium and hence the presence of other non-specific proteins. These would compete with LCAT for the Talon resin making it less available for binding. One way to overcome this problem is a 2-stage procedure involving an initial purification step using octyl-Sepharose column chromatography to remove a major proportion of protein contaminants before using Talon resin to isolate H6LCAT from large volumes of medium. This is described in the next section (section 4.9).

Table 4.7 Purification of H6LCAT using a Talon resin gravity-flow column

Samples	1st		2nd		3rd		4th	
	LCAT (μg)	**Recovery (%)**	**LCAT (μg)**	**Recovery (%)**	**LCAT (μg)**	**Recovery (%)**	**LCAT (μg)**	**Recovery (%)**
Start	**19.7**	100	**40.1**	100	**87.8**	100	**104.0**	100
Flow-through	0	0	10.8	26.9	16.0	18.2	7.5	7.2
Eluate	10.4	**53.9**	26.7	**66.7**	47.5	**54.1**	49.1	**47.2**

Four separate collections of CD-CHO.H6LCAT medium were passed through individual Talon resin column (single use). The flow-through and eluate were collected and the amount of LCAT activity in the start, flow-through and eluate was estimated by standard assay (expressed as micrograms). The percentage recovery of LCAT in the two fractions is also shown.

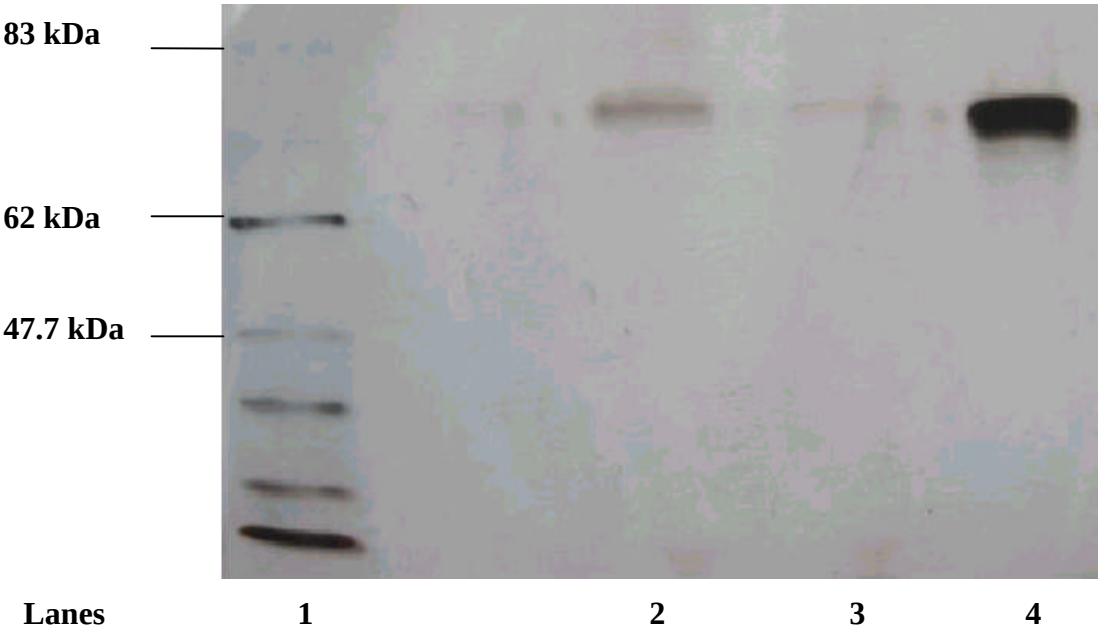

Figure 4.4 Electrophoretic purity of H6LCAT during each stage of isolation by Talon resin affinity chromatography

Samples were taken at each stage of purification using Talon resin gravity column, and run on a 8-16% Tris-Glycine gel followed by silver staining to ascertain the purity of LCAT. ***Lane 1*** *show the broad range molecular weight markers (kDa),* ***Lane 2*** *start medium, CD-CHO containing H6LCAT as represented by a faint band above 62 kDa,* ***Lane 3*** *flow-through as shown by a very light band above 62 kDa indicating some loss of LCAT in the flow-through.* ***Lane 4*** *eluate as indicated by a marked dark band above 62kDa signifying pure LCAT. As typified by the analysis shown in Lane 4, this isolation procedure consistently produce pure LCAT.*

4.9 An optimized two-step purification of H6LCAT using octyl-Sepharose chromatography and a Talon resin column

4.9.1 Introduction

In order to purify a large stock of H6LCAT for injection into LCAT-deficient mice, large volumes of CD-CHO LCAT medium would be used. Purification of LCAT by HIC–octyl-Sepharose column would be an ideal first step for a preliminary purification and concentration. Following this, Talon resin purification method would be an effective second step procedure as it gave a satisfactory recovery and high-purity LCAT, as described in section 4.8.

4.9.2 Materials and Methods

The Equipment set-up has previously been described in section 4.4.2. After the column was equilibrated with 300 ml of PBS, 1.35 L of CD-CHO H6LCAT medium (1.4 μg/ml) pooled from several collections was thawed and passed through the column overnight. The pump flow rate was set at 53 (1.6 ml/min) and the chart recorder set at 100 mV and a speed at 1 mm/min; the absorbance of the detector was 0.2. The next day, after the medium had been pumped through, the column was washed with an excess of 10 mM sodium phosphate (pH 7.5). Finally the column was eluted with water (48 ml) which showed a sharp peak in absorbance on the chart recorder as protein was eluted. When the elution was complete, the absorbance indicator returned to a stable baseline, and the collected eluate was concentrated to 20 ml using a 10,000 MWCO Vivaspin concentrator at 2,500g and 4 ^{0}C.

This concentrate was then incubated with 2 ml of primed Talon resin at 4 ^{0}C for 2 h on a roller mixer. Next, the resin was washed with 40 ml of extraction buffer for 10 min at 4 ^{0}C, centrifuged at 700 g for 10 min and after discarding the supernatant and the whole wash process repeated. Subsequently, the resin was transferred to the gravity-flow column and eluted with 10 ml of elution buffer.

A second purification was carried out in an identical manner using a new batch of Talon resin (2 ml), except that a smaller volume of CD-CHO.H6LCAT medium was fractionated (350 ml). For both purifications, the amount of protein and LCAT at each stage of the isolation was determined by Bradford (section 2.5.5) and LCAT assays (section 2.2.3) and the purities assessed by SDS-PAGE (section 2.5.6).

4.9.3 Results and Discussion

For the 1st purification, there was 1890 μg of LCAT in the CD-CHO medium (Table 4.8). Binding of LCAT was efficient as LCAT could not be detected in the flow-through. This appears better than the previous result (Table 4.3) where 21.6 % of LCAT was found in the same fraction after 500 μg of LCAT was loaded onto the column. In the eluate, 322 μg (17%) of LCAT was recovered and this amount proportionally is less than previously (37%) using a smaller LCAT load (500 μg) (Table 4.3). The eluate was further purified using Talon resin and there was 52 μg (2.8%) of LCAT in the flow-through and 260.9 μg (an overall recovery 13.8%) in the eluate. In the 2nd run, when the starting volume of CD-CHO medium was much smaller (350 ml containing 490 μg of LCAT), there was a small amount of LCAT in the flow-through 5 μg (1 %). However, in the eluate there was 129.4 μg (26.4 %) of LCAT, an improved recovery compared with the 1st run. This result may reflect the smaller amount of LCAT loaded onto the column and the relative increased proportional binding of LCAT. Using Talon resin, there was 3.5 μg (0.7 %) of LCAT in the flow-through and 53.2 μg (10.9 %) of LCAT in the eluate. The proportions of LCAT recovered relative to the amounts loaded on the Talon resin, were 81% and 41% for the 1st and 2nd runs, respectively.

The amount of total protein in 1.35 L of CD-CHO medium was 34.6 mg. After passing through the octyl-Sepharose column, there was 3.45 mg (10%) of protein in the eluate. When eluted from the Talon resin, there was 0.77 mg (2.2%) of protein present. In the 2nd run, the CD-CHO medium contained 9 mg of total protein, which was reduced to 2.1 mg (23.3%) of protein after octyl-Sepharose chromatography and to 0.5 mg (5.6%) after Talon resin purification.

Overall, a combined total of 451 μg (19 %) of LCAT was recovered from octyl-Sepharose column, 314 μg (13.2 %) after elution from the Talon resin. Although gel-electrophoresis showed that the LCAT recovered was of high purity similar to that in Fig 4.4, there was a significant loss of LCAT (> 85%) during this process.

4.9.4 Conclusion

The problem with the 2-step octyl-Sepharose chromatography and talon resin column is that % LCAT protein recovered is low (1st run: 13.8 % i.e. 260.9 μg / 1890 μg; 2nd run: 10.9 % i.e. 53.2 μg / 490 μg see Table 4.8). Recovery of protein by the

Talon resin step in the 1st run was 22.3 % (i.e. 0.77 mg / 3.45 mg) and in the 2nd run , 23.8 % (i.e. 0.5 mg / 2.1mg). The combined % LCAT protein was 24.2% (314.1 μg / 1300 μg see Table 4.9). Similar results with low % LCAT protein yield were observed using Ni-NTA column (14.6 % i.e. 6.8 μg / 46.6 μg see Table 4.4) and and octyl-Sepharose column (11.6 % i.e. 184.8 μg / 1600 μg see Table 4.3). This raises the probability that LCAT may be inactivated during the process of purification since no obvious contamination was seen on my gels e.g. Fig 4.4. This is further substantiated by the high recovery of "active and inactive" LCAT of 53.4% (% ratio of total protein in eluate [770 + 500 μg] to total LCAT [2380 μg]). Another possible explanation for the high protein yield in the eluate may be due to an over-estimation of protein concentration based on the Bradford assay whose standard is the bovine serum albumin (BSA). As there are many different types of proteins in the culture medium, the concentration of protein derived from one protein standard may not be accurately reflect the true amount of protein present.

Mercaptoethanol reduces disulfide bonds and preserve the active sulfur-hydroxyl groups in LCAT. One way to prevent unwanted interaction between contaminant proteins and His_6tagged LCAT is to add β-mercaptoethanol to the buffers during purification. Recycling of flow-throughs (although no LCAT here) increases the binding time and thus could potentially recover some LCAT lost (e.g. 21.6%, see Table 4.3) at this stage.

In conclusion, purifying LCAT from small volumes of medium was found to be feasible using Talon resin. Scaling up this purification to larger volumes of medium using a two-step procedure was inefficient, even though very pure LCAT was recovered. Further work will need to focus on this area, perhaps using Talon resin in a larger column to purify higher amounts of LCAT. For my subsequent *in vivo* work on protein therapy, I adopted the method described in section 4.8 to purify LCAT.

Table 4.8 Large-scale purification of LCAT using a combination of octyl-Sepharose and Talon resin column chromatography

Octyl-sepharose	1st Run (1.35 L)				2nd Run (0.35 L)			
	LCAT (μg)	LCAT Recovery (%)	Total Protein (mg)	Protein Recovery (%)	LCAT (μg)	LCAT Recovery (%)	Total Protein (mg)	Protein Recovery (%)
Start	1890.0	100	34.6	100	490	100	9.0	100
Flow through	0	0	–	–	5.0	1.0	–	–
Eluate	322.0	**17.0**	3.45	10.0	129.4	**26.4**	2.1	23.3
Talon resin								
Flow through	52.0	2.8	–	–	3.5	0.7	–	–
Eluate	260.9	**13.8**	0.77	2.2	53.2	**10.9**	0.5	5.6

Two separate purifications of CD-CHO medium were carried out (1.35 L and 0.35 L). For both runs, the amount of LCAT (μg) in the start, flow-through and eluate was determined after passing through the octyl-sepharose column and the Talon resin. Protein contents in the start and eluate of both stages were determined by Bradford assays but not in the flow-throughs.

Table 4.9 The combined result of the large volume purification of LCAT using octyl-sepharose column and Talon resin

Octyl-Sepharose	LCAT (μg)	LCAT Recovery (%)	Total Protein (mg)	Protein Recovery (%)
Start	2380	100	43.5	100
Flow through	5.0	0.2		
Eluate	451.4	**19**	5.5	**12.6**
Talon resin				
Flow through	55.5	2.3		
Eluate	314.1	**13.2**	1.3	**3.0**

The combined data from the large scale purification of LCAT is shown. After passing through the octyl-Sepharose column, 19 % of LCAT and 12.6 % of protein were eluted. Elution from Talon resin yielded 13.2 % of LCAT and 3 % of total protein were recovered.

CHAPTER 5

IN VIVO STUDIES

5. IN VIVO STUDIES

5.1 Protein Therapy

5.1.1 Introduction

Protein therapy refers to the ability to deliver therapeutic proteins in humans. The major potential uses of proteins include direct replacement of deficient protein or enzyme and the augmentation of a pre-existing pathway leading to reduced levels of a toxic metabolite.

Live proteins extracts have been used to treat hepatitis and cirrhosis. One such protein is the thymus protein that is being used to increase host's resistance and is responsible for modulation of cell-mediated immunity (Zeman *et al*., 1991). Hepatocyte Growth Factor (HGF) is another live protein that has been employed to improve the regenerative capabilities of the liver. It has been identified as one of the many active proteins and growth factors found in the liquid liver extract that is said to stimulate liver regeneration, accelerate hepatic function and reverse fibrosis and cirrhosis (Kaido *et al.,* 1998).

One approach to treat the lipoprotein abnormality in liver disease is by direct injection of pure LCAT via either intravenous route or intraperitoneal cavity. I have evaluated this method by performing a series of pilot experiments with LCAT $^{-/-}$ mice. The latter were kindly provided by Dr Eddy Rubin from Berkeley (Ng *et al.,* 1997). Homozygous LCAT$^{-/-}$ mice were healthy and, like their human counterparts, have markedly reduced plasma concentrations of cholesterol, HDL cholesterol, apoAI and apoAII making them ideal for my studies.

5.1.2 Intravenous Injection

I report here a pilot study infusing H6LCAT into LCAT $^{-/-}$ mice via the tail vein and then measuring LCAT activity at three time intervals post-injection.

Materials and Methods

Pure LCAT was freshly prepared as described in section 4.8 using Talon resin and was then frozen. An activity assay on the day of injection showed the concentration of active enzyme was 189 ng/μl. One female LCAT $^{-/-}$ mouse, 20 months old and

weighing 26 g was injected with 70 μl (13.23 μg) of pure LCAT intravenously via the tail vein. This amount was based on the fact that the LCAT concentration in human plasma is 6 μg/ml and that the approximate blood volume in a mouse is 78 ml/kg. Therefore, a 26 g mouse has an estimated circulatory volume of approximately 2.0 ml. As its haematocrit or packed cell volume is 40, the plasma volume is 0.8 ml. Hence, it would require approximately 4.8 μg equivalent of LCAT in order to achieve a plasma concentration of 6 μg/ml. An arbitrary excess amount of LCAT (13.23 μg) was used to compensate for any loss of LCAT during preparation and injection (e.g. LCAT remaining in syringe and needle).

A tail bleed was taken prior to injection and at 0.5, 3 and 22 h intervals. Home Office guidelines require that mice are not bled more than 15 % of their blood volume per month. Assuming a 26 g mouse has a blood volume of 2ml, the maximum volume permitted is 300 μl and therefore, I have limited each bleed to a safe volume of 30-40 μl. Collected blood in plain Eppendorfs was immediately transferred onto ice and centrifuged at 13000 rpm at 4 ^{0}C. The plasma was temporarily stored at –20^{0}C and subsequently assayed for LCAT (section 2.2.3).

Results and Discussion

As expected, plasma from the LCAT $^{-/-}$ mouse did not contain any endogenous LCAT as demonstrated by undetectable LCAT activity in the pre-bleed sample. A peak of 11 μg/ml of LCAT (Fig 5.1) was detected in the mouse plasma 30min after tail-vein injection which was more than the estimated LCAT concentration (6-7 μg/ml) predicted. This could be explained by an overestimation of the mouse plasma volume as discussed later. A further plasma sample taken at 3 h, showed that 8.9 μg/ml of LCAT was present. The last sample at 22 h recorded 2.23 μg/ml of LCAT thus demonstrating a substantial decline in activity.

Haematocrit is defined as the ratio of the volume occupied by packed red blood cells to the volume of the whole blood. Assuming that the plasma volume is 1 ml, the total blood volume in a mouse with a normal haematocrit (35-40 %) would be approximately 1.5-1.7 ml. This value is nearly equivalent to the total blood volume (1.8 ml) of a 26 g mouse. This would explain the unexpected high peak concentration of 11 μg/ml of LCAT at 30 min. Further more, 70 μl LCAT infused is ~ 4 % of the blood volume and may increase the viscosity of the blood in the mouse thus impair the heart to pump effectively. It results in abnormal distribution of LCAT which may account for

this high LCAT concentration. However, infusion of normal saline would dilute the blood and reduce the viscosity to normality.

After 22 h, there was a significant reduction (80 %) in LCAT concentration compared to its peak value. This suggests that LCAT was rapidly cleared and is most likely due to normal rate of clearance e.g. perhaps due to HDL catabolism. Of specific importance is that human LCAT was still enzymically active in mouse plasma.

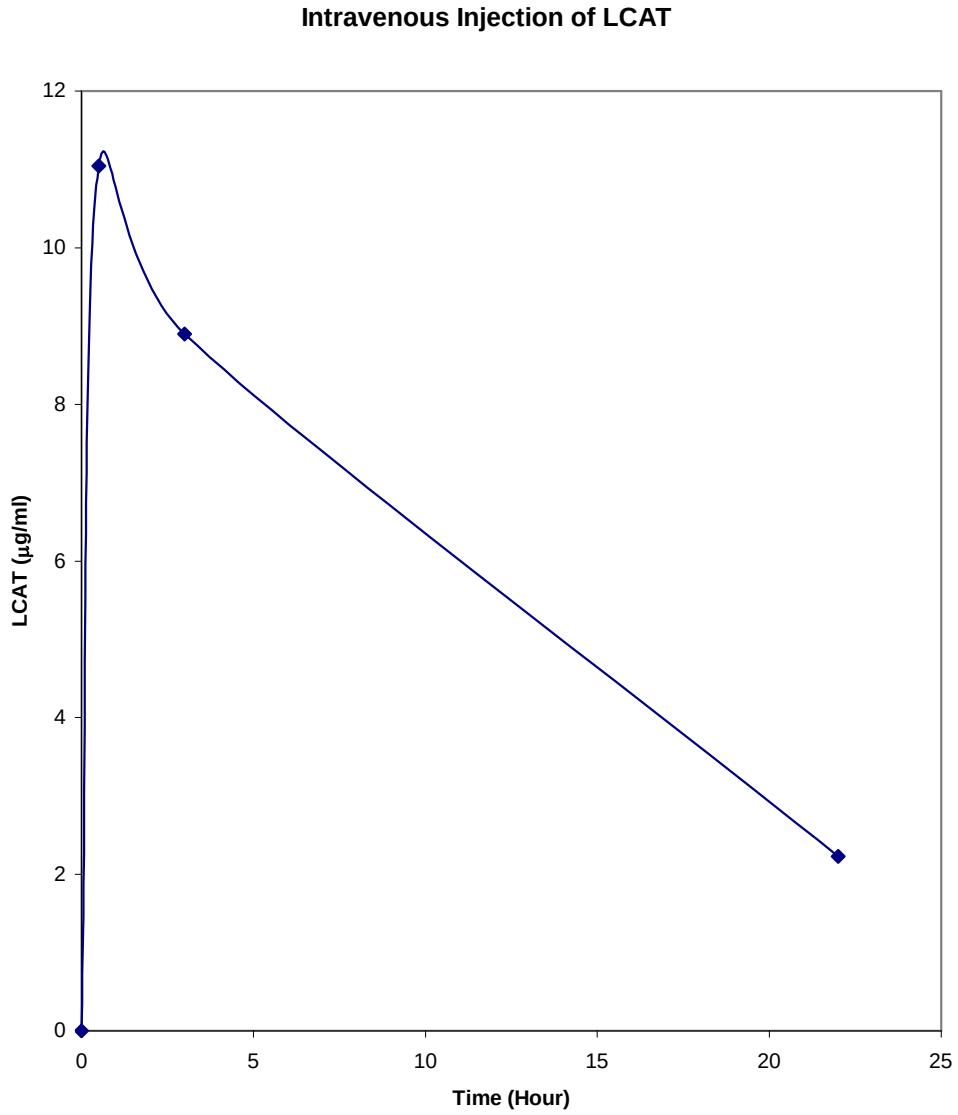

Figure 5.1 Plasma LCAT concentration after a bolus tail-vein injection of purified LCAT in one LCAT $^{-/-}$ mice.

A bolus of purified LCAT (13.23 µg) was administered into the tail-vein of a LCAT $^{-/-}$ mouse. Mouse plasma was sampled at 0.5, 3 and 22 h. The plasma was assayed for LCAT activity as described in section 2.2.3. The % CE calculated was converted to an equivalent LCAT mass in µg/ml.

5.1.3 Intraperitoneal Injection (IP)

An alternative method using the intraperitoneal route was chosen to deliver LCAT into the LCAT $^{-/-}$ mice. This route was of interest as it would be a prelude to implanting encapsulated cells into the peritoneal cavity once this stage of the study was deemed feasible. No advantage has been demonstrated of one needle size over another, quadrant of injection, or investigator (Miner *et al.,* 1969).

Materials and Methods

Two healthy female LCAT $^{-/-}$ mice, both about 19 months old and weighing 36 g, were used in this experiment. The 1 ml syringes with 26-gauge needles were used for IP injections. LCAT with a concentration of active enzyme of 189 ng/μl was used in this experiment (section 4.1.1). Both LCAT $^{-/-}$ mice were injected with 100 μl (18.9 μg) of pure LCAT into their peritoneal cavities. Tail bleeds of 20-50 μl were taken prior to injection and at 0.5, 1, 2, 4 and 22 h intervals. The plasma collected was assayed for LCAT activity, free and total cholesterol as described in sections 2.2.3 and 2.5 respectively.

Results and Discussion

In both mice, there was detectable LCAT in their plasma within 0.5 h in mouse (2) and 1 h in mouse (1) (Fig 5.2). In mouse (2), the plasma LCAT was 13.2 μg/ml at 1 h post injection followed by the highest concentration recorded, 14.9 μg/ml at 2 h. At the 4th hour, the plasma LCAT was 13.3 μg/ml. It may have peaked even further between 1 and 4 h but it was not possible to collect blood samples at more frequent intervals as it would have made the animal unwell and also have exceeded the recommended guidelines for bleeding. The concentration of LCAT in mouse (2) was high. This could be explained by the small circulatory plasma volume in these mice (~1.26 ml); whereas the total blood volume with a normal haematocrit (0.35) would be approximately 1.9 ml. It is plausible that this picture could be representative of the way in which LCAT could behave when secreted from encapsulated cells.

At 22 h, 5.3 μg/ml of LCAT was still present in the plasma. In mouse (1), a maximum of 3.26 μg/ml of LCAT was present in the plasma at 4 h. Although the LCAT level was much less than in mouse (2), it was maintained at 3.20 μg/ml even at 22 h. This could be a result of a delay in absorption and or the amount absorbed was less than

expected. The peritoneal cavity blood barrier could be abnormal from previous inflammatory process causing impaired absorption of LCAT into the blood stream.

Apart from mouse (1), where there was insufficient plasma at 1 h to do the free cholesterol assay, cholesteryl ester was calculated as a percentage as described before (section 2.5). An apparent decrease in % CE/TC in mice (2) one hour post injection (34 %) was noted, followed by a significant rise at 22 h (51 %) (Fig 5.3). There was a similar decrease in % CE/TC in mice (1) at 2 h (27 %), but a smaller rise at the 22 h (41 %).

Intravenous injection of LCAT into mice provides a relatively rapid route for administration of the protein and achieves a high plasma level in a short time. However, intraperitoneal injection as demonstrated here is an alternative that is easily accessible and just as effective even though there is lag time of absorption for the LCAT to traverse into the bloodstream. More importantly, it produces a physiological response by increasing the esterification of cholesterol. However, the peak levels of LCAT in the mice plasma do not correspond to the maximal levels of esterified cholesterol. It appears that there was delay in esterification and this process may be slow and cumulative in effect.

An additional advantage here is that the peritoneal cavity could act as a reservoir, slowly releasing LCAT into the circulation after only a single injection. There were no adverse effects suffered by both animals following administration of LCAT and blood sampling.

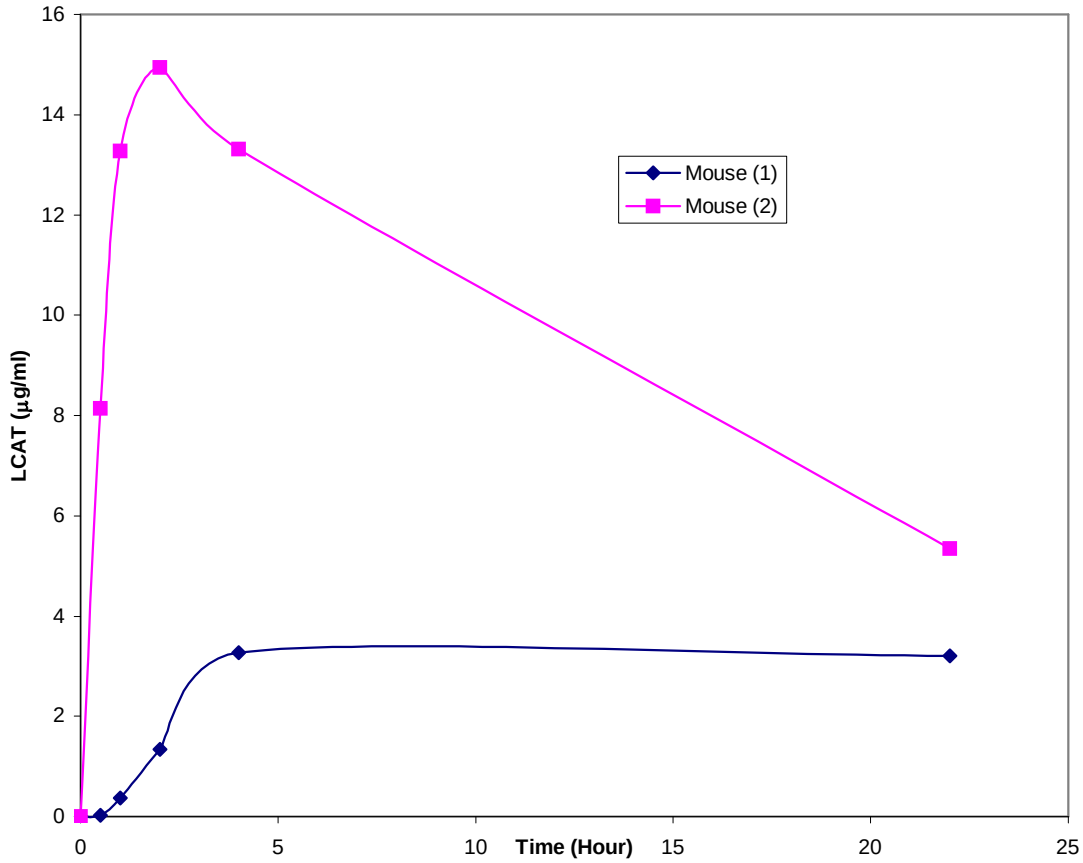

Figure 5.2 Plasma LCAT concentration in LCAT $^{-/-}$ mice following IP injection of pure LCAT.

A bolus of pure LCAT (18.9 µg) was administered to both LCAT $^{-/}$ mice via IP route. Tail bleeds were taken at 0, 0.5, 1, 2 and 22 h and plasma collected were checked for LCAT activity as described in section 2.3.3. The results were converted to LCAT mass expressed as µg/ml.

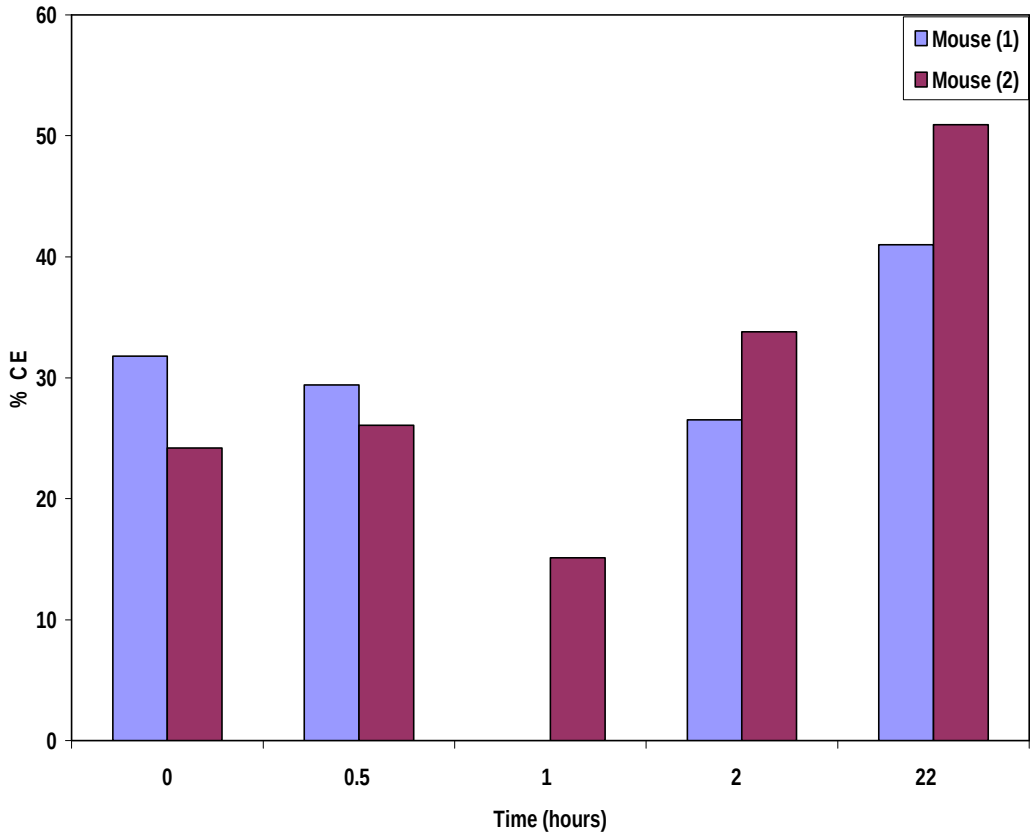

Figure 5.3 The percentage esterified cholesterol in two LCAT $^{-/-}$ mice plasma following IP injections of LCAT.

After each LCAT $^{-/-}$ mouse (mouse (1) and mouse (2)) was given a bolus IP injection of pure LCAT (18.9 μg), tail bleeds were taken at 0, 0.5, 1, 2 and 22 h. The concentration of free and total cholesterol was estimated in the standard manner as described in section 2.5. Cholesteryl ester concentrations were derived by subtracting the free cholesterol values from those of the total cholesterol measurements. The percentage of total cholesterol as cholesteryl esters was then calculated as shown in the bar graph.

.

5.1.4 Bolus injection of LCAT

With the initial apparent success with IP administration, I decided to do a follow-up study using more LCAT $^{-/-}$ mice. Unfortunately, as there were problems with in-house breeding, I was limited to 3 mice to verify the pilot study.

Materials and Methods

Three female LCAT $^{-/-}$ mice, all 3 months old and weighing 18-20 g, were each given a bolus injection of 15.2 μg of LCAT into their peritoneal cavities. Tail bleeds were taken just before the single injection and 1, 2, 4, 6 and 22 h post-injection. The samples were collected on ice and centrifuged at 13,000 rpm at 4 ^{0}C. The supernatant plasma was aliquoted for LCAT, total and free cholesterol assays as described in sections 2.3.3 and 2.5. Plasma was analysed by agarose gel electrophoresis (section 2.5.4) to monitor changes in the lipoprotein profile (results described on page 150 and shown in Fig. 5.10).

Results and Discussion

In this experiment, all the pre-bleed plasma of the LCAT $^{-/-}$ mice showed the absence of basal LCAT. There was a significant increase in LCAT concentration in all 3 mice at 1 h (Fig 5.4). The highest level of LCAT concentration 2 h post injection was 15.6 μg/ml in mouse (2) and 14.3 μg/ml in mouse (3). At 6 h, LCAT concentration in mouse (1) was 14.9 μg/ml. As before, the plasma LCAT concentration in mouse (2) at 2h exceeded the bolus dose (15.2 μg). The average peak plasma LCAT concentration achieved was 14.7 μg/ml at 2 h. LCAT concentration remained relatively constant from 2-6 h except for mouse (3). In the latter, there was a more rapid decline in LCAT concentration after its peak concentration. Due to limitations of collecting blood, I was unable to obtain more samples between the time intervals. As a result, the point at which LCAT concentration began to decline rapidly could not be accurately determined. It is likely to be between 6 and 22 h. Even at 22 h, the plasma LCAT concentration was ~ 6 μg/ml. This represents a 60 % drop from its peak LCAT concentration and thus suggests that rapid clearance of LCAT may have occurred. All 3 mice behaved similarly as the peak LCAT concentrations were achieved within 6 h of injection followed by a rapid decline in LCAT concentration to 22 h. The mean plasma LCAT concentration of all 3 LCAT $^{-/-}$ mice following single bolus IP injection is shown in Fig 5.5. The average peak LCAT concentration was 14.7 ± 0.3 μg/ml at 2 h post injection and followed by a

gradual decline to 6 ± 1.2 μg/ml at 22 h. The plasma half life of LCAT (t ½) was 7.35 μg/ml at 18.5 h.

The LCAT $^{-/-}$ mice being homozygous for LCAT deficiency, have an intrinsic basal level of esterified cholesterol in the mice expressed as 25.5 ± 1.5 % CE (Fig 5.6). This is a marked difference to the homozygotes for classic familial LCAT deficiency where the LCAT activity is either severely reduced (~ 5-9% of normal) or not detectable and esterification of cholesterol is virtually absent (Glomset *et al.,* 1995, Kuivenhoven *et al.,* 1995). The residual cholesteryl esters still present in LCAT $^{-/-}$ mice plasma most likely originate from intracellular pools formed by acylcoenzyme A:cholesterol acyltransferase (Sakai *et al*., 1997). Chylomicrons which are produced in the intestinal mucosa may also account for the basal cholesteryl esters level. They transport dietary cholesteryl esters from intestine into the general circulation via the thoracic duct. Another source of basal cholesteryl esters is the liver where the former are synthesized and are transported as VLDL.

The plasma LCAT concentration in mouse (2) (15.6 μg/ml) was greater than the bolus dose (15.2 μg) injected. Although such high plasma LCAT concentration could be explained by the small circulatory plasma volume in these mice (~1 ml), most mice with a weight greater than 25 g would have a plasma volume exceeding 1 ml. Re-activation or re-naturation of enzyme in circulation seems likely to explain the discrepancy between the amount of LCAT injected and the mice plasma LCAT. The LCAT assay has been validated (see Chap 2.3) and there is no reason to suggest that the method employed here was inaccurate. The role of glycan chains is not known with certainty. One possibility is that alteration of glycan chains of purified human LCAT in mouse plasma can lead to a change in reactivity of the enzyme with HDL substrates. In Chapter 4, where the steps for purification of LCAT were described, the total protein in the eluent greatly exceeds the LCAT mass as determined by activity even though the LCAT in the eluent was pure by SDS-PAGE (Fig 4.4). This suggests that activation of human LCAT in mouse plasma is possible.

A statistically significant increase in % CE/TC was detected 4 h post injection and very significant after 22 h (see Table 5.1, Fig 5.6). Again it appears that peak LCAT levels do not correspond to high levels of cholesteryl esters. One can infer that there was a lag phase and a gradual increase in esterification although the peak level could not be certain due to the relatively wide time intervals.

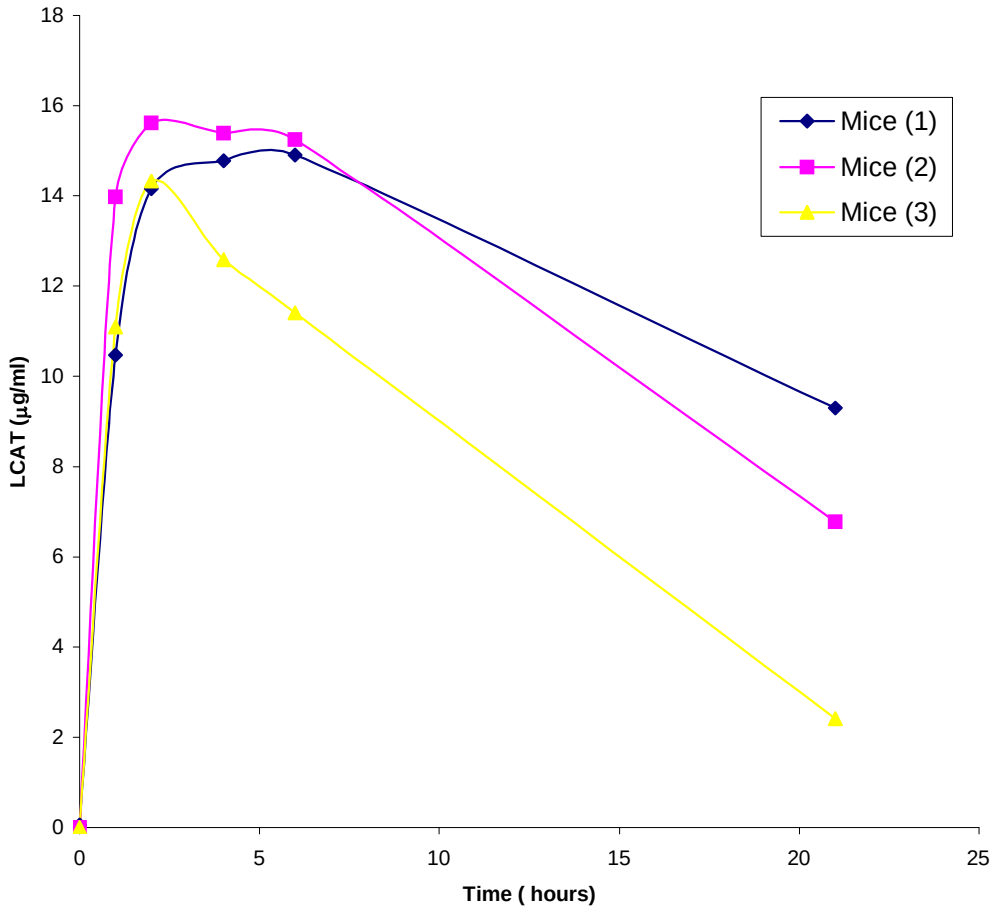

Figure 5.4 Plasma LCAT concentrations following a single bolus IP injection of pure LCAT in 3 individual LCAT $^{-/-}$ mice.

A bolus of pure LCAT (15.2 µg) was injected into the peritoneal cavities of 3 LCAT $^{-/-}$ mice. At various time intervals (0, 1, 2, 4, 6 and 22 h) following injection, tail bleeds were taken. The plasma collected was assayed for LCAT activity as described in 2.2.3. The results were converted to its equivalent LCAT mass expressed in µg/ml indicated on the y-axis.

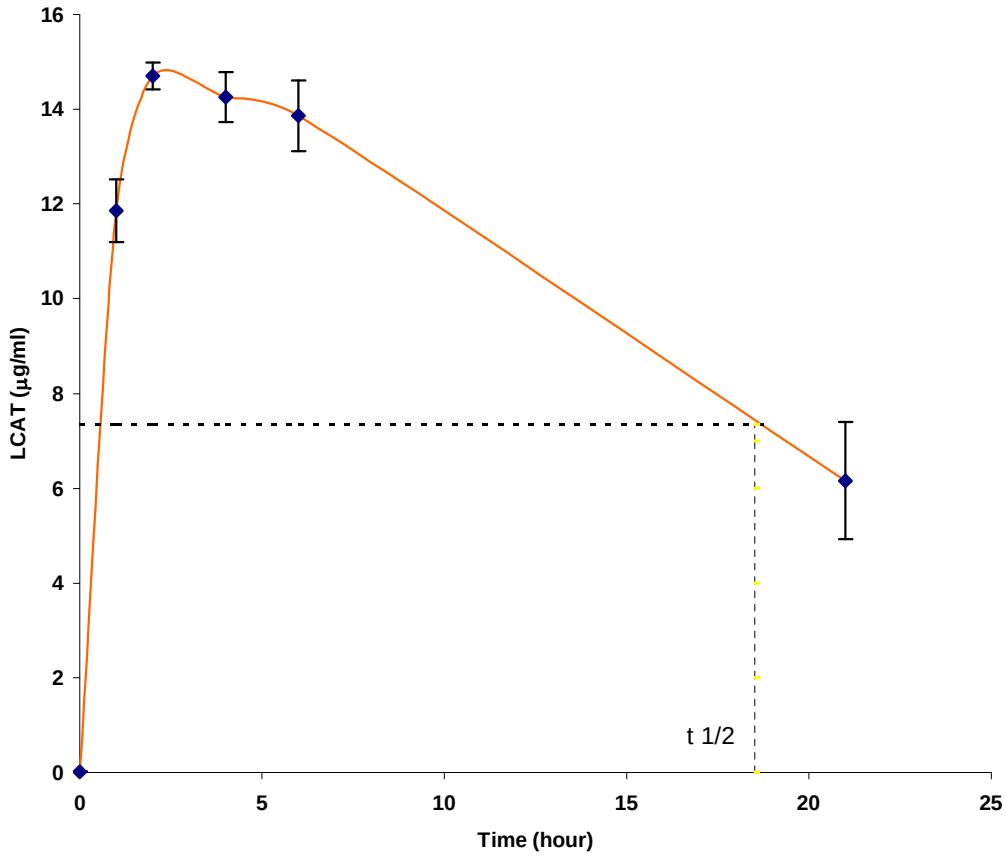

Figure 5.5 Mean plasma LCAT concentration of 3 LCAT $^{-/-}$ mice following single bolus IP injection.

LCAT concentration was calculated from its LCAT activity assay. The values are expressed as means ± SD The average peak LCAT level (14.7 µg/ml) was achieved at approximately 2 h post injection and followed by an initial gradual decline (2-6 h) before the last observed value, 6 µg/ml of LCAT at 22 h. This is estimated to be approximately 40 % of the dose of LCAT injected. The plasma half-life (t ½) of LCAT was 7.35 µg/ml at 18.5 h.

Table 5.1 The percentage of esterified cholesterol in the 3 LCAT $^{-/-}$ mice following IP injection of pure LCAT.

Hour	Mouse 1 (%CE/TC)	Mouse 2 (%CE/TC)	Mouse 3 (%CE/TC)
0	**24.9**	**27.9**	**23.6**
1	23.0	43.8	33.1
2	35.9	54.4	26.0
4	**46.1**	**56.6**	**41.5**
6	**57.5**	**54.2**	**47.0**
22	**55.9**	**52.0**	**54.4**

After each LCAT $^{-/-}$ mice was given a bolus IP injection of LCAT (15.2 μg), tail bleeds were taken at 0, 1, 2, 4, 6 and 22 h. The concentration of free and total cholesterol was estimated in the standard manner as described in 2.5. The percentage of total cholesterol as cholesteryl esters was then calculated. The % CE/TC highlighted in all 3 mice at 4, 6 and 22h was statistically significant when compared with the basal esterification at 0 h.

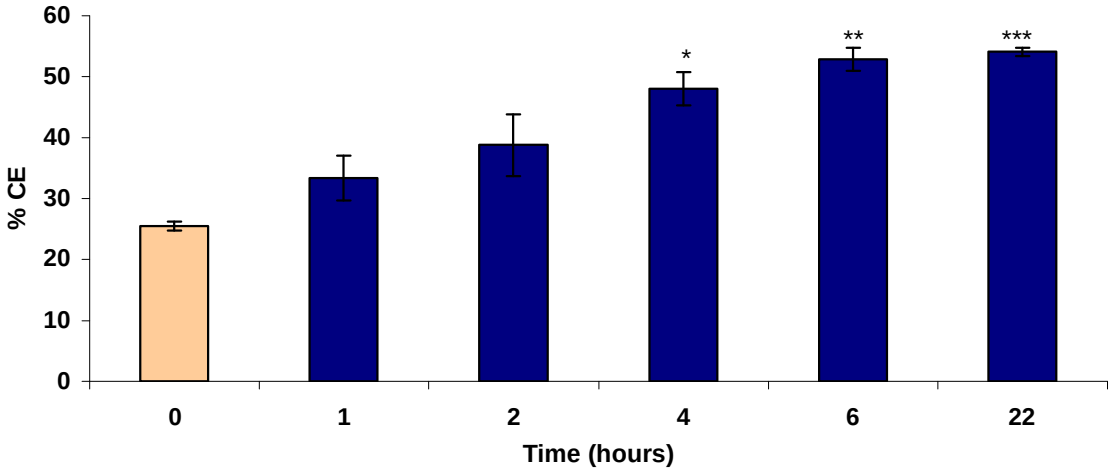

Figure 5.6 The percentage esterified cholesterol in plasma of three LCAT $^{-/-}$ mice following IP injection of LCAT.

*Bar graph represents the % CE/TC means ± SD. The background basal esterification (0 h) is represented in grey, whilst the % CE at 1, 2, 4, 6 and 22 h is represented in black.. Asterisk * denotes $p < 0.05$, ** $p < 0.01$ and *** $p < 0.0001$.*

5.1.5 Repeated Injections

Based on my previous results, there was enough evidence to suggest that human LCAT is active in LCAT $^{-/-}$ mice with a high-dose single injection. To determine if a smaller repeat dose produces a similar or enhanced effect, the same number of mice was used for this study over 4 days.

Materials and Method

Three male mice, 2 months old and weighing 18-20 g each, were injected with 4.5 μg of pure LCAT into their peritoneal cavities every 24 h for 3 consecutive days. A tail bleed was taken prior to injection and at every 24 h post-injection for 3 consecutive days when the experiment was terminated. The samples were collected on ice and centrifuged at 13,000 rpm at 4 ^{0}C. The supernatant plasma was aliquoted for LCAT, total cholesterol and free cholesterol assays. Plasma was run on ready-to-use agarose gel provided in the Hydragel-Mini Lipo Kit (Sebia) to observe the changes in lipoprotein profile (section 2.5.4).

Results and Discussion

After the 1st 24 h post injection, 2.8 μg/ml LCAT was detectable in mouse (A) and 3.0 μg/ml in mouse (B) (Fig 5.7). However, LCAT was undetectable in mouse (C) (Fig 5.7). It is possible that for mouse (C), LCAT was administered into the subcutaneous tissues instead of the peritoneal cavity and thus did not show a demonstrable rise in plasma LCAT concentration. However, after the 2nd injection, ~ 3.1 μg/ml of LCAT was detectable in the plasma of mouse (C) 24 h later.

Again, the amount of LCAT detectable in plasma (~ 3 μg/ml) at 24 h compared with the amount of LCAT injected (4.5 μg) is very high. There was a relatively steady plasma LCAT concentration (2 μg/ml to 3.1 μg/ml) over the remaining test period for all 3 mice (Fig 5.8). These results suggest that LCAT may be consistently activated in mouse plasma on repeated injections in order to account for the high LCAT in mouse plasma. Indeed, % CE/TC in plasma of all 3 mice was statistically significant after 24 h and remained so at day 2 and 3 (Fig 5.9). These data show that repeat injections can give more stable and sustained LCAT levels in the plasma (Fig 5.8) and hence provide a steady rate of esterification (Fig 5.9).

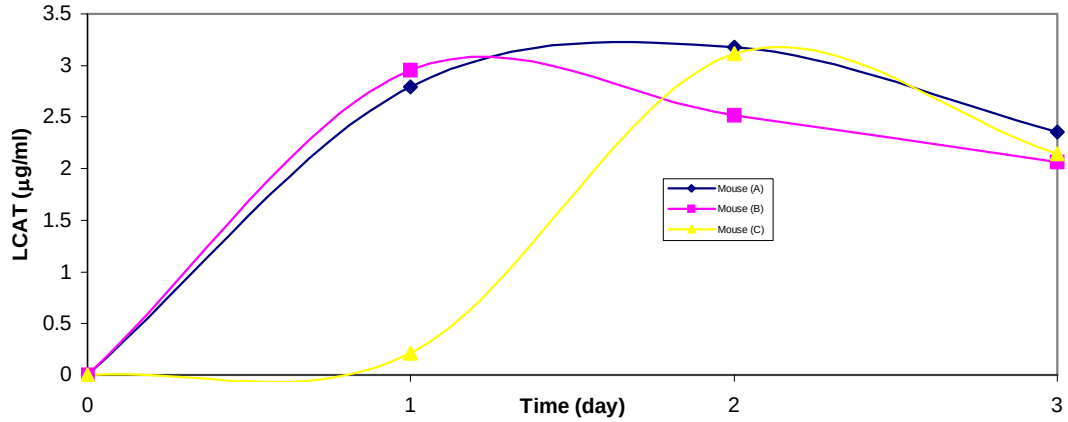

Figure 5.7 Plasma concentration of LCAT in LCAT $^{-/-}$ mice following 3 repeated injections at 24 hour intervals.

Three LCAT $^{-/-}$ mice were each given IP injection of 4.5 µg of LCAT over 3 consecutive 24 h interval. Tail bleeds were taken at each 24 h interval and plasma was assayed for LCAT activity in the standard way (section 2.3.3) with the results expressed as µg/ml.

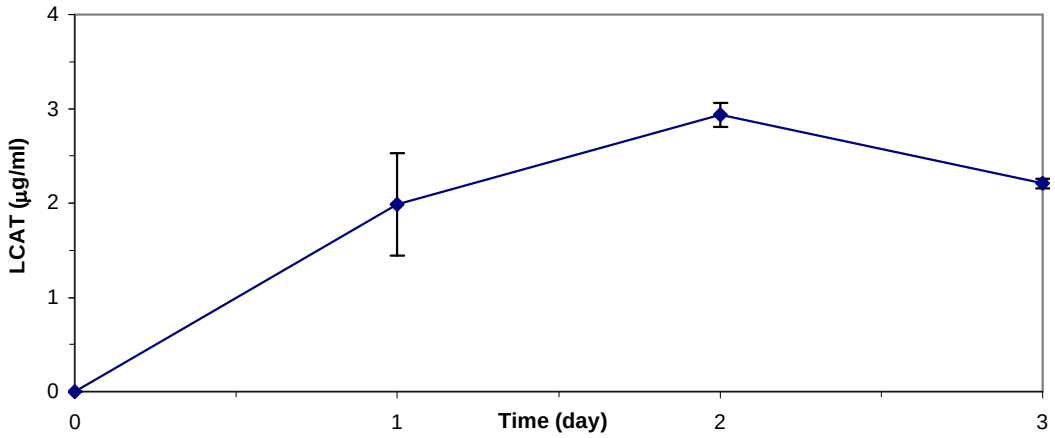

Figure 5.8 The combined result of plasma LCAT concentration following repeated injections in 3 LCAT $^{-/-}$ mice.

The plasma LCAT concentration is expressed as means ± SD at 0-3 days. A satisfactory LCAT level (2 µg/ml) was achieved after 24 h post injection. Thereafter, a steady plasma level was maintained by consecutive 24 h injection of LCAT.

Table 5.2 The percentage of esterified cholesterol in plasma following repeated LCAT injections in 3 LCAT $^{-/-}$ mice.

Day	Mouse A (%CE/TC)	Mouse B (%CE/TC)	Mouse C (%CE/TC)
0	44.4	49.2	47.2
1	**57.6**	**59.8**	52.6
2	**56.0**	**61.0**	**56.2**
3	**63.2**	**63.9**	**63.5**

The three mice represented by (A), (B) and (C) were administered 4.5 μg LCAT every 24 h for 3 consecutive days. Tail bleeds were taken at 24 h interval and the plasma assayed for total and free cholesterol described in 2.5. From this result, the cholesteryl esters were quantified and % CE/TC calculated. The values highlighted in bold demonstrated a statistically significant increase in esterification following repeated LCAT injection.

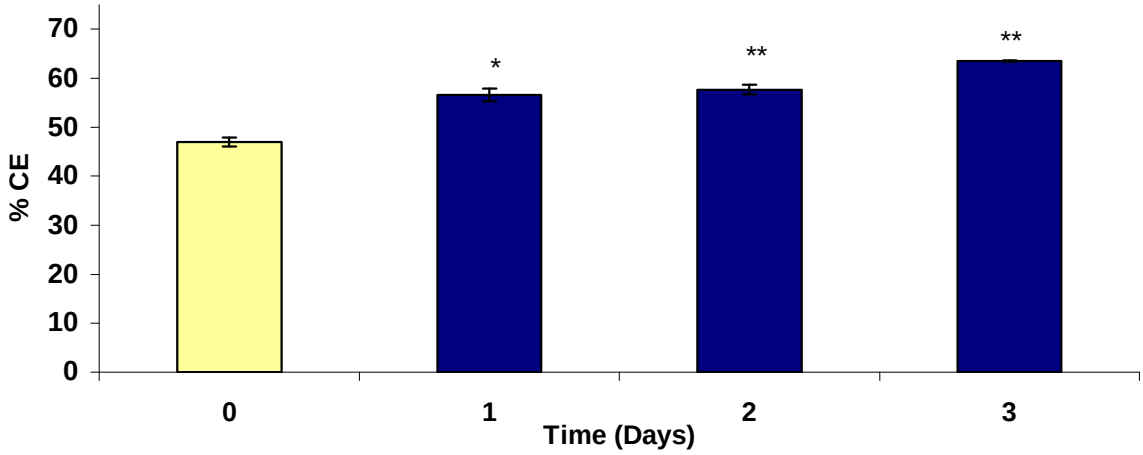

Figure 5.9 Mean percentage esterified cholesterol in plasma from 3 LCAT $^{-/-}$ mice following repeated IP injection of LCAT.

*Bar graph represents the % CE/TC means ± SD. The background basal esterification (0 h) is represented in grey and whilst the % CE at 1, 2 and 3rd day is represented by black. Asterisk * denote statistically significant differences in comparison to pre-injected estrification level using the Student's t-test, with * $p < 0.05$, ** $p < 0.01$.*

A comparison of lipoprotein profiles following single or repeat intraperitoneal injections of LCAT, as determined by agarose gel electrophoresis

Corresponding lipoprotein profile of single LCAT bolus injected (section 5.1.4) versus smaller repeated injected mice (section 5.1.5) were compared. Plasma taken from mice at various time intervals were examined by running 2 μl of each test sample on agarose gel (section 2.5.4), which was then stained with Sudan black. Human plasma was used as a positive control (C). All the LCAT $^{-/-}$ mice had virtually absent HDL bands in their plasma prior to the start of experiment. The VLDL and LDL bands were merged. When LCAT $^{-/-}$ mice were given a single bolus dose injection of purified LCAT, the HDL band progressively became more visible and broader from 1 to 21 h post-injection (Fig 5.10) suggesting some restoration of HDL in plasma. Moreover, changes in VLDL and LDL were noted, but at shorter time intervals (4-6 h) compared with HDL (4-22 h). Levels of VLDL and LDL bands were reduced at 4 and 6 h post injection in mouse (1) and (2) and at 4 h in mouse (3) demonstrating a reduction in level. These findings corresponded with a significant increase in cholesterol esterification from 4 h to 22 h post injection (Fig 5.6). However, there was also evidence for a rebound effect of VLDL/LDL i.e. at 22 h increased compared to 4 and 6 h (Fig 5.10). Interestingly, HDL holds up (most apparent in mice 1 and 2).

When given repeated injections with lower doses of LCAT, there was some evidence of increased HDL appearing during the 1st day until the 3rd day, in particular mice (2) and (3) (Fig 5.11). There was insufficient plasma from mouse (1) on days 2 and 3 for this agarose gel electrophoresis. However, the bands were less prominent compared with the ones with single injections. VLDL and LDL bands did not show any obvious changes on agarose gel electrophoresis. Although repeated injections do work, LCAT $^{-/-}$ mice may need a higher dose of human LCAT (at least 10 μg or more) in order to increase their capacity for cholesterol esterification. The changes in the lipoprotein profile which exhibit a clear increase in HDL (and sometimes a corresponding decrease in VLDL and LDL) suggests that replacement LCAT therapy may have a beneficial effect and could be a practical method for correcting lipoproteins abnormalities.

Figure 5.10

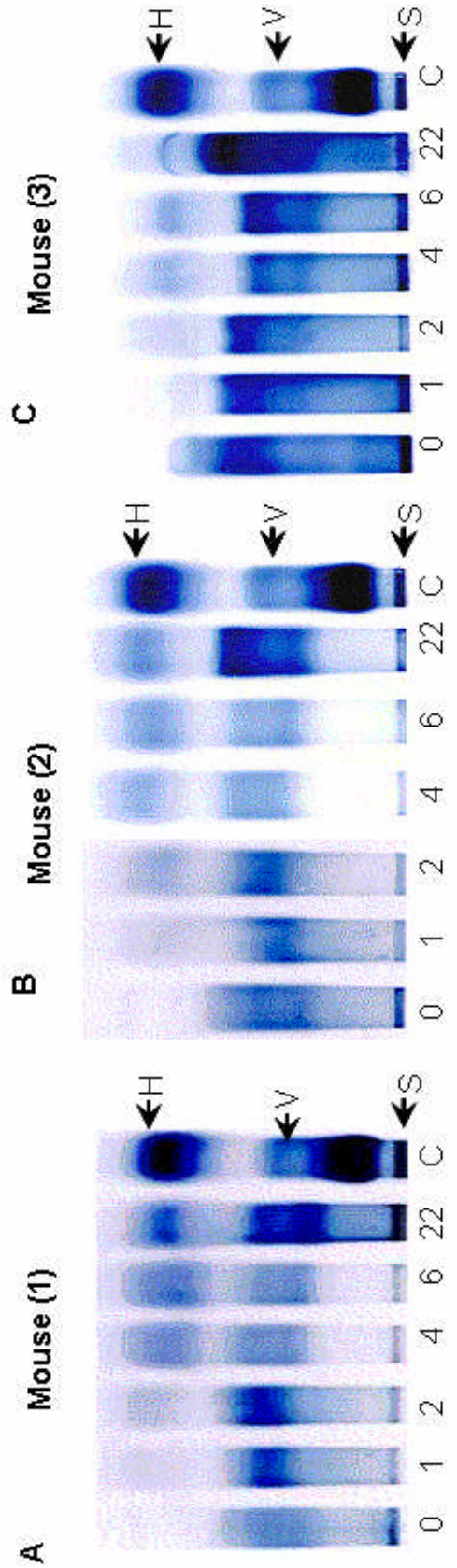

Figure 5.10 Agarose gel electrophoresis following bolus injection of LCAT

Plasma taken from LCAT bolus injected mice (Section 5.1.4) were analysed. Equal 2 µl volumes of plasma obtained from (A) mouse (1), (B) mouse (2) and (C) mouse (3) were taken at various indicated time points and loaded onto the Hydragel and stained with Sudan black. Time points 0, 1, 2, 4, 6, and 22 indicated beneath each lane represents the time 0 hr, 1 hr, 2 hr, 4 hr, 6 hr and 22 hr respectively following bolus injection. C represents the positive control of an equivalent volume of human plasma. The start mark (S) was the lowest level, followed by LDL and VLDL (V) in the 1st migratory level and HDL (H) being the highest mark. HDL bands become broader with time (2-22 h) following injection of LCAT. On the other hand, VLDL and LDL bands become weaker from 2-6 h post- injection but return to darker bands at 22 h in all 3 mice.

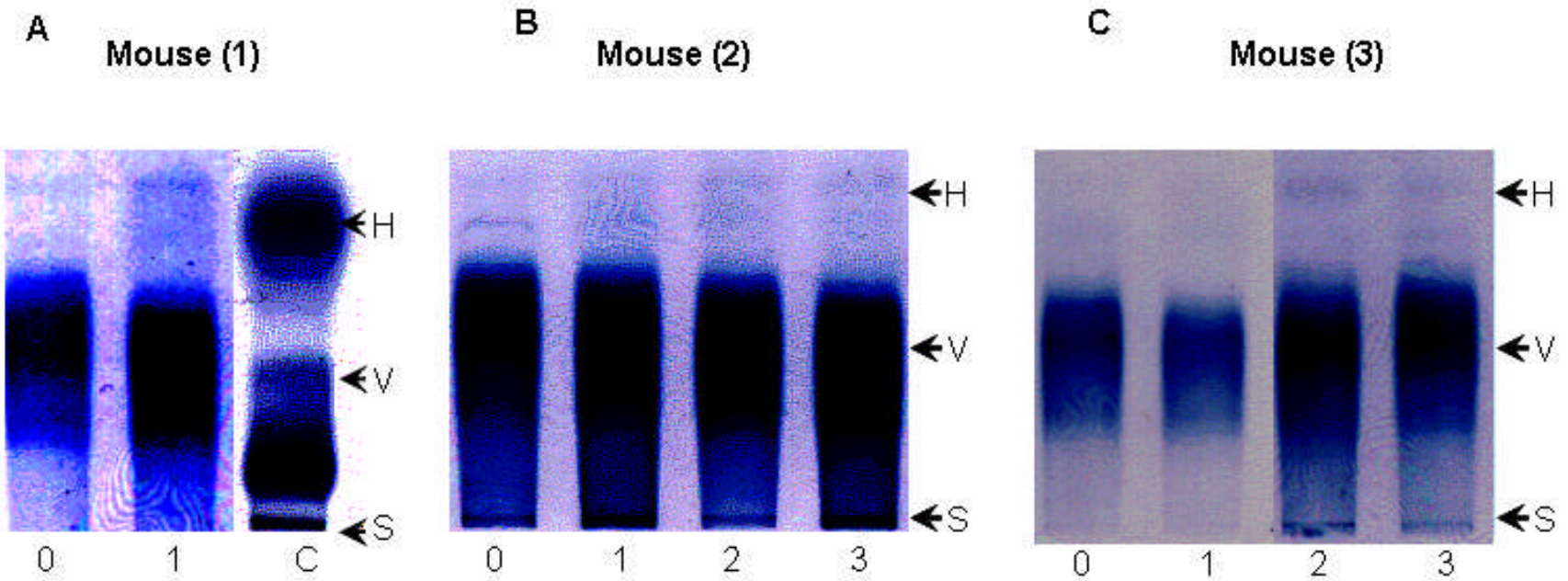

Figure 5.11 Agarose gel electrophoresis of plasma obtained from LCAT-/- mice following repeated injections of LCAT

Plasma from repeated injections of LCAT in LCAT$^{-/-}$ mice (Section 5.1.5) were studied. Equal 2 µl plasma volumes from (A) mouse (1), (B) mouse (2) and (C) mouse (3) were loaded onto a hydragel gel and visualized with Sudan black. Lanes marked 0, 1, 2 and 3 represented prebleed, 1st , 2nd and 3rd day post injection. There was insufficient plasma from mouse (1) on 2nd and 3rd day post injection. As a result only the 1st day was sampled. Human plasma was used as a control. The start mark (S) was the lowest level, followed by LDL and VLDL (V) in the 1st migratory level and HDL (H) being the highest mark. There were faint bands in the HDL region corresponding to human control, C, forming on the 2nd and 3rd days post- injection suggesting limited HDL formation after repeated injection of LCAT in all three mice but there were no discernible changes in the VLDL and LDL bands.

5.1.6 General Discussion

Proteins when used as therapeutic agents have many advantages over chemical compounds. By nature, proteins are specific in their function and thus have less potential to interfere with unrelated pathways, and hence are less likely to produce unwanted side-effects. LCAT's mode of action is very specific and it acts exclusively in the circulatory system. As it cannot be administered orally, the routes of administering were either intravenous or intraperitoneal. Even though the intravenous route gave comparable results with one mouse, the intraperitoneal route was pursued as the route for implanting encapsulated cells. It was interesting to note that LCAT was equally well absorbed from the peritoneal cavity into the portal venous system and then into the general systemic circulation. Intermittent administration when compared with daily bolus injection maintains a steady plasma concentration and significantly improves efficacy of treatment. However, there is a time lag of at least 4 h before esterification of cholesterol becomes significant. This is demonstrated in the bolus injection study and may be related to the time taken for LCAT to be absorbed into the systemic circulation.

We used mammalian (CHO) cells for LCAT expression because it can be stably transfected with an expression vector which produces fully glycosylated LCAT. Unlike the immature high-mannose type LCAT produced by insects which is rapidly cleared by the hepatic mannose receptor (Taylor, 1993), the glycosylated LCAT from CHO cells is postulated to have an extended circulating half-life due to the presence sialic-acid terminated N-glycans to prevent premature clearance. Glycan chains may have a role in increasing the solubility of enzyme in plasma, prevent non-specific binding to cell membranes and may facilitate removal of old desialylated enzyme from plasma. In addition, the glycan chains are necessary for the efficient secretion of LCAT from cultured cells. Removal of individual glycan chains has been shown to affect the enzymic activity (Francone *et al*., 1993, Qu *et al*., 1993, OK *et al*., 1993).

Due to time constraints and the limited number of mice, I have only been able to show the amelioration of reduced esterified cholesterol and low HDL. Other areas of interest which could be looked at in the future include assessing cell membrane abnormalities and kinetic studies of the enzyme. Of importance is also the investigation into any emergence of neutralising antibodies against human LCAT which acts as a neoantigen here since $LCAT^{-/-}$ mice was used. It would not provoke adverse immune responses in cirrhotic mouse or $LCAT^{+/-}$ mouse since human LCAT has very high homology with mouse

In conclusion, LCAT protein will normalize lipoproteins and predict correct membrane lipids. Hence, work from $LCAT^{-/-}$ mouse should equate to liver disease. Patients with liver failure may benefit from short-term intravenous LCAT therapy to reverse lipoprotein abnormalities in order to optimize their condition prior to transplant surgery.

5.2 Microencapsulation

5.2.1 Encapsulation of CHO-H6LCAT cells in Alginate Microspheres

Introduction

Microencapsulation of cells offers a safe method for the systemic delivery of therapeutic protein from genetically engineered cells (Chang, 1997; Chang, 1998). Sodium alginate, a polyanion when mixed with polymers such as poly-L-lysine (PLL), supports growth of cells (Koch *et al*., 2003) in an encapsulated environment. The high porosity of alginate allows for high diffusion rates of macromolecules. Nutrients and oxygen can cross this barrier and desired gene product can be secreted unhindered. Here I encapsulate recombinant CHO cells expressing human LCAT in alginate-based microcapsules and confirm that LCAT protein is secreted and is biologically active *in vitro.*

Materials and Methods

PLL with a MW 25,000 Da (cat no P2636) was purchased from Sigma-Aldrich, and sodium alginate (mannuronic:guluronic, 1:1) from Kelco International. The cells used were CHO-H6LCAT prepared as described in section 2.2.1. The protocol for encapsulation of the CHO-H6LCAT cells was developed by Dr K.A Heald, Worcester Royal infirmary.

The required solutions were prepared according to provided recipes as follows:

(a) Gelling solution

	Weight (g)	**Concentration (mM)**
KCl	0.15	2
$CaCl_2$	14.70	100
HEPES	2.38	10

pH was adjusted to 7.4 with NaOH before making up to the final volume of 1 litre.

(b) Krebs Ringer Buffer (KRB) with Ca^{2+}

	Weight (g)	**Concentration (mM)**
NaCl	6.72	115
$NaHCO_3$	2.02	24
KCl	0.37	5
$MgCl_2$	0.2	1
$CaCl_2$. $2H_2O$	0.367	2.5
HEPES	2.38	10

pH was adjusted to 7.4 with NaOH before making up to the final volume of 1 litre.

(c) Calcium-free Krebs Ringer Buffer (Ca^{2+} -free KRB)

	Weight (g)	**Concentration (mM)**
NaCl	7.89	115
$NaHCO_3$	2.02	24
KCl	0.37	5
$MgCl_2$	0.20	1
HEPES	2.38	10

pH was adjusted to 7.4 with NaOH before making up to final volume of 1 litre.

(d) Ethylene glycol-bis(beta-aminoethyl ether)-N,N,N',N'-tetra-acetic acid (EGTA) solution was prepared by dissolving 19 mg EGTA in 50 ml Ca^{2+}-free KRB

(e) PLL was made up to 0.1% in saline i.e. 0.1 g of PLL in 100 ml normal saline. This was then filtered, aliquoted and stored at –20 ^{0}C until required

(f) Alginate solution was made up to 2-3 % in normal saline.

CHO-H6LCAT cells were grown to confluency in two T75 culture flasks. CHO-*dhfr* $^-$ cells were grown in a separate T75 flask as a negative control. An estimated 12 x 10^6 cells in each flask were suspended in 2 ml of 2 % purified alginate. Large air bubbles were removed and the alginate/cell mixture was loaded into a syringe. The plunger was re-inserted and was attached to a syringe driver (Fig 5.12). The nozzle of the syringe was then connected to the air jacket and the tubing from the air-flow meter

to the air jacket. A collecting vat was placed underneath the syringe. The air flow was 1.5 ml/min upon switching on the syringe pump.

Alginate droplets gelled in 0.1 M $CaCl_2$ solution. These beads were collected in a 50 ml tube and washed 3 times in KRB with Ca^{2+} (each time allowing the beads to settle, decanting supernatant and refilling to 25 ml mark). After the final wash, the beads were suspended in 10 ml KRB with Ca^{2+}. PLL (10 ml) was then added to the suspension and incubated for 9 mins (final concentration of PLL: 0.05 %). The beads were washed 3 times in Ca^{2+} -free KRB solution followed by incubation in 0.2 % alginate for 5 min. Finally, the beads were incubated in 1 mM EGTA (5 mls) for 10 min to liquify inner alginate. They were washed once in Ca^{2+} -free KRB, twice in KRB with calcium, and once in fresh culture medium. Encapsulated CHO-H6LCAT and CHO-*dhfr* $^-$ cells were grown in respective growth medium and 24 h collections were carried out. The samples were centrifuged and the supernatant was assayed for LCAT activity (section 2.2.3), converting the results to its equivalent LCAT mass. Viability of the cells was checked 10 days later with trypan blue staining.

Results and Discussion

Several attempts were made to encapsulate the CHO-H6LCAT cells with PLL of MW 25,000 Da. However, LCAT assays on the samples collected over a period of 4 weeks did not show any LCAT in the medium. Nevertheless, the cells within the capsules had been proliferating when viewed under the microscope. Trypan blue stained the outer coat of the capsules but was unable to enter the capsules and did not stain the cells within. When the capsules were ruptured, the cells adhered to the cell culture flask and proliferated. We know from our laboratory *in vitro* studies on encapsulation of apoE recombinant CHO cells (Tagalakis *et al.*, 2005), that the small apoE molecule (34-kDa) was secreted into the medium. My results suggest that the pore size of the capsules prevented the larger 64-kDa LCAT molecule from being excreted, but did not prevent nutrients from entering the capsule as the cells remained viable. Perhaps there was also a feedback inhibition mechanism to reduce LCAT secretion as the concentration of LCAT built up within the microcapsule, but the proliferation of cells was not restricted.

It has been shown previously that the molecular weight cut-off values of the capsule membrane can be controlled by varying the molecular weight (the lower the molecular weight of PLL, the less permeable the capsules) and the concentration of PLL, as well as the contact time between alginate and PLL (Goosen *et al.*, 1999).

Alginate gels made from high guluronic acid content are more porous and exhibit high diffusion rates for proteins (Thu *et al*., 1996). The charge on a protein can also influence its rate of diffusion from an alginate based capsule. A protein with a high pH and overall net positive charge can potentially interact with the negatively charged alginate polymer, thus inhibiting diffusion from the capsules.

Further attempts were made to increase the pore size of the microcapsules by encapsulating LCAT-CHO cells using a higher molecular weight of PLL (50,000 Da) and reducing the incubation time from 9 min to 8 min. The encapsulation was performed using duplicate T75 flasks of CHO-H6LCAT cells and one T-75 flask of CHO-*dhfr* $^{-}$ cells as control. The encapsulated cells were transferred back into their respective flasks containing 15 ml of normal growth medium. For the first month, medium was collected every 24 h and in the second month, every 48 h and a final collection at the end of the 3rd month. LCAT was detected in the medium by performing the radioactive cholesterol esterification assay (section 2.2.3).

During the initial 2 days, LCAT production increased as the encapsulated cells adapted to their new environment. After the third day post-encapsulation, the LCAT production was steady at approximately 1 μg/24 h for 2 weeks and this was followed by a gradual rise to 1.5 - 2 μg/24 h towards the end of the 1st month (Fig. 5.13). In the 2nd month of study, as I anticipated a fall in LCAT production, I collected the medium over a 48 h period so that the LCAT concentration in the medium was measurable. It showed in principle that LCAT was still being secreted with Flask (1) generating 1.3-2.1 μg/48 h (Fig 5.14). The production in Flask (2) was ~1.0 μg/ml/48 h during the first 2 weeks of the 2nd month but declined to ~0.7 μg/ml/48 h at the end of the 2nd month (Fig. 5.14). After 12 weeks, LCAT was still detectable with each flask of encapsulated cells giving ~0.6-0.8 μg/48 h. Unencapsulated and encapsulated CHO-*dhfr* $^{-}$ cells acting as controls, were grown simultaneously in T75 flask containing growth medium with hypoxanthine and thymidine supplements and without Mtx. Throughout the period of encapsulation study, there was no LCAT activity detectable in the controls. Western blot (section 2.5.7) confirmed that LCAT was secreted by encapsulated cells and it displayed the same migration properties as LCAT from non-encapsulated cells (Fig 5.15).

LCAT production of the encapsulated cells increased during the latter half of the 1st month. This could be due to the proliferation of cells within the microcapsules. However, after 6 weeks, the LCAT production seemed to have decreased in both flasks. One explanation would be the physical limitation of the microcapsules as cells reached a state of full occupancy and proliferation of cells was halted. Soon a critical state arose

where some cells within the centre of the microcapsules could not receive adequate gas exchange and supply of nutrients and hence they began to die. Flask 1 also shows a fall and then a rise in LCAT production in 2nd month. One possibility is that the cells may die off but the space gets re-populated with proliferating cells again which continue to secrete LCAT and hence may explain the rise in LCAT production in the later in the 2nd month. Nevertheless, there was a sustainable amount of LCAT being secreted by the encapsulated cells to proceed with implanting these encapsulated cells into the peritoneal cavities of LCAT $^{-/-}$ mice and study its effects.

Syringe Pump

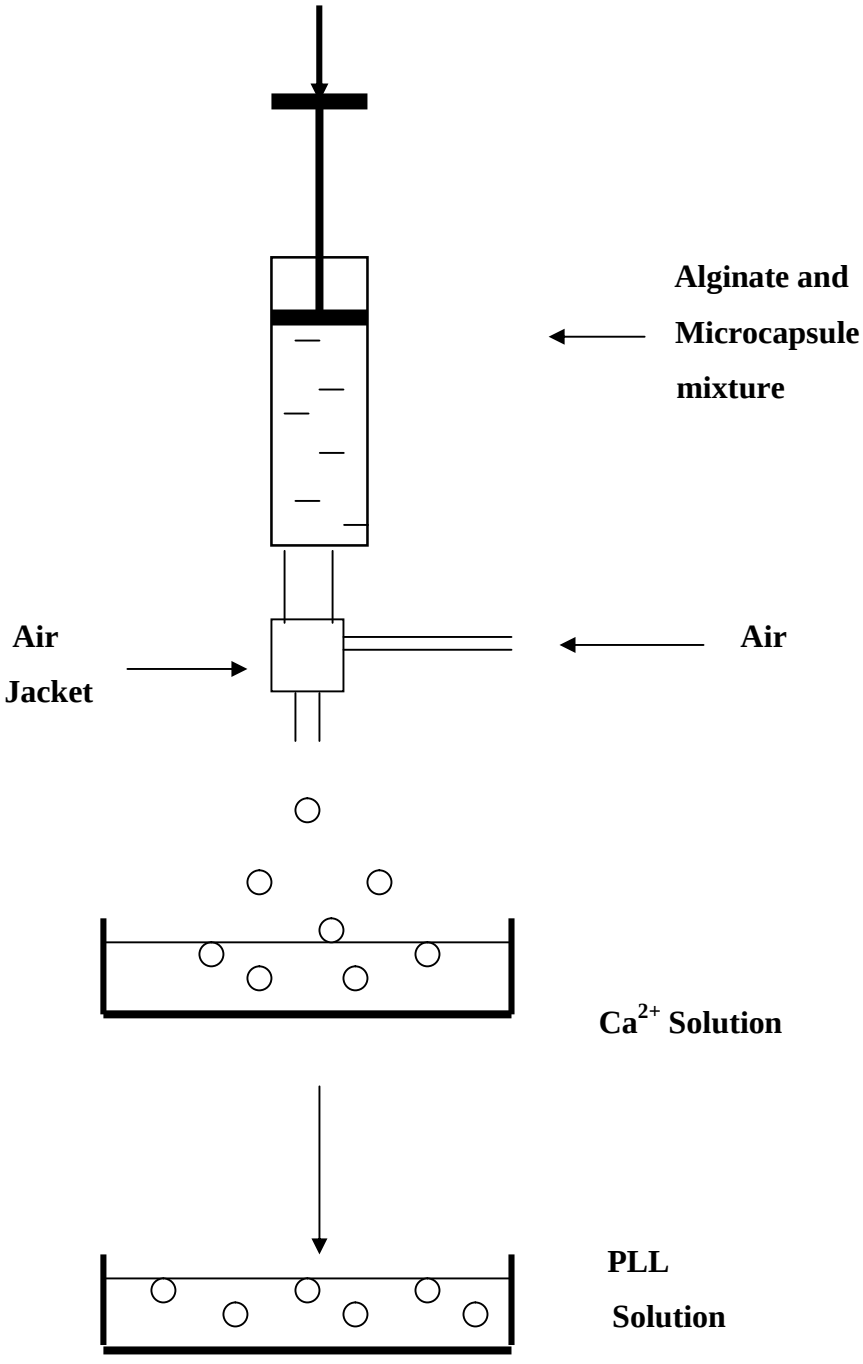

Figure 5.12 Technique of encapsulating cells

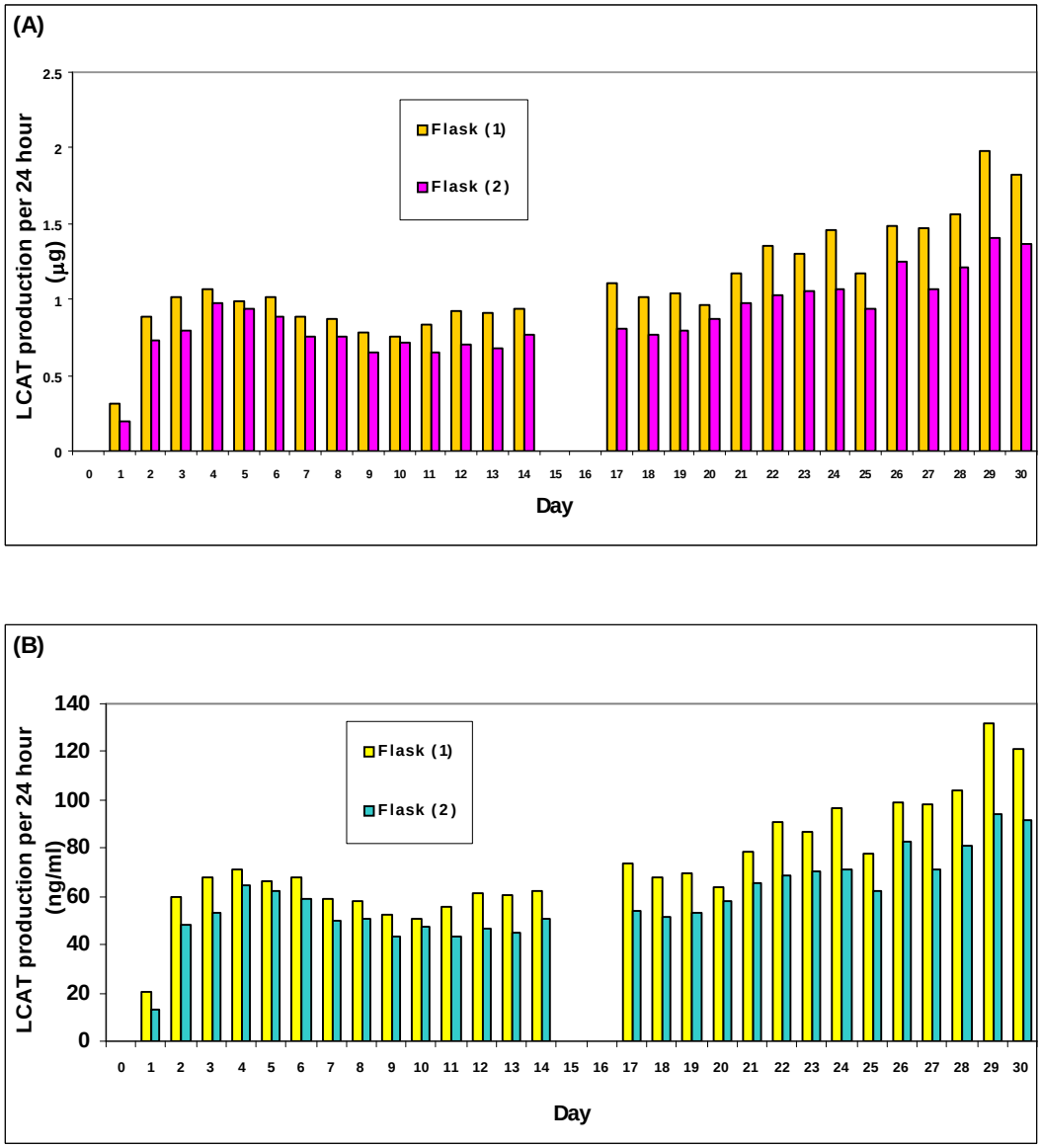

Figure 5.13 LCAT production by encapsulated CHO-H6LCAT cells during the 1st month

Encapsulated CHO-H6LCAT cells were grown in a T75 flask containing 15 ml normal growth medium. Collections of medium were made every 24 h throughout the 1st month except days 15 and 16. Medium collected was assayed for LCAT activity (see 2.2.3) and the result was converted to (A) its equivalent LCAT mass expressed as µg/24 h/flask in the top bar chart and (B) ng/ml/24 h in the bottom bar chart.

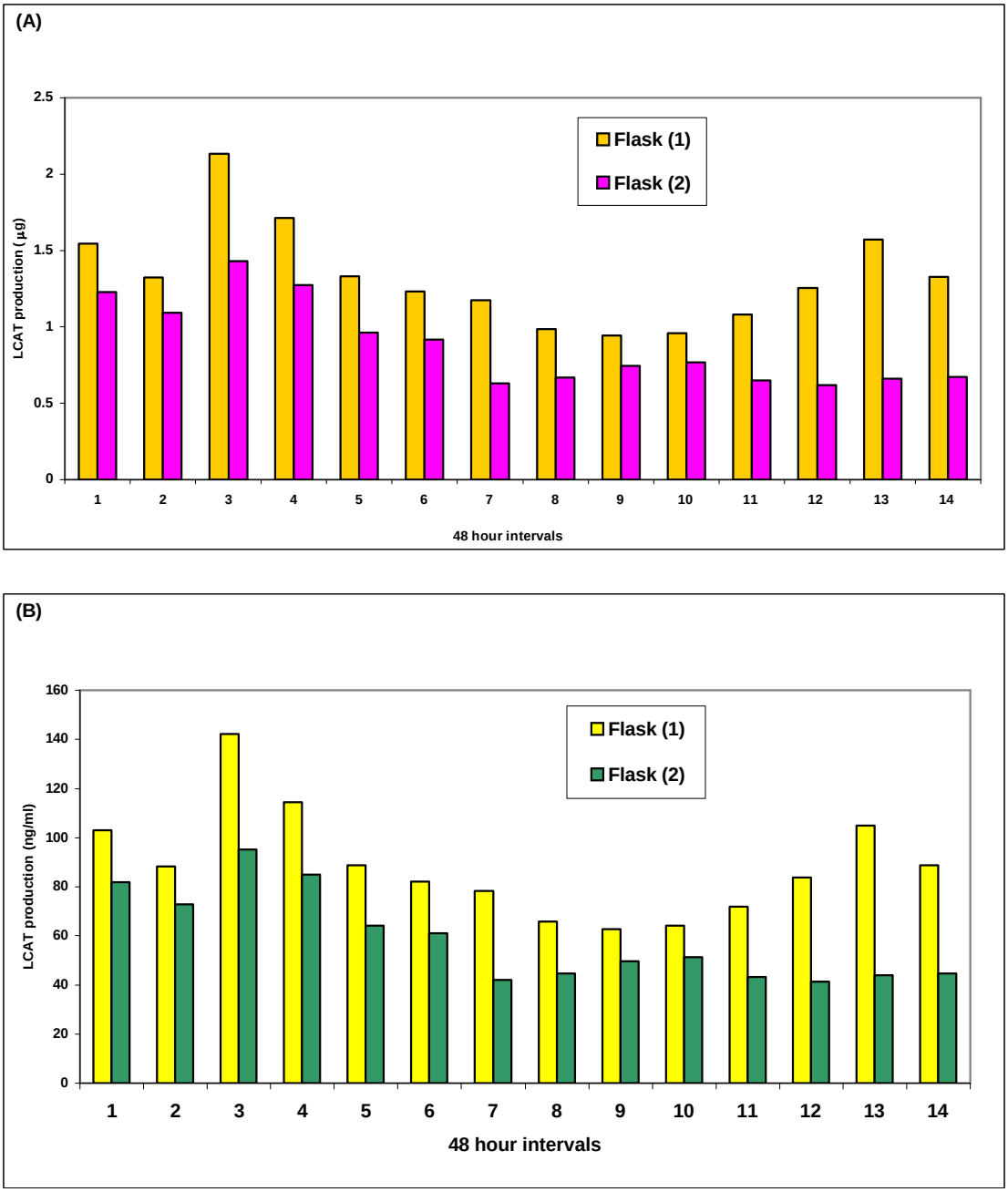

Figure 5.14 LCAT production by encapsulated CHO-H6LCAT cells during the 2nd month

The encapsulated cells continued to be grown in a T75 flask containing 15 ml normal growth medium. Collections were every 48 h and the medium assayed for LCAT. (A) Graph shows the amount of LCAT secreted per flask (µg/24 h). (B) Graph shows the concentration of LCAT (ng/ml) secreted each day.

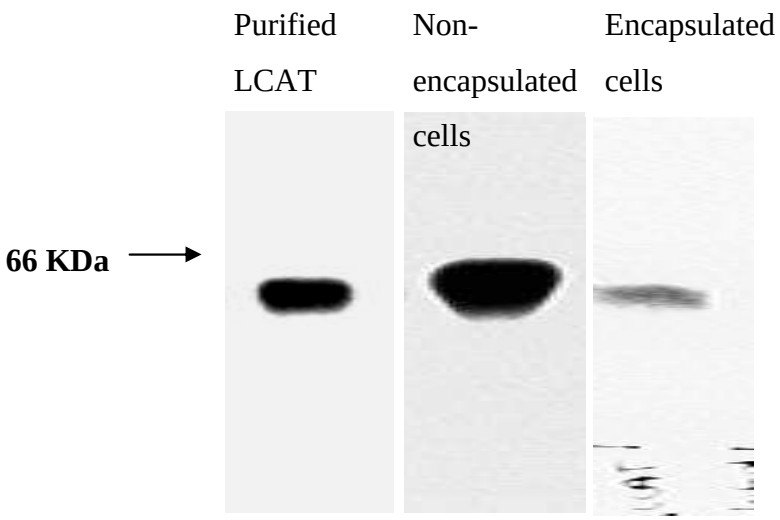

Figure 5.15 Western blot showing LCAT secretion by non-encapsulated and encapsulated cells

With the purified LCAT acting as a control, LCAT secreted from non-encapsulated and encapsulated cells were loaded onto agarose gel. All migrate to the same level.

5.2.2 Cell therapy - implantation of microencapsulated cells into peritoneal cavities of mice

<u>Study A</u> – a 4 day pilot study

This study was designed to determine if LCAT was secreted when implanted into LCAT $^{-/-}$ mice. The ability of the secreted LCAT to restore some of the plasma lipid abnormalities was also investigated.

Materials and Methods

CHO-H6LCAT cells were encapsulated as before (5.2.1) by suspending ~12 x 10^6 cells in 2 ml of alginate. The encapsulated cells were transported to the animal laboratory in normal growth media. The latter was removed and the microcapsules were washed with PBS several times to remove any remaining medium that might cause subsequent antigenic reaction. Microcapsules were then drawn into a 2 ml syringe via a large bore 18G needle. Three 18 months old female LCAT $^{-/-}$ mice were implanted with microcapsules in their peritoneal cavity. Two were injected with 1 ml of microcapsules secreting 7.4 μg/ml of LCAT. The third (control) mouse was injected with encapsulated CHO cells. Tail bleeds were taken prior to injection and at 4 h, 1, 2, and 4 days following injection. LCAT, total cholesterol and free cholesterol assays were performed as described in section 2.2.3 and 2.5.

Results and Discussion

Following the injection of the microcapsules, a small amount of LCAT (54 ng/ml) was detected in mouse (1) after 4 h (Fig 5.16-A). On the 1st and 2nd day, LCAT was found in the plasma of both mice implanted with LCAT secreting cells. It was higher on the second day rising to approximately 270 ng/ml in mouse (2) (Fig 5.16-A). However, LCAT was not detectable on the 4th day. Throughout the period of study, the control LCAT $^{-/-}$ mice did not have any detectable LCAT in its plasma. The plasma of mouse (1) showed an increase in esterified cholesterol on the 4th day (Fig 5.16-B) but there was no detectable esterified cholesterol on 2nd day again suggesting the possibility of a lag phase in esterification as demonstrated in section 5.1.4. Alternatively, this could be due to an error in sampling or the assay not working for this sample. Agarose gel electrophoresis demonstrated HDL formation in the plasma of the mice injected with microcapsules secreting LCAT, but no visible HDL band in the control mice (data not

shown). Therefore implantation of encapsulated cells secreting LCAT appears to be feasible therapy for LCAT $^{-/-}$ mice but will need further evaluation and optimization.

A

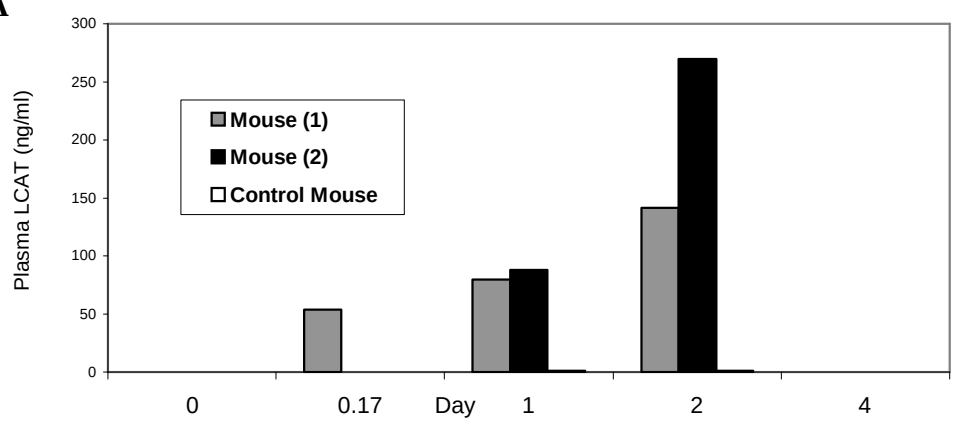

B

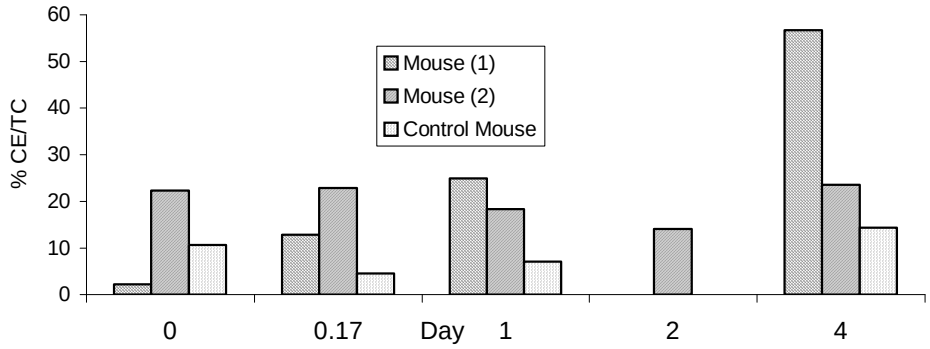

Figure 5.16 Study A – 4 day pilot study

(A) Plasma LCAT concentration (ng/ml) following peritoneal implantation of encapsulated CHO-H6LCAT cells in LCAT$^{-/-}$ mice. One ml of encapsulated CHO-H6LCAT cells was injected into the peritoneal cavity of two LCAT $^{-/-}$ mice (mouse 1 (grey) and 2 (black)) but control mouse (white) received only encapsulated CHO cells which did not secrete LCAT. Blood was collected pre- and 4 h, 1, 2 and 4 days post implantation and assayed for LCAT activity. The plasma LCAT concentration was expressed as ng/ml. (B) Esterification of cholesterol following implantation of CHO-H6LCAT cells in LCAT$^{-/-}$ mice. One ml of encapsulated CHO-H6LCAT cells was injected into the peritoneal cavity of two LCAT $^{-/-}$ mice, mouse 1 (grey)) and mouse 2 (black) with control mouse (white) receiving encapsulated CHO cells. Tail bleeds were taken from the three mice at 0, 4 24 48 h and 4th day and plasma collected was assayed for free and total cholesterol. The plasma cholesteryl ester content was calculated and expressed as a percentage of the cholesterol.

Pilot Study B – a second short-term (4 day) study

In order to verify the results of the first pilot study, a further second study with four LCAT $^{-/-}$ mice were undertaken.

Materials and Methods

CHO-H6LCAT cells were encapsulated as before (5.2.1) by suspending ~12 x 10^6 cells in 2 ml of 2 % alginate to produce microcapsules with the same cell density per capsule as in pilot study A. The encapsulated cells were placed in normal growth medium before injection. The following day LCAT secretion was confirmed by proteoliposome assay. Three female LCAT $^{-/-}$ mice, 2 months of age, were each injected with 1 ml of microencapsulated CHO-H6LCAT cells. One mouse was injected with empty capsules. Tail bleeds were taken prior to injection and at daily intervals for 4 consecutive days. The samples were centrifuged and aliquoted for LCAT assay (section 2.2.3), total cholesterol, free cholesterol (section 2.5) and agarose gel (section 2.5.4) analysis.

Results and Discussion

Mouse (A) recorded a small increase in plasma LCAT concentration from 47 ng/ml on the 1st day to 89 ng/ml on the 3rd day (Fig. 5.17-A). In mouse (B) LCAT was detected on the 2nd day and there was sustained level of LCAT concentration, ~50 ng/ml till 4th day. However, in mouse (C), there was a modest increase in LCAT concentration on 1st day (120 ng/ml) to 3rd day (280 ng/ml) but this declined to ~ 50 ng/ml on the 4th day (Fig. 17-A). No LCAT was detectable in the control mouse throughout the 4 day period.

The percentage of esterification in mouse (A) increased on 3rd and 4th day (Fig 5.17-B) which weakly corresponded to the small increase in LCAT concentration seen (Fig 5.17-A). Mouse (B) basal esterifcation was 26 % and increased to 33 % on the 1st day before returning to its basal level. Mouse (C) showed a steady basal esterification of 39 % but fell to less than 20 % on day 4. Analysis by agarose gel electrophoresis (Fig 5.18) showed some HDL formation from day 2-4 in mouse (A). Although mouse (B) demonstrate the presence of LCAT, it was probably insignificant to cause any real change in the percentage of esterification which corresponded to the absence of HDL on agarose gel (Fig 5.18). Mouse (C) with the biggest rise in LCAT concentration, showed HDL formation from day 1-4 on agarose gel.

A

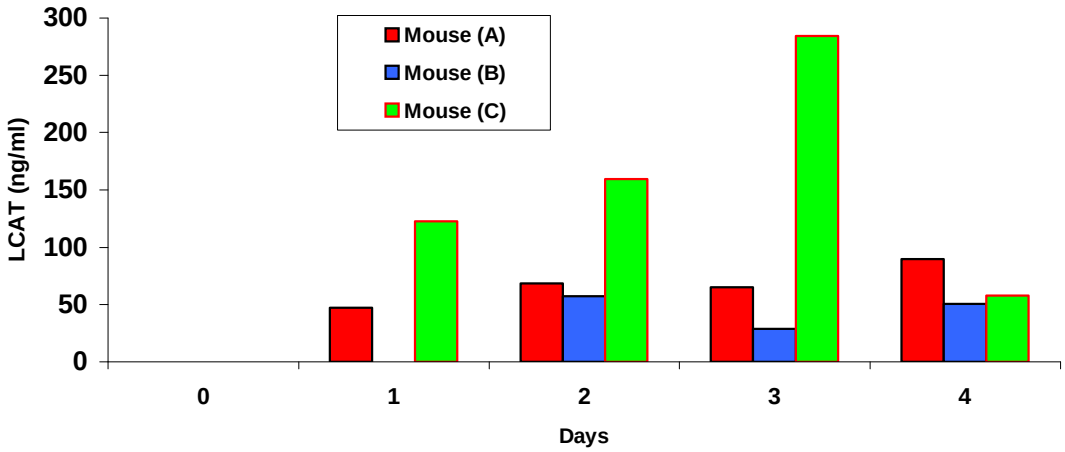

B

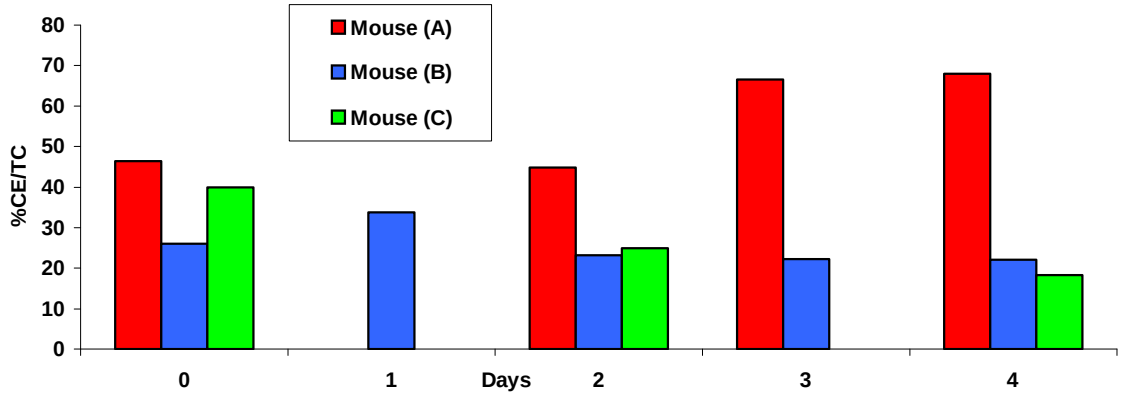

Figure 5.17 Study B – second 4 day study

(A) Plasma LCAT concentration (ng/ml) following peritoneal cavity implantation of encapsulated CHO-H6LCAT cells Three LCAT$^{-/-}$ mice were each injected with 1 ml of encapsulated CHO-H6LCAT cells. Tail bleeds were taken prior to injection and on the 1st, 2nd 3rd and 4th days post- injection. The plasma was assayed for LCAT activity and the corresponding LCAT mass was calculated. The bar chart above shows the plasma LCAT concentration in ng/ml. Control mouse (not shown) did not show any LCAT activity in its plasma on all test days (B) Three LCAT$^{-/-}$ mice were each injected with 1 ml of encapsulated CHO-H6LCAT cells. Tail bleeds were taken prior to injection and on the 1st, 2nd 3rd and 4th days post-injection. Free and total cholesterol assay were performed on the plasma. Cholesteryl ester was indirectly determined and the percentage of esterified cholesterol in the plasma is shown.

Figure 5.18

Figure 5.18 Detection of HDL by agarose gel electrophoresis

Plasma from all three LCAT-/- mice that were injected with 1 ml of encapsulated CHO-H6LCAT cells was obtained from tail bleeds at pre-injection and post-injection (1st-4th day). Equal volumes (2 μl) of plasma from mouse (A), (B) and (C) were loaded onto a Hydragel following electrophoresis, and stained with Sudan black. Pre-injection, day 1-4 were represented by 0-4 (S) at the bottom of the gel. Human plasma denoted by C was used as a control marker. The presence of HDL (H) and VLDL/LDL (V) was determined by comparing the migratory pattern in the control. Note that for mouse (A) on the 1st day, insufficient plasma was available so this lane was left empty.

Study C – a longer-term (14 day) study

Based on the initial 4 day studies, a greater number of mice were implanted with the encapsulated cells to verify the feasibility of enzyme delivery over a longer time period (14 days).

Materials and Methods

The maximum volume permitted per injection in mice is about 1 ml. In an attempt to boost the level of plasma LCAT in the $LCAT^{-/-}$ mice, the cell density in each microcapsule was nearly doubled by suspending ~24 x 10^6 cells in 2 ml of alginate. CHO-H6LCAT cells were encapsulated using the same method as described before (section 5.2.1). The encapsulated cells were placed in normal growth medium before injection. The following day the medium was collected and assayed for LCAT. Having confirmed that LCAT was secreted, the encapsulated cells were washed with PBS and 1 ml of the encapsulated cells was transferred into individual syringes. Empty capsules were also prepared in the same manner.

The remaining encapsulated cells were placed back into a T75 flask containing 15 ml of normal growth medium and were cultured in the incubator. The medium was collected at 24 h intervals from the 2^{nd} to 15^{th} day. The 1^{st} day was omitted because there was less than 20 h of incubation. New growth medium (15 ml) was added every 24 h. LCAT secretion was monitored by the LCAT assay. These acted as an additional control for the encapsulated cells, but in an *in vitro* environment.

In this experiment, five (2 months old) male $LCAT^{-/-}$ mice were selected. Unfortunately, no female $LCAT^{-/-}$ mice, which were used in studies A and B, were available. Tail bleeds were performed one day before the injection. The mice were starved of food for 4 h before each bleed throughout the period of study, but had free access to water. Immediately after the injection, they were fed with their normal diet.

Four mice (A-D) were injected with 1 ml of encapsulated cells and mouse (E) with 1 ml of empty capsules as a control. Tail bleeds were performed on the 1^{st}, 4^{th}, 8^{th} and 14^{th} days following injection. When the bleeds were collected, they were immediately transferred onto ice. The samples were then centrifuged at 13,000 rpm for 10 min. The plasma was separated and aliquoted for LCAT, free and total cholesterol assays. The remainder was set aside for agarose gel electrophoresis. At the end of the experiment, all the mice were killed by CO_2 inhalation and the microcapsules were retrieved through a small abdominal incision by washing the peritoneal cavity with sterile saline.

Results and Discussion

On the 2nd day, ~ 0.9 μg/ml of LCAT was being secreted by the *in vitro* control (encapsulated) cells (Fig 5.19). After one week, this declined to ~ 0.6 μg/ml, but increased to 0.7-0.8 μg/ml of LCAT being secreted into the medium towards the end of 2 weeks. Despite a higher cell density in each microcapsule, the LCAT production was slightly lower than my previous *in vitro* study (section 5.2.1). Due to the high cell density, encapsulated cells may not be receiving sufficient oxygen and nutrient supply. In addition a new batch of PLL (cat no 1274) purchased from Sigma-Aldrich with higher molecular weight (70, 000 Da) was used. As a result, the pore size may have changed and thus limited the amount of LCAT secreted out of the microcapsules.

Plasma assays prior to implantation (Fig 5.20) showed a small amount of LCAT was present in mouse (A) (125 ng/ml) and mouse (C) (111 ng/ml). This was an unexpected finding as there may be an error in the sampling or that LCAT assay is not reliable at very low values. However, LCAT was not present in the prebleed samples of mouse (B) and (D) and the control (E).

On the 1st day following the implantation, there was ~ 234 ng/ml of LCAT in mouse (A) plasma (Fig 5.20). On the 4th day, the serum of mouse (A) recorded a peak LCAT concentration of ~ 1.3μg/ml. And by the 8th and 14th day, LCAT concentration had declined to ~ 240 ng/ml and 32 ng/ml respectively. In mouse (B), no LCAT was detectable on the 1st day but 361 ng/ml of LCAT was demonstrated on the 4th day. More than 80 ng/ml of LCAT was detected on 8th and 14th day of study. Mouse (C) had ~ 100 ng/ml of LCAT on the 1st day, which increased to 234 ng/ml on the 4th day before declining to 138 ng/ml and 31 ng/ml on the 8th and 14th days. Apart from the 4th day (195 ng/ml), LCAT was not detected in mouse (D) throughout the study. For all the four mice (A-D), day 4 was the peak of plasma LCAT activity. Nevertheless, the amount of LCAT in mouse plasma secreted from the encapsulated CHO-H6LCAT cells secretion was poor except for mouse (A) though mice (B-D) were consistent with studies A and B.

In terms of plasma esterified cholesterol, mouse (A) showed a substantial increase in percentage, achieving more than 60 % compared with 20 % in the control mouse on the 4th day (Fig 5.21). The remaining mice did not show any changes. Agarose gel electrophoresis (Fig 5.22) was performed on plasma samples from all four mice following implantation of microcapsules. Human serum was used as a control marker. The presence of HDL and VLDL/LDL was determined by comparing the migratory pattern in the control. There was some formation of HDL in mouse (A) and

mouse (D) as indicated by weak bands (Figure 5.22). In mouse (A), VLDL and LDL bands were weaker on 4^{th} and 8^{th} day suggesting a reduction in level and this correspond with the timing of increased plasma LCAT. Mouse (B) and mouse (C) as well as the control showed no changes.

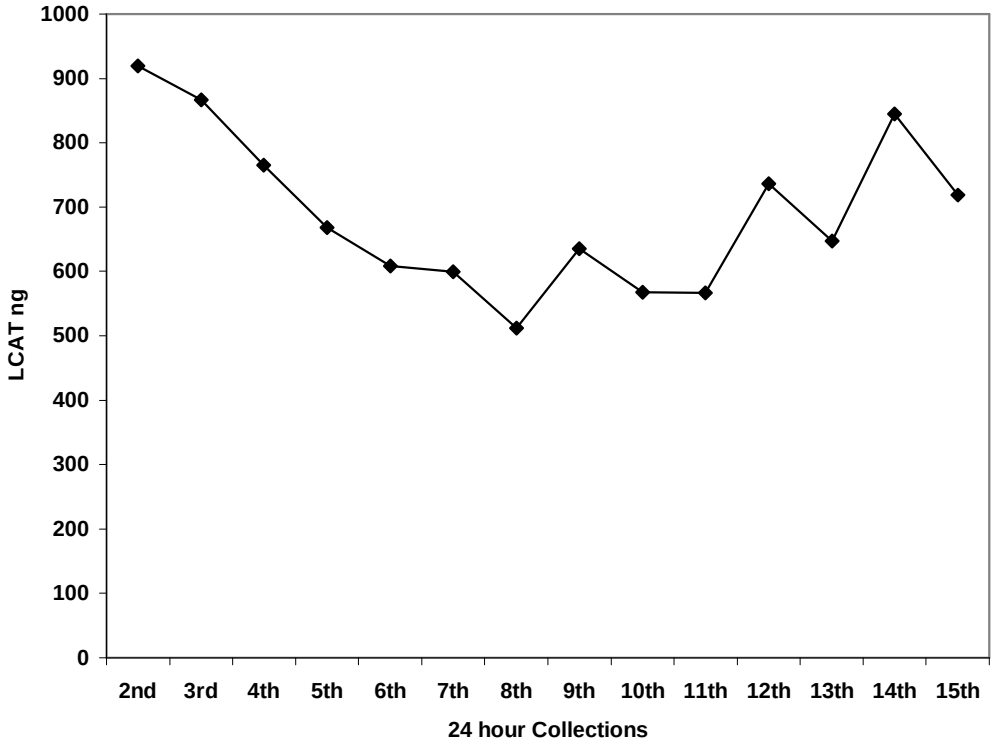

Figure 5.19 Expression and release of LCAT from encapsulated CHO-H6LCAT cells *in vitro*.

One milliliter of encapsulated cells was grown in a T75 flask containing 15 ml of normal growth medium. Daily collections of the medium were made and assayed for LCAT. It was expressed as LCAT mass (ng).

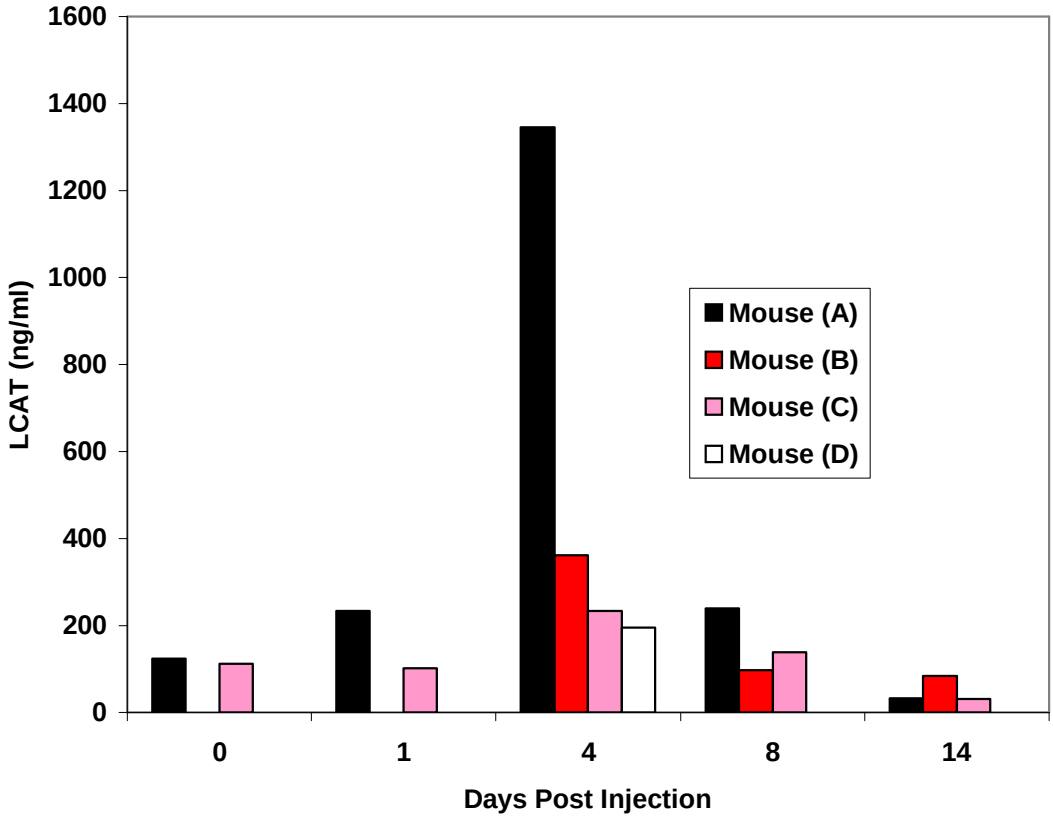

Figure 5.20 Plasma LCAT concentration following implantation of encapsulated CHO-H6LCAT cells

Equal volumes (1 ml) of encapsulated CHO-H6LCAT cells were injected into four LCAT$^{-/-}$ mice. Plasma was obtained through tail bleeds taken at 0 (pre-injection), 1, 4, 8 and 14 day following implantation. The samples were assayed for LCAT activity and the final results expressed as ng/ml.

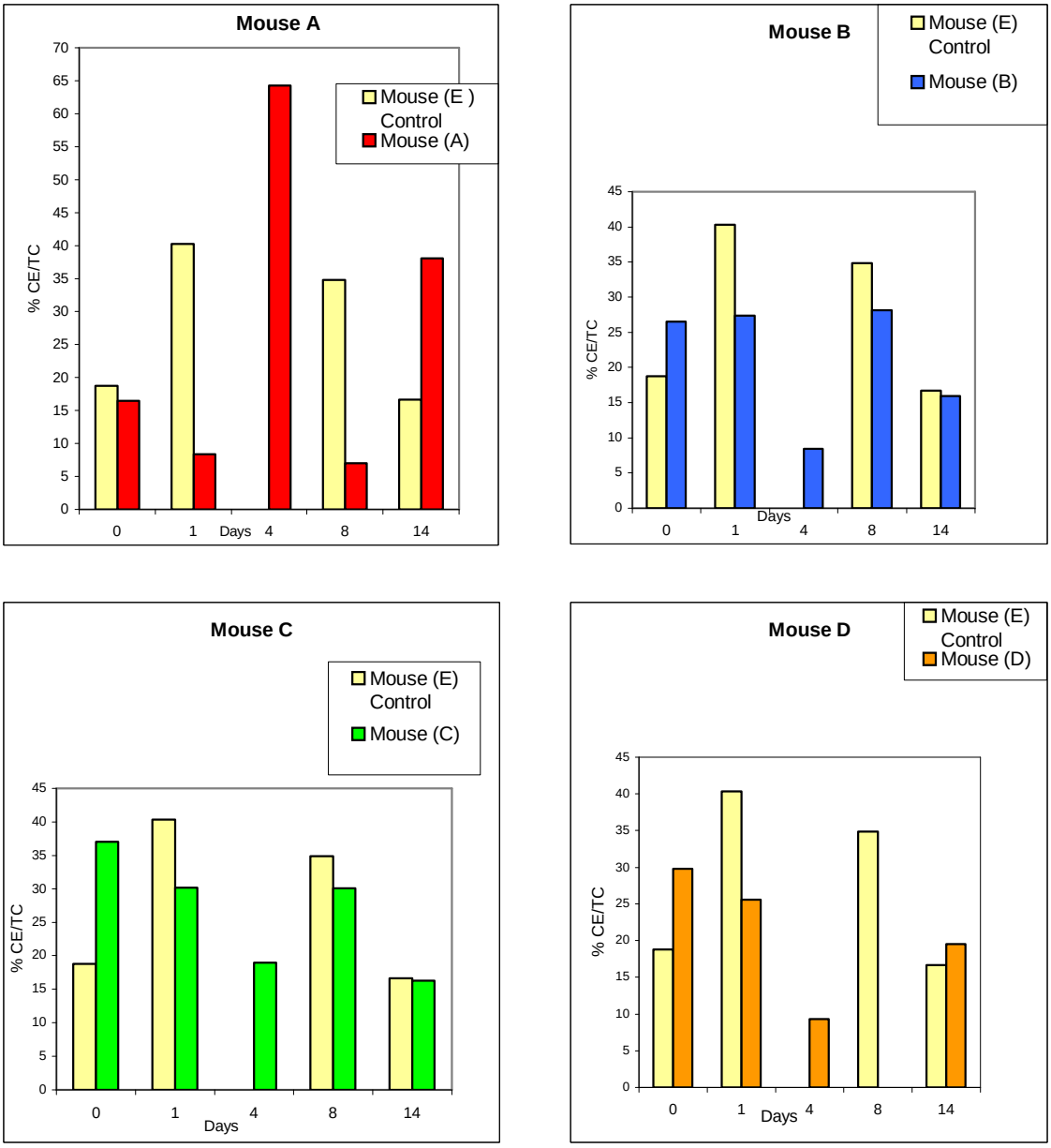

Figure 5.21 Percentage of esterified cholesterol in plasma following implantation of encapsulated CHO-H6LCAT cells

After 1 ml of encapsulated CHO-H6LCAT cells were injected into 4 LCAT$^{-/-}$ mice, tail bleeds were taken at pre-injection, 1, 4, 8 and 14 days post-implantation. The amount of free and total cholesterol was measured and the percentage as cholesteryl esters was calculated. The % CE/TC of each mouse (A to D) is shown in separate bar charts and compared to the control mouse (E).

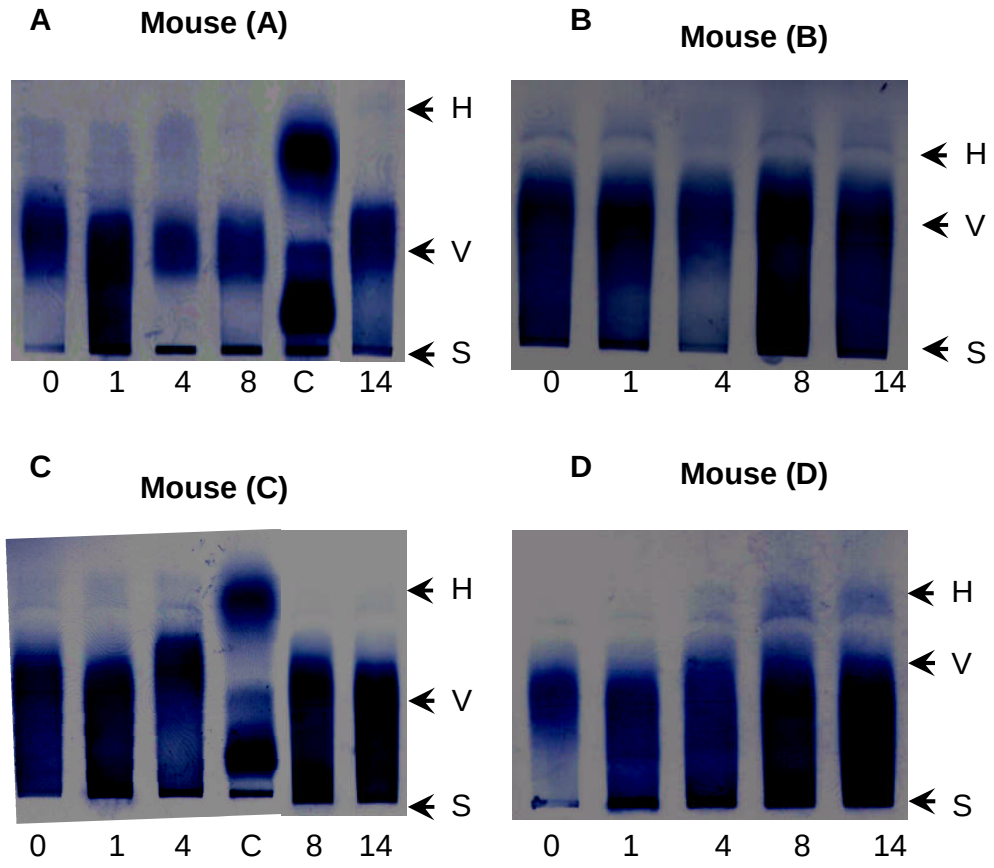

Figure 5.22 Agarose gel electrophoresis

Plasma (2 μl) taken from each of the four LCAT-/- mice following implantation of microcapsules, was separated on (agarose) Hydragel and stained with Sudan black. Pre-injection, day 1, 4, 8 and 14 samples were represented by 0, 1, 4, 8 and 14 at the bottom of each lane. Human serum denoted by C was used as a control marker. The presence of HDL(indicated by H) and VLDL/LDL (indicated by V) was determined by comparing the migratory pattern in the control. There was some formation of HDL in mouse (A) and mouse (D) as indicated by the appearance a faint band. The rest of the mice as well as the human control, showed no changes.

5.2.3 Histological Examination

Pre-implantated capsules are macroscopically clear and spherical in shape. Under microscopy, they appear as round capsules surrounding numerous cells (Fig 5.23-A, B and C). An increased aggregation of cells was observed within the microcapsules (Fig 5.23-B) indicating that cell proliferation had taken place. On average, the diameter of the microcapsules was 650-700 μm before and after implantation. Under higher magnification, the outer layer of PLL and inner layer of alginate can be visualized (Fig 5.23-D).

At autopsy of the mice most of the microcapsules examined had retained their original shape except for a few misshapen capsules mainly from mouse (C) and (D). Microcapsules retrieved from control mice (second short-term 4 day study) showed some empty capsules coated in varying degrees by a layer of cells (Fig 5.24-A,B). A magnified view of the coated microcapsule is shown in Fig 5.24-C.

In those mice injected with encapsulated cells, some of the microcapsules retrieved showed increased in cell density and multiple groups of cells appear within the capsules, consistent with cell proliferation (Fig 5.25-A,B). However in Fig 5.25-C, two microcapsules showing early signs of external coating with thin layer of cells compared with 3 other normal looking microcapsules although some degree of cell proliferation had occurred.

In the longer-term (14 day) study, microcapsules retrieved from implanted mice at day 14, were found in big clumps within the peritoneal cavity (Fig 5.25-D). Macroscopically, the contents of the microcapsules appeared opaque and coated with a thick layer consisting of coagulated cell debris, secreted extracellular matrix or inactivated proteins from the ascitic fluid in the peritoneal cavity which was absent from pre-implanted capsules (Fig 5.23). When these capsules were ruptured, there were no viable cells observed in *in-vitro* culture medium.

Under microscopy, a thin layer of cells is seen coating the empty microcapsule that was retrieved from control mouse. Haematoxlyin and eosin which stain nucleus (blue) and cytoplasm (pink) confirm a layer of cells covering the surface of the microcapsules (Fig 5.26-A,B). Those microcapsules which had encapsulated cells showed more intense fibrous overgrowth on the surface. With haematoxlyin and eosin stain, a thicker layer of cells is seen coating externally (Fig 5.26-C,D). Mr John Auld, senior scientific officer in the Histopathology Department, Royal Free Hospital, characterised these cells further using markers for fibroblasts (CD34), monocytes

(CD15) and macrophages (CD68); they were positive for all three cells. Many of the retrieved microcapsules showed a fibrous overgrowth on the surface.

When the microcapsules were retrieved from the peritoneal cavities especially from mice (B), (C) and (D) (14 day study), microscopic examination revealed that many had lysed and were empty of cells. Only some of the retrieved CHO-H6LCAT cells remained viable and proliferated, whilst the majority were non-viable as confirmed by trypan blue staining.

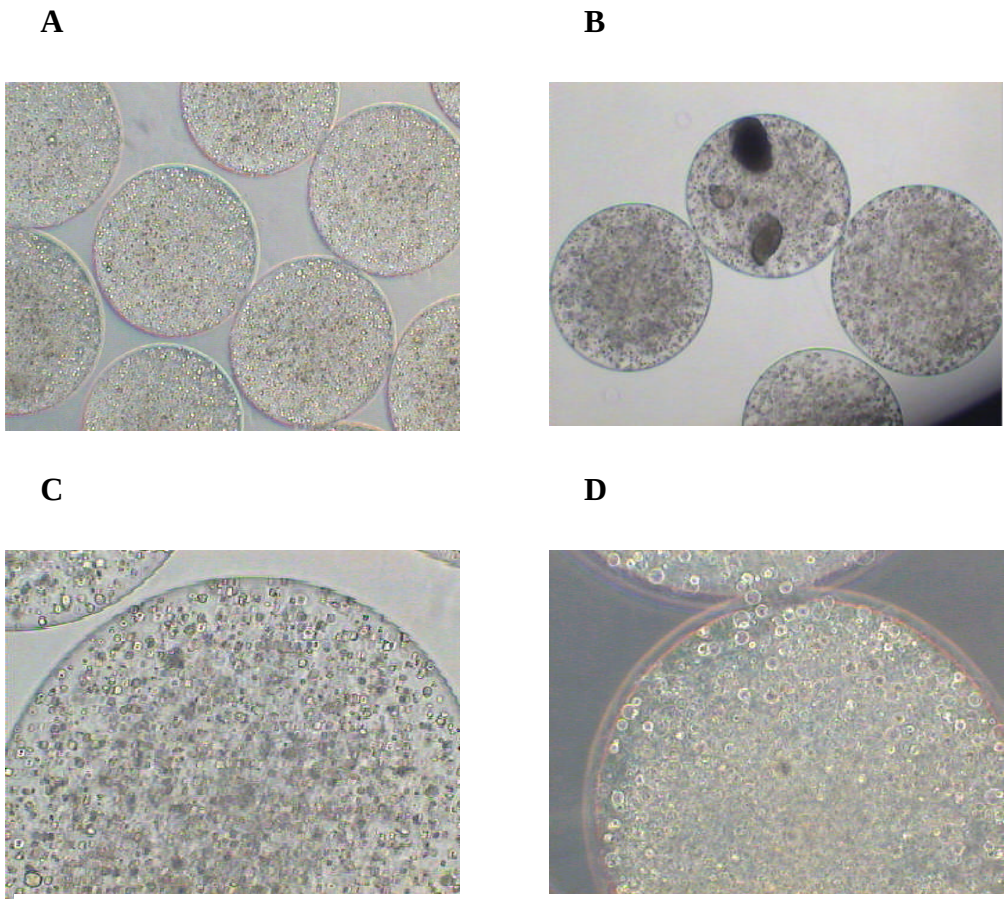

Figure 5.23 Microscopic appearance of encapsulated cells prior to implantation into mice

(A) Encapsulated cells at x 10 magnification. (B) Increased density of cells within microscapsule demonstrating proliferation of cells. (C) The microcapsule magnified x 20 and shows that the cells were evenly distributed within (D) shows the microcapsule magnified x 40 showing an outer layer of PLL and an inner layer of alginate.

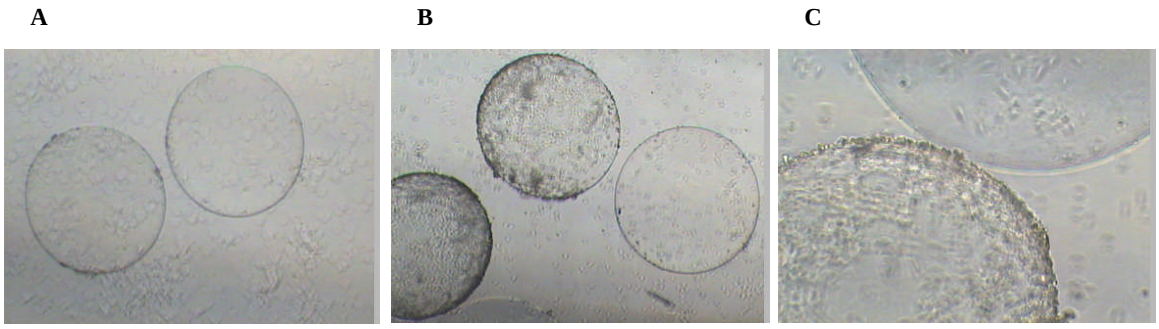

Figure 5.24 Empty microcapsules obtained from control mouse

(A), ***(B)*** *and* ***(C)*** *show empty microcapsules at x 10, x 10, and x 20 magnification, respectively.* ***(A)***, ***(B)*** *and* ***(C)*** *were microcapsules retrieved from control mouse after 3 days and some showed a layer of cells coating their surfaces.*

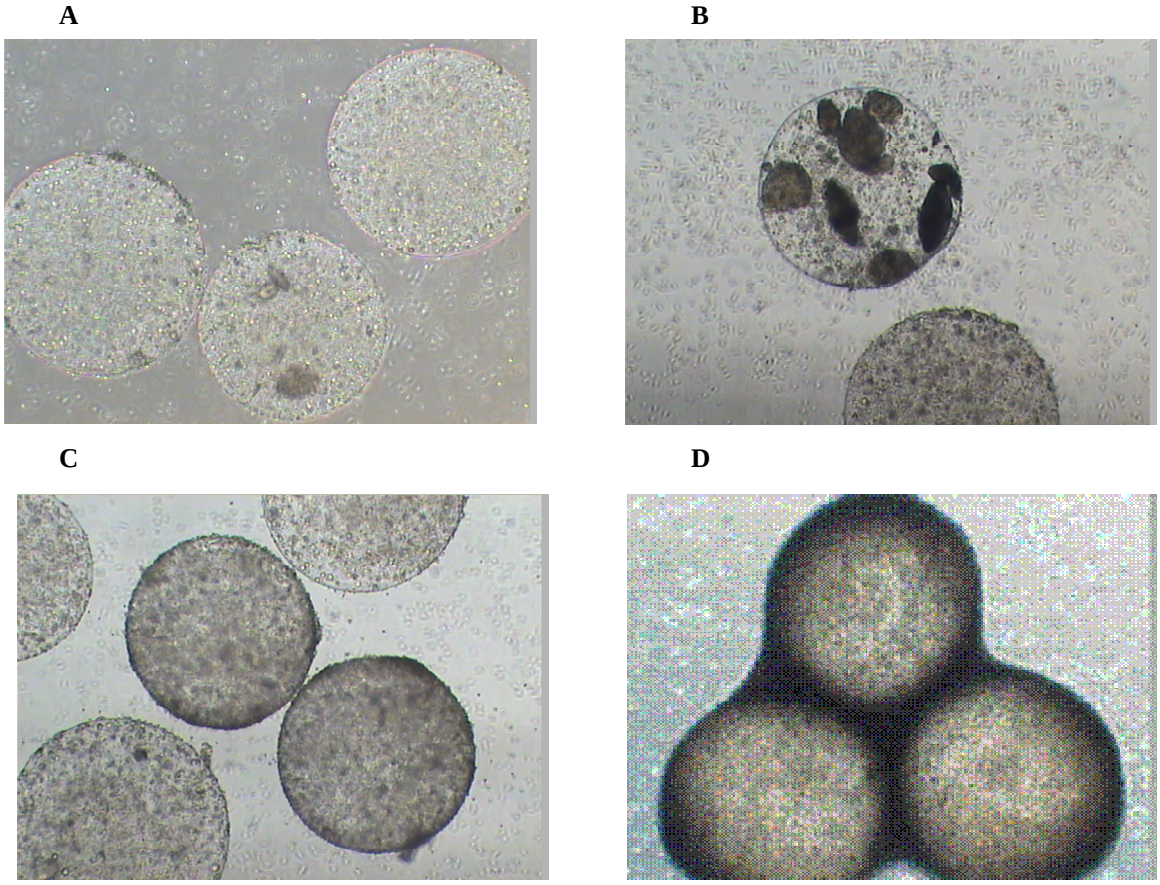

Figure 5.25 Microcapsules retrieved 3 and 14 days after implanted into LCAT $^{-/-}$ mice.

(A) *Microcapsules with x 10 magnification showing early stage of cell proliferation.* ***(B)*** *Multiple clumps of proliferated cells in implanated microcapsule.* ***(C)*** *Two microcapsules showing early signs of external coating with thin layer of cells compared with 3 other normal looking microcapsules.* ***(D)*** *Intense aggregation of microcapsules when they were retrieved from the mice at day 14. They were coated with a thick layer cells and do not show viable cells within.*

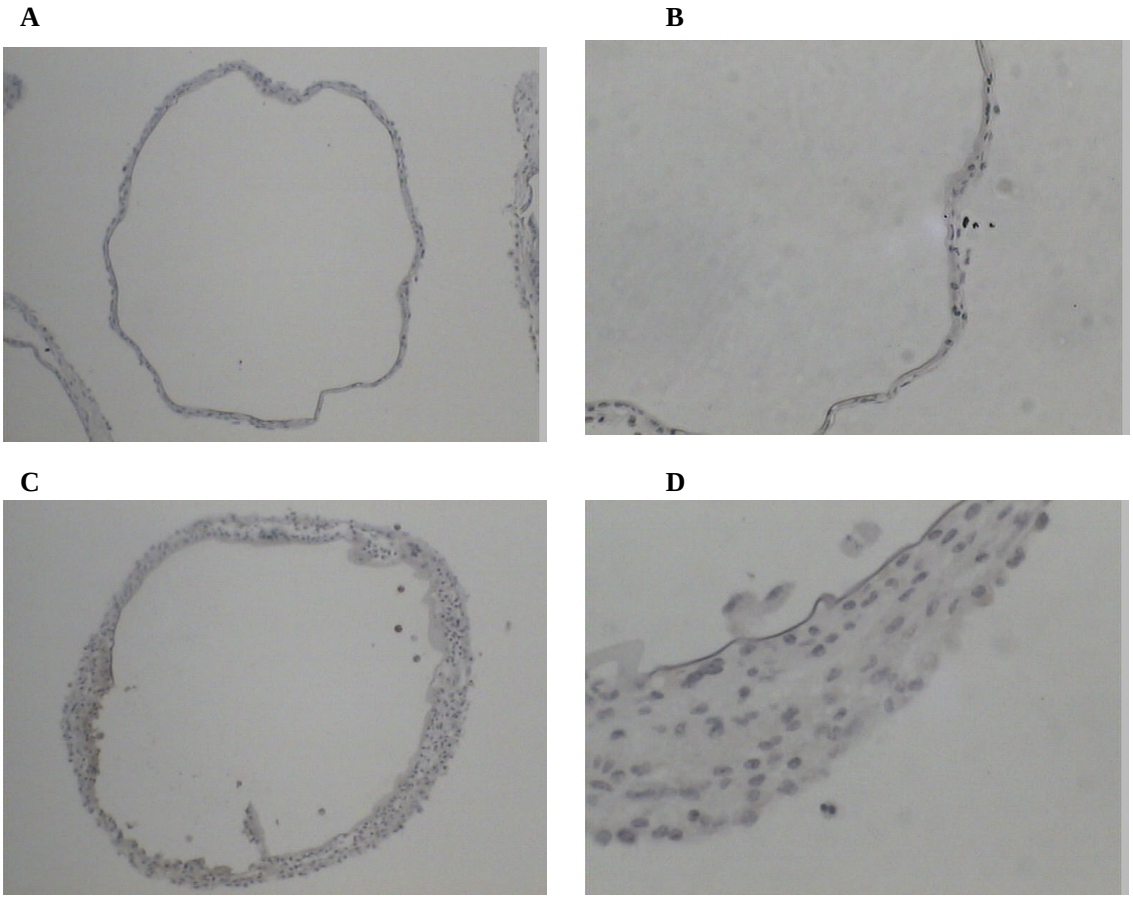

Figure 5.26 Histology of microcapsules after implantation into LCAT$^{-/-}$ mice

(A and (B) were empty microcapsules recovered from the control mice. (A) Shows an empty microcapsule magnified x 10 and being coated with a thin layer of cells. (B) The same microcapsule magnified x 20. (C) This microcapsule with encapsulated cells was retrieved from an experimental mouse peritoneal cavity. The capsule with its external thick layer of cells was stained with haematoxylin and eosin. (D The wall of the microcapsule magnified x 40 showing nuclei of cells within the capsule and those coating the capsule, staining blue whilst the cytoplasm of cells stain pink.

5.2.4 Discussion

The LCAT$^{-/-}$ mouse is a valuable experimental model of human LCAT deficiency. No LCAT is secreted and this results in the near absence of HDL in the circulatory system. Therefore, this circulatory deficiency allows us to investigate the feasibility of two alternative methods of delivery of gene product, namely direct infusion of purified recombinant LCAT from CHO-H6LCAT cells and the peritoneal implantation of non-autologous recombinant cells protected in alginate capsules.

Purified recombinant LCAT can be administered to LCAT$^{-/-}$ mouse either as a bolus or as multiple repeated injections. A sustained plasma LCAT concentration and prolonged cholesterol esterification is seen in LCAT$^{-/-}$ mice being given repeated injections. HDL lipoprotein is formed in plasma proving that this strategy of enzyme replacement in principle does work in the short-term. Larger studies of longer duration involving a larger cohort of LCAT$^{-/-}$ mice will be needed to evaluate whether there would be any immune response to prolonged repeated injections of recombinant LCAT and hence its effectiveness.

From the three animal studies (section 5.2.2), some of the treated LCAT$^{-/-}$ mice demonstrated that encapsulated cells can survive and secrete LCAT, which then gets absorbed and enters the circulatory system. In addition, the LCAT secreted showed biological activity by increasing the percentage of esterified cholesterol and raising the level of HDL in some mice. However, these physiological changes only lasted for a few days. I was unable to repeat the experiment on a larger scale due to time constraints and the shortage of mice as a result of difficulties with in-house breeding.

In the course of this study, it was interesting to note that the preparation of perfect capsules was far from simple. The quality of the capsule varied from one preparation to the next. Capsule strength may play an important role for studies *in vivo*. When capsules were weak, they would tend to collapse a few days after implantation and this probably explained why a number of microcapsules had lysed and was empty of cells.

The size of the capsule is also critical for the prolonged survival of the encapsulated cells. We now understand that in a vascularised tissue, the maximum distance for an effective diffusion of oxygen and nutrients from capillary to cells is 200 μm (Mueller-Klieser et al., 1986; Dionne et al., 1993). As there is no convection movement within the microcapsule, the principle driving force for the transfer of nutrients to encapsulated cells is the concentration gradient. The latter is proportional to the distance between the capsular surface and the centre of the oxygen-consuming cell

(Schrezenmeir *et al*., 1992; Schrezenmeir *et al*., 1994). Furthermore, there is a significant reduction in pericapsular reaction when using microcapsules as small as 185 μm in diameter when compared to using microcsapsules of a standard size (Hallé et al ., 1994; Robitaille et al ., 1999). Some authors have suggested that the critical diameter for optimal function and biocompatibility of the microcapsules is between 400-450 μm (Hunkeler, 2001; Orive et al., 2003).

Viscosity of the alginate solution and the alginate-polylysine reaction time from cross-linking must be strictly tested and controlled; otherwise capsule strength and smoothness of the capsular membrane will not be ideal. As no biomaterial is 100% biocompatible, it is inevitable that some capsules will eventually attract cell overgrowth. Many factors can promote overgrowth if inadequately controlled, notably spheroidicity, smoothness of the capsular surface, strength and volume of the microcapsules, viscosity, composition and purity of the alginate.

Alginate, a linear polysaccharide with gel forming properties, is composed of 1, 4 linked β-D-mannuronic acid (M), αL-glucuronic acid (G) and alternating MG blocks. Some studies have shown that mitogenic impurities, which are found in commercial alginate but not in purified alginate, are solely responsible for the side effects observed, including cytokine release and inflammatory reactions (Orive *et al.*, 2006). Other groups have shown that alginate rich in mannuronic acid is a potent stimulator of cytokines (IL-1 and TNF-α). In my study, the alginate used was manufactured commercially by Kelco International. Due to some fibroproliferative connective tissue observed on the outer surface of the microcapsules and the short-lived production of LCAT, there is some doubt about the purity of alginate used.

Non-specific host inflammatory reactions to capsule components, related to immune response mounted by the host, include lymphocyte and macrophage adhesion to the microcapsule surface and early fibrotic overgrowth. These will reduce effective LCAT secretion whilst at the same time impair metabolic functions of the encapsulated cells by decreasing the transfer of oxygen, nutrients and metabolites and ultimately causing cell death.

Encapsulation therapy has many advantages over systemic injections in that it can provide a sustained systemic therapy. The mode of delivery is also clinically benign, potentially economical, highly versatile and amenable to industrial-scale production. The microcapsules also have the potential of being retrievable, particularly when implanted subcutaneously. Although the clinical efficacy has not been proven

here, further studies are warranted to investigate the potential of microencapsulated cells as a clinical treatment of LCAT deficiency.

CHAPTER 6

GENERAL DISCUSSION

6. General Discussion

Aims of the project

Liver disease is frequently complicated by widespread cellular and metabolic disturbances in other tissues and organs. These include heart and vascular dysfunctions, abnormal handling of salt and water by the kidney, leading to swollen legs and ascites, and increased susceptibility to infections. The reasons are poorly understood, but increasing evidence suggests that many of these metabolic disturbances are caused by an imbalance of cholesterol and other fats present in patient's blood and cell membranes. LCAT, the principal cholesterol-esterifying enzyme, is manufactured in the liver and is a key regulator of fat metabolism. In liver disease and familial LCAT deficiency, reduced LCAT activity leads to marked changes in the lipid and apolipoprotein composition of circulating lipoproteins which in turn leads to altered lipid composition and fluidity of cell membranes throughout the body. This cause cells to malfunction, through adverse effects on the receptors, transport proteins and enzymes, which are embedded in their membranes.

The major aim of my studies was to develop two new approaches to treat plasma LCAT deficiency, namely protein therapy and encapsulated cell technology. As well as being important for the treatment of the small number of patients with familial LCAT deficiency, it has major clinical implications for correcting the lipoprotein abnormalities in liver diseases. Thus normalising LCAT activity would improve the widespread cellular dysfunctions caused or exacerbated by abnormal lipoproteins and so help in the management of severe hepatitis or in the preparation of patients with metabolic liver disease or severe liver disease for surgery or transplantation, by improving associated cellular dysfunctions.

Establishing stably producing clones

CHO cells have been used extensively in the industry for the production of proteins. Protein produced from these cell lines has appropriate post-translational modification such as glycosylation, whereas E. coli or insect cell lines are incapable of this (Kim et al 1998, Grabenhorst et al 1999). A clonal cell line of productive CHO cells secreting LCAT cDNA tagged with six histidine residues (CHO.H6LCAT) was selected from amongst numerous clones and was further subjected to increasing concentration of Mtx. This increased the LCAT yield in a T75 flask by 14 fold from ~600 ng/ml/48h to 8.7 μg/ml/48h. LCAT activity was confirmed by using our laboratory modified

radioactive LCAT assay as discussed below. The LCAT expression CHO-H6LCAT cells was relatively high compared to LCAT production in other studies using mammalian and insect cell lines (Chawla and Owen, 1995, Miller *et al*., 1996, Jin *et al.,* 1997, Vinogradov *et al.,* 1998, Jeffrey *et al*., 1999). This was an important step towards ensuring the success of the proposed treatments. In future studies the recombinant LCAT produced here can be further characterised for particle sizing, and in addition, use of electron microscopy can help to assess the shape of the particles.

More recently, human LCAT has been cloned and expressed in a human lung cell line (Lane *et al.,* 2004). The scaled-up LCAT production of this cell line yielded approximately 5 μg/ml of conditioned medium. The enzymatic properties and the carbohydrate components of the recombinant LCAT were similar to those of the circulating human plasma enzyme, suggesting that this source of LCAT may be more suitable for use in some form of enzyme replacement.

LCAT assay

Measurement of plasma LCAT mass was difficult. During the course of my experiments, the proteoliposome substrate method used allowed the assay of LCAT activity to be optimised and standardised for plasma. However, the quality of substrate varied with each preparation and it lacked specificity and sensitivity especially when the LCAT activity was low. Nevertheless, this substrate has been reported to have excellent correlation between LCAT activity in normal plasma and LCAT protein by radioimmunoassay (Albers *et al.,* 1981). The isolation of pure H6LCAT would in the future allow us to produce in-house antibodies and develop an ELISA assay for the quantification of serum LCAT.

Purifying LCAT

The presence of foetal bovine serum in normal growth medium would inevitably contain a small amount of LCAT enzyme. Published reports had revealed marked similarities between human and other mammalian LCAT (Mclean *et al.,* 1986; Warden *et al.,* 1989). To avoid the likely event of co-purifying bovine LCAT from culture medium and subsequent contamination of the final preparation, I had to use an alternative serum-free medium. After testing the LCAT production from cells grown in three other media (SFM, PFM and CD-CHO), CD-CHO was found to support a similar LCAT production as in normal growth medium after an initial lag phase. Another advantage of using this medium was that it would simplify the purification of LCAT, as

it had the least contaminating amount of protein. Hundreds of mls of this medium containing LCAT were produced with ease.

The use of pre-charged mini-columns with nickel-nitrotriacetic acid and nickel resin did not yield pure LCAT. Isolating LCAT with octyl-sepharose column as an extra step improved the efficiency of recovery (37%), but still had contaminants. Therefore, this eluate was passed through another nickel column with success in getting a high purity on SDS-page gel electrophoresis but sacrificing efficiency. Further attempts to improve the quality by using cobalt-based IMAC resin (Talon resin) yielded good results. On average at least 50% pure LCAT was recovered but this only allowed a small scale purification (100 ml). Therefore, I attempted to scale up the purification process to 1 L by loading the LCAT medium onto an octyl-sepharose column first and then passing the smaller volume of LCAT-enriched eluent through a Talon column. Although pure LCAT was eluted, less than 10 % of LCAT was recovered and thus this two-step procedure was not justified. Hence, I made multiple small-scale purifications using the Talon resin.

Protein therapy

Having obtained pure LCAT, the next step was to evaluate the routes of administration. As expected, intravenous injection gave a direct route into the systemic circulation of the $LCAT^{-/-}$ mice achieving a high LCAT plasma concentration within 30 min. It is envisaged that administration of LCAT into systemic circulation will not be a problem in humans as veins are easily accessible in the peripheral tissues.

A pilot study using the intraperitoneal route gave encouraging results, which led to a more detailed study with a bolus injection of pure LCAT into the peritoneal cavities of $LCAT^{-/-}$ mice. A high concentration of plasma LCAT was detected in the circulation within 2 h of injection. After a delay of several hours, the LCAT secreted proved to be functionally active since it increased the amount of esterified cholesterol in the plasma. A sustained level of LCAT concentration and esterification took place when the $LCAT^{-/-}$ mice were given repeated injections. More importantly, all injected mice had increased levels of HDL as detected by agarose gel electrophoresis. LCAT had been shown to be primarily responsible for HDL particle maturation as well as maintenance of HDL plasma concentration (Séguret-Macé *et al.*, 1988). Further work with larger number of mice would be needed to evaluate the plasma, erythrocyte lipid compositions and lipoprotein profiles.

Cell therapy

Studies *in vitro* showed that encapsulated recombinant CHO cells secreted biologically active human H6LCAT for 3 months. The *in vivo* study of the feasibility of cell therapy was hampered by only having limited number of mice available due to in-house breeding difficulties. However, some mice did show that LCAT was secreted by the microcapsules and absorbed into the circulation to produce a certain normalisation of the lipoprotein profile. Compared to the *in vitro* study, LCAT secretion by encapsulated CHO cells in $LCAT^{-/-}$ mice is reduced. The transfer of the encapsulated cells from the incubator to the peritoneum of $LCAT^{-/-}$ mice could decrease LCAT production, but it would be difficult to know.

A second reason may be due to the over proliferation of cells in the microcapsules resulting in poor nutrient supply, hence less viable cells available for LCAT secretion. One way to overcome excess cell proliferation and diminished secretion is to encapsulate recombinant mouse C2C12 myoblasts (Deglon *et al.*, 1996; Regulier *et al.*, 1997, Orive *et al.*, 2005). These terminally differentiate into myotubes in low FCS, allowing implantation of non-dividing cells and thereby permitting controlled LCAT production. Another approach to overcome low yield in LCAT production in encapsulated cells is to use a more productive cell line for encapsulation.

Finally, other factors may include limited activation of human enzyme. Potential explanations are differences in the size and composition of mouse versus human HDL, the different specificities of the 2 enzymes for available esters as well as limited availability of FC as substrate (Vaiseman *et al.*, 1995). Differences in mouse and human apoA1 (Karathanasis *et al.*, 1983; Stoffel *et al.*, 1992) could lead to reduced activation of human LCAT by mouse co-factor.

These studies also highlight the need to improve capsule biocompatibility. In my short-term *in vivo* studies, implantation of the microcapsules in $LCAT^{-/-}$ mice appear to cause non-specific hosts inflammatory reactions to the microcapsules leading to fibrotic overgrowth on the surface of the capsules and further compromising the long-term viability of the CHO-H6LCAT cells. Biocompatibility will not be a problem in capsules implanted over the short term as ultra-pure alginate can now be obtained and uniform capsules can be produced by automated machines (Anilkumar *et al.*, 2001). However, it is clear that a number of issues still need to be addressed for implanting capsules for longer periods. These include toxicology, bio-safety and the type of polymer to be used, although progress is being made in developing immune-compatible cross-linking coating polymers (Orive *et al.*, 2003, 2004).

Conclusions

In many regards, the aims of this thesis have been satisfied even though many issues remained unanswered. As compared to viral gene therapy, studies on non-viral strategies for LCAT replacement are still at present limited. The results presented in this thesis could hopefully provide further insights into the feasibility of delivering therapeutic proteins by protein injection and encapsulated cell technology.

BIBLIOGRAPHY

Aebischer P, Pochon NA, Heyd B, Deglon N, Joseph JM, Zurn AD, Baetge EE, Hammang JP, Goddard M, Lysaght M, Kaplan F, Kato AC, Schluep M, Hirt L, Regli F, Porchet F, and De Tribolet N (1996) Gene therapy for amyotrophic lateral sclerosis (ALS) using a polymer encapsulated xenogenic cell line engineered to secrete hCNTF. *Hum.Gene Ther.* **7**:851-860.

Agorastos J, Fox C, Harry DS, and McIntyre N (1978) Lecithin--cholesterol acyltransferase and the lipoprotein abnormalities of obstructive jaundice. *Clin.Sci.Mol.Med.* **54**:369-379.

Albers JJ, Chen CH, and Adolphson JL (1981) Lecithin:cholesterol acyltransferase (LCAT) mass; its relationship to LCAT activity and cholesterol esterification rate. *J.Lipid Res.* **22**:1206-1213.

Albers JJ, Bergelin RO, Adolphson JL, and Wahl PW (1982) Population-based reference values for lecithin-cholesterol acyltransferase (LCAT). *Atherosclerosis* **43**:369-379.

Allain CC, Poon LS, Chan CS, Richmond W, and Fu PC (1974) Enzymatic determination of total serum cholesterol. *Clin.Chem.* **20**:470-475.

Ambrosino G, Varotto S, Basso SM, Cecchetto A, Carraro P, Naso A, De Silvestro G, Plebani M, Abatangelo G, Donato D, Cestrone A, Giron G, and D'Amico DF (2003) Hepatocyte transplantation in the treatment of acute liver failure: microencapsulated hepatocytes versus hepatocytes attached to an autologous biomatrix. *Cell Transplant.* **12**:43-49.

Anilkumar AV, Lacik I, and Wang TG (2001) A novel reactor for making uniform capsules. *Biotechnol.Bioeng.* **75**:581-589.

Arad Y, Ramakrishnan R, and Ginsberg HN (1990) Lovastatin therapy reduces low density lipoprotein apoB levels in subjects with combined hyperlipidemia by reducing the production of apoB-containing lipoproteins: implications for the pathophysiology of apoB production. *J.Lipid Res.* **31**:567-582.

Aron L, Jones S, and Fielding CJ (1978) Human plasma lecithin-cholesterol acyltransferase. Characterization of cofactor-dependent phospholipase activity. *J.Biol.Chem.* **253**:7220-7226.

Arroyo V, Planas R, Gaya J, Deulofeu R, Rimola A, Perez-Ayuso RM, Rivera F, and Rodes J (1983) Sympathetic nervous activity, renin-angiotensin system and renal excretion of prostaglandin E2 in cirrhosis. Relationship to functional renal failure and sodium and water excretion. *Eur.J.Clin.Invest* **13**:271-278.

Assmann G and Jabs HU (1985) Enzymology of lecithin:cholesterol acetyltransferase. *Biochem.Soc.Trans.* **13**:19-20.

Balladur P, Crema E, Honiger J, Calmus Y, Baudrimont M, Delelo R, Capeau J, and Nordlinger B (1995) Transplantation of allogeneic hepatocytes without immunosuppression: long-term survival. *Surgery* **117**:189-194.

Barter PJ and Rye KA (1994) High-density lipoproteins and coronary heart disease. *J.Cardiovasc.Risk* **1**:217-221.

Basic D, Vacek I, and Sun AM (1996) Microencapsulation and transplantation of genetically engineered cells: a new approach to somatic gene therapy. *Artif.Cells Blood Substit.Immobil.Biotechnol.* **24**:219-255.

Benoist S and Nordlinger B (2001) [The internal bioartifical liver]. *J.Soc.Biol.* **195**:91-96.

Berard AM, Foger B, Remaley A, Shamburek R, Vaisman BL, Talley G, Paigen B, Hoyt RF, Jr., Marcovina S, Brewer HB, Jr., and Santamarina-Fojo S (1997) High plasma HDL concentrations associated with enhanced atherosclerosis in transgenic mice overexpressing lecithin-cholesteryl acyltransferase. *Nat.Med.* **3**:744-749.

Bienz-Tadmor B, Dicerbo PA, Tadmor G, and Lasagna L (1992) Biopharmaceuticals and conventional drugs: clinical success rates. *Biotechnology (N.Y.)* **10**:521-525.

Bingle C, Ghazi S, Owen JS, and Srai SK (1991) LCAT mRNA in liver disease. *Lancet* **338**:1531.

Blitzer BL, Waggoner JG, Jones EA, Gralnick HR, Towne D, Butler J, Weise V, Kopin IJ, Walters I, Teychenne PF, Goodman DG, and Berk PD (1978) A model of fulminant hepatic failure in the rabbit. *Gastroenterology* **74**:664-671.

Borysiewicz LK, Soutar AK, Evans DJ, Thompson GR, and Rees AJ (1982) Renal failure in familial lecithin: cholesterol acyltransferase deficiency. *Q.J.Med.* **51**:411-426.

Bradford MM (1976) A rapid and sensitive method for the quantitation of microgram quantities of protein utilizing the principle of protein-dye binding. *Anal.Biochem.* **72**:248-254.

Brousseau ME, Santamarina-Fojo S, Zech LA, Berard AM, Vaisman BL, Meyn SM, Powell D, Brewer HB, Jr., and Hoeg JM (1996) Hyperalphalipoproteinemia in human lecithin cholesterol acyltransferase transgenic rabbits. In vivo apolipoprotein A-I catabolism is delayed in a gene dose-dependent manner. *J.Clin.Invest* **97**:1844-1851.

Brown MS and Goldstein JL (1983) Lipoprotein metabolism in the macrophage: implications for cholesterol deposition in atherosclerosis. *Annu.Rev.Biochem.* **52**:223-261.

Bruce C and Tall AR (1995) Cholesteryl ester transfer proteins, reverse cholesterol transport, and atherosclerosis. *Curr.Opin.Lipidol.* **6**:306-311.

Bush GL, Tassin AM, Friden H, and Meyer DI (1991) Secretion in yeast. Purification and in vitro translocation of chemical amounts of prepro-alpha-factor. *J.Biol.Chem.* **266**:13811-13814.

Cai ZH, Shi ZQ, Sherman M, and Sun AM (1989) Development and evaluation of a system of microencapsulation of primary rat hepatocytes. *Hepatology* **10**:855-860.

Candido EP, Reeves R, and Davie JR (1978) Sodium butyrate inhibits histone deacetylation in cultured cells. *Cell* **14**:105-113.

Carlson LA (1979) A further case of fish-eye disease. *Lancet* **2**:1376-1377.

Carlson LA and Philipson B (1979) Fish-eye disease. A new familial condition with massive corneal opacities and dyslipoproteinaemia. *Lancet* **2**:922-924.

Carlson LA (1982) Fish eye disease: a new familial condition with massive corneal opacities and dyslipoproteinaemia. *Eur.J.Clin.Invest* **12**:41-53.

Carlson LA and Holmquist L (1985) Evidence for deficiency of high density lipoprotein lecithin: cholesterol acyltransferase activity (alpha-LCAT) in fish eye disease. *Acta Med.Scand.* **218**:189-196.

Carlson LA and Holmquist L (1985) Paradoxical esterification of plasma cholesterol in fish eye disease. *Acta Med.Scand.* **217**:491-499.

Chang PL (1997) Microcapsules as bio-organs for somatic gene therapy. *Ann.N.Y.Acad.Sci.* **831**:461-473.

Chang TM (1964) Semipermeable microcapsules. *Science* **146**:524-525.

Chang TM (1992) Artificial liver support based on artificial cells with emphasis on encapsulated hepatocytes. *Artif.Organs* **16**:71-74.

Chang TM (1998) Artificial cells with emphasis on cell encapsulation of genetically engineered cells. *Artif.Organs* **22**:958-965.

Chang TM and Malave N (2000) The development and first clinical use of semipermeable microcapsules (artificial cells) as a compact artificial kidney. 1970. *Ther.Apher.* **4**:108-116.

Chang TM, Powanda D, and Yu WP (2003) Analysis of polyethylene-glycol-polylactide nano-dimension artificial red blood cells in maintaining systemic hemoglobin levels and prevention of methemoglobin formation. *Artif.Cells Blood Substit.Immobil.Biotechnol.* **31**:231-247.

Chawla D and Owen JS (1995) Secretion of active human lecithin-cholesterol acyltransferase by insect cells infected with a recombinant baculovirus. *Biochem.J.* **309 (Pt 1)**:249-253.

Chen CH and Albers JJ (1982) Characterization of proteoliposomes containing apoprotein A-I: a new substrate for the measurement of lecithin: cholesterol acyltransferase activity. *J.Lipid Res.* **23**:680-691.

Chen CH and Albers JJ (1983) Interspecies activation of lecithin-cholesterol acyltransferase by apolipoprotein A-I isolated from the plasma of humans, horses, sheep, goats and rabbits. *Biochim.Biophys.Acta* **753**:40-46.

Chen CH, Forte TH, Cahoon BE, Thrift RN, and Albers JJ (1986) Synthesis and secretion of lecithin-cholesterol acyltransferase by the human hepatoma cell line HepG2. *Biochim.Biophys.Acta* **877**:433-439.

Chia MC, Shi W, Li JH, Sanchez O, Strathdee CA, Huang D, Busson P, Klamut HJ, and Liu FF (2004) A conditionally replicating adenovirus for nasopharyngeal carcinoma gene therapy. *Mol.Ther.* **9**:804-817.

Chisholm JW, Gebre AK, and Parks JS (1999) Characterization of C-terminal histidine-tagged human recombinant lecithin:cholesterol acyltransferase. *J.Lipid Res.* **40**:1512-1519.

Chu FC, Kuwabara T, Cogan DG, Schaefer EJ, and Brewer HB, Jr. (1979) Ocular manifestations of familial high-density lipoprotein deficiency (Tangier disease). *Arch.Ophthalmol.* **97**:1926-1928.

Cirone P, Bourgeois JM, Shen F, and Chang PL (2004) Combined immunotherapy and antiangiogenic therapy of cancer with microencapsulated cells. *Hum.Gene Ther.* **15**:945-959.

Clayton HA, London NJ, Colloby PS, Bell PR, and James RF (1991) The effect of capsule composition on the biocompatibility of alginate-poly-l-lysine capsules. *J.Microencapsul.* **8**:221-233.

Clifton PM, Barter PJ, and Mackinnon AM (1988) High density lipoprotein particle size distribution in subjects with obstructive jaundice. *J.Lipid Res.* **29**:121-135.

Cohen SN and Chang AC (1973) Recircularization and autonomous replication of a sheared R-factor DNA segment in Escherichia coli transformants. *Proc.Natl.Acad.Sci.U.S.A* **70**:1293-1297.

Cooper AD (1985) Role of the liver in the degradation of lipoproteins. *Gastroenterology* **88**:192-205.

Coromili V and Chang TM (1993) Polydisperse dextran as a diffusing test solute to study the membrane permeability of alginate polylysine microcapsules. *Biomater.Artif.Cells Immobilization Biotechnol.* **21**:427-444.

Cullen SN and Chapman RW (2005) Review article: current management of primary sclerosing cholangitis. *Aliment.Pharmacol.Ther.* **21**:933-948.

Cullen SN and Chapman RW (2006) The medical management of primary sclerosing cholangitis. *Semin.Liver Dis.* **26**:52-61.

Date I, Ohmoto T, Imaoka T, Shingo T, and Emerich DF (1996) Chromaffin cell survival from both young and old donors is enhanced by co-grafts of polymer-encapsulated human NGF-secreting cells. *Neuroreport* **7**:1813-1818.

Day RC, Harry DS, Owen JS, Foo AY, and McIntyre N (1979) Lecithin-cholesterol acyltransferase and the lipoprotein abnormalities of parenchymal liver disease. *Clin.Sci.(Lond)* **56**:575-583.

De Castro M, Orive G, Hernandez RM, Gascon AR, and Pedraz JL (2005) Comparative study of microcapsules elaborated with three polycations (PLL, PDL, PLO) for cell immobilization. *J.Microencapsul.* **22**:303-315.

Deckelbaum RJ, Ramakrishnan R, Eisenberg S, Olivecrona T, and Bengtsson-Olivecrona G (1992) Triacylglycerol and phospholipid hydrolysis in human plasma lipoproteins: role of lipoprotein and hepatic lipase. *Biochemistry* **31**:8544-8551.

Deglon N, Heyd B, Tan SA, Joseph JM, Zurn AD, and Aebischer P (1996) Central nervous system delivery of recombinant ciliary neurotrophic factor by polymer encapsulated differentiated C2C12 myoblasts. *Hum.Gene Ther.* **7**:2135-2146.

DeMatteo RP, Chu G, Ahn M, Chang E, Burke C, Raper SE, Barker CF, and Markmann JF (1997) Immunologic barriers to hepatic adenoviral gene therapy for transplantation. *Transplantation* **63**:315-319.

Desai K, Mistry P, Bagget C, Burroughs AK, Bellamy MF, and Owen JS (1989) Inhibition of platelet aggregation by abnormal high density lipoprotein particles in plasma from patients with hepatic cirrhosis. *Lancet* **1**:693-695.

Dionne KE, Colton CK, and Yarmush ML (1993) Effect of hypoxia on insulin secretion by isolated rat and canine islets of Langerhans. *Diabetes* **42**:12-21.

Dionne KE, Cain BM, Li RH, Bell WJ, Doherty EJ, Rein DH, Lysaght MJ, and Gentile FT (1996) Transport characterization of membranes for immunoisolation. *Biomaterials* **17**:257-266.

Dyson JE, Daniel J, and Surrey CR (1992) The effect of sodium butyrate on the growth characteristics of human cervix tumour cells. *Br.J.Cancer* **65**:803-808.

Farber JL, Gill G, and Konishi Y (1973) Prevention of galactosamine-induced liver cell necrosis by uridine. *Am.J.Pathol.* **72**:53-62.

Farooqui JZ, Wohl RC, Kezdy FJ, and Scanu AM (1988) Identification of the active-site serine in human lecithin: cholesterol acyltransferase. *Arch.Biochem.Biophys.* **261**:330-335.

Felgner PL and Rhodes G (1991) Gene therapeutics. *Nature* **349**:351-352.

Fielding CJ and Fielding PE (1971) Purification and substrate specificity of lecithin-cholesterol acyl transferase from human plasma. *FEBS Lett.* **15**:355-358.

Fielding CJ, Shore VG, and Fielding PE (1972) Lecithin: cholesterol acyltransferase: effects of substrate composition upon enzyme activity. *Biochim.Biophys.Acta* **270**:513-518.

Fielding PE, Miida T, and Fielding CJ (1991) Metabolism of low-density lipoprotein free cholesterol by human plasma lecithin-cholesterol acyltransferase. *Biochemistry* **30**:8551-8557.

Floren CH and Gustafson A (1985) Apolipoproteins A-I, A-II and E in cholestatic liver disease. *Scand.J.Clin.Lab Invest* **45**:103-108.

Floren CH, Chen CH, Franzen J, and Albers JJ (1987) Lecithin: cholesterol acyltransferase in liver disease. *Scand.J.Clin.Lab Invest* **47**:613-617.

Foger B, Chase M, Amar MJ, Vaisman BL, Shamburek RD, Paigen B, Fruchart-Najib J, Paiz JA, Koch CA, Hoyt RF, Brewer HB, Jr., and Santamarina-Fojo S (1999) Cholesteryl ester transfer protein corrects dysfunctional high density lipoproteins and reduces aortic atherosclerosis in lecithin cholesterol acyltransferase transgenic mice. *J.Biol.Chem.* **274**:36912-36920.

Folkert VW, Yunis M, and Schlondorff D (1984) Prostaglandin synthesis linked to phosphatidylinositol turnover in isolated rat glomeruli. *Biochim.Biophys.Acta* **794**:206-217.

Francone OL and Fielding CJ (1991) Effects of site-directed mutagenesis at residues cysteine-31 and cysteine-184 on lecithin-cholesterol acyltransferase activity. *Proc.Natl.Acad.Sci.U.S.A* **88**:1716-1720.

Francone OL, Evangelista L, and Fielding CJ (1993) Lecithin-cholesterol acyltransferase: effects of mutagenesis at N-linked oligosaccharide attachment sites on acyl acceptor specificity. *Biochim.Biophys.Acta* **1166**:301-304.

Friend C, Zajac-Kaye M, Holland JG, and Pogo BG (1987) Recent studies on the mechanism of induction of differentiation in murine erythroleukemia cells. *Haematologica* **72**:75.

Fritschy WM, De Vos P, Groen H, Klatter FA, Pasma A, Wolters GH, and van Schilfgaarde R (1994) The capsular overgrowth on microencapsulated pancreatic islet grafts in streptozotocin and autoimmune diabetic rats. *Transpl.Int.* **7**:264-271.

Furukawa Y and Nishida T (1979) Stability and properties of lecithin-cholesterol acyltransferase. *J.Biol.Chem.* **254**:7213-7219.

Gao GP, Yang Y, and Wilson JM (1996) Biology of adenovirus vectors with E1 and E4 deletions for liver-directed gene therapy. *J.Virol.* **70**:8934-8943.

Gershwin ME and Mackay IR (1991) Primary biliary cirrhosis: paradigm or paradox for autoimmunity. *Gastroenterology* **100**:822-833.

Gillet and Owen. Cholesterol esterifying enzymes - lecithin:cholesterol acyltransferase (LCAT) and acylcoenzyme A:cholesterol acyltransferase (ACAT). Converse and Skinner. Lipoprotein Analysis. A practical approach. 187-201. 1992. IRL, Oxford.
Ref Type: Generic

Gjone E, Blomhoff JP, and Wiencke I (1971) Plasma lecithin: cholesterol acyltransferase activity in acute hepatitis. *Scand.J.Gastroenterol.* **6**:161-168.

Gjone E (1974) Familial lecithin:cholesterol acyltransferase deficiency--a clinical survey. *Scand.J.Clin.Lab Invest Suppl* **137**:73-82.

Gjone E, Blomhoff JP, and Skarbovik AJ (1974) Possible association between an abnormal low density lipoprotein and nephropathy in lecithin: cholesterol acyltransferase deficiency. *Clin.Chim.Acta* **54**:11-18.

Gjone E, Blomhoff JP, Holme R, Hovig T, Olaisen B, Skarbovik AJ, and Teisberg P (1981) Familial lecithin:cholesterol acyltransferase deficiency. Report of a fourth family from northwestern Norway. *Acta Med.Scand.* **210**:3-6.

Glomset JA (1962) The mechanism of the plasma cholesterol esterification reaction: plasma fatty acid transferase. *Biochim.Biophys.Acta* **65**:128-135.

Glomset JA (1963) Further studies of the mechanism of the plasma cholesterol esterification reaction. *Biochim.Biophys.Acta* **70**:389-395.

Glomset JA and Wright JL (1964) Some properties of a cholesterol esterifying enzyme in human plasma. *Biochim.Biophys.Acta* **89**:266-276.

Glomset JA, Assmann G, Gjone E, and Norum KR (1995) Lecithin:Cholesterol Acyltransferase Deficiency and Fish Eye Disease. *The Metabolic and Molecular Bases of Inherited Disease* **2** :1933-1951.

Goldstein JL and Brown MS (1984) Progress in understanding the LDL receptor and HMG-CoA reductase, two membrane proteins that regulate the plasma cholesterol. *J.Lipid Res.* **25**:1450-1461.

Goldstein JL and Brown MS (1985) The LDL receptor and the regulation of cellular cholesterol metabolism. *J.Cell Sci.Suppl* **3**:131-137.

Goosen MF (1999) Physico-chemical and mass transfer considerations in microencapsulation. *Ann.N.Y.Acad.Sci.* **875**:84-104.

Gotto AM, Jr., Pownall HJ, and Havel RJ (1986) Introduction to the plasma lipoproteins. *Methods Enzymol.* **128**:3-41.

Grabenhorst E, Schlenke P, Pohl S, Nimtz M, and Conradt HS (1999) Genetic engineering of recombinant glycoproteins and the glycosylation pathway in mammalian host cells. *Glycoconj.J.* **16**:81-97.

Graham FL (2000) Adenovirus vectors for high-efficiency gene transfer into mammalian cells. *Immunol.Today* **21**:426-428.

Gunzburg WH and Salmons B (1996) Development of retroviral vectors as safe, targeted gene delivery systems. *J.Mol.Med.* **74**:171-182.

Guo LS, Hamilton RL, Ostwald R, and Havel RJ (1982) Secretion of nascent lipoproteins and apolipoproteins by perfused livers of normal and cholesterol-fed guinea pigs. *J.Lipid Res.* **23**:543-555.

Gupta S, Alpini G, Vemuru RP, Hurston E, and Shafritz DA (1994) Butyrate synchronization of hepatocytes: modulation of cycling and cell cycle regulated gene expression. *Growth Factors* **10**:171-180.

Haegel-Kronenberger H, Haanstra K, Ziller-Remy C, Ortiz Buijsse AP, Vermeiren J, Stoeckel F, Van Gool SW, Ceuppens JL, Mehtali M, De Boer M, Jonker M, and Boon L (2004) Inhibition of

costimulation allows for repeated systemic administration of adenoviral vector in rhesus monkeys. *Gene Ther.* **11**:241-252.

Halbert DN, Cutt JR, and Shenk T (1985) Adenovirus early region 4 encodes functions required for efficient DNA replication, late gene expression, and host cell shutoff. *J.Virol.* **56**:250-257.

Halle JP, Leblond FA, Pariseau JF, Jutras P, Brabant MJ, and Lepage Y (1994) Studies on small (< 300 microns) microcapsules: II--Parameters governing the production of alginate beads by high voltage electrostatic pulses. *Cell Transplant.* **3**:365-372.

Hamilton RL, Williams MC, Fielding CJ, and Havel RJ (1976) Discoidal bilayer structure of nascent high density lipoproteins from perfused rat liver. *J.Clin.Invest* **58**:667-680.

Henneberry RC and Fishman PH (1976) Morphological and biochemical differentiation in HeLa cells. Effects of cycloheximide on butyrate-induced process formation and ganglioside metabolism. *Exp.Cell Res.* **103**:55-62.

Herz J and Gerard RD (1993) Adenovirus-mediated transfer of low density lipoprotein receptor gene acutely accelerates cholesterol clearance in normal mice. *Proc.Natl.Acad.Sci.U.S.A* **90**:2812-2816.

Higashi H, Yanaga K, Shimada M, Makowka L, Van Thiel DH, and Starzl TE (1990) Plasma lecithin/cholesterol acyltransferase (LCAT) activity in multiple-organ donors: a predictor of allograft viability in clinical liver transplantation. *Transplant.Proc.* **22**:433-434.

Hill JS, O K, Wang X, Paranjape S, Dimitrijevich D, Lacko AG, and Pritchard PH (1993) Expression and characterization of recombinant human lecithin:cholesterol acyltransferase. *J.Lipid Res.* **34**:1245-1251.

Hochuli E, Dobeli H, and Schacher A (1987) New metal chelate adsorbent selective for proteins and peptides containing neighbouring histidine residues. *J.Chromatogr.* **411**:177-184.

Hoeg JM, Santamarina-Fojo S, Berard AM, Cornhill JF, Herderick EE, Feldman SH, Haudenschild CC, Vaisman BL, Hoyt RF, Jr., Demosky SJ, Jr., Kauffman RD, Hazel CM, Marcovina SM, and Brewer HB, Jr. (1996) Overexpression of lecithin:cholesterol acyltransferase in transgenic rabbits prevents diet-induced atherosclerosis. *Proc.Natl.Acad.Sci.U.S.A* **93**:11448-11453.

Hortelano G, Al Hendy A, Ofosu FA, and Chang PL (1996) Delivery of human factor IX in mice by encapsulated recombinant myoblasts: a novel approach towards allogeneic gene therapy of hemophilia B. *Blood* **87**:5095-5103.

Hovig T and Gjone E (1973) Familial plasma lecithin: cholesterol acyltransferase (LCAT) deficiency. Ultrastructural aspects of a new syndrome with particular reference to lesions in the kidneys and the spleen. *Acta Pathol.Microbiol.Scand.[A]* **81**:681-697.

Hunkeler D (2001) Allo transplants xeno: as bioartificial organs move to the clinic. Introduction. *Ann.N.Y.Acad.Sci.* **944**:1-6.

Imai J, Katagiri H, Yamada T, Ishigaki Y, Ogihara T, Uno K, Hasegawa Y, Gao J, Ishihara H, Sasano H, Mizuguchi H, Asano T, and Oka Y (2005) Constitutively active PDX1 induced efficient insulin production in adult murine liver. *Biochem.Biophys.Res.Commun.* **326** :402-409.

Imbasciati E, Paties C, Scarpioni L, and Mihatsch MJ (1986) Renal lesions in familial lecithin-cholesterol acyltransferase deficiency. Ultrastructural heterogeneity of glomerular changes. *Am.J.Nephrol.* **6**:66-70.

Jahn CE, Schaefer EJ, Taam LA, Hoofnagle JH, Lindgren FT, Albers JJ, Jones EA, and Brewer HB, Jr. (1985) Lipoprotein abnormalities in primary biliary cirrhosis. Association with hepatic lipase inhibition as well as altered cholesterol esterification. *Gastroenterology* **89**:1266-1278.

Jin L, Lee YP, and Jonas A (1997) Biochemical and biophysical characterization of human recombinant lecithin: cholesterol acyltransferase. *J.Lipid Res.* **38**:1085-1093.

Jin L, Shieh JJ, Grabbe E, Adimoolam S, Durbin D, and Jonas A (1999) Surface plasmon resonance biosensor studies of human wild-type and mutant lecithin cholesterol acyltransferase interactions with lipoproteins. *Biochemistry* **38**:15659-15665.

Joki T, Machluf M, Atala A, Zhu J, Seyfried NT, Dunn IF, Abe T, Carroll RS, and Black PM (2001) Continuous release of endostatin from microencapsulated engineered cells for tumor therapy. *Nat.Biotechnol.* **19**:35-39.

Jonas A (1991) Lecithin-cholesterol acyltransferase in the metabolism of high-density lipoproteins. *Biochim.Biophys.Acta* **1084**:205-220.

Jonas A (1998) Regulation of lecithin cholesterol acyltransferase activity. *Prog.Lipid Res.* **37**:209-234.

Jonas A (2000) Lecithin cholesterol acyltransferase. *Biochim.Biophys.Acta* **1529**:245-256.

Kaido T, Yoshikawa A, Seto S, Yamaoka S, Sato M, Ishii T, and Imamura M (1998) Portal branch ligation with a continuous hepatocyte growth factor supply makes extensive hepatectomy possible in cirrhotic rats. *Hepatology* **28**:756-760.

Karathanasis SK, Zannis VI, and Breslow JL (1983) A DNA insertion in the apolipoprotein A-I gene of patients with premature atherosclerosis. *Nature* **305**:823-825.

Kasher MS, Wakulchik M, Cook JA, and Smith MC (1993) One-step purification of recombinant human papillomavirus type 16 E7 oncoprotein and its binding to the retinoblastoma gene product. *Biotechniques* **14**:630-641.

Kawata S, Chitranukroh A, Owen JS, and McIntyre N (1987) Membrane lipid changes in erythrocytes, liver and kidney in acute and chronic experimental liver disease in rats. *Biochim.Biophys.Acta* **896**:26-34.

Keppler D, Lesch R, Reutter W, and Decker K (1968) Experimental hepatitis induced by D-galactosamine. *Exp.Mol.Pathol.* **9**:279-290.

Keppler D and Decker K (1969) Studies on the mechanism of galactosamine-1-phosphate and its inhibition of UDP-glucose pyrophosphorylase. *Eur.J.Biochem.* **10**:219-225.

Keppler D and Decker K (1971) [Mechanism of action of D-galactosamine in the liver]. *Verh.Dtsch.Ges.Inn.Med.* **77**:1182-1185.

Kim NS, Kim SJ, and Lee GM (1998) Clonal variability within dihydrofolate reductase-mediated gene amplified Chinese hamster ovary cells: stability in the absence of selective pressure. *Biotechnol.Bioeng.* **60**:679-688.

Kim YM, Jeon YH, Jin GC, Lim JO, and Baek WY (2004) Immunoisolated chromaffin cells implanted into the subarachnoid space of rats reduce cold allodynia in a model of neuropathic pain: a novel application of microencapsulation technology. *Artif.Organs* **28**:1059-1066.

Koch S, Schwinger C, Kressler J, Heinzen C, and Rainov NG (2003) Alginate encapsulation of genetically engineered mammalian cells: comparison of production devices, methods and microcapsule characteristics. *J.Microencapsul.* **20**:303-316.

Kostner GM, Laggner P, Prexl HJ, and Holasek A (1976) Investigation of the abnormal low-density lipoproteins occurring in patients with obstructive jaundice. *Biochem.J.* **157**:401-407.

Kostner GM, Knipping G, Groener JE, Zechner R, and Dieplinger H (1987) The role of LCAT and cholesteryl ester transfer proteins for the HDL and LDL structure and metabolism. *Adv.Exp.Med.Biol.* **210**:79-86.

Krieger M (2001) Scavenger receptor class B type I is a multiligand HDL receptor that influences diverse physiologic systems. *J.Clin.Invest* **108**:793-797.

Kuivenhoven JA, van Voorst tot Voorst EJ, Wiebusch H, Marcovina SM, Funke H, Assmann G, Pritchard PH, and Kastelein JJ (1995) A unique genetic and biochemical presentation of fish-eye disease. *J.Clin.Invest* **96**:2783-2791.

Kuivenhoven JA, Stalenhoef AF, Hill JS, Demacker PN, Errami A, Kastelein JJ, and Pritchard PH (1996) Two novel molecular defects in the LCAT gene are associated with fish eye disease. *Arterioscler.Thromb.Vasc.Biol.* **16**:294-303.

Kuivenhoven JA, Pritchard H, Hill J, Frohlich J, Assmann G, and Kastelein J (1997) The molecular pathology of lecithin:cholesterol acyltransferase (LCAT) deficiency syndromes. *J.Lipid Res.* **38**:191-205.

Laffi G, La Villa G, Pinzani M, Ciabattoni G, Patrignani P, Mannelli M, Cominelli F, and Gentilini P (1986) Altered renal and platelet arachidonic acid metabolism in cirrhosis. *Gastroenterology* **90**:274-282.

Lager DJ, Rosenberg BF, Shapiro H, and Bernstein J (1991) Lecithin cholesterol acyltransferase deficiency: ultrastructural examination of sequential renal biopsies. *Mod.Pathol.* **4** :331-335.

Lambert G, Sakai N, Vaisman BL, Neufeld EB, Marteyn B, Chan CC, Paigen B, Lupia E, Thomas A, Striker LJ, Blanchette-Mackie J, Csako G, Brady JN, Costello R, Striker GE, Remaley AT, Brewer HB, Jr., and Santamarina-Fojo S (2001) Analysis of glomerulosclerosis and atherosclerosis in lecithin cholesterol acyltransferase-deficient mice. *J.Biol.Chem.* **276**:15090-15098.

Lambert G, Sakai N, Vaisman BL, Neufeld EB, Marteyn B, Chan CC, Paigen B, Lupia E, Thomas A, Striker LJ, Blanchette-Mackie J, Csako G, Brady JN, Costello R, Striker GE, Remaley AT, Brewer HB, Jr., and Santamarina-Fojo S (2001) Analysis of glomerulosclerosis and atherosclerosis in lecithin cholesterol acyltransferase-deficient mice. *J.Biol.Chem.* **276**:15090-15098.

Lane SB, Tchedre KT, Nair MP, Thigpen AE, and Lacko AG (2004) Characterization of lecithin:cholesterol acyltransferase expressed in a human lung cell line. *Protein Expr.Purif.* **36** :157-164.

Lanza RP and Chick WL (1997) Transplantation of encapsulated cells and tissues. *Surgery* **121**:1-9.

Lanza RP and Cooper DK (1998) Xenotransplantation of cells and tissues: application to a range of diseases, from diabetes to Alzheimer's. *Mol.Med.Today* **4**:39-45.

Lee SS, Marty J, Mantz J, Samain E, Braillon A, and Lebrec D (1990) Desensitization of myocardial beta-adrenergic receptors in cirrhotic rats. *Hepatology* **12**:481-485.

Lee YM and Kaplan MM (1995) Primary sclerosing cholangitis. *N.Engl.J.Med.* **332**:924-933.

Leibovitch MP and Kruh J (1979) Effect of sodium butyrate on myoblast growth and differentiation. *Biochem.Biophys.Res.Commun.* **87**:896-903.

Lim F and Sun AM (1980) Microencapsulated islets as bioartificial endocrine pancreas. *Science* **210**:908-910.

Liu H, Gaskari SA, and Lee SS (2006) Cardiac and vascular changes in cirrhosis: pathogenic mechanisms. *World J.Gastroenterol.* **12**:837-842.

Lohr M, Hoffmeyer A, Kroger J, Freund M, Hain J, Holle A, Karle P, Knofel WT, Liebe S, Muller P, Nizze H, Renner M, Saller RM, Wagner T, Hauenstein K, Gunzburg WH, and Salmons B (2001) Microencapsulated cell-mediated treatment of inoperable pancreatic carcinoma. *Lancet* **357**:1591-1592.

Ma Z, Meddings JB, and Lee SS (1994) Membrane physical properties determine cardiac beta-adrenergic receptor function in cirrhotic rats. *Am.J.Physiol* **267**:G87-G93.

Manzato E, Fellin R, Baggio G, Walch S, Neubeck W, and Seidel D (1976) Formation of lipoprotein-X. Its relationship to bile compounds. *J.Clin.Invest* **57**:1248-1260.

McIntyre N, Calandra S, and Pearson AJ (1974) Lipid and lipoprotein abnormalities in liver disease: the possible role of lecithin: cholesterol acyltransferase deficiency. *Scand.J.Clin.Lab Invest Suppl* **137**:115-120.

McIntyre N (1978) Plasma lipids and lipoproteins in liver disease. *Gut* **19**:526-530.

McLean J, Fielding C, Drayna D, Dieplinger H, Baer B, Kohr W, Henzel W, and Lawn R (1986) Cloning and expression of human lecithin-cholesterol acyltransferase cDNA. *Proc.Natl.Acad.Sci.U.S.A* **83**:2335-2339.

McLean J, Wion K, Drayna D, Fielding C, and Lawn R (1986) Human lecithin-cholesterol acyltransferase gene: complete gene sequence and sites of expression. *Nucleic Acids Res.* **14**:9397-9406.

McLean J, Wion K, Drayna D, Fielding C, and Lawn R (1986) Human lecithin-cholesterol acyltransferase gene: complete gene sequence and sites of expression. *Nucleic Acids Res.* **14**:9397-9406.

Medghalchi S, Padmanabhan R, and Ketner G (1997) Early region 4 modulates adenovirus DNA replication by two genetically separable mechanisms. *Virology* **236**:8-17.

Miller KR, Wang J, Sorci-Thomas M, Anderson RA, and Parks JS (1996) Glycosylation structure and enzyme activity of lecithin:cholesterol acyltransferase from human plasma, HepG2 cells, and baculoviral and Chinese hamster ovary cell expression systems. *J.Lipid Res.* **37**:551-561.

Miner NA, Koehler J, and Greenaway L (1969) Intraperitoneal injection of mice. *Appl.Microbiol.* **17**:250-251.

Morsy MA and Caskey CT (1999) Expanded-capacity adenoviral vectors--the helper-dependent vectors. *Mol.Med.Today* **5**:18-24.

Mount JD, Herzog RW, Tillson DM, Goodman SA, Robinson N, McCleland ML, Bellinger D, Nichols TC, Arruda VR, Lothrop CD, Jr., and High KA (2002) Sustained phenotypic correction of hemophilia B dogs with a factor IX null mutation by liver-directed gene therapy. *Blood* **99**:2670-2676.

Mueller-Klieser W, Freyer JP, and Sutherland RM (1986) Influence of glucose and oxygen supply conditions on the oxygenation of multicellular spheroids. *Br.J.Cancer* **53**:345-353.

Mullen CA, Snitzer K, Culver KW, Morgan RA, Anderson WF, and Blaese RM (1996) Molecular analysis of T lymphocyte-directed gene therapy for adenosine deaminase deficiency: long-term expression in vivo of genes introduced with a retroviral vector. *Hum.Gene Ther.* **7**:1123-1129.

Narayanan S (1984) Biochemistry and clinical relevance of lipoprotein X. *Ann.Clin.Lab Sci.* **14**:371-374.

Nevens F (1997) Acute liver failure. *Acta Gastroenterol.Belg.* **60**:298-301.

Ng DS, Francone OL, Forte TM, Zhang J, Haghpassand M, and Rubin EM (1997) Disruption of the murine lecithin:cholesterol acyltransferase gene causes impairment of adrenal lipid delivery and up-regulation of scavenger receptor class B type I. *J.Biol.Chem.* **272**:15777-15781.

Nordby G, Berg T, Nilsson M, and Norum KR (1976) Secretion of lecithin: cholesterol acyltransferase from isolated rat hepatocytes. *Biochim.Biophys.Acta* **450**:69-77.

Norum KR and Gjone E (1967) Familial serum-cholesterol esterification failure. A new inborn error of metabolism. *Biochim.Biophys.Acta* **144**:698-700.

Norum KR, GLOMSET JA, Nichols AV, and Forte T (1971) Plasma lipoproteins in familial lecithin: cholesterol acyltransferase deficiency: physical and chemical studies of low and high density lipoproteins. *J.Clin.Invest* **50**:1131-1140.

O'Grady JG, Schalm SW, and Williams R (1993) Acute liver failure: redefining the syndromes. *Lancet* **342**:273-275.

O K, Hill JS, Wang X, McLeod R, and Pritchard PH (1993) Lecithin:cholesterol acyltransferase: role of N-linked glycosylation in enzyme function. *Biochem.J.* **294 (Pt 3)**:879-884.

Okada N, Miyamoto H, Yoshioka T, Katsume A, Saito H, Yorozu K, Ueda O, Itoh N, Mizuguchi H, Nakagawa S, Ohsugi Y, and Mayumi T (1997) Cytomedical therapy for IgG1 plasmacytosis in human interleukin-6 transgenic mice using hybridoma cells microencapsulated in alginate-poly(L)lysine-alginate membrane. *Biochim.Biophys.Acta* **1360**:53-63.

Oram JF and Lawn RM (2001) ABCA1. The gatekeeper for eliminating excess tissue cholesterol. *J.Lipid Res.* **42**:1173-1179.

Orive G, Hernandez RM, Gascon AR, Igartua M, and Pedraz JL (2003) Survival of different cell lines in alginate-agarose microcapsules. *Eur.J.Pharm.Sci.* **18**:23-30.

Orive G, Hernandez RM, Rodriguez GA, Calafiore R, Chang TM, De Vos P, Hortelano G, Hunkeler D, Lacik I, and Pedraz JL (2004) History, challenges and perspectives of cell microencapsulation. *Trends Biotechnol.* **22**:87-92.

Orive G, De Castro M, Ponce S, Hernandez RM, Gascon AR, Bosch M, Alberch J, and Pedraz JL (2005) Long-term expression of erythropoietin from myoblasts immobilized in biocompatible and neovascularized microcapsules. *Mol.Ther.* **12**:283-289.

Orive G, Tam SK, Pedraz JL, and Halle JP (2006) Biocompatibility of alginate-poly-L-lysine microcapsules for cell therapy. *Biomaterials* **27**:3691-3700.

Osuga T and Portman OW (1971) Origin and disappearance of plasma lecithin: cholesterol acyltransferase. *Am.J.Physiol* **220**:735-741.

Owen JS, Hutton RA, Day RC, Bruckdorfer KR, and McIntyre N (1981) Platelet lipid composition and platelet aggregation in human liver disease. *J.Lipid Res.* **22**:423-430.

Owen JS, Bruckdorfer KR, Day RC, and McIntyre N (1982) Decreased erythrocyte membrane fluidity and altered lipid composition in human liver disease. *J.Lipid Res.* **23**:124-132.

Owen JS and Gillett MP (1983) Plasma lipids, lipoproteins and cell membranes. *Biochem.Soc.Trans.* **11**:336-339.

Owen JS, Goodall H, Mistry P, Harry DS, Day RC, and McIntyre N (1984) Abnormal high density lipoproteins from patients with liver disease regulate cholesterol metabolism in cultured human skin fibroblasts. *J.Lipid Res.* **25**:919-931.

Owen JS (1990) Extrahepatic cell membrane lipid abnormalities and cellular dysfunction in liver disease. *Drugs* **40 Suppl 3**:73-83.

Owen JS, Wiebusch H, Cullen P, Watts GF, Lima VL, Funke H, and Assmann G (1996) Complete deficiency of plasma lecithin-cholesterol acyltransferase (LCAT) activity due to a novel homozygous mutation (Gly-30-Ser) in the LCAT gene. *Hum.Mutat.* **8**:79-82.

Owen JS and Mulcahy JV (2002) ATP-binding cassette A1 protein and HDL homeostasis. *Atheroscler.Suppl* **3**:13-22.

Packard CJ, Munro A, Lorimer AR, Gotto AM, and Shepherd J (1984) Metabolism of apolipoprotein B in large triglyceride-rich very low density lipoproteins of normal and hypertriglyceridemic subjects. *J.Clin.Invest* **74**:2178-2192.

Palmer TD, Rosman GJ, Osborne WR, and Miller AD (1991) Genetically modified skin fibroblasts persist long after transplantation but gradually inactivate introduced genes. *Proc.Natl.Acad.Sci.U.S.A* **88**:1330-1334.

Perez-Ayuso RM, Arroyo V, Camps J, Rimola A, Gaya J, Costa J, Rivera F, and Rodes J (1984) Evidence that renal prostaglandins are involved in renal water metabolism in cirrhosis. *Kidney Int.* **26**:72-80.

Picariello L, Benvenuti S, Recenti R, Formigli L, Falchetti A, Morelli A, Masi L, Tonelli F, Cicchi P, and Brandi ML (2001) Microencapsulation of human parathyroid cells: an "in vitro" study. *J.Surg.Res.* **96**:81-89.

Porath J, Carlsson J, Olsson I, and Belfrage G (1975) Metal chelate affinity chromatography, a new approach to protein fractionation. *Nature* **258**:598-599.

Porath J (1992) Immobilized metal ion affinity chromatography. *Protein Expr.Purif.* **3**:263-281.

Puthenveetil G and Malik P (2004) Gene therapy for hemoglobinopathies: are we there yet? *Curr.Hematol.Rep.* **3**:298-305.

Qu SJ, Fan HZ, Blanco-Vaca F, and Pownall HJ (1993) Roles of cysteines in human lecithin:cholesterol acyltransferase. *Biochemistry* **32**:3089-3094.

Qu SJ, Fan HZ, Blanco-Vaca F, and Pownall HJ (1993) Effects of site-directed mutagenesis on the N-glycosylation sites of human lecithin:cholesterol acyltransferase. *Biochemistry* **32**:8732-8736.

Ramond MJ, Comoy E, and Lebrec D (1986) Alterations in isoprenaline sensitivity in patients with cirrhosis: evidence of abnormality of the sympathetic nervous activity. *Br.J.Clin.Pharmacol.* **21**:191-196.

Rashid S, Trinh DK, Uffelman KD, Cohn JS, Rader DJ, and Lewis GF (2003) Expression of human hepatic lipase in the rabbit model preferentially enhances the clearance of triglyceride-enriched versus native high-density lipoprotein apolipoprotein A-I. *Circulation* **107**:3066-3072.

Regulier E, Schneider BL, Deglon N, Beuzard Y, and Aebischer P (1998) Continuous delivery of human and mouse erythropoietin in mice by genetically engineered polymer encapsulated myoblasts. *Gene Ther.* **5**:1014-1022.

Riggs MG, Whittaker RG, Neumann JR, and Ingram VM (1977) n-Butyrate causes histone modification in HeLa and Friend erythroleukaemia cells. *Nature* **268**:462-464.

Riordan SM and Williams R (2000) Acute liver failure: targeted artificial and hepatocyte-based support of liver regeneration and reversal of multiorgan failure. *J.Hepatol.* **32**:63-76.

Ritter T, Lehmann M, and Volk HD (2002) Improvements in gene therapy: averting the immune response to adenoviral vectors. *BioDrugs.* **16**:3-10.

Robitaille R, Pariseau JF, Leblond FA, Lamoureux M, Lepage Y, and Halle JP (1999) Studies on small (<350 microm) alginate-poly-L-lysine microcapsules. III. Biocompatibility Of smaller versus standard microcapsules. *J.Biomed.Mater.Res.* **44**:116-120.

Sagot Y, Tan SA, Baetge E, Schmalbruch H, Kato AC, and Aebischer P (1995) Polymer encapsulated cell lines genetically engineered to release ciliary neurotrophic factor can slow down progressive motor neuronopathy in the mouse. *Eur.J.Neurosci.* **7**:1313-1322.

Saitoh Y, Taki T, Arita N, Ohnishi T, and Hayakawa T (1995) Cell therapy with encapsulated xenogeneic tumor cells secreting beta-endorphin for treatment of peripheral pain. *Cell Transplant.* **4 Suppl 1**:S13-S17.

Sakai N, Vaisman BL, Koch CA, Hoyt RF, Jr., Meyn SM, Talley GD, Paiz JA, Brewer HB, Jr., and Santamarina-Fojo S (1997) Targeted disruption of the mouse lecithin:cholesterol acyltransferase (LCAT) gene. Generation of a new animal model for human LCAT deficiency. *J.Biol.Chem.* **272**:7506-7510.

Schaefer EJ and Levy RI (1985) Pathogenesis and management of lipoprotein disorders. *N.Engl.J.Med.* **312**:1300-1310.

Schimke RT, Kaufman RJ, Alt FW, and Kellems RF (1978) Gene amplification and drug resistance in cultured murine cells. *Science* **202**:1051-1055.

Schrezenmeir J, Gero L, Laue C, Kirchgessner J, Muller A, Huls A, Passmann R, Hahn HJ, Kunz L, Mueller-Klieser W, and . (1992) The role of oxygen supply in islet transplantation. *Transplant.Proc.* **24**:2925-2929.

Schrezenmeir J, Kirchgessner J, Gero L, Kunz LA, Beyer J, and Mueller-Klieser W (1994) Effect of microencapsulation on oxygen distribution in islets organs. *Transplantation* **57**:1308-1314.

Sealy L and Chalkley R (1978) The effect of sodium butyrate on histone modification. *Cell* **14**:115-121.

Seguret-Mace S, Latta-Mahieu M, Castro G, Luc G, Fruchart JC, Rubin E, Denefle P, and Duverger N (1996) Potential gene therapy for lecithin-cholesterol acyltransferase (LCAT)-deficient and hypoalphalipoproteinemic patients with adenovirus-mediated transfer of human LCAT gene. *Circulation* **94**:2177-2184.

Seidel D, Alaupovic P, and Furman RH (1969) A lipoprotein characterizing obstructive jaundice. I. Method for quantitative separation and identification of lipoproteins in jaundiced subjects. *J.Clin.Invest* **48**:1211-1223.

Seidel D, Greten H, Geisen HP, Wengeler H, and Wieland H (1972) Further aspects on the characterization of high and very low density lipoproteins in patients with liver disease. *Eur.J.Clin.Invest* **2**:359-364.

Seidel D (1987) Lipoproteins in liver disease. *J.Clin.Chem.Clin.Biochem.* **25**:541-551.

Sgoutas DS (1972) Fatty acid specificity of plasma phosphatidylcholine: cholesterol acyltransferase. *Biochemistry* **11**:293-296.

Shimada M, Yanaga K, Makowka L, Kakizoe S, Van Thiel DH, and Starzl TE (1989) Significance of lecithin:cholesterol acyltransferase activity as a prognostic indicator of early allograft function in clinical liver transplantation. *Transplantation* **48**:600-603.

Shinozuka H, Farber JL, Konishi Y, and Anukarahanonta T (1973) D-galactosamine and acute liver cell injury. *Fed.Proc.* **32**:1516-1526.

Silman NJ and Fooks AR (2000) Biophysical targeting of adenovirus vectors for gene therapy. *Curr.Opin.Mol.Ther.* **2**:524-531.

Silver DL, Wang N, Xiao X, and Tall AR (2001) High density lipoprotein (HDL) particle uptake mediated by scavenger receptor class B type 1 results in selective sorting of HDL cholesterol from protein and polarized cholesterol secretion. *J.Biol.Chem.* **276**:25287-25293.

Simon M and Brissot P (1988) The genetics of haemochromatosis. *J.Hepatol.* **6**:116-124.

Smidsrod O and Skjak-Braek G (1990) Alginate as immobilization matrix for cells. *Trends Biotechnol.* **8**:71-78.

Soon-Shiong P, Lu ZN, Grewal I, Lanza R, and Clark W (1990) Prevention of CTL and NK cell-mediated cytotoxicity by microencapsulation. *Horm.Metab Res.Suppl* **25**:215-219.

Soon-Shiong P, Otterlie M, Skjak-Braek G, Smidsrod O, Heintz R, Lanza RP, and Espevik T (1991) An immunologic basis for the fibrotic reaction to implanted microcapsules. *Transplant.Proc.* **23**:758-759.

Soon-Shiong P, Feldman E, Nelson R, Komtebedde J, Smidsrod O, Skjak-Braek G, Espevik T, Heintz R, and Lee M (1992) Successful reversal of spontaneous diabetes in dogs by intraperitoneal microencapsulated islets. *Transplantation* **54**:769-774.

Soon-Shiong P (1999) Treatment of type I diabetes using encapsulated islets. *Adv.Drug Deliv.Rev.* **35**:259-270.

Spector T (1978) Refinement of the coomassie blue method of protein quantitation. A simple and linear spectrophotometric assay for less than or equal to 0.5 to 50 microgram of protein. *Anal.Biochem.* **86**:142-146.

Steinmetz A and Utermann G (1985) Activation of lecithin: cholesterol acyltransferase by human apolipoprotein A-IV. *J.Biol.Chem.* **260**:2258-2264.

Stillman B (1986) Functions of the adenovirus E1B tumour antigens. *Cancer Surv.* **5**:389-404.

Stoffel W, Muller R, Binczek E, and Hofmann K (1992) Mouse apolipoprotein AI. cDNA-derived primary structure, gene organisation and complete nucleotide sequence. *Biol.Chem.Hoppe Seyler* **373**:187-193.

Stokke KT, Bjerve KS, Blomhoff JP, Oystese B, Flatmark A, Norum KR, and Gjone E (1974) Familial lecithin:cholesterol acyltransferase deficiency. Studies on lipid composition and morphology of tissues. *Scand.J.Clin.Lab Invest Suppl* **137**:93-100.

Strand BL, Ryan TL, In't VP, Kulseng B, Rokstad AM, Skjak-Brek G, and Espevik T (2001) Poly-L-Lysine induces fibrosis on alginate microcapsules via the induction of cytokines. *Cell Transplant.* **10**:263-275.

Strand BL, Ryan TL, In't VP, Kulseng B, Rokstad AM, Skjak-Brek G, and Espevik T (2001) Poly-L-Lysine induces fibrosis on alginate microcapsules via the induction of cytokines. *Cell Transplant.* **10**:263-275.

Strom SC, Fisher RA, Thompson MT, Sanyal AJ, Cole PE, Ham JM, and Posner MP (1997) Hepatocyte transplantation as a bridge to orthotopic liver transplantation in terminal liver failure. *Transplantation* **63**:559-569.

Struck MM (1994) Biopharmaceutical R&D success rates and development times. A new analysis provides benchmarks for the future. *Biotechnology (N.Y.)* **12**:674-677.

Subbaiah PV, Albers JJ, Chen CH, and Bagdade JD (1980) Low density lipoprotein-activated lysolecithin acylation by human plasma lecithin-cholesterol acyltransferase. Identity of lysolecithin acyltransferase and lecithin-cholesterol acyltransferase. *J.Biol.Chem.* **255**:9275-9280.

Sun AM, Cai Z, Shi Z, Ma F, O'Shea GM, and Gharapetian H (1986) Microencapsulated hepatocytes as a bioartificial liver. *ASAIO Trans.* **32**:39-41.

Sun AM (1997) Microencapsulation of cells. Medical applications. *Ann.N.Y.Acad.Sci.* **831**:271-279.

Sun Y, Ma X, Zhou D, Vacek I, and Sun AM (1996) Normalization of diabetes in spontaneously diabetic cynomologus monkeys by xenografts of microencapsulated porcine islets without immunosuppression. *J.Clin.Invest* **98**:1417-1422.

Tagalakis AD, Diakonov IA, Graham IR, Heald KA, Harris JD, Mulcahy JV, Dickson G, and Owen JS (2005) Apolipoprotein E delivery by peritoneal implantation of encapsulated recombinant cells improves the hyperlipidaemic profile in apoE-deficient mice. *Biochim.Biophys.Acta* **1686 3**:190-199.

Tall AR (1990) Plasma high density lipoproteins. Metabolism and relationship to atherogenesis. *J.Clin.Invest* **86**:379-384.

Taylor ME (1993) Recognition of complex carbohydrates by the macrophage mannose receptor. *Biochem.Soc.Trans.* **21**:468-473.

Teisberg P, Gjone E, and Olaisen B (1975) Genetics of LCAT (lecithin: cholesterol acyltransferase) deficiency. *Ann.Hum.Genet.* **38**:327-331.

Terblanche J and Hickman R (1991) Animal models of fulminant hepatic failure. *Dig.Dis.Sci.* **36**:770-774.

Thu B, Bruheim P, Espevik T, Smidsrod O, Soon-Shiong P, and Skjak-Braek G (1996) Alginate polycation microcapsules. II. Some functional properties. *Biomaterials* **17**:1069-1079.

Thu B, Bruheim P, Espevik T, Smidsrod O, Soon-Shiong P, and Skjak-Braek G (1996) Alginate polycation microcapsules. I. Interaction between alginate and polycation. *Biomaterials* **17**:1031-1040.

Thu B, Bruheim P, Espevik T, Smidsrod O, Soon-Shiong P, and Skjak-Braek G (1996) Alginate polycation microcapsules. II. Some functional properties. *Biomaterials* **17**:1069-1079.

Tripathy SK, Goldwasser E, Lu MM, Barr E, and Leiden JM (1994) Stable delivery of physiologic levels of recombinant erythropoietin to the systemic circulation by intramuscular injection of replication-defective adenovirus. *Proc.Natl.Acad.Sci.U.S.A* **91**:11557-11561.

Uludag H, De Vos P, and Tresco PA (2000) Technology of mammalian cell encapsulation. *Adv.Drug Deliv.Rev.* **42**:29-64.

Vaisman BL, Klein HG, Rouis M, Berard AM, Kindt MR, Talley GD, Meyn SM, Hoyt RF, Jr., Marcovina SM, Albers JJ, and . (1995) Overexpression of human lecithin cholesterol acyltransferase leads to hyperalphalipoproteinemia in transgenic mice. *J.Biol.Chem.* **270**:12269-12275.

van Schilfgaarde R and De Vos P (1999) Factors influencing the properties and performance of microcapsules for immunoprotection of pancreatic islets. *J.Mol.Med.* **77**:199-205.

Van Wijk R, Tichonicky L, and Kruh J (1981) Effect of sodium butyrate on the hepatoma cell cycle: possible use for cell synchronization. *In Vitro* **17**:859-862.

Vandenbossche GM, Bracke ME, Cuvelier CA, Bortier HE, Mareel MM, and Remon JP (1993) Host reaction against alginate-polylysine microcapsules containing living cells. *J.Pharm.Pharmacol.* **45**:121-125.

Vinogradov DV, Hongqun L, and Owen JS (1998) C-terminal His6-tagged lecithin-cholesterol acyltransferase (LCAT) is catalytically active. *Biochem.Soc.Trans.* **26**:S146.

Wang L, Nichols TC, Read MS, Bellinger DA, and Verma IM (2000) Sustained expression of therapeutic level of factor IX in hemophilia B dogs by AAV-mediated gene therapy in liver. *Mol.Ther.* **1**:154-158.

Wang N, Lan D, Chen W, Matsuura F, and Tall AR (2004) ATP-binding cassette transporters G1 and G4 mediate cellular cholesterol efflux to high-density lipoproteins. *Proc.Natl.Acad.Sci.U.S.A* **101**:9774-9779.

Warden CH, Langner CA, Gordon JI, Taylor BA, McLean JW, and Lusis AJ (1989) Tissue-specific expression, developmental regulation, and chromosomal mapping of the lecithin: cholesterol acyltransferase gene. Evidence for expression in brain and testes as well as liver. *J.Biol.Chem.* **264**:21573-21581.

Weber CJ, Zabinski S, Koschitzky T, Wicker L, Rajotte R, D'Agati V, Peterson L, Norton J, and Reemtsma K (1990) The role of CD4+ helper T cells in the destruction of microencapsulated islet xenografts in nod mice. *Transplantation* **49**:396-404.

Wickham TJ, Mathias P, Cheresh DA, and Nemerow GR (1993) Integrins alpha v beta 3 and alpha v beta 5 promote adenovirus internalization but not virus attachment. *Cell* **73**:309-319.

Wilson JM (2001) Adenovirus-mediated gene transfer to liver. *Adv.Drug Deliv.Rev.* **46**:205-209.

Winn SR, Hammang JP, Emerich DF, Lee A, Palmiter RD, and Baetge EE (1994) Polymer-encapsulated cells genetically modified to secrete human nerve growth factor promote the survival of axotomized septal cholinergic neurons. *Proc.Natl.Acad.Sci.U.S.A* **91**:2324-2328.

Wong H and Chang TM (1986) Bioartificial liver: implanted artificial cells microencapsulated living hepatocytes increases survival of liver failure rats. *Int.J.Artif.Organs* **9**:335-336.

Wong H and Chang TM (1988) The viability and regeneration of artificial cell microencapsulated rat hepatocyte xenograft transplants in mice. *Biomater.Artif.Cells Artif.Organs* **16**:731-739.

Wright JA (1973) Morphology and growth rate changes in Chinese hamster cells cultured in presence of sodium butyrate. *Exp.Cell Res.* **78**:456-460.

Xu W, Liu L, and Charles IG (2002) Microencapsulated iNOS-expressing cells cause tumor suppression in mice. *FASEB J.* **16**:213-215.

Yang CY, Manoogian D, Pao Q, Lee FS, Knapp RD, Gotto AM, Jr., and Pownall HJ (1987) Lecithin:cholesterol acyltransferase. Functional regions and a structural model of the enzyme. *J.Biol.Chem.* **262**:3086-3091.

Yang Y, Nunes FA, Berencsi K, Furth EE, Gonczol E, and Wilson JM (1994) Cellular immunity to viral antigens limits E1-deleted adenoviruses for gene therapy. *Proc.Natl.Acad.Sci.U.S.A* **91**:4407-4411.

Yang Y, Haecker SE, Su Q, and Wilson JM (1996) Immunology of gene therapy with adenoviral vectors in mouse skeletal muscle. *Hum.Mol.Genet.* **5**:1703-1712.

Zannis VI, Chroni A, and Krieger M (2006) Role of apoA-I, ABCA1, LCAT, and SR-BI in the biogenesis of HDL. *J.Mol.Med.* **84**:276-294.

Zeman K, Dworniak D, Tchorzewski H, Pokoca L, and Majewska E (1991) Effect of thymic extract on allogeneic MLR and mitogen-induced responses in patients with chronic active hepatitis B. *Immunol.Invest* **20**:545-555.

ACKNOWLEDGEMENTS

I would like to express my gratitude to Prof. James S. Owen for giving me an opportunity to do an MD under his supervision. His patience, guidance, support, encouragement throughout this project and his critical review of this manuscript has been invaluable.

I am very grateful to all my friends and work colleagues at the Royal Free and Royal Holloway who have contributed directly and indirectly to this project. I would like to thank Prof. M. Winslet for arranging the RMO job to fund this project; Dr. D. Riddell who showed me the rudiments of laboratory work; Dr. A. Stannard for her help in cell culture; Dr. A. D. Tagalakis for his help in radioactive assays, cell maintenance when I was on duty and proof reading my thesis; Dr. S. Schepelmann for her help and training in molecular biology and protein purification techniques ; Dr. J. Auld for his help with histology of my specimens; Dr. I. R. Graham for his help and access to animal work. I am also grateful to Dr. K. Heald at the Worcester Royal Infirmary for her expertise and help in microencapsulation.

Very special thanks to my dearest wife Yanning for her patience, love, understanding and encouragement throughout. I am grateful for her assistance in computing skills especially in the preparation of this manuscript.

Lastly, I would like to thank my mother, sisters and brothers especially Jee Ming who constantly ask “Have you finished writing your thesis yet?”

Jee Low, January 2008.